

**MODULATION OF DNA TRIPLEX STABILITY THROUGH
CHEMICAL MODIFICATIONS**

**THESIS
SUBMITTED TO
THE UNIVERSITY OF POONA**

TH-1089

**FOR
THE DEGREE OF DOCTOR OF PHILOSOPHY
IN CHEMISTRY**

**BY
K. G. RAJEEV**

**NATIONAL CHEMICAL LABORATORY
PUNE-411 008
APRIL 1997**

TH-1089

Dedicated to My Parents

CERTIFICATE

Certified that the work incorporated in the thesis entitled "**Modulation of DNA Triplex Stability Through Chemical Modifications**" submitted by **Mr. K. G. RAJEEV** was carried out by the candidate under my supervision. Such materials as obtained from other sources have been duly acknowledged in the thesis.


(K. N. GANESH)

April 1997

Research Guide

Head, Division of Organic Chemistry (Synthesis)

National Chemical laboratory

Pune-411 008.

CANDIDATE'S DECLARATION

I hereby declare that the thesis entitled "**Modulation of DNA Triplex Stability Through Chemical Modifications**" submitted for the degree of Doctor of Philosophy in Chemistry to the University of Poona has not been submitted by me for a degree to any other university or institution.

National Chemical Laboratory

Pune- 411 008.

April 1997


(K. G. RAJEEV)

ACKNOWLEDGMENTS

It gives me great pleasure to place on record my deep sense of gratitude to my research guide Dr. K. N. Ganesh for introducing me to the chemistry and biology of Nucleic Acids, the fascinating area of bioorganic chemistry. His receptive attitude, constant encouragement and enthusiasm will always remain a source of inspiration.

I am greatly thankful to Dr. M. S. Shashidhar for his timely help and encouragement. I owe him much not only for his help in scientific guidance but also for his care and concern in the lab. In fact a part of the thesis is an outcome of my interaction with him.

I am thankful to Dr. S. Rajappa for providing me the opportunity to start my research career with Dr. K. N. Ganesh. I take this opportunity to thank the Director, National Chemical Laboratory, for allowing me to work in this laboratory and providing necessary facilities.

My sincere thanks are due to:

Prof. A. D. Hamilton, University of Pittsburgh, USA; Prof. C. Switzer, University of California, USA and Dr. Vairamani, IICT, Hyderabad for providing MS of key compounds.

Dr. P. Chakrabarti and Mr. U. Samanta, the Division of Physical Chemistry, NCL for X-Ray crystal structure analysis.

Dr. K. Pius, M. G. University, Kottayam for AM1 calculations.

I gratefully acknowledge and thank Mr. A. G. Samuel, Dr. G. J. Sanjayan, Dr. R. Krishnakumar and Mrs. U. Phalgune for their assistance in recording and analyzing NMR spectra. My thanks are also due to Mrs. S. S. Kunte, Mrs. M. V. Mane for HPLC analysis and the library staff for excellent facilities. I am thankful to Mrs. A. Gunjal for her assistance in oligonucleotide synthesis.

I take this opportunity to place my sincere thank to Dr. D. A. Barawkar and Dr. (Mrs.) V. A. Kumar for their valuable scientific discussion during the course of this work.

I am grateful to Dr. T. Pathak and Dr. A. A. Natu for their help and suggestions.

It is a great pleasure to thank my friends Gopal, Vasant and Anand for their invaluable help inside and outside the lab during the course of my Ph. D. work.

I take this opportunity to thank my colleagues Tanya, Gangamani, Sanjib, Praveen, Nagamani, Bindu, Pradeep, Vipul, Ramesh, Moneesha, Vallabh, Leena and Meena.

I am grateful to Drs. R. R Joshi, T. P. Prakash, M. Renil and K. Sakthivel for their encouragement.

I am indebted to Dr. (Ms) Anita Bhargava, S. N. College, Kannur for providing me financial assistance for my higher education. I am very much thankful to Mr. E. Prasannan, S. N. College, Kannur and Prof. Padmanabhan Nambiar, P. R. N. S. S. College Mattanur for their invaluable help during my early stage of education.

I would like to thank Jayashree Gopal not only for taking trouble in bringing out the thesis but also for providing homely atmosphere away from home.

I thank Makhar, Prakash, Sunil and Bhumkar for their help and cooperation.

I am thankful to Santhosh, Anuj, Radha, Vijay, Rajesh, Saumen, Deepak, Karthikeyan, Suresh, Prasad, Gawande, Jayaprakash and Anil for providing me a cheerful hostel atmosphere. I will be failing in my duties if I forget to thank my MSc. friends Vinod, Asok and Sam for their support and encouragement.

I am indebted to my family members for their sacrifice and encouragement.

Finally I acknowledge CSIR (INDIA) for valuable support in the form of fellowship.

CONTENTS

PUBLICATIONS	i
ABSTRACT	ii
ABBREVIATIONS	X
CHAPTER 1. INTRODUCTION	
1.1 Introduction	1
1.1.1 Polymorphism in DNA structures	4
1.1.2 Molecular recognition in the major and minor groove of DNA	8
1.1.3 Scope and aims	8
1.2 DNA triple helix: General features	8
1.2.1 Triple helical motifs	9
1.2.2 Triplex structures	11
1.2.3 Triplex grooves	12
1.2.4 Sequence control of triplex stability	12
1.2.5 Kinetics of triple helix formation	14
1.3 Nucleobase modification	16
1.3.1 Pyrimidine modification to alter N3 pK _a	16
1.3.2 C5-substituted pyrimidines	16
1.3.3 Neutral mimics of C ⁺	20
1.4 Triplex stabilization by backbone modifications	23
1.5 Biological applications of triple helix forming ODNs	24
1.6 Present work	25
1.7 References	28
CHAPTER 2. CHEMICAL SYNTHESIS AND CHARACTERIZATION OF (I) dC-N ⁴ -(ALKYLAMINO/ALKOXY) AND (II) 2-AMINO-dA-N ⁶ -(ALKYLAMINO) ANALOGUES FOR APPLICATION IN DNA TRIPLEX STABILIZATION	
2.1 Target molecules and rationale	34
2.2 Synthesis of N -(alkylamino/alkoxy)-dC and 2-amino-N -(spermino)-dA	36
2.2.1 General synthetic strategy	36
2.2.2 Substituted amines for linking to N ⁴ of dC	37
2.2.3 N ⁴ -(alkylamino/alkoxy)-dC	42

2.2.4 2-Amino-N ⁶ -(spermine)-dA	52
2.3 pK _a determination of modified dC analogues	53
2.4 Conclusions	56
2.5 Experimental	57
2.6 References	69
CHAPTER 3. BIOPHYSICAL STUDIES ON THE MOLECULAR ORIGIN OF TRIPLEX STABILIZATION BY DC-N⁴-(SUBSTITUTED) OLIGONUCLEOTIDE FORMING TRIPLEXES.	
3.1 Introduction	71
3.2 Results	71
3.2.1 Synthesis and characterization of <i>sp</i> -ODNs	71
3.2.2 Triplex formation by <i>sp</i> -ODN	74
3.2.3 pH dependence of <i>sp</i> -ODN	75
3.2.4 Protonation status of N3: UV spectral study	77
3.2.5 Sequence specificity	83
3.2.6 Hysteresis in triplex transition and effect of ionic strength	85
3.3 Discussion	88
3.3.1 Effect of pK _a	88
3.3.2 Effect of mismatch	90
3.3.3 Counter-ion effect	91
3.3.4 Electrostatic neutrality	92
3.3.5 Effect of spermine on dissociation/association	92
3.4 Stabilization of triplex by <i>teg</i> -ODN: A comparative study with <i>sp</i> -ODN triplexes	93
3.4.1 Thermal stability of <i>teg</i> -ODN duplexes and triplexes	94
3.4.2 Effect of PEG on macromolecular physical properties	96
3.4.3 Hysteresis in <i>teg</i> -ODN triplexes	97
3.4.4 Effect of salt on <i>teg</i> -ODN triplex stability	98
3.4.5 Gel electrophoresis of <i>sp</i> -ODN and <i>teg</i> -ODN	102
3.4.6 Primer extension reaction with <i>sp</i> -ODNs and <i>teg</i> -ODNs	103
3.5 Origin of triplex stability: <i>sp</i> -ODN versus <i>teg</i> -ODN	103
3.6 Conclusions	106
3.7 Materials and methods	107
3.8 References	112

CHAPTER 4. CONFORMATIONALLY RESTRAINED CHIRAL ANALOGUES OF SPERMINE: CHEMICAL SYNTHESIS AND IMPROVEMENTS IN DNA TRIPLEX STABILITY		
4.1	Introduction	115
4.1.1	Polyamine-DNA interaction	115
4.1.2	Structurally Modified polyamines	118
4.1.3	Design of pyrrolidyl polyamines	118
4.2	Synthesis of pyrrolidyl polyamines	120
4.3	DNA duplex and triplex stabilization with modified amines	135
4.3.1	Interaction of spermine with DNA	135
4.3.2	Present results	135
4.4	Conclusions	139
4.5	Experimental	140
4.6	References	149
CHAPTER 5. RING-CHAIN TAUTOMERISM OF 2-FORMYLBENZENE-SULFONAMIDES: THEIR STRUCTURES IN SOLID, SOLUTION AND GAS PHASES		
5.1	Introduction	152
5.2	Reaction of 2-formylbenzenesulfonamides with amines	156
5.3	Structure of 2-(N-alkyl/aryl-imino)-methylbenzenesulfonamides	160
5.4	Structure of 2-formylbenzenesulfonamides	163
5.4.1	IR spectroscopy	163
5.4.2	NMR spectroscopy	165
5.4.3	X-ray Crystallography	177
5.4.4	Mass spectroscopy	184
5.5	Conclusions	189
5.6	Experimental	190
5.7	References	196

LIST OF PUBLICATIONS

1. Reaction of normal and pseudo 2-formylbenzenesulfonyl chlorides with amines: Experimental and theoretical studies on the structure of 2-formylbenzenesulfonamides in solid, solution and gas phases. **Rajeev K. G.**, Shashidhar M. S., Pius, K. and Bhatt V. M., *Tetrahedron*, **1994**, *50*, 5425-5438.
2. Triplex formation at physiological pH by 5-Me-dC-N⁴-(spermine) [X] oligonucleotides: Non protonation of N3 in X of X*GC triad and effect of base mismatch/ionic strength on triplex stabilities. Barawkar D. A., **Rajeev K. G.**, Kumar V. A., and Ganesh K. N., *Nucleic Acids Research*, **1996**, *24*, 1229-1237.
3. Modulation of DNA triplex stability through nucleobase modifications. Ganesh K. N., **Rajeev K. G.**, Pallan P. S., Rana V. S., Barawkar D. A., and Kumar V. A., *Nucleosides and Nucleotides* **1997** (in Press).
4. Enhancing DNA triplex stability via nucleobase modifications Ganesh K. N., Kumar V. A., Barawkar D. A., **Rajeev K. G.** and Rana V. S., *Pure. Appl. Chem.* **1997** (in Press).
5. Molecular association of 2,3-dihydro-2-alkyl-3-hydroxy-benzisothiazole-1,1-dioxides: Formation of novel bicyclic dimers containing 12/14 membered rings. **Rajeev K. G.**, Samanta U., Chakrabarti P., Shashidhar M. S. and Samuel A. G., (Communicated to *J. Org. Chem.*).
6. Conformationally restrained chiral analogues of spermine: Chemical synthesis and improvements in DNA triplex stability. **Rajeev, K. G.**, Sanjayan, G. J., Ganesh, K. N. (Communicated to *J. Org. Chem.*).
7. The molecular origin of triplex stability: Comparative studies of *sp*-ODN and *teg*-ODN triplexes. **Rajeev K. G.**, Jadhav, V. R. and Ganesh K. N. (Manuscript under preparation for communicating to *Nucleic Acids Research*)

ABSTRACT

Chapter 1: Introduction

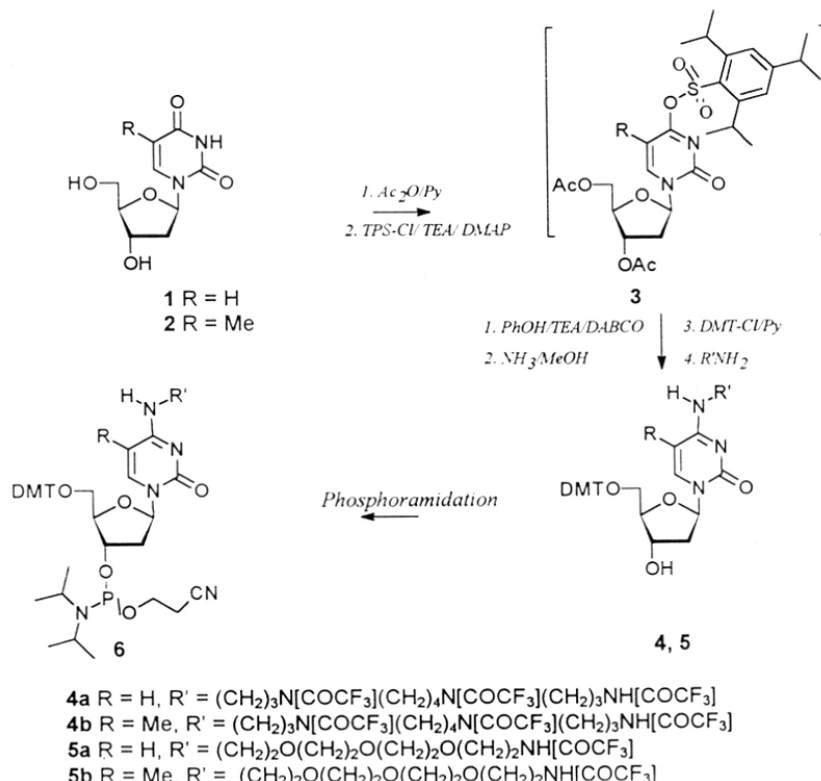
The discovery of triple stranded DNA and its potential applications is an exciting development in the field of DNA molecular recognition. Strategies to recognize a double stranded DNA using another single strand oligodeoxyribonucleotide have far reaching implications in the field of genetics, biochemistry and medicine. Triple helix formation by association of a third oligonucleotide strand with Watson-Crick (W-C) base paired DNA duplex through Hoogsteen base pairing, can in principle inhibit transcription (antigene strategy). Development of designer oligonucleotides through chemical modifications to achieve improved stabilization of DNA triplexes under physiological conditions is therefore currently an active area of research.

Polypyrimidine and polypurine oligonucleotides bind in the major groove of W-C double stranded DNA with polypurine stretches resulting in triple helices. Triplexes are formed by the formation of Hoogsteen hydrogen bonds of third strand with purines of the Watson-Crick duplex and are of two distinct types *viz*: (i) the 'pyrimidine motif' in which the third strand is parallel to the central purine strand where AT base pair recognizes neutral T and GC base pair recognizes protonated C and (ii) the 'purine motif' in which the third strand is antiparallel to the central purine strand where AT base pair recognizes A and GC recognizes G. Common features of both motifs are the necessity of purine bases in the central strand and base specificity. The triplex formation also depends on structural environment, cation concentration, temperature and backbone composition. In order to realize the full potential of DNA triplexes, there is a wide spread interest in expanding the scope of triplex stabilization using different approaches. These approaches center on the use of unnatural synthetic heterocycles as bases, chemically modified backbones and also applications of various DNA binding and intercalating agents. This chapter gives an overview of the importance of chemical modifications in triplex stabilization with a focus on nucleobases and their emerging applications.

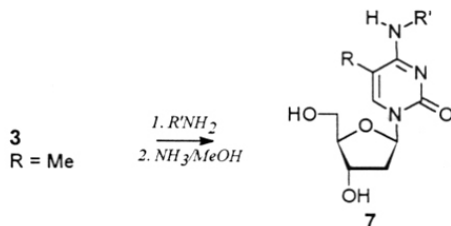
Chapter 2. Chemical Synthesis and Characterization of (i) dC-N⁴-(alkylamino/alkoxy) and (ii) 2-Amino-dA-N⁶-(alkylamino) Analogues for Application in DNA Triplex Stabilization.

Polyamines are known to interact with and stabilize duplex and triplex DNA. Spermine, a naturally occurring polyamine, in millimolar concentration stabilizes DNA duplexes and triplexes. The effectiveness of polyamines is due to their preponderant protonation at physiological pH and such polycations favorably interact with DNA polyanions. Thus covalently linked polyamine-oligonucleotide conjugates may have good prospects in antigen/antisense applications.

This chapter describes (i) the synthesis of various N⁴-substituted dC and 5-Me-dC nucleosides which can provide insight into the effect of charge and steric factors on the N3 pK_a, (ii) design and synthesis of desired N⁴-substituents, (iii) conjugation of spermine to purine bases and (iv) pK_a determination of N⁴-substituted dC analogues.



Syntheses of different N⁴- alkylamino, alkoxy, alkoxy-amino and polyamino substituted 2'-deoxy-cytidines of choice were accomplished starting from naturally occurring nucleobases (T and dU) as shown in **Schemes 1 and 2**.



7a $R = \text{Me}$, $R' = n\text{-propyl}$,

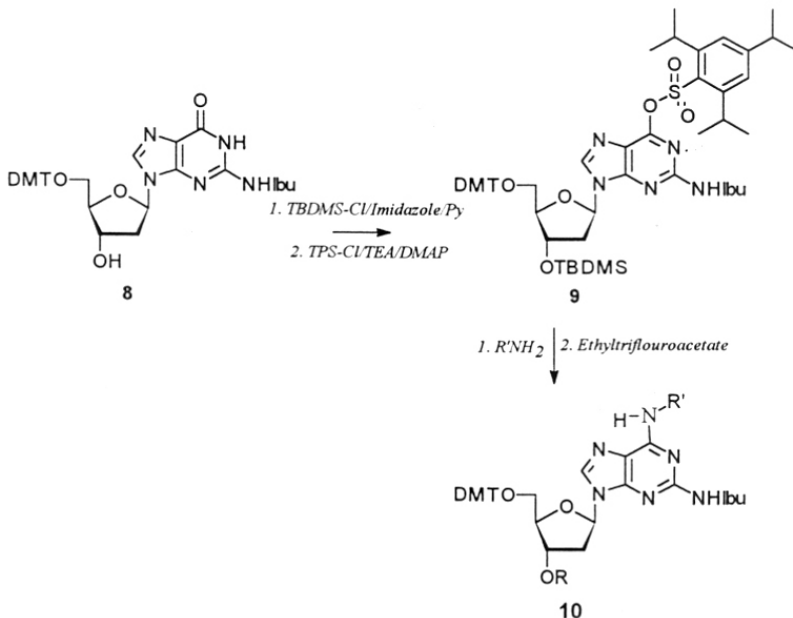
7b $R = \text{Me}$, $R' = n\text{-C}_{12}\text{H}_{25}$

7c $R = \text{Me}$, $R' = (\text{CH}_2)_2\text{O}(\text{CH}_2)_2\text{O}(\text{CH}_2)_2\text{O}(\text{CH}_2)_2\text{OTBDMS}$

Scheme 2

Synthesis of phosphoramidites of suitably protected derivatives of such modified bases are accomplished by following literature procedure. All the phosphoramidites are characterized by ³¹P NMR and later incorporated into oligonucleotides at desired sites for biophysical studies (Chapter 3).

N⁶-Spermine conjugated 2-amino-2'-deoxyadenosine is also synthesized from protected 2'-deoxyguanosine as shown in **Scheme 3**.



$R = \text{TBDMS}$, $R' = (\text{CH}_2)_3\text{N}[\text{COCF}_3](\text{CH}_2)_4\text{N}[\text{COCF}_3](\text{CH}_2)_3\text{NH}[\text{COCF}_3]$

Scheme 3

pK_a determination of modified dC analogues: The pK_a of the ring nitrogen (N3) of modified dC analogues is an important factor of triplex stability. Therefore, the N3 pK_a of modified dC analogues were determined by acid-base titration. It is found that in the case of amine conjugated dC analogues the N3 pK_a is shifting more towards the acidic side compared to unmodified dC (pK_a = 4.3).

Chapter 3: Biophysical Studies on the Molecular Origin of Triplex Stabilization by dC-N⁴-(substituted) Oligonucleotides Containing Triplex.

Oligonucleotide directed triplex formation has therapeutic importance and depends on Hoogsteen base pairing between a duplex DNA and a third DNA strand. Preliminary studies on spermine conjugated oligonucleotides (sp-ODNs) had shown that spermine conjugation on oligonucleotides stabilizes triple helix. The present studies on *sp*-ODN triplexes are focused on (i) the effect of N⁴-substitution on N3 pK_a of dC ODNs (ii) the contribution of appended spermine on triplex stability, (iii) the role of appended spermine on the dissociation and association of triplexes at neutral pH (hysteresis and salt effect) and (iv) the molecular origin of triplex stabilization by *sp*-ODNs.

The outcome of experiments designed and carried out to investigate the role of spermine conjugation on triplex stability indicated that for triplex formation, N3 protonation of C is not a necessary requirement in the spermine conjugated oligonucleotides. Triplex formation of oligonucleotides with unmodified C (C⁺-GC triplex) is favored at acidic pH due to the necessity of N3 protonation of C with optimum pH at 5.6. In comparison, *sp*-ODNs stabilize the DNA triplex at neutral pH (7.0). Hysteresis experiments have shown that rate of association and dissociation of *sp*-ODN triplex are close to each other whereas the control, unmodified C⁺-GC triplex, shows incomplete association, leading to a noticeable hysteresis under identical conditions.

Both spermine and ω,ω' -dideoxydiaminotetraethyleneglycol have very close molecular mass and atom chain length and hence provide a close comparison between *sp*-ODN and ω,ω' -dideoxydiaminotetraethyleneglycol (*teg*-ODN) triplexes. Towards understanding the role of tetraprotonated spermine side chain in causing the triplex stability, the appendage at C4 of 5-Me-dC was replaced with ω,ω' -dideoxydiaminotetraethyleneglycol that has only one protonation site.

1 C G G T T C T T T T T C T T T T C T G C G d
 2 d G C C A A G A A A A A A G A A A A A A G A C G C
 3 d - T T X T T T T T Y T T T T T Z T
 3a. X, Y, Z = dC 3f X, Y = dC & Z = 5-Me-dC-N⁴-(ω -amino-TEG)
 3b X, Y = dC & Z = 5-Me-dC-N⁴-(spermine) 3f X, Z = dC & Y = 5-Me-dC-N⁴-(ω -amino-TEG)
 3c X, Z = dC & Y = 5-Me-dC-N⁴-(spermine) 3h Y = dC & X, Z = 5-Me-dC-N⁴-(ω -amino-TEG)
 3d Y = dC & X, Z = 5-Me-dC-N⁴-(spermine) 3i X, Y, Z = 5-Me-dC-N⁴-(ω -amino-TEG)
 3e X, Y, Z = 5-Me-dC-N⁴-(spermine)

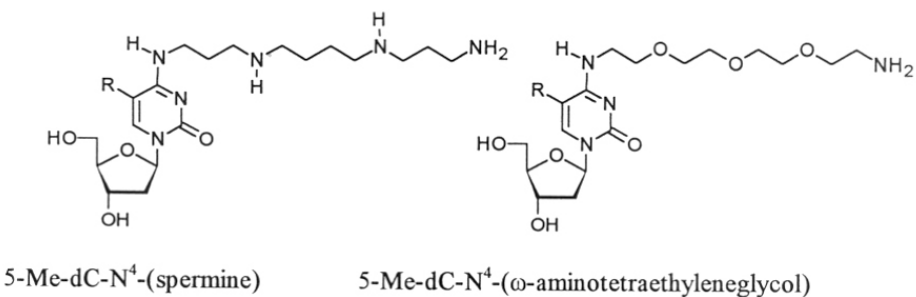


Figure 1. Oligonucleotides sequence, modified and unmodified, used for studying the effect of conjugated spermine on triplex stability.

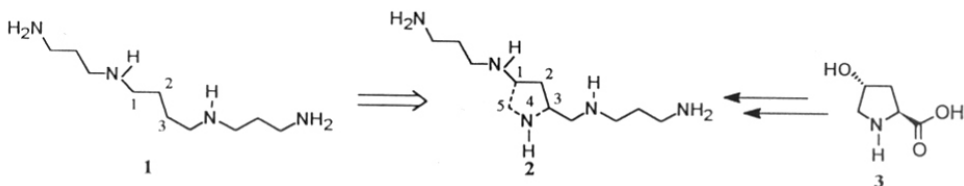
The experimental results presented in this chapter clearly indicate that ODNs with a spermine or a ω,ω' -dideoxymethyltetraethyleneglycol amine side chain appended at C4 of 5-Me-dC form stable triplexes under different salt concentrations. The stability of *sp*-ODN triplexes under low salt concentration is mostly due to enhanced reassociation of duplex and third strand, accelerated by ionic interactions of conjugated cationic spermine with anionic phosphate backbone and possible hydrogen bonding interaction with bases in adjacent strands. In case of *teg*-ODN triplexes lacking a polycationic side chain, the triplex stability arises from a fine tuning of microenvironment by the polyether side chain in terms of desolvation, facilitating a hydrophobic interaction.

Chapter 4. Conformationally Restricted Chiral Analogues of Spermine: Chemical Synthesis and Improvements in DNA Triplex Stability.

Linear polyamines, putrescine, spermidine and spermine, are biological cations ubiquitously found in all cells with a diverse role in physiological processes. Studies on these polyamine analogues revealed that spermine in millimolar concentration stabilize DNA duplex

and triplex structures. To modulate this property of spermine, several structural modifications were made to the polyamine backbone and their activity have been studied in detail. However most of these modifications are through N-substitutions and are achiral. Since many of the polyamine receptor sites (nucleic acids, membranes) are chiral in nature, it was reasoned that introduction of asymmetry into polyamine backbone may be beneficial to their activity. Thus syntheses of Conformationally constrained analogues of spermine and their interaction with DNA are found to be interesting.

A retrosynthetic analysis reveals that constrained analogues of spermine with a pyrrolidine backbone having two asymmetric centers can be derived from *trans*-4-hydroxy-L-proline as shown in **Scheme 1**. The two asymmetric centers can generate four stereo isomers viz. (a) *cis* 2*S*,4*S*; (b) *cis* 2*S*,4*R*; (c) *trans* 2*S*,4*R* and (d) *trans* 2*R*,4*S* isomers, with introduction of an additional N-atom to the polyamine backbone. In addition to the interaction with DNA, these newer analogs of spermine find potential applications as drugs or drug delivery agents.

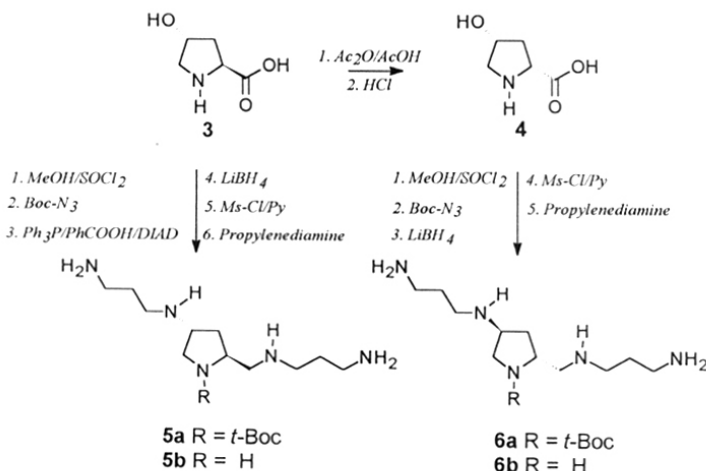


Scheme 1

The synthesis of two of the four stereo isomers (2*S*, 4*R* and 2*R*, 4*S*) were accomplished from *trans*-4-hydroxy-L-proline as shown in **Scheme 2**.

Binding studies of these polyamine analogues with DNA duplexes and triplexes showed that the constrained analogues of spermine with an additional N-atom substantially improves DNA triplex stability over that by spermine. However the duplex stability was not affected considerably when compared to its natural analogue, spermine. The topology of polyamine DNA interactions in duplexes differ considerably from that in triplexes where polyamine structural variation have profound effect on stability. The magnitude of observed stability with the constrained polyamine analogues cannot be solely attributed to the effect of the additional positive charge in them as compared to spermine. It is more likely that the rigid conformations of the constrained polyamine analogues are more suitable for triplex binding

than the flexible conformations of spermine. These studies suggest that the rational fine tuning of the stereochemistry in the polyamine analogues may lead to improvement in DNA duplex/triplex binding/stability and such approaches have potential to design/develop more efficient and selective DNA binding agents.



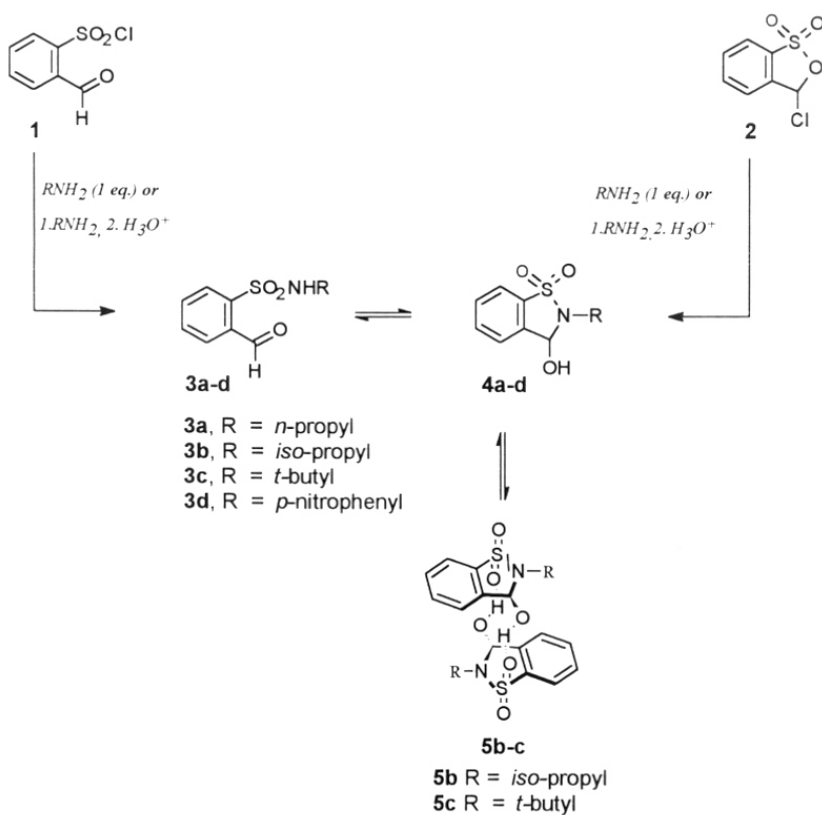
Scheme 2

Chapter 5: Ring-chain tautomerism of 2-formylbenzenesulfonamides: Their Structure in Solid, Solution and Gas Phases.

The reaction of 2-formylbenzenesulfonyl chlorides **1** and its pseudo isomer **2** with one equivalent of primary amines or with excess primary amines followed by acid treatment (**Scheme 1**) gives the corresponding 2-formylbenzenesulfonamides. These derivatives exist as an equilibrium mixture of the 2-formylbenzenesulfonamide and 2-alkyl-3-hydroxybenzisothiazole-1,1-dioxide. Spectroscopic studies suggest that 2-formylbenzenesulfonamides exist completely as benzisothiazole-1,1-dioxide in the solid state, as a mixture of 2-formylbenzenesulfonamide and the corresponding 3-hydroxybenzisothiazole-1,1-dioxide in solution and as 2-formylbenzenesulfonamide in the gas phase. X-ray crystallographic studies of these compounds confirm the existence of N-alkyl-2-formylbenzenesulfonamides exclusively as 3-hydroxybenzisothiazoles in the solid state.

3-Hydroxybenzisothiazole-1,1-dioxides constitute a self - complementary hydrogen bond donor - acceptor system. The intermolecular association of these molecules through

S-O.....H-O interactions resulting in the formation of novel hydrogen bonded dimers containing 12/14-membered bicyclic bridge is revealed by NMR spectroscopy as well as X-ray crystallography. 2,3-Dihydro- 2 - isopropyl- 3 -hydroxybenzisothiazole -1,1-dioxide exhibits interesting concentration and temperature dependent NMR spectra due to association in solution. Perhaps, this is the first report on hydrogen bonding interactions between a sulfonyl group and a hydroxyl group resulting in the formation of a 12/14-membered ring. Delineation of these interactions could help design and synthesis of supramolecular structures with interesting properties.



Scheme 1

ABBREVIATIONS

A	: Adenine
AC ₂ O	: Acetic anhydride
aq	: Aqueous
t-Boc	: <i>t</i> -Butyloxycarbonyl
CAP	: Catabolite activator protein
CH ₃ CN	: Acetonitrile
CHCl ₃	: Chloroform
Cys	: Cysteine
dA	: Deoxyadenosine
DABCO	: 1,4-diazabicyclo-[2.2.2]-octane
dC	: Deoxycytidine
DCC	: Dicyclohexylcarbodiimide
DCE	: Dichloroethane
DCM	: Dichloromethane
dG	: Deoxyguanosine
DHP	: 2,3-dihydropyran
DIAD	: Diisopropylazodicarboxylate
DMAP	: 4-N,N-dimethylaminopyridine
DMF	: Dimethylformamide
DMT-Cl	: 4,4'-Dimethoxytrityl chloride
DNA	: Deoxyribonucleic acid
dU	: Deoxyuridine
EDTA	: Ethylenediaminetetraacetic acid
EtOH	: Ethanol
FAB MS	: Fast atom bombardment mass spectroscopy/spectrum
FPLC	: Fast protein purification liquid chromatography
FTO	: Functionally tethered oligonucleotide
g	: grams
μg	: microgram
h	: hour
His	: Histidine
HOAc	: Acetic acid
HOBT	: Hydroxybenzotriazole
HPLC	: High performance liquid chromatography
HRMS	: High resolution mass spectrum
Hz	: Hertz
IR	: Infrared
μl	: microliter
μM	: micromolar
M	: molar
MeCN	: Acetonitrile
MeOH	: Methanol
Met	: Methionine

Mhz	: Megahertz
min	: minute (s)
mM	: millimolar
mmol	: millimole
MS	: Mass spectrum/spectroscopy
MsCl	: Methanesulfonyl chloride
NaOAc	: Sodium acetate
nm	: nanometer
NMR	: Nuclear magnetic resonance
ODN	: oligodeoxynucleotide
PAGE	: Polyacrylamide gel electrophoresis
PFP	: Pentafluorophenol
Ph ₃ P	: Triphenylphosphine
PNA	: Peptide nucleic acid
py	: Pyridine
RNA	: Ribonucleic acid
RPC	: Reverse phase chromatography
<i>sp</i> -ODN	: Spermine conjugated deoxyoligonucleotide
T	: Thymine
TBDMS-Cl	: t-Butyldimethylsilyl chloride
TEA	: Triethylamine
TEAA	: Triethyl ammonium acetate
TEAB	: Triethyl ammonium bicarbonate
<i>teg</i> -ODN	: ω,ω' -dideoxydiaminotetraethyleneglycol conjugated oligodeoxynucleotide
TFA	: Trifluoroacetic acid
THF	: Tetrahydrofuran
THP	: Tetrahydropyran
TLC	: Thin layer chromatography
TPS-Cl	: 2,4,6-Triisopropylbenzenesulfonylchloride.
Tris	: Tris(hydroxymethyl)methylamine(2-amino-2-(hydroxymethyl)-1,3-propanediol
Trp	: Tryptophan repressor
UV	: Ultraviolet

CHAPTER 1.

INTRODUCTION

TH - 1089

1.1 INTRODUCTION

Nucleic acids (DNA, RNA) are the most important of all biopolymers. DNA is primarily responsible for the storage of genetic information, while its expression occurs through the participation of RNA. Nucleic acids perform their vital functions in cell replication and the regulation of biological activity through interaction with a variety of small and large molecules with specific molecular recognition. Indeed, nature has reached evolutionary perfection in endowing nucleic acids with structures highly optimized for the self-recognition and interaction with other molecules so essential for information storage and transfer within the cell. Accurate DNA replication is most necessary for survival of the cell, and at a molecular level this is achieved through Watson-Crick (WC) specific hydrogen bonding between the complementary base pairs TA (T = thymine, A = adenine) and CG (C = cytosine, G = guanine).¹ The mutual specific recognition of bases by use of two hydrogen bonds in TA and three hydrogen bonds in CG (Figure 1) primarily ensures the fidelity of DNA transcription and translation. The four possible purine-pyrimidine base pair combinations AT, TA, CG and GC are geometrically isomorphous, and when linked through the sugar phosphate backbone lead to the classical antiparallel double-helical structure for DNA in which two strands held together by hydrogen bonds are twisted around each other (Figure 2). The backbones of the two strands are crossed to each other at the edge of the base pairs, giving rise to major and minor grooves in a double-stranded helix. From a functional point of view the grooves play key roles, as the most specific interactions of the DNA duplex with other species such as proteins, drugs, water and metal ions take place in these grooves.² Three modes of interactions (Figure 3) are possible for DNA recognition: (1) surface binding by interionic interactions with positively charged ligands; (2) specific recognition in major and minor grooves via hydrophobic and hydrogen-bonding interactions; and (3) intercalation of polycyclic aromatic rings in between the base stacks. Among the three basic components of DNA- sugar, phosphate

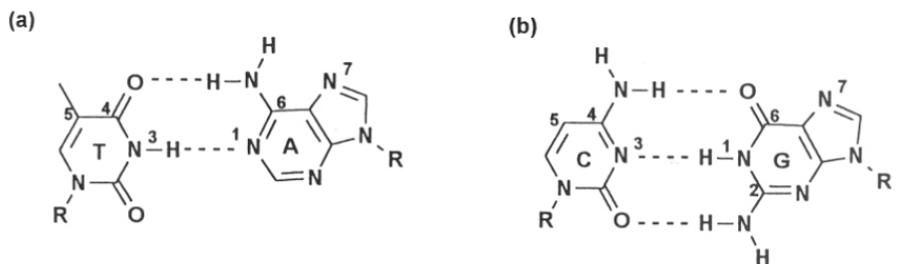


Figure 1. Watson-Crick hydrogen-bonding schemes for (a) TA and (b) CG base pair.

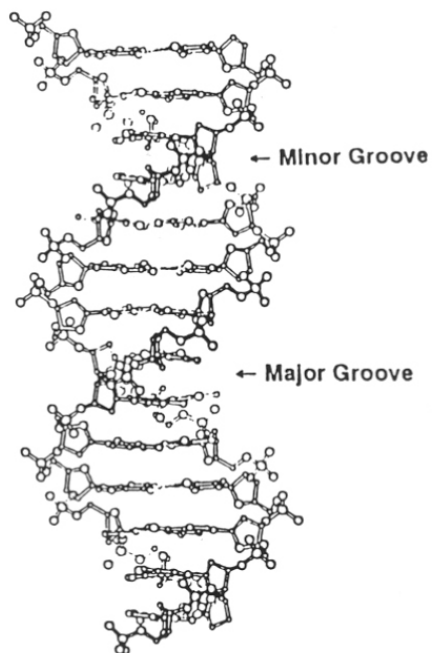


Figure 2. Structure of B-DNA depicting the major and minor grooves.

and heterocyclic bases - the sugar and phosphate provide sites for nonspecific hydrophobic and electrostatic interactions, respectively, while the heterocyclic bases are responsible for specific hydrogen-bonding (H-bonding) interactions in the major and minor grooves. Many molecules use combinations of the above modes to generate high sequence specificity in DNA recognition.

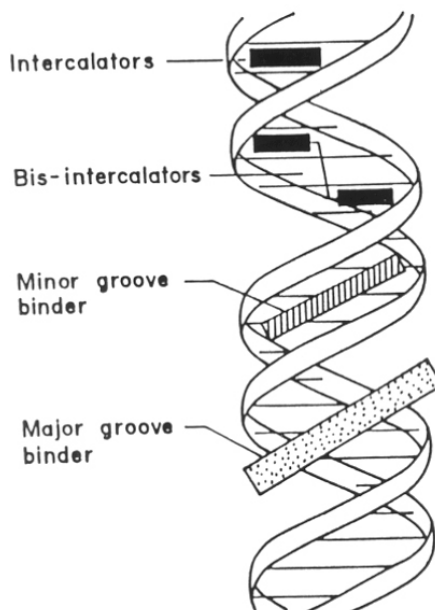


Figure 3. DNA-ligand interactions: intercalation and groove binding.

Among other patterns of hydrogen bonding, the Hoogsteen (HG)³ and wobble^{4,5} base pairs are the most significant (Figure 4). Hoogsteen base pairing is not isomorphous with Watson-Crick base pairing and has importance in triple-helix formation. In wobble base pairing, a single purine (Pu) is able to recognize a noncomplementary pyrimidine (Py)

(e.g. GU, where U = uracil). Wobble base pairs have importance in the interaction of messenger RNA (m-RNA) with transfer RNA (t-RNA) on the ribosome during protein synthesis (codon-anticodon interactions). Several mismatched base pairs and anomalous H-bonding patterns have been seen in X-ray studies of synthetic oligodeoxynucleotides (ODN).^{6,7}

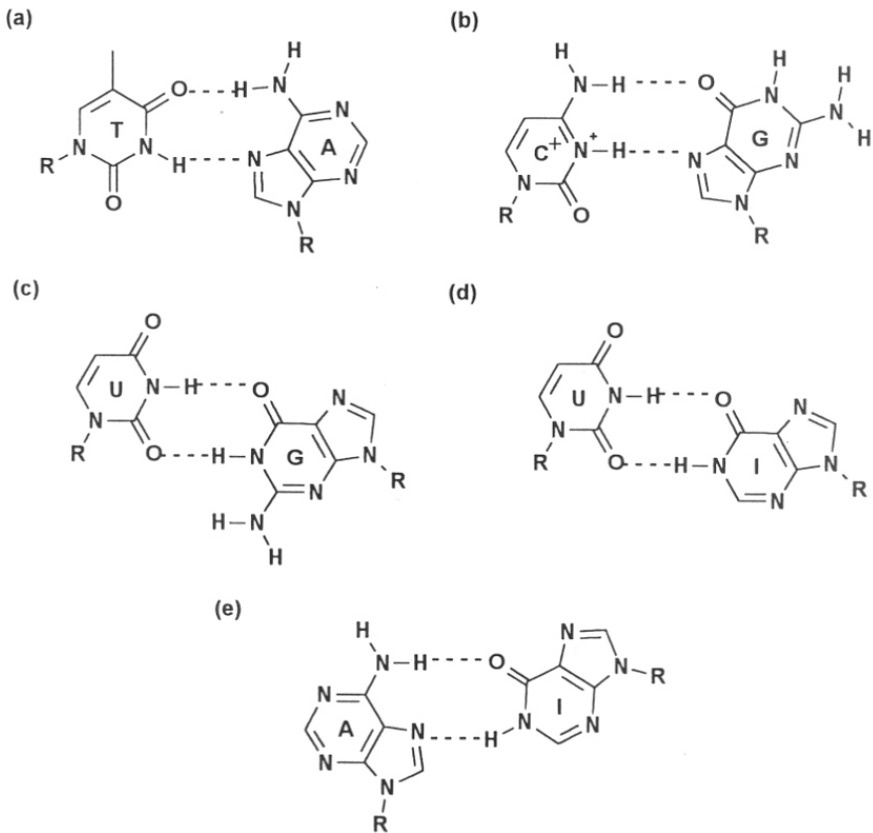


Figure 4. (a, b) Hoogsteen and (c-e) wobble base-pairing schemes. I = inosine.

1.1.1. Polymorphism in DNA Structure

Depending upon the base sequence and environment, the DNA duplex can exist in three major conformations: A-DNA, B-DNA and Z-DNA (Figure 5). A-DNA and B-DNA are regular major secondary structures with right-handed double helices. B-DNA has a wide major groove and a narrow minor groove and the structure is maintained by an *anti*-

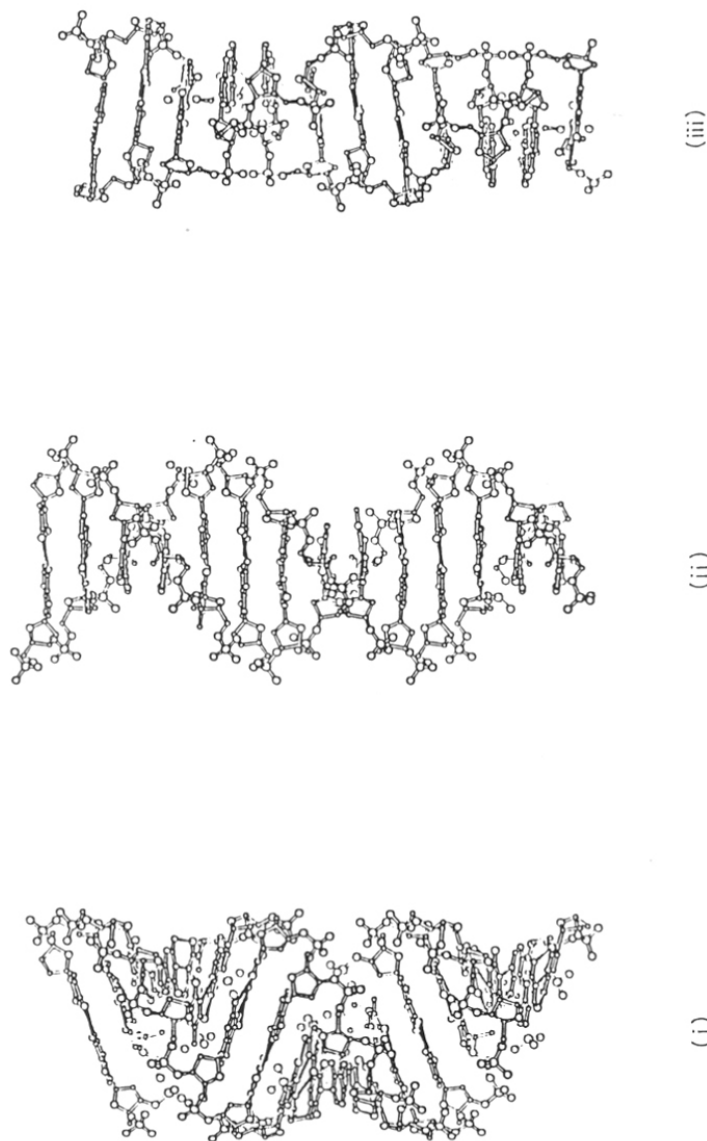


Figure 5. DNA structural polymorphs: (i) A-DNA, (ii) B-DNA and (iii) Z-DNA.

glycosidic conformation with a C2'-*endo*-sugar pucker (Figure 6).^{8,9} In contrast, A-DNA has a more rigid structure with a deep, narrow major groove and a broad, shallow minor groove, showing little sequence-dependent variation in structure. The structure comprises *anti*-glycosidic torsion with a C2'-*endo*-sugar geometry. Z-DNA is a left-handed double helix which is favored by alternating GC sequences and stabilized by high concentrations of salt and ethanol.¹⁰ Z-DNA has a zig zag phosphate backbone in which purines adopt a *syn*-conformation with a C3'-*endo*-sugar pucker. Structural transitions from one form of DNA to another are possible as a response to a change in environment such as salt, solvent and pH, and easily monitored by optical spectroscopic techniques, in particular circular dichroism.²

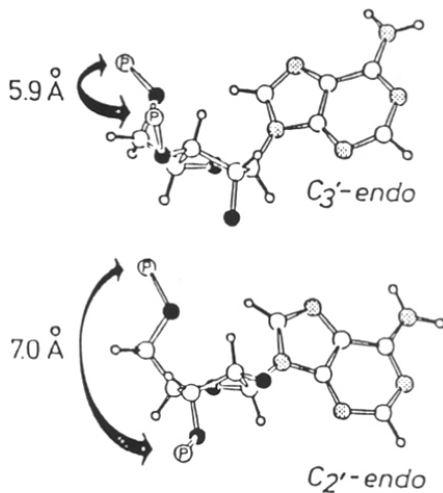


Figure 6. Sugar puckers and glycosidic torsions in DNA structure.

1.1.2. Molecular Recognition in the Major and Minor Grooves of Duplex DNA

The major and minor grooves of DNA differ significantly in their electrostatic potential, H-bonding character,¹¹ steric effects, hydration¹² and dielectric strength.¹³ Hydrogen bonds can be accepted by AT and TA base pairs from ligands bound in the major groove via the C4 carbonyl of T and N7 of A, while in the minor groove H-bonding occurs through the C2 carbonyl of T and N3 of A (Figure 7). The only hydrogen bond

donor in the major groove for the AT base pair is the N6 amino of A, while none exists in the minor groove. The picture is different for CG and GC duplets, the H-bond acceptors in the major groove being N7 and O6 of G, and in the minor groove C2 of C and N3 of G. The H-bond donor in the major groove for CG is the N4 amino of C, and in the minor groove it is the N2 amino of G.

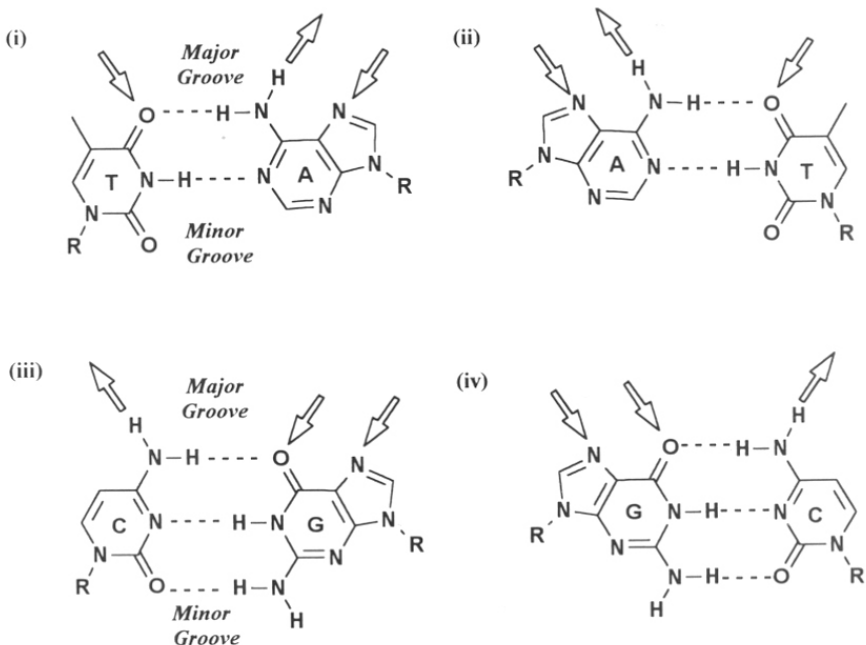


Figure 7. Hydrogen bond donor and acceptor sites in the major groove of duplex DNA at (i) TA, (ii) AT, (iii) CG and (iv) GC base pairs. Arrows pointing to the atoms indicate acceptor sites; arrows pointing away from the atoms indicate donor sites.

The salient outcome of this distribution of H-bond donors and acceptors in the naturally occurring base pairs is that the binding molecules can discriminate the AT base pair from CG efficiently from the major groove side but not so well in the minor groove.¹¹ Two further features of molecular discrimination are noteworthy. In AT and TA base pairs, the C5 methyl of T offers substantial hydrophobic recognition in the major groove which is absent for CG and GC base pairs. However in the CG and GC duplets, the N2 amino of G presents a steric block to hydrogen bond formation at N3 of G and the C2 carbonyl of C in the minor groove. It is possible to distinguish AT from TA and CG from

GC in the major groove since the horizontally ordered arrays of H-bonding sites and hydrophobic centers differ among the four pairs (Figure 7). The negative electrostatic potential due to phosphate charges is greater in the AT minor groove than in GC-rich regions, and this provides an additional important source for AT-specific minor groove recognition.¹²

1.1.3. Scope and Aims

An understanding of the macrostructural organization of nucleic acids at a molecular level becomes important in discerning the three-dimensional recognition codes and allows the design of new supramolecular systems of practical importance. In DNA, a vertical combination of the horizontally ordered hydrogen bond donor and acceptor sites characteristic of each base pair in a helix generates a three-dimensional grid which is unique to each DNA sequence. This pattern is recognized in the major or minor groove by ligands possessing complementary sites. When the ligand is another strand of DNA having Hoogsteen or reverse Hoogsteen complementarity to the duplex in the major groove, the binding leads to formation of a DNA triplex. The synthetic control of the structure and stability of such a triplex can be exercised either by varying the sequence of bases, giving rise to different motifs, or by a chemical modification of the nucleobase or phosphate backbone within a particular motif. In this section, a brief description of the general features of triplex structure is followed by examples of specific chemical modifications (with a special emphasis on chemical modifications of nucleobases) and their emerging biological applications.

1.2. DNA TRIPLE HELIX: GENERAL FEATURES

A few years after the discovery of the double helix structure of DNA,¹ it was shown that a triple helix could be formed by polynucleotides.¹⁴ This is perhaps one of the most exciting developments in DNA molecular recognition with a high potential for practical utility. Moser and Dervan¹⁵ were the earliest to demonstrate site-specific binding of an oligonucleotide to the major groove of a DNA duplex (Figure 8). Le Doan *et. al.*¹⁶ simultaneously reported the formation of a triplex between an unnatural α -

oligonucleotide and its cognate DNA duplex sequence. This new strategy for the recognition of double - stranded DNA sequences has fueled studies unabated, with far - reaching implications in the fields of genetics, biochemistry and medicine.¹⁷

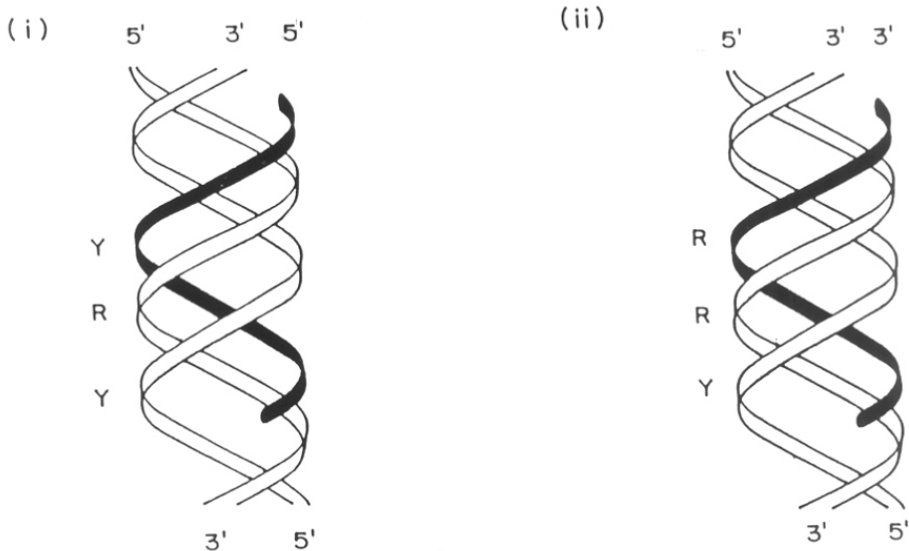


Figure 8. DNA triple helices with the third-strand ODN in the major groove (i) parallel (YRY motif) and (ii) antiparallel (RRY motif).

1.2.1. Triple - Helical Motifs

Pyrimidine oligonucleotides bind in the major groove of Watson-Crick double-stranded DNA with polypurine stretches resulting in triple-stranded structures.¹⁵ The specificity in triple-helix formation is derived from Hoogsteen hydrogen bonding in which thymine recognizes the AT base pair (TAT triplet) and protonated cytosine the GC base pair (C^+ GC triplet) (Figure 9). The notable features of this motif, called the “pyrimidine motif” (YRY), are that (i) while AT base pairs are recognized by neutral T, the base pair GC requires protonated C (C^+) for triad formation, and (ii) the third strand (HG) is parallel to the central purine strand. In the “purine motif” (RRY),^{18,19} oligodeoxyribopurines are capable of forming triplexes, but again through interaction with

a homopurine tract of double-stranded DNA. These triplexes are characterized by A:AT and G:GC triplets, and unlike in the pyrimidine motif, no protonation of purine is required for GC recognition; in addition, the third strand is antiparallel to the central purine strand (Figure 10).

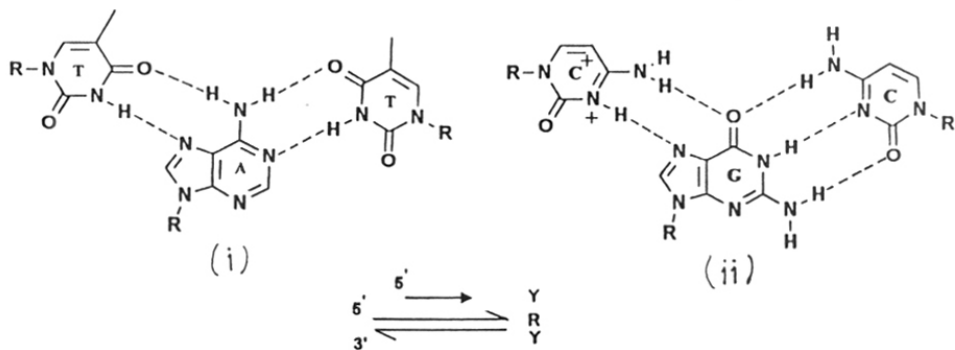


Figure 9. Base-pairing schemes in YRY motif: (i) T:AT and (ii) C⁺:GC triads. The arrows indicate the relative 5'→3' directionalities of the three strands.

A common feature of both motifs is the necessity of a purine in the central position of the triad. Thus, among the four possible duplets AT, GC, CG and TA, only the first two are “allowed” to recognize the incoming purine or pyrimidine third strand. In addition to the formation of specific base triplets, triple-helix formation is also sensitive to several structural and environmental factors such as the length of the third strand, single mismatches, cation concentration and valency, temperature, and backbone composition of the three strands.¹⁵ In order to realize the full potential of triplex formation, there is widespread interest in expanding the scope of triplex recognition to all four duplex base pairs within a single triple-helical motif. These approaches have mainly involved invention and use of several synthetic heterocycles which are either mimics of protonated C or provide complementary neutral hydrogen-bonding sites to the duplex base pair. Synthetic control of DNA structures via chemical modifications of backbones and heterocyclic base components provides an innovative strategy for triplex stabilization.¹⁷

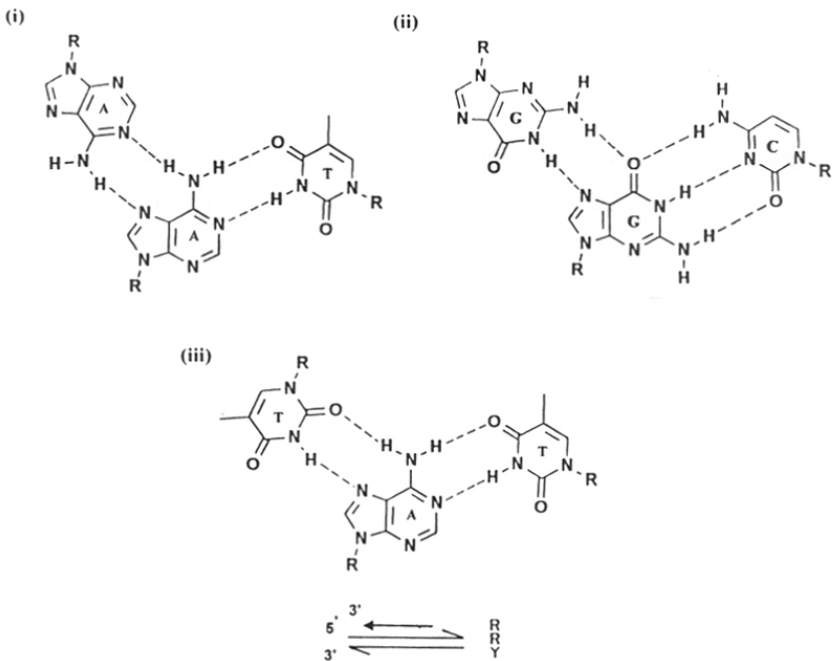


Figure 10. Base-pairing schemes in RRY motif. (i) A'AT, (ii) GGC and (iii) T'AT triads. Note the reverse HG mode for the third-strand Tin (iii) as compared to T'AT in Figure 9.

1.2.2. Triplex Structure

Triplex formation with natural bases is limited by several important structural requirements. Recognition of any sequence in one of the WC strands is achieved by the formation of specific sets of hydrogen bonds (Hoogsteen or reverse Hoogsteen) with complementary base pairs in the other strand (Figure 7). Because of steric and electrostatic considerations, interaction of a third-strand nucleic acid with a double-stranded target site occurs almost exclusively within the major groove with sequence restrictions. Pyrimidine bases provide only one hydrogen-bonding site at C4 in the major groove of a WC-type duplex, whereas purine bases afford two sites at C6 and N7. The 5-methyl group on T in DNA can sterically block hydrogen-bonding interactions within the major groove. The donor and acceptor patterns in the major groove for A and G are distinct from each other, and therefore sequence-specific recognition through the formation of pairs of hydrogen bonds occurs only at purine bases. A regular placement of a third strand in the major grooves requires that all purine complements of WC base pairs

are on the same strand. Hence triplex formation is limited to polypyrimidine-polypurine duplex sites.

Considerable progress in understanding the structure of triple-stranded oligonucleotides has been achieved in recent years. The complexity of the problem has demanded a wide variety of approaches to the solution, ranging from biochemical (gel electrophoresis,¹⁹ footprinting and affinity cleavage¹⁵) and biophysical (spectroscopy, mainly NMR²⁰), and calorimetry for energetics¹⁷ to molecular biology (gene inhibition) techniques.^{18b,21}

1.2.3. Triplex Grooves

The binding of the third strand in the YRY motif induces global conformational changes in the WC-paired duplex region of the triplex. As a result, WC pairs move towards the minor groove by 1 Å to overcome the nonbonded interactions with the incoming third strand in the major groove, accompanied by a slight unwinding of the helix. The third strand partitions the major groove of DNA, leading to three distinct grooves in triple helices (Figure 11).²⁰ Among these, in the YRY motif, the Crick-Hoogsteen (CH) groove is quite narrow (2-3 Å) with an ordered, interconnected network of water molecules. These water molecules not only solvate the macromolecule but also screen the repulsive interactions between negatively charged phosphate groups in the narrow groove. The Watson-Hoogsteen (WH) groove is wide (>7 Å) and somewhat hydrophobic owing to the presence of the 5-methyl groups of T moieties. The Watson-Crick (WC) groove (6-7 Å) is similar to the minor groove of B-DNA with hydration sites located near H2 of A. The CH groove in the RRY motif is narrow (3 Å) and somewhat shallow with extensive hydration. The WH groove, despite its width (8 Å), has water molecules positioned along the inner edges close to the phosphate oxygens. Thus, hydration is an important determinant in the stability of RRY duplexes.

1.2.4. Sequence Control of Triplex Stability

There are four different ways (Figure 12) to assemble YRY triple helices from oligonucleotides (ODNs): (i) mixing of appropriate homopurine and homopyrimidine

ODNs in a stoichiometry of 1:2;²² (ii) addition of a complementary homopyrimidine guest strand to a host hairpin duplex with a polypurine-polypyrimidine stem;²³ (iii) adding a complementary homopurine strand to a palindromic pyrimidine sequence²⁴ and (iv) successive folding of a single contiguous ODN to shield an intramolecular triplex.²⁵ Depending on the nature of the ODNs chosen, the relative contributions of various thermodynamic parameters for triplex stabilization differ.

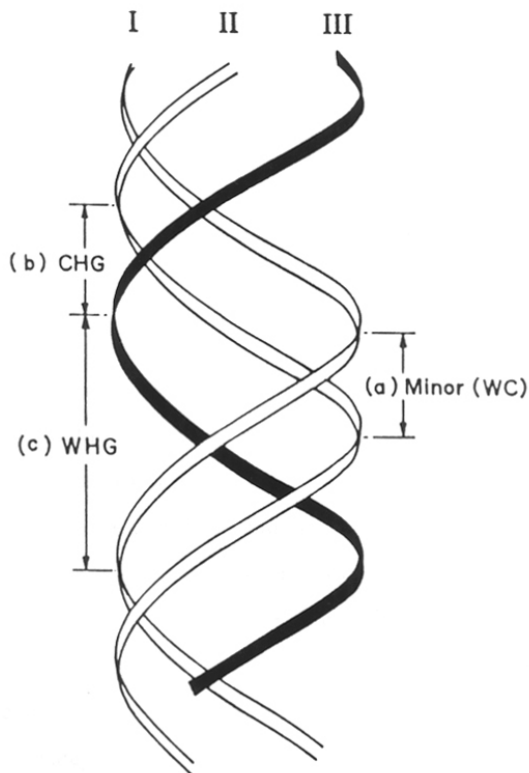


Figure 11. Triple-helix grooves: (a) the Watson-Crick (strands I and II) minor groove of the duplex; (b) the Crick-Hoogsteen (strands II and III) groove and (c) the Watson-Hoogsteen (strands I and III) groove. The grooves in (b) and (c) are formed by partition of the major groove of the DNA duplex by a Hoogsteen strand.

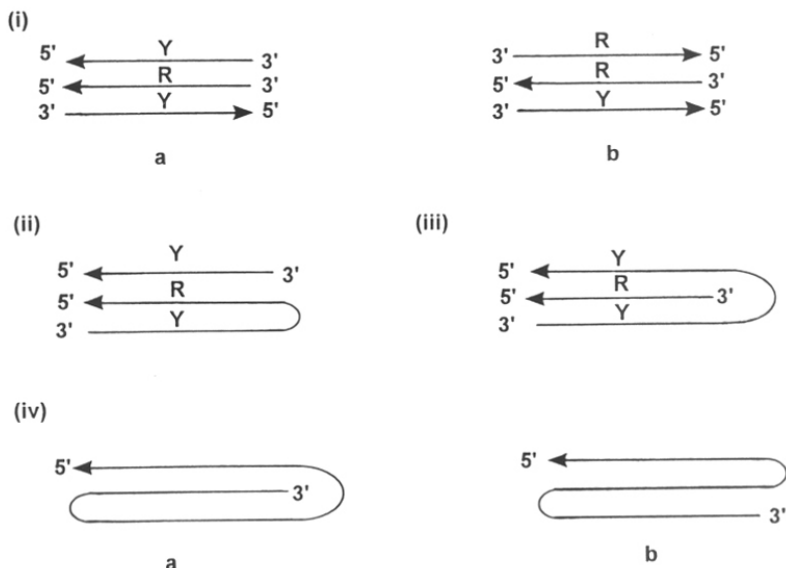


Figure 12. Schematic illustration of modes of inter- and intramolecular triple-helix formation: (i) intermolecular YRY and RRY motifs; (ii) bimolecular from a hairpin duplex (RY) and a single strand (Y); (iii) bimolecular from a hairpin loop (YY) and a single strand (R) and (iv) a and b single-strand intramolecular.

1.2.5. Kinetics of Triple-Helix Formation

A knowledge of the kinetics of triple-helix formation is important since triple-helix-forming ODNs have to compete with other duplex-DNA-binding agents *in vivo* such as proteins, transcription activators and so on. Studies on the thermal denaturation-renaturation kinetics of a 22-base third strand with a 22-mer duplex have indicated a hysteresis effect with nonsuperimposable heating and cooling curves.²⁶ The association constant K_{on} is independent of the nature of the base and the presence of mismatches, but decreases linearly with salt concentration. The dissociation constant K_{off} shows an opposite trend, being independent of salt concentration but dependent on the nature of the base in the third strand and increasing with the presence of base mismatches. These features are characteristic of the presence of a quasistable intermediate, supporting a nucleation zipper model for the formation of a triplex from a duplex and a third strand.^{26,27} Their association is a slower process compared to duplex formation from two single strands (Figure 13).

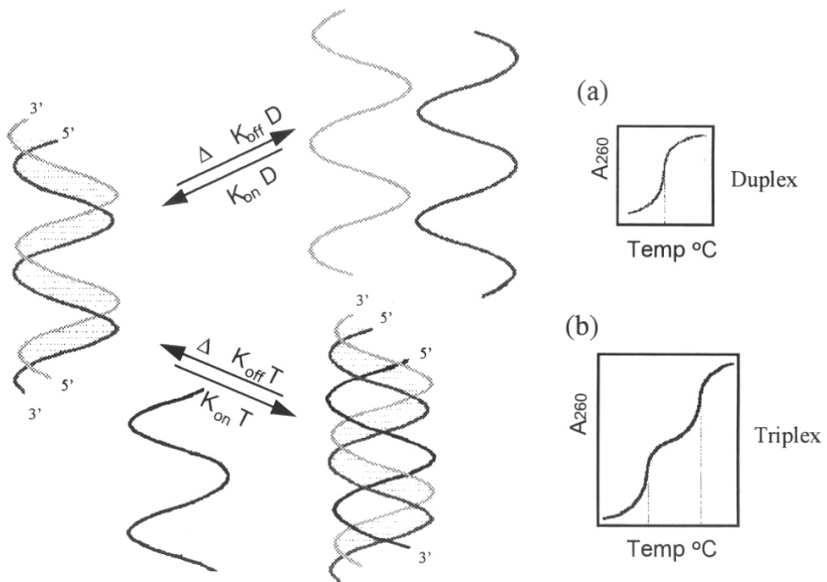


Figure 13. Schematic representation of thermal dissociation and association of DNA double and triple helices. In the right side, boxes (a) and (b) represent the UV-melting profiles of the duplex and triplex DNA monitored at $\lambda_{260\text{ nm}}$. Mid point of the transition (dotted line) corresponds to the melting temperature (T_m). Duplex DNA melting is accompanied by a single transition (a) whereas the triplex DNA melting is accompanied by two transitions (b) *viz.* (i) triplex \rightarrow duplex + single strand and (ii) duplex \rightarrow single strand.

The energies of activation for association (E_{on}) and dissociation (E_{off}) also show opposing behaviors, with the overall activation energy being negative and corresponding to the formation of three to five base triplets in nucleation. The replacement of a single base pair in the YRY motif is highly detrimental to triple strand binding, with a mismatch at the end less destabilizing.²⁶ Nucleation requires about five base triplets, the remaining complexation being formed in a highly cooperative way. A mismatch in the center disrupts the cooperativity between neighboring base triplets.

1.3. NUCLEOBASE MODIFICATIONS²⁸

1.3.1. Pyrimidine Modifications to alter N3 pK_a :

In general, the stability of YRY triplexes containing cytosine residues in the third strand decreases as the pH of the solution is raised from acidic to alkaline values.^{29,30} This is due to a decreased protonation at the N3 of C with increasing pH. The triplex stability reaches a maximum around pH 5.8, close to the pK_a of the N3 of C. Various approaches have been described to overcome this pH limitation (Figure 14), since any triplex-dependent *in vivo* applications demand stable triplexes at physiological pH. Since the RRY motif does not involve any charged triad bases, its stability is independent of pH.

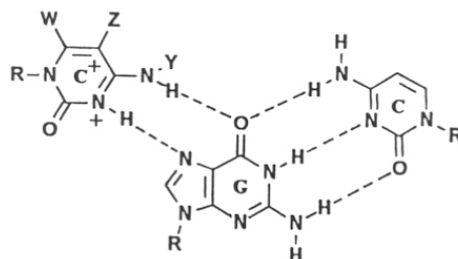


Figure 14. The C^+ -GC triad with various base modifications in the third strand. Possibilities include $W = Y = H$, $Z = Me$ or H ; $W = Y = H$, $Z = C\equiv CMe$; $W = Z = H$, $Y = n\text{-Bu}$, $(\text{CH}_2)_2\text{COOH}$ or $(\text{CH}_2)_4\text{NH}_2$; $W = H$, $Z = Me$, $Y = (\text{CH}_2)_3\text{NH}(\text{CH}_2)_4\text{NH}(\text{CH}_2)_3\text{NH}_2$.

1.3.2. C5-substituted pyrimidines

The first category of modifications involved substitutions at C5 of the pyrimidine nucleobase (Figures 14 and 15).³¹ It is well known that C5 substitutions control the pK_a of the N3 of C in nucleosides. An electron-withdrawing substituent (e.g. bromine) increases

the acidity of the N3 amino (making it a better hydrogen bond donor) but decreases the electron-donating properties of the carbonyl lone pair, making it a poorer hydrogen bond acceptor. An electron-donating substituent such as a methyl would have the opposite effect of stabilizing protonation at N3, which is thus favorable for triplex formation.

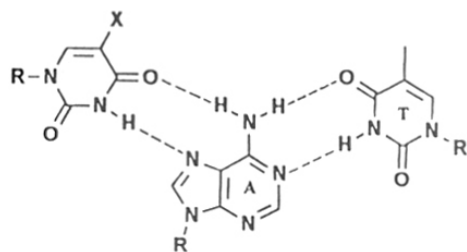


Figure 15. The Y'AT triad with various substitution in the third-strand pyrimidine. Possibilities include X = Br, C=CMe and Me.

The pH-dependent affinity cleavage experiments with ODNs incorporating 5-Br-dU and 5-Me-C in the third strand have indicated that (1) substitution of 5-Br-U for T increases the binding affinity without changing the pH profile greatly, (2) incorporation of 5-Me-C for C increases the triplex binding only marginally but extends the pH range to 7 and substitution of both 5'Me-C and 5-Br-U results in a large increase in binding over an extended pH range.³¹ The relative stabilities of base triplets are in the order 5-Br-U'AT > TAT > U'AT and 5-Me-C'GC > C'GC, suggesting that 5-methylation in general increases the binding affinity irrespective of the methylated pyrimidine. Thus, the substitution of methyl for hydrogen at C5 promotes binding by a hydrophobic effect, while bromine substitution strengthens binding by increasing acidity at N3 or hydrophobicity or both.

Thermodynamic analysis has indicated that the additional stability imparted to the triplex by 5-methylcytosine is entropic in origin.^{22a,32} The methyl group should fill a space in the major groove, causing a release of hydrating water molecules from the double helix to bulk solvent, a source of positive entropy change. In addition to hydrogen bonding and solvation, another likely source of stabilization is the increased base-stacking interactions. Methyl substitution increases the molecular polarizability and thereby the free energy of

stacking, and may stabilize the complex through increased stacking energy without directly influencing the protonation event. Thus, 5-Me-C has become an important structural element for inducing stabilization of C⁺GC-containing triple helices under physiological conditions.

C5-(1-propynyl)-2'-dC: The logic of entropic and stacking stabilization provided by 5-Me-C has been extended to investigate the effect of 1-propynyl substituent at C5.³³ The propyne modification (Figure 14) is planar with respect to the heterocycles and allows for increased stacking of bases. It is also more hydrophobic than the methyl group, allowing a further increase in the entropy of binding. The increased hydrophobicity of propyne analogues relative to dT and 5-Me-C may also facilitate permeation of ODNs into cells, with potential therapeutic applications.

5-Methyl-2'-O-methylcytidine: The 2'-O-methyl oligoribonucleotides are chemically more stable and relatively nuclease resistant compared to unmodified RNAs. It was recently demonstrated that the triplex of a 2'-O-methylpyrimidine RNA oligomer with a duplex DNA is thermally more stable than the corresponding DNA triplex.³³ It was also observed that while 5-methyl-2'-O-methyluridine formed a more stable triple helix with double-stranded DNA than the 5-unmodified parent probe, the corresponding cytidine analogue destabilized the triplex.

Carbocyclic 5-Me-C: The carbocyclic analogue (Figure 16) of 5-Me-C (c5-Me-C), having a higher pK_a of 4.8 than the parent nucleoside with a pK_a of 4.5 facilitates protonation at N3. It was found that incorporation of c5-Me-C into the third strand resulted in an increase in T_m by 3.9 °C per substitution over strands containing c5-Me-C at pH 7.2.³⁴ Interestingly, carbocyclic T (cT) showed an opposite trend, with a decrease in T_m of 1.7 °C per substitution at pH 6.6 relative to the ODN containing T.

1.3.2a. N⁴ - Alkyl C: Another site for easy modification of cytosine is N⁴, which can be derivatised by means of sulfate - catalysed transamination reaction.^{35,36} Oligonucleotides

which carry side chains at N⁴ of dC form triplexes (Figure 14) with double-stranded ODN target molecules. The transaminated oligomers were found to be capable of forming triplexes with a double-stranded DNA target, but the triplexes were considerably more destabilized than those formed with an unmodified third-strand oligomer. The decrease in triplex stability was attributed to either steric interactions between the side chain and the components of the major groove or a lower pK_a of the modified cytosine, which decreases the N3 protonation ability.

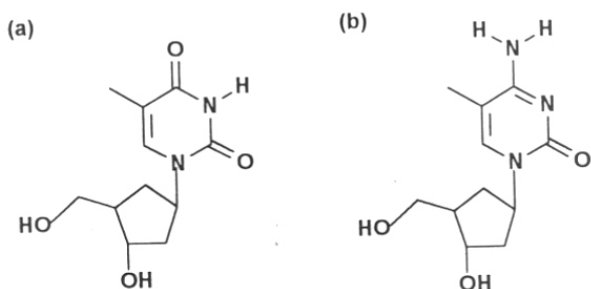


Figure 16. Carbocyclic pyrimidines (a) cT and 5-Me-cT.

N⁴-ethano-C: Substitution of N⁴-ethano-5-Me-dC in the third strand in place of a C⁺ residue resulted in an irreversibly crosslinked stable DNA triplex. This reaction does not require light or addition of any external reagent and occurs at physiological conditions (Figure 17a).³⁷

6-Amino-C: 6-Amino-2'-O-methyl-C having pK_a 6.8 was incorporated as a substitute for protonated cytidine for triplex binding.³⁸ These ODNs showed significantly lowered binding to duplex DNA relative to control 2'-O-methyl-C.

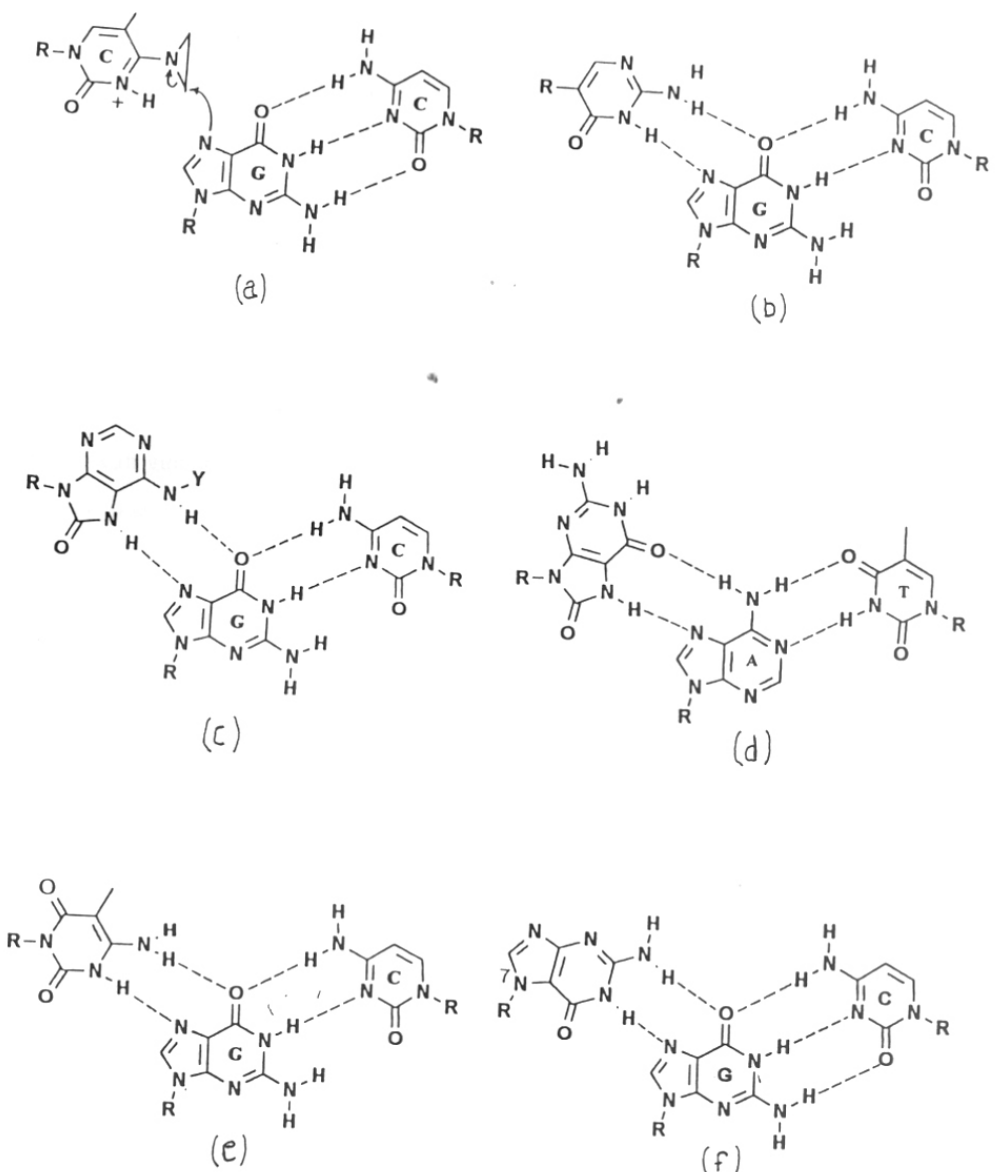


Figure 17. (a) $\text{N}^4\text{-ethano-}\text{C}^+$ GC triad, (b) ψiC GC triad in the YRY motif, (c) 8-oxo-dA GC triad, where $\text{Y} = \text{H}$ or Me , (d) 8-oxo-dG AT triad in the YRY motif, (e) 6-oxo-5-Me- C^+ GC triad and (f) N7-dG GC triad in the YRY motif.

1.3.3. Neutral mimics of C⁺

Charge repulsion disfavors protonation at N3 of C in continuous stretches of C⁺GC and 5-Me-C⁺GC triplexes. The pK_a value of N3 of C in C⁺GC and 5-Me-C in 5-Me-C⁺GC triads are sequence dependent, limiting the utility of 5-Me-C for ODN-directed triplex formation for G-rich sequences. Also N3 protonation of C seems to be a critical factor in determining the triplex stability and this has led to a search for neutral, nonprotonated C⁺ mimics. These may not only reduce the pH dependence but also eliminate the destabilization of the triplex due to charge repulsions between cations on neighboring protonated C or 5-Me-C bases.

Pseudoisocytidine: Pseudoisocytidine derivative (Ψ iC) has the ability to form both Hoogsteen - type and Watson-Crick - type (Figure 17b & 17c) base pairing to hydrogen bond with guanine under neutral conditions.³⁹ This is possible since Ψ iC has a hydrogen at N3 position for H - bonding with N7 of G, leading to the Ψ iC'GC triad in neutral conditions (Figure 17b). The uncharged base containing ODN would be helpful in forming a triplex with double - stranded DNA containing a 2'-dG cluster.

8-Oxo-dA: ODNs with 8-oxo-adenine (Figure 17d) were found to be capable of forming stable triplexes with GC of double - stranded DNA under neutral and basic pH, eliminating the necessity of protonation of the base in the third strand.^{40,41,42}

8-Oxo-dG: Incorporation of 8-oxo-dG into the third strand ODN of a triplex exhibited both high thermal stability like those of the triplex containing G.AT triad.⁴³ The stabilization of triplex possibly arises from two H - bonds viz. the H - bonding between O6 of 8-oxo-dG and the 6-amino of dA and that of between the N7 hydrogen of 8-oxo-dG and N7 of dA (Figure 17e).

6-oxo-5-Me-C: 4-amino-5-methyl-2,6-[1H,3H]pyrimidione (6-oxo-5-Me-C) a 6-keto derivative of 5-Me-C can act as a bidentate hydrogen bond donor to O6 and N7 of G base through its imido and amino groups (Figure 17f) and can be better mimic for C in the third

Table* 1. Third-strand base modifications and duplex recognition specificity.^a

	R or Y	AT	TA	CG	GC	UA	Reference
1	T	+		+		+	14, 49, 26a, 53
2	U			+			53
3	A		+			ΨUA	54
4	C				+	+	53
5	G			+		+	15, 52
6	5-Me-dC				+		53
7	5-(1-propynyl)-2'-dC				+		48
8	carbocyclic 5-Me-dC				+		34
9	2-Methoxy-5-Me-dC				-		32
10	cT (carbocyclic T)	-					34
11	N ⁴ -alkyl-C				-		35, 36
12	N ⁴ -(Spermine)-5-Me-dC				+		50
13	6-Ethano-C				+		37
14	6-Amino-C				-		38
15	ΨiC (pseudoisocytidine)				+		39
16	8-Oxo-dA				+		39
17	8-Oxo-dG	+					43
18	6-Oxo-5-Me-dC				+		44
19	N7-dG			+	+		45
20	N ⁴ -(6-Aminopyridimyl)-dC	+		+			46
21	P1, P2 (Pyrazole analogues)			+	+		47
22	4-Phenylimidazole (D2)			+			51
23	2'-Deoxynebularine (N)	+		+			55
24	2-Deoxyformycin A			+			56
25	7/9-Deaza-2'-dG			+			57, 58
26	7-Deaza-dX	+					57a
27	6-Thio-G				+		58
28	Pyridopyrimidone	+					59b
29	2-Aminopyridyl			+			60
30	2-(4-Aminobuty-1-yl)-1,3-propanediol	-		-			61

* Adopted from Ganesh *et. al.*²⁸ ^aThe entries + and - indicate stabilization and destabilization of triplexes consisting of specific triads relative to control triads having no chemical modifications.

strand of Y'RY triplex.⁴⁴ Compared to C and 5-Me-C analogues, 6-oxo-5-Me-C ODNs show triplex T_m values which are largely pH independent in the range 6.4-8.5.

N7-dG: 7-(2'-Deoxy- β -D-erythro-pentafuranosyl)guanine is N7-glycosylated guanine which, upon incorporation into a pyrimidine ODN, binds to W-C GC duplexes (Figure 17g) with remarkable specificity.⁴⁵ The third-strand orientation in such N7-G:GC triplets is reversed compared to the conventional R'RY motif and becomes parallel to the purine WC strand. Most of the modified bases and their ability to form/stabilize triplets when they are present in the third strand ODN of the triplet are summarized in Table 1.

1.4 TRIPLEX STABILIZATION BY BACKBONE MODIFICATIONS

Delineation of all factors contributing triplex stability is pivotal to the application of ODN-directed, sequence-specific recognition of duplexes for *in vivo* applications. Structural modifications of the sugar phosphate backbones in ODN provide an excellent opportunity to alter the conformations of triplex components to enhance stability, which introduce nuclease resistance and increase the cellular permeability of ODNs. While the use of RNA strands instead of DNA is the simplest variation in backbone structure,⁶² chemical modifications of the natural system include introduction of methyl phosphonates⁶³ and phosphorothioates.⁶⁴ Phosphorothioates are successfully emerging as first-generation antisense lead compounds. Currently, several dephosphono analogues which are nonionic and neutral are being designed, synthesized and studied as potential antigene and antisense agents. The most promising backbone modification involves the newly emerged peptide nucleic acids (PNA)⁶⁵ which have nucleobases on an achiral peptide backbone (Figure 18).

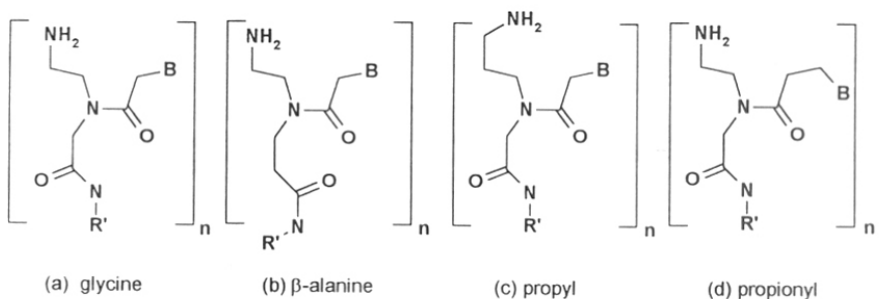


Figure 18. Peptide nucleic acid backbones: (a) glycine-ethylenediamine, (b) β -alanine-ethylenediamine and (c) glycine-propylenediamine. All have bases (B) linked by acetyl group, except for (d) which has a propionyl linker.

1.5. BIOLOGICAL APPLICATIONS OF TRIPLE HELIX FORMING OLIGO-NUCLEOTIDES

The most potential therapeutic application of triple helix strategy is known as “antigene approach” in which DNA transcription is inhibited by third strand binding⁶⁶ (Figure 19). The triplex forming ODNs can be perceived to affect biological processes which involve the use of duplex DNA as a matrix.^{17b,66} These are replication, transcription, DNA repair, recombination, action of topoisomerases and alteration in chromatin superstructure. When the triplex-forming site overlaps with the recognition binding sites of one of the components such as the transcription activator, RNA polymerase or replication machinery, competition for this site by the ODN exerts a direct effect on the biological processes.^{17,67} The DNA conformational change accompanying triplex formation, such as bending, may perturb the binding of protein. These changes may extend to distant regions outside the triplex-forming site and modulate the biological processes. Initiation of transcription and replication may be inhibited by a triplex-forming ODN bound close to a promoter site or origin of replication, thus interfering in the function of DNA or RNA polymerase (Figure 19).

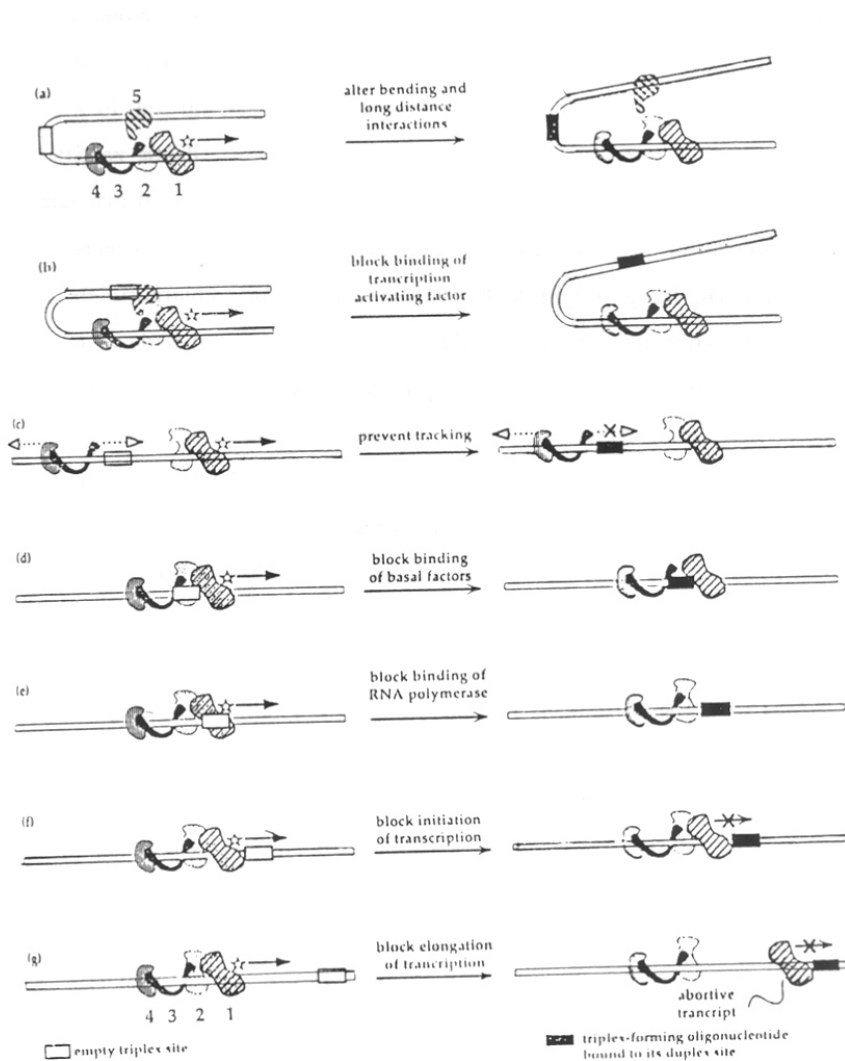


Figure 19. Schematic representation of different mechanisms by which triplex-forming oligonucleotides can block transcription. (Adopted from Thoung and Helene^{17b})

1.6. PRESENT WORK

The above resume outlines the utility of chemical modifications in triple helix stabilization and biological application of triple helices if they are stable at physiological pH. In view of this, the major work in the present thesis is focused on understanding the basis of triplex stabilization by polyamine linked oligodeoxynucleotides at neutral pH. Polyamines and their bio-conjugates have potential as biological effector molecules with bright prospects for medicinal developments.⁶⁷ The naturally occurring polyamines, spermine and spermidine are largely protonated at physiological pH and exhibit net positive charge close to +4 and +3 respectively.⁶⁸ Their inherent polycationic nature and conformational mobility of chain, encourage electrostatic interaction with the anionic phosphates of polynucleotides resulting in specific molecular interaction with duplex DNA.⁶⁹ Spermine is also known to favor triple helix formation when present in millimolar concentrations⁷⁰ and it was recently shown^{50,71} that spermine conjugation to oligonucleotides (see *Chapter 2, section 2.1* for details) leads to improved triple helix stability. It was indeed found that incorporation of 5-Me-dC-N⁴-(spermine) into the Hoogsteen strand of a DNA triplex remarkably stabilized the triplexes at desirable physiological pH, even without Mg²⁺, as compared to non-formation of triplexes with unmodified third strand.⁵⁰

Chapter 2: In view of the fact that spermine conjugation at C4 of 5-Me-dC leads to stabilization of triplexes involving GC W-C duplex pair (C⁺GC triplex) at neutral pH, (which is normally stable at acidic pH), it was though worthwhile to examine the role of spermine side chain on the N3 pK_a of the modified base. To understand the effect of substituent at N⁴ of 5-Me-dC, different N⁴ substituted 5-Me-dC analogues are needed. This chapter describes the syntheses of different N⁴ substituted 5-Me-dC analogues and the determination of N3 pK_a of the modified bases. It also describes the successful attachment of spermine to the C6 of suitably protected purine, dG to get 2-amino-dA analogue.

Chapter 3: This chapter deals with studies directed towards understanding the molecular origin of stabilization of triplets by spermine conjugated oligonucleotides (*sp*-ODN). The present work involves study of the effect of mismatches and the possible role of conjugated spermine in affecting the N3 protonation and association/dissociation equilibrium. To gain further insights towards engineering better triplet systems, comparative studies are conducted on triplets derived from *sp*-ODN with those containing ODNs conjugated with ω,ω' -dideoxydiaminotetraethyleneglycol at C4 of 5-Me-dC (*teg*-ODN). The results are described in terms of thermal stability, salt effect and hysteresis (thermal dissociation and association behavior).

Chapter 4: Spermine is well known to bind both DNA duplex and triplet structures when added externally (see *Chapter 4, section 4.1* for details). However, the exact role of the conformationally flexible backbone of spermine to the nature of binding is not fully understood. Introduction of asymmetry in the spermine backbone may give insight into the mechanisms of its binding to DNA duplex and triplet structures. This chapter first describes the syntheses of conformationally constrained spermine analogues (pyrrolidine analogues) starting from *trans*-4-hydroxy-L-proline, a naturally occurring amino acid followed by DNA binding studies. These new spermine analogues carry two asymmetric centers and an additional nitrogen atom.

Chapter 5: In this chapter the syntheses of different 2-formylbenzenesulfonamides and 2-(N-alkyl/aryl-imino)methyl-benzenesulfonamides from normal and pseudo 2-formylbenzenesulfonylchlorides are described. Both the 2-formylbenzenesulfonamides and 2-(N-alkyl/aryl-imino)methyl-benzenesulfonamides, synthesized, exhibited ring-chain tautomerism and a detailed study on the tautomeric structure of these compounds in solid solution and gas phases were carried out using NMR, IR and MASS spectrometry and also by X-ray crystal structure analysis in the solid state.

1.7. REFERENCES

1. Watson, J. D.; Crick, F. H. C. *Nature*, **1953**, *171*, 737.
2. Saenger, W. *Principles of Nucleic Acids Structure*, **1984**, Springer, New York.
3. Hoogsteen, K. *Acta Crystallogra.*, **1963**, *16*, 907.
4. Crick, F. H. C. *J. Mol. Biol.*, **1966**, *19*, 548.
5. Soll, D.; Cherayil, J. D.; Bock, R. M. *J. Mol. Biol.*, **1966**, *19*, 97.
6. Dickerson, R. E. in *Unusual DNA Structures* (eds. Wells, R. D.; Harvey Sr., S. C.), **1988**, Springer, New York.
7. Kennard, O.; Hunter, W. N. *Q. Rev. Biophys.*, **1989**, *22*, 337.
8. Wing, R. M.; Drew, H. R.; Takano, T.; Broka, C.; Tanaka, S.; Itakura, K.; Dickerson, R. E. *Nature*, **1980**, *287*, 755.
9. Drew, H. R.; Wing, R. M.; Takano, T.; Broka, C.; Tanaka, S.; Itakura, K.; Dickerson, R. E. *Proc. Natl. Acad. Sci. USA.*, **1981**, *78*, 2179.
10. Wang, A. J.-H.; Quigley, G. J.; Kolpak, F. J.; van der Marel, G.; van Boom, J. H.; Rich, A. *Science*, **1980**, *211*, 171.
11. Seeman, N. C.; Rosenberg, J. M.; Rich, A. *Proc. Natl. Acad. Sci. USA.*, **1976**, *73*, 804.
12. (a) Saenger, W.; Hunter, W. N.; Kennard, O. *Nature*, **1986**, *324*, 385. (b) Westhof, E. *Int. J. Biol. Macromol.*, **1987**, *9*, 185.
13. Jin, R.; Breslauer, K. G. *Proc. Natl. Acad. Sci. USA.*, **1988**, *85*, 8939. (b) Barawkar, D. A.; Ganesh, K. N. *Nucleic Acids. Res.*, **1995**, *23*, 159.
14. Felsenfeld, G.; Davies, D. R.; Rich, A. *J. Am. Chem. Soc.*, **1957**, *79*, 2023.
15. Moser, H. E.; Dervan, P. B. *Science*, **1987**, *238*, 645.
16. (a) Le Doan, T.; Perrouault, L.; Praseuth, D.; Habhou, N.; Decout, J. L.; Thoung, N. T.; Lhomme, J.; Helene, C. *Nucleic Acids. Res.*, **1987**, *15*, 7749. (b) Praseuth, D.; Perrouault, L.; Le Doan, T.; Chasseigne, M.; Thoung, N. T.; Helene, C. *Proc. Natl. Acad. Sci. USA.*, **1988**, *85*, 1349.
17. (a) Wells, R. D.; Collier, D. A.; Harvey, J. C.; Schimizu, M.; Wohlrat, F. *FASEB J.*, **1988**, *2*, 2931. (b) Thoung, N. T.; Helene, C. *Angew. Chem. Int. Ed. Engl.*, **1993**, *32*, 666.

18. (a) Cooney, M.; Czernszowsky, G.; Postel, E. H.; Flink, S. J.; Hogan, M. E. *Science*, **1988**, *241*, 456. (b) Beal, P. A.; Dervan, P. B. *Science*, **1991**, *251*, 1360.
19. Yoon, K.; Hobbs, C. A.; Koch, J.; Sandaro, M.; Kunty, R.; Weis, A. *Proc. Natl. Acad. Sci. USA*, **1992**, *89*, 3840.
20. Radhakrishnan, I. R.; Patel, D. J. *Biochemistry*, **1994**, *33*, 11405.
21. Maher, L. J.; Wold, B.; Dervan, P. B. *Science*, **1989**, *245*, 725.
22. (a) Plum, G. E.; Park, Y. W.; Singleton, S. F.; Dervan, P. B.; Breslauer, K. J. *Proc. Natl. Acad. Sci. USA*, **1990**, *87*, 9436. (b) Pilch, D. S.; Brousseau, R.; Shafer, R. H. *Nucleic Acids Res.*, **1990**, *18*, 5743. (c) Shea, R. G.; Ng, P.; Bischofberger, N. *Nucleic Acids Res.*, **1990**, *18*, 4859. (d) Pilch, D. S.; Levenson, C.; Shafer, R. H. *Biochemistry*, **1991**, *30*, 6051. (e) Singleton, S. F.; Dervan, P. B. *J. Am. Chem. Soc.*, **1992**, *114*, 6957. (f) Singleton, S. F.; Dervan, P. B. *J. Am. Chem. Soc.*, **1994**, *116*, 10376.
23. (a) Mooren, M. M. W.; Pulleybank, D. E.; Wijmenga, S. S.; Blommers, M. J. J.; Hilbers, C. W. *Nucleic Acids Res.*, **1990**, *18*, 6523. (b) Xodo, L. E.; Manzini, G.; Quadrifoglio, F. *Nucleic Acids Res.*, **1990**, *18*, 3557.
24. (a) Cheng, A.-J. Van Dyke, M. W. *Nucleic Acids Res.*, **1994**, *22*, 4742. (b) Xodo, L. E.; Manzini, G.; Quadrifoglio, F.; van der Marel, G. A.; van Boom, J. H. *Nucleic Acids Res.*, **1991**, *19*, 5625.
25. (a) Chen, F. M. *Biochemistry*, **1991**, *30*, 4472. (b) Volker, J.; Botes, D. P.; Lindsey, G. G., Klump, H. H. *J. Mol. Biol.*, **1993**, *230*, 1278. (c) Plum, G. E.; Breslauer, K. J. *J. Mol. Biol.*, **1995**, *248*, 679.
26. (a) Mergny, J. -L.; Sun, J. -S.; Rougee, M.; Garestier, T. -M.; Barcelo, F.; Comilier, J.; Helene, C. *Biochemistry*, **1991**, *30*, 9791. (b) Rougee, M.; Faucon, B.; Mergny, J. -L.; Barcelo, F.; Giovannangeli, C.; Garestier, T. -M.; Helene, C. *Biochemistry*, **1992**, *31*, 9269.
27. Porschke, D.; Eigen, M. *J. Mol. Biol.* **1971**, *62*, 361-381.
28. Ganesh, K. N.; Kumar, V. A.; Barawkar, D. A. in *Perspective in Supramolecular Chemistry (Vol 3)*, **1996**, p 263, Hamilton, A. (ed.), John Wiley & Sons Ltd.
29. Lee, J. S.; Woodsworth, M. L.; Latimer, L. J. P.; Morgan, A. R. *Nucleic Acids. Res.*, **1984**, *12*, 6603.
30. Lee, J. S.; Woodsworth, M. L.; Latimer, L. J. P. *Biochemistry*, **1984**, *23*, 3277.
31. Povsic, T. J.; Dervan, P. B. *J. Am. Chem. Soc.*, **1989**, *111*, 3059.
32. Maher III, L. J.; Dervan, P. B.; Wold, B. *Biochemistry*, **1990**, *29*, 8820.

33. Shimizu, M.; Koizumi, T.; Inoue, H.; Ohtsuka, E. *Bioorg. Med. Chem. Lett.*, **1994**, *4*, 1029.
34. Froehler, B. C.; Ricca, D. J. *J. Am. Chem. Soc.*, **1992**, *114*, 8320.
35. Miller, P. S.; Cushman, C. D. *Bioconj. Chem.*, **1992**, *3*, 74.
36. Huang, C.-Y.; Cushman, C. D.; Miller, P. S. *J. Org. Chem.*, **1992**, *58*, 5048.
37. Shaw, J. -P.; Milligan, J. F.; Krawczyk, S. H.; Matteucci, M. *J. Am. Chem. Soc.*, **1991**, *113*, 7765.
38. Pudlo, J. S.; Wadwani, S.; Milligan, J. F.; Matteucci, M. D. *Bioorg. Med. Chem. Lett.*, **4**, 1025.
39. Ono, A.; Ts' O, P. O. P.; Kan, L. -S. *J. Org. Chem.*, **1992**, *57*, 3265.
40. Jetter, M. C.; Hobbs, F. W. *Biochemistry*, **1992**, *32*, 3249.
41. Miller, P. S.; Bhan, P.; Cushman, C. D.; Trapane, T. L. *Biochemistry*, **1992**, *31*, 6788.
42. Davison, e. C.; Johnsson, K. *Nucleosides Nucleotides*, **1993**, *12*, 237.
43. Shimizu, M.; Inoue, H.; Ohtsuka, E. *Biochemistry*, **1994**, *33*, 606.
44. Xiang, G.; Soussou, W.; McLaughlin, L. W. *J. Am. Chem. Soc.*, **1994**, *116*, 11155.
45. Hunziker, J.; Presley, E. S.; Brunav, H.; Dervan, P. B. *J. Am. Chem. Soc.*, **1995**, *117*, 2421.
46. Huang, C. -Y.; Miller, P. S. *J. Am. Chem. Soc.*, **1993**, *115*, 10456.
47. (a) Koh, J. S.; Dervan, P. B. *J. Am. Chem. Soc.*, **1992**, *114*, 1470. (b) Priestley, E. S.; Dervan, P. B. *J. Am. Chem. Soc.*, **1995**, *117*, 4761.
48. Froehler, B. C.; Wadwani, S.; Terhost, T. J.; Gerrard, S. R. *Tetrahedron Lett.*, **1992**, *33*, 5307.
49. Best, G. C.; Dervan, P. B. *J. Am. Chem. Soc.*, **1995**, *117*, 1187.
50. Barawkar, D. A.; Kumar, V. A.; Ganesh, K. N. *Biochem. Biophys. Res. Commun.*, **1994**, *205*, 1665.
51. Griffin, L. C.; Kiessling, L. L.; Beal, P. A.; Gillespie, P.; Dervan, P. B. *J. Am. Chem. Soc.*, **1992**, *114*, 7976.
52. Griffin, L. C.; Dervan, P. B. *Science*, **1989**, *245*, 967.
53. Miller, P. S.; Cushman, C. D. *Biochemistry*, **1993**, *32*, 2999.
54. Bandaru, R.; Hashimoto, H.; Switzer, C. *J. Org. Chem.*, **1995**, *60*, 786.
55. Stilz, H. U.; Dervan, P. B. *Biochemistry*, **1993**, *32*, 2177.
56. Rao, T. S.; Hogan, M. E.; Revankar, G. R. *Nucleosides Nucleotides*, **1994**, *13*, 95.
57. (a) Milligan, J. F.; Krawczyk, S. H.; Wadwani, S.; Matteucci, M. D. *Nucleic Acids Res.*, **1993**, *21*, 327. (b) Cheng, A. -J.; van Dyke, M. W. *Nucleic Acids Res.*, **1993**, *21*, 5630. (c)

- Olivas, W. M.; Maher, L. J. *Biochemistry*, **1993**, *34*, 278. (d) Rao, T. S.; Lewis, A. F.; Durland, R. H.; Revankar, G. R. *Tetrahedron Lett.*, **1993**, *34*, 6709.
58. (a) Rao, T. S.; Durland, R. H.; Seth, D. M.; Myrick, M. A.; Bodepudi, V.; Revankar, G. R. *Biochemistry*, **1995**, *34*, 765. (b) Rao, T. S.; Lewis, A. F.; Hill, T. S.; Revankar, G. R. *Nucleosides Nucleotides*, **1995**, *14*, 1.
59. (a) Bhattacharya, B. K.; Chari, M. V.; Durland, R. H.; Revankar, G. R. *Nucleosides Nucleotides*, **1995**, *14*, 45. (b) Staubli, A. B.; Dervan, P. B. *Nucleic Acids Res.*, **1994**, *22*, 2637.
60. Hildbrand, S.; Leumann, C. *Angew. Chem. Int. Ed. Engl.*, **1996**, *35*, 1968.
61. Kandimalla, E. R.; Manning, A. N.; Venkataraman, G.; Sasisekharan, V.; Agrawal, S. *Nucleic Acids Res.*, **1995**, *23*, 4510.
62. (a) Chou, S. -H.; Flynn, P.; Reid B. *Biochemistry*, **1989**, *28*, 2435. (b) Macaya, R. F.; Wang, E.; Schultze, P.; Sklenar, V.; Feigon, J. *J. Mol. Biol.*, **1990**, *225*, 755. (c) Macaya, R. F.; Schultze, P.; Feigon, J. *J. Am. Chem. Soc.*, **1992**, *114*, 7811. (d) Roberts, R. F.; Crothers, D. M. *Science*, **1992**, *258*, 1463. (e) Han, H.; Dervan, P. B. *Proc. Natl. Acad. Sci. USA.*, **1993**, *90*, 3806. (f) Escude, C.; Francois, J. C.; Sun, J. S.; Ott, G.; Sprinze, M.; Gareshier, T., Helene, C. *Nucleic Acids Res.*, **1993**, *21*, 5547. (g) Semerad, C. L.; Maher, L. J. *Nucleic Acids Res.*, **1994**, *22*, 5321.
63. (a) Callahan, D. E.; Trapane, T. L.; Miller, P. S.; Ts' O, P. O. P.; Kan, L. -S. *Biochemistry*, **1991**, *30*, 1650. (b) Herzog, L. -K.; Keil, B.; Zon, G.; Shinozuka, K.; Mizan, S.; Wilson, W. D. *Nucleic Acids Res.*, **1990**, *18*, 3545.
64. Xodo, L.; Alunnifabroni, M.; Manzini, G.; Quadrifoglio, F. *Nucleic Acids Res.*, **1994**, *22*, 3322.
65. (a) Egholm, M.; Buchardt, O.; Nielsen, P. E.; Berg, R. H. *J. Am. Chem. Soc.*, **1992**, *114*, 1895. (b) Egholm, M.; Buchardt, O.; Christensen, L.; Behrens, C.; Frier, S. M.; , Driver, D. A.; Berg, R.; Norden, B.; Nielsen, P. E. *Nature*, **1993**, *365*, 566. (c) Kim, S.; Nielsen, P. E., Egholm, M.; Buchrdt, O.; Norden, B. *J. Am. Chem. Soc.*, **1994**, *116*, 785. (d) Nielsen, P. E.; Egholm, M.; Berg, R. H.; Buchardt, O. *Science*, **1991**, *254*, 1497. (e) Nielsen, P. E.; Egholm, M.; Buchardt, O. *Bioconj. Chem.*, **1994**, *5*, 3.
66. (a) Helene, C. *Anti-Cancer Drug Des.*, **1991**, *6*, 569. (b) Maher, L. J. *Bioessays*, **1992**, *14*, 807

67. (a) Ganem, B. *Acc. Chem. Res.*, **1982**, *15*, 290. (b) Tabor, C. W.; Tabor, H. *Annu Rev. Biochem.*, **1984**, *53*, 749. (c) Behr, J. P. *Acc. Chem. Res.*, **1993**, *26*, 274.
68. Takeda, Y.; Samesima, K.; Nagano, K.; Watanabe, M.; Sugeta, H.; Kyogoko, Y. *Eur. J. Biochem.*, **1983**, *130*, 383.
69. (a) Feurstein, B. G.; Pattabiraman, N.; Marton, L. J. *Nucleic Acids Res.*, **1990**, *18*, 1271. (b) Jain, S.; Zon, G.; Sunderalingam, M. *Biochemistry*, **1989**, *28*, 2360. (c)
70. Hampel, K. J.; Crosson, P.; Lee, J. S. *Biochemistry*, **1991**, *30*, 4455. (b) Thomas, T.; Thomas, T. J. *Biochemistry*, **1993**, *32*, 14068.
71. Tung, C.; Breslauer, K.; Stein, S. *Nucleic Acids Res.*, **1993**, *21*, 5489-5494. (b) Schmid, N.; Behr, J. P. *Tetrahedron Lett.*, **1995**, *36*, 1447-1450. (c) Bigey, P.; Pratveil, G.; Meunier, B. *J. Chem. Soc., Chem. Comm.*, **1995**, 181-182. (d) Sund, C.; Puri, N.; Chattopadhyaya, J. *Tetrahedron*, **1996**, *52*, 12275-12290.

CHAPTER 2.

CHEMICAL SYNTHESIS AND CHARACTERIZATION OF
(i) dC-N⁴-(ALKYLAMINO/ALKOXY) AND
(ii) 2-AMINO-dA-N⁶-(ALKYLAMINO) ANALOGUES FOR
APPLICATION IN DNA TRIPLEX STABILIZATION

2.1 TARGET MOLECULES AND RATIONALE

The studies directed towards DNA nucleobase modifications to achieve better duplex and triplex specificity desired for antisense/antigene applications have been discussed in Chapter 1. Among several approaches, polyamine conjugations to DNA have shown utility in stabilization of DNA triple helices.¹⁻⁷ Externally added spermine is well known to stabilize DNA duplex and triplex.^{8,9} Polyamines are required for natural growth of cells and spermine is the most abundant polyamine present in animal cells.¹⁰ These aspects raised our interest in spermine conjugated oligonucleotides as potential non-toxic candidates for the antisense and antigene strategies. A few reports on spermine conjugated oligodeoxynucleotides (ODNs) have emerged over recent years and the various site of conjugation employed are 5'-terminus, 2'-O-position and nucleobases. Tung *et. al.*¹ introduced spermine at the 5'-terminus (Figure 1) of oligonucleotides in a post synthetic step by reacting 5'-iodoacetamidoalkyl linked oligo-DNA with N1-(3-mercaptopropyl)spermine (1) in aqueous solution. Prakash *et. al.*² conjugated spermine to the C4 of 5-Me-dC moiety, as in 2, and introduced it into ODN through the phosphoramidite based solid-phase synthesis. Schmid and Behr³ conjugated spermine to C2 of a guanine base, as in 3, in a post-synthetic procedure by using protected 2-fluoro-2'-deoxyinosine phosphoramidite block in the solid-phase synthesis. Bigey *et. al.*⁴ introduced spermine as a linker between the 5'-hydroxyl of their ODN and a tris(methylpyridiniumyl)porphyrinato-manganese (III) motif (4) in a post synthetic procedure. Recently, Sund *et. al.*⁵ introduced C-branched spermine to C2' and to C5' through a phosphate linker. Irrespective of the site of conjugation of spermine on oligonucleotides, it was shown that such conjugation to DNA, generally provides positive contribution to triplex stability.

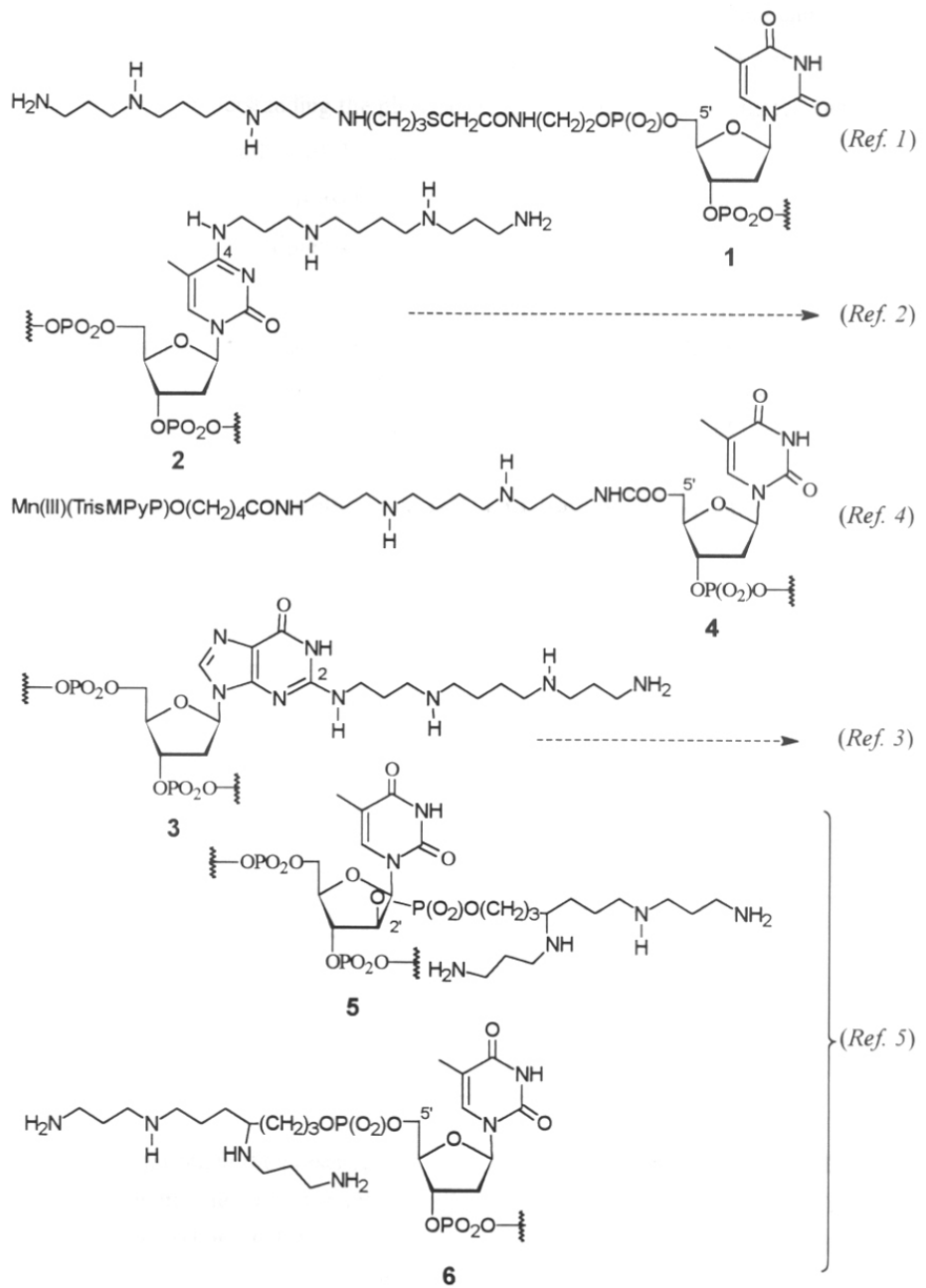


Figure 1

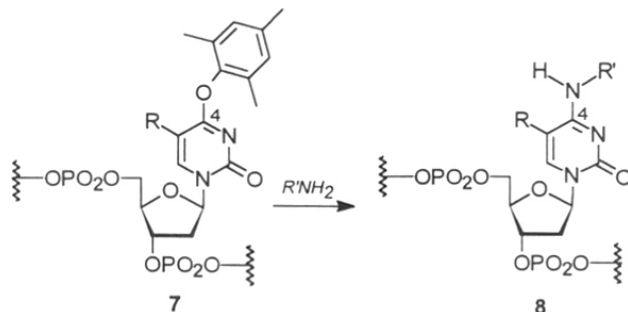
Conjugation of spermine at N⁴ of dC of ODNs has shown not only enhancement in triplex stability but also facilitated its formation at physiological pH.⁶ In view of this remarkable effect, understanding the physical/structural role of N⁴-conjugated spermine on triplex stability and the effect of the tetracationic spermine side chain on the pK_a of N3 of dC assumes significance. It is well known that N3 pK_a of dC is one of the important factors that determine the triplex stability of C⁺GC triad (see *Chapter 1* for details).

The objectives of this chapter are (i) synthesis of various N⁴-substituted dC and 5-Me-dC nucleosides which can provide insight into the effect of charge and steric factors on the N3 pK_a, (ii) design and synthesis of desired N⁴-substituents, (iii) conjugation of spermine to purine base and (iv) pK_a determination of N⁴-substituted dC derivatives.

2.2. Synthesis of N⁴-(alkylamino/alkoxy)-dC and 2-amino-N⁶-(spermido)-dA

2.2.1. General Synthetic Strategy

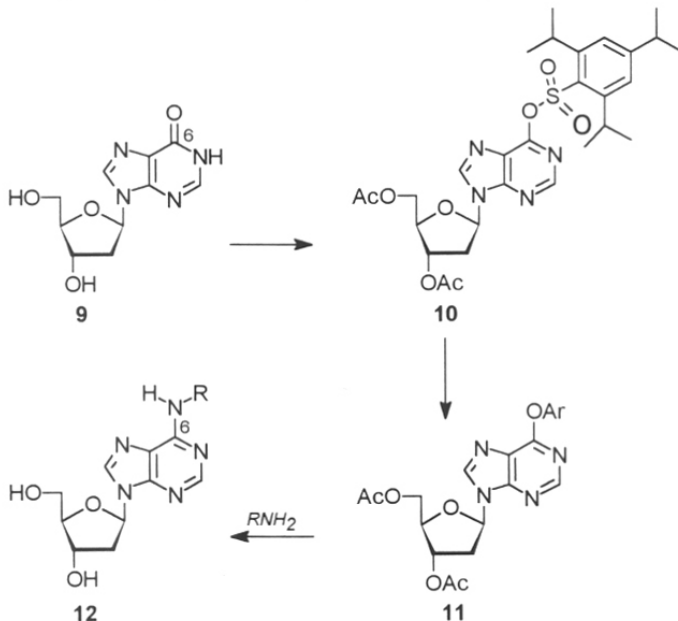
For the synthesis of functionally tethered oligonucleotides (FTOs) MacMillan and Verdine¹¹ have incorporated a convertible nucleoside, O⁶-(2,4,6-trimethylphenyl)-2'-deoxy-uridine (**7**) at specific sites of the oligonucleotide (ODN) sequence (Scheme 1).



Scheme 1

In this approach the presence of a convertible nucleoside such as **7** in ODN allows the tether to be attached after the DNA synthesis. FTO **7** derived from U or T undergoes aminolytic conversion at C4 to give N⁴-substituted cytidines, **8**. The treatment of corresponding monomer with different amines before incorporation into ODN can lead to various N⁴-substituted cytidines. This approach and a slight modification of the same are presently used for synthesis of the desired N⁴-alkyl, alkoxy and alkylamino substituted dC

analogues (see section 2.2.3). Ferentz and Verdine¹² later extended the same strategy to purines to obtain FTOs as shown in **Scheme 2**. In this extended approach, the convertible nucleoside O⁶-phenyl and O⁶-*p*-nitrophenyl - deoxyinosine **11** are used for conversion to N⁶-substituted 2'-deoxyadenosine **12**, by reaction with amine at the oligonucleotide level. The precursor for the synthesis of O⁶-aryl-2'-deoxyinosine is the sulfonate ester **10**, prepared from 2'-deoxyinosine by acetyl protection of the 3' and 5' hydroxy functions and subsequent treatment with 2,3,6-triisopropylbenzenesulfonylchloride (TPS-Cl) in presence of triethylamine (TEA). Similar intermediate of 2'-deoxyguanosine derivative is used for the attachment of spermine at C-6 of dG (see section 2.2.4).



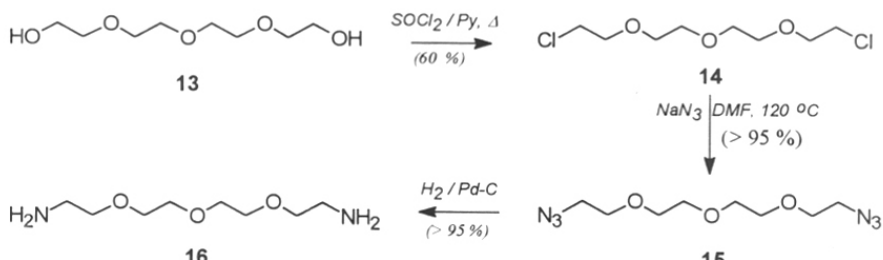
Scheme 2

2.2.2 Synthesis of Substituted Amines for Linking to dC-N⁴

To obtain different N⁴- alkoxy and alkylaminoxy substituted dC analogues, different amines of interest are needed to be synthesized. the conversion of terminal hydroxy functions of tetraethyleneglycol to amino group leads to mono and diaminotetraethyleneglycols depending on the reaction conditions.¹³ Both these derivatives are similar to spermine in terms of molecular mass and atom chain length and are good substitutes to investigate the role of spermine amino groups. Thus, the attachment of 1,11-diamino-3,6,6-trioxaundecane (ω,ω' -didehydroxy-diaminotetraethyleneglycol) at N⁴ of dC

and its incorporation into ODNs can provide close comparison with spermine conjugated ODNs (see *Chapter 3*).

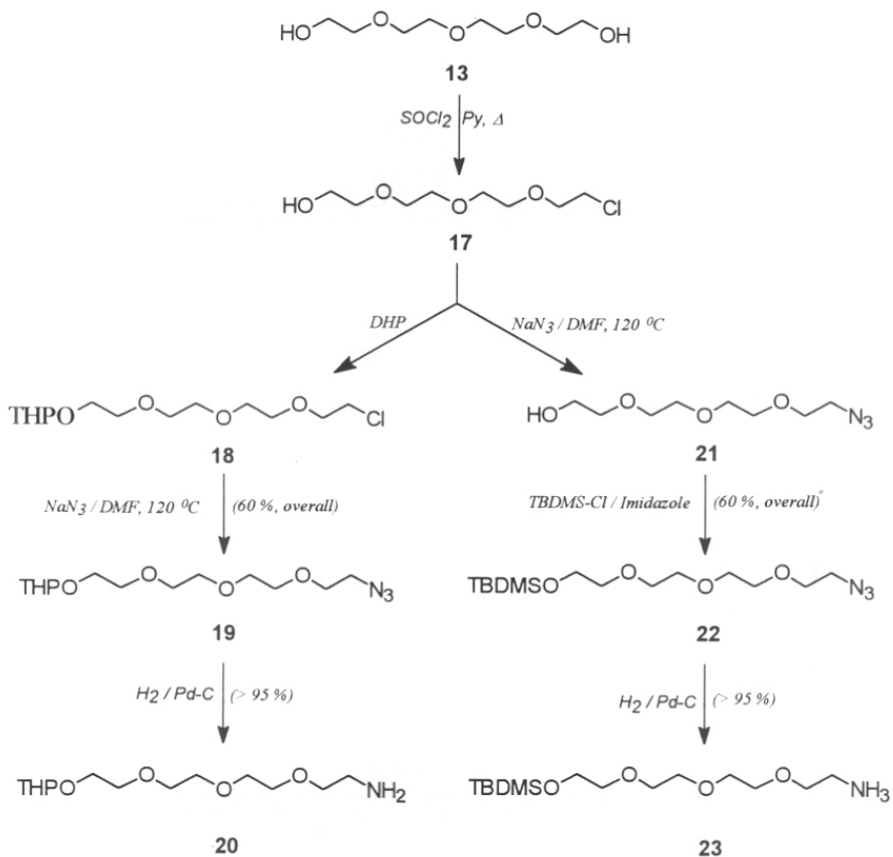
Tetraethyleneglycol **13** (TEG) after azeotropic drying over toluene and treatment with excess of thionylchloride in pyridine under reflux in toluene gave the ω,ω' -dichloro derivative **14** (**Scheme 3**).¹³ This was passed through a column of activated alumina to remove trace amount of sulfur contamination from thionylchloride, followed by reaction with sodium azide in DMF to give the diazide, 1,11-diazido-3,6,9-trioxaundecane (**15**) in quantitative yield. The formation of the azide was confirmed by a strong band at 2100 cm^{-1} for azide stretching in its IR spectrum and a characteristic triplet at 3.43 ppm in its ^1H NMR spectrum. The catalytic hydrogenation of azide **15** using 10 % Pd-C catalyst¹³ afforded the desired 1,11-diamino-3,6,9-trioxaundecane (**16**) in quantitative yield.



Scheme 3

The synthesis of differentially O-protected monoamino derivatives, **20** and **23** were accomplished as shown in **Scheme 4**. One pot reaction of TEG with one equivalent of thionylchloride followed by addition of 2,3-dihydropyran (DHP), yielded mono-THP derivative **18**. The reaction was complete without the addition of pyridinium-*p*-toluenesulfonate (PPTS)¹⁴ (normally used catalyst for THP etherification) or any other catalyst. The presence of traces of pyridiniumhydrochloride equivalent to PPTS, a byproduct of the acid chloride reaction, is thought to be involved in the THP etherification reaction. The reaction of the monochloro derivative **18** with sodium azide in DMF gave 1-azido-11-O-tetrahydropyranyl-3,6,9-trioxaundecane (**19**) in 80 % yield along with the diazide **15** (20 %) as a side product. The catalytic reduction of the azide **19** over Pd-C (10 %) in methanol yielded the amino derivative, 1-amino-11-O-tetrahydropyranyl-3,6,9-trioxaundecane (**20**) in quantitative yield. The formation of the azide **19** and its reduction into the corresponding amine **20** were confirmed by IR and NMR spectroscopy.

The monochloroderivative **17** on treatment with sodium azide in DMF at 120 °C gave the azide **21**.¹³ This upon reaction with TBDMS-Cl and imidazole gave 1-azido-11-O-*t*-butyldiemethylsilyl-3,6,9-trioxaundecane **22** in moderate yield.¹⁵ As in the case of the azide **19** about 20 % of the diazide **15** was isolated from the reaction mixture by silica gel column chromatography. The catalytic reduction of **22** yielded the desired monoamine, 1-amino-11-O-*t*-butyldimethylsilyl-3,6,9-trioxaundecane (**23**) in quantitative yield (Scheme 4). Compounds **22** and **23** were characterized by IR and NMR (see Figure 2 and 3) spectroscopy techniques.



Scheme 4

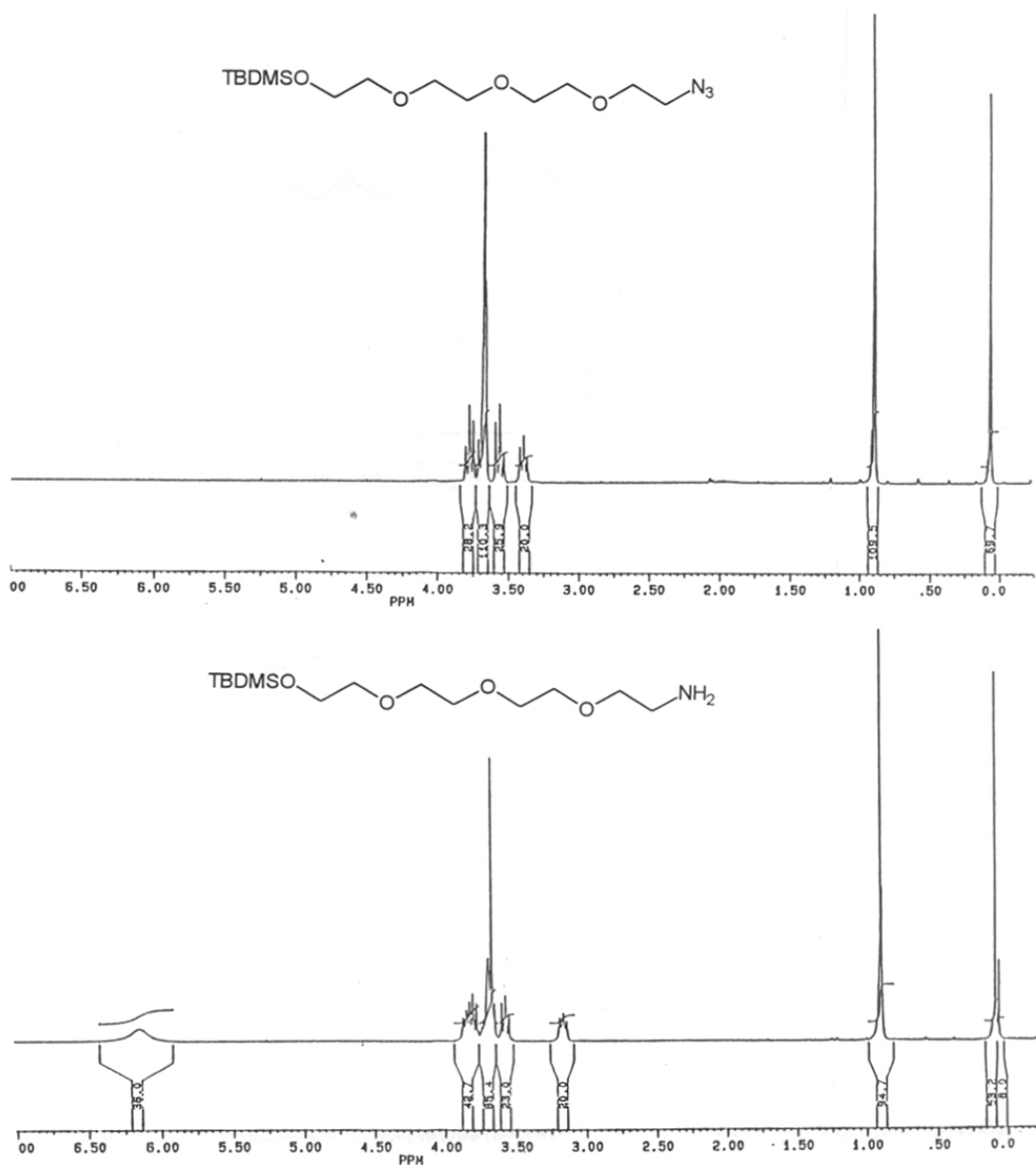


Figure 2. ¹H NMR spectra of (a) 22 and (b) 23 in CDCl₃.

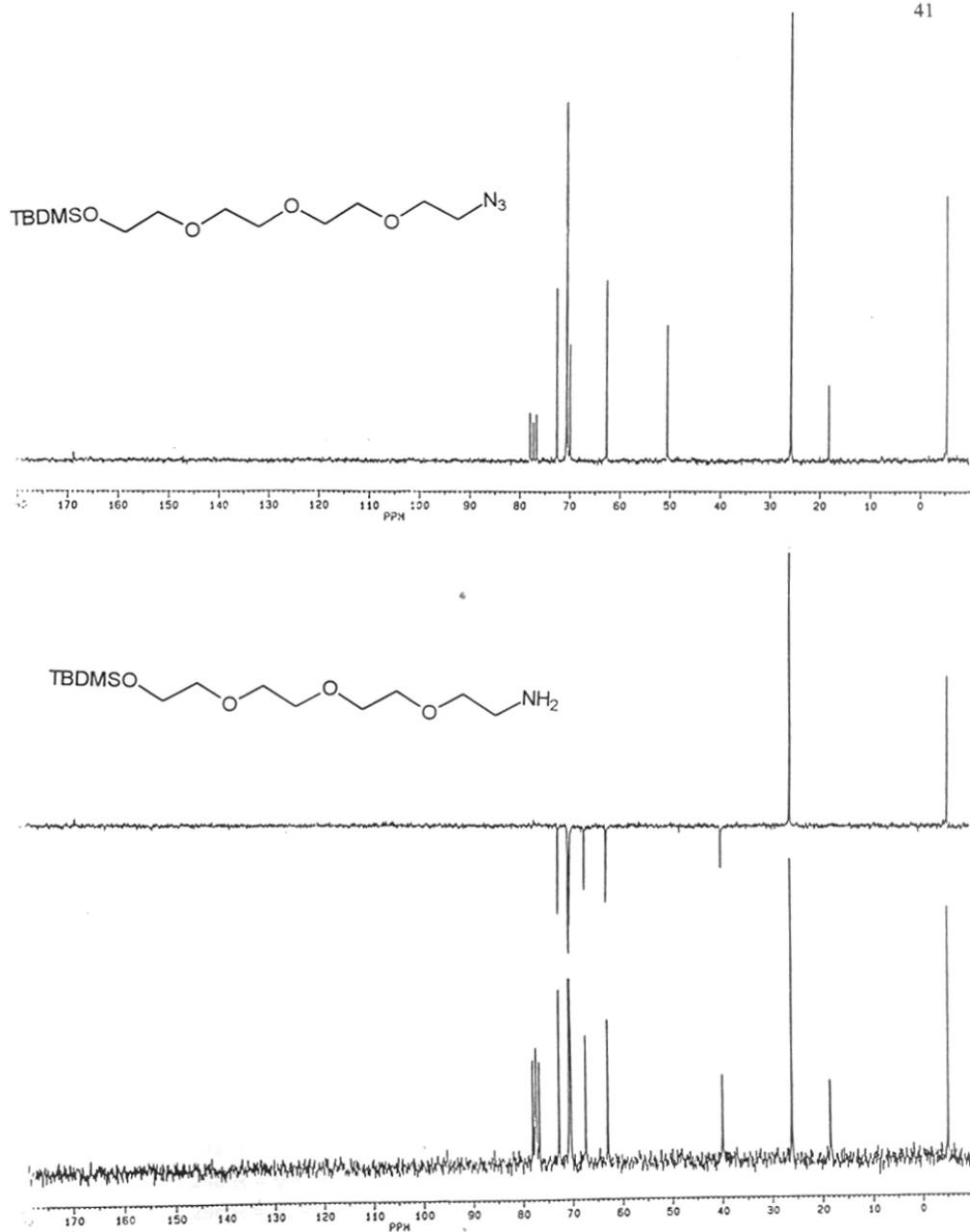
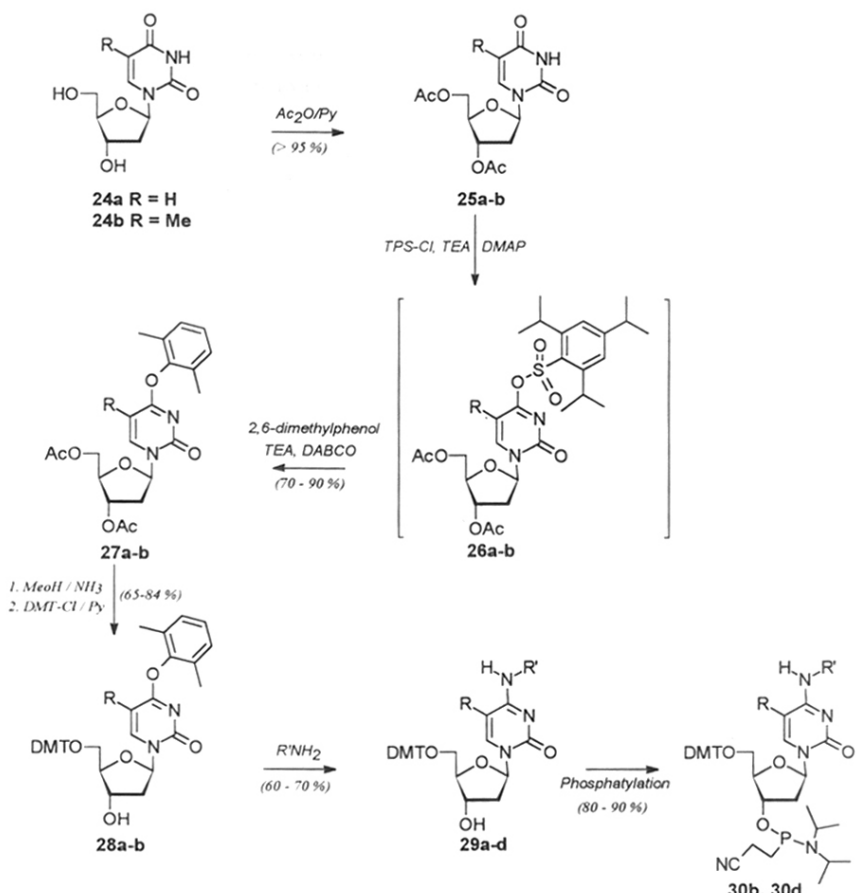


Figure 3. ^{13}C NMR spectra of (a) 22 and (b) 23 in CDCl_3 .

2.2.3. Synthesis of N^4 -alkyl/alkylamino/alkoxy substituted dC:

The convertible nucleoside approach¹¹ and a modification of this approach were used for accomplishing the synthesis of various N^4 -substituted dC analogues.



29a R = H, R' = $(CH_2)_3N[COCF_3](CH_2)_4N[COCF_3](CH_2)_3NH[COCF_3]$

29b R = Me, R' = $(CH_2)_3N[COCF_3](CH_2)_4N[COCF_3](CH_2)_3NH[COCF_3]$

29c R = H, R' = $(CH_2)_2O(CH_2)_2O(CH_2)_2O(CH_2)_2NH[COCF_3]$

29d R = Me, R' = $(CH_2)_2O(CH_2)_2O(CH_2)_2O(CH_2)_2NH[COCF_3]$

Scheme 5

*5'-O-4,4'-Dimethoxytrityl-4-O-(2,6-dimethylphenyl) derivatives of 2'-deoxyuridine **28a** and of thymidine **28b** were synthesized (Scheme 5) from 2'-deoxycytidine (**24a**) and thymidine (**24b**), respectively. Upon treatment with acetic anhydride in pyridine, **24a** and **24b** gave the diacetates **25a** and **25b**, which were converted to **27a** and **27b** in one pot via the non-isolated sulfonate intermediate **26a-b**.^{11,16} The diacetates when reacted with TPS-Cl in the presence of equivalent amount of TEA and catalytic amount of 4-N,N-dimethylaminopyridine (DMAP) formed the sulfonate intermediate **26**, which was then directly treated with 2,6-dimethylphenol/TEA/DABCO to get the C4 functionalised derivatives **27a-b**. The 3',5'-di-O-acetate groups of **27a-b** were removed by treatment with methanolic ammonia for 1 h at ambient temperature without affecting the C4-O-substituent followed by protection of 5' hydroxy function as 4,4'-dimethoxytrityl by treatment with 4,4'-dimethoxy-tritylchloride in pyridine¹⁷ to afford convertible nucleoside analogues **28a** and **28b**. These convertible nucleosides on treatment with amines of interest gave different N⁴-substituted cytidine derivatives as shown in Scheme 5.*

The reaction of the convertible nucleoside **28b** with excess spermine at 60 °C gave *5'-O-4,4'-dimethoxytrityl-5-methyl-2'-deoxycytidine-N⁴-(spermine)* which was converted to the trifluoroacetamide derivative **29b** by treatment with ethyltrifluoroacetate.² The reaction of the convertible nucleoside **28b** with diamine **16** under identical conditions gave the alkoxyderivative, *5'-O-4,4'-dimethoxytrityl-4-N-(11-trifluoroacetamido-3,6,9-trioxaundecyl)-5-methyl-2'-deoxycytidine* (**29d**). This was characterized by NMR (¹H and ¹³C) and mass spectroscopy (Figure 4, 5 and 6). It was interesting to see that in addition to the expected molecular ion peak at 814 m/z ($M^+ + 1 = 815.3$ m/z, obtained) in NMBA/MeOH matrix, the FAB MS of the compound **29d** gave a peak at 837.3 m/z ($M^+ + Na^+$) when it was recorded in NMBA/MeOH/NaCl matrix (Figure 6). This is probably due to the polyoxyethylene side chain present at N⁴ of the modified base which can chelate with Na⁺ ion, like crown ethers. The synthesis of *5'-O-4,4'-dimethoxytrityl-4-N-(8-amino-3,6-dioxaoctyl)-2'-deoxycytidine*, an analogue of compound **29d** via the N⁴-tosylate of protected cytidine has been reported by Markiewicz *et. al.*¹⁸ Synthesis of 2'-deoxycytidine derivatives **29a** and **29c** were completed from the convertible nucleoside **28a** by treatment with spermine and 1,11-diamino-3,6,9-trioxaundecane (**16**) respectively followed by trifluoroacetylation as described above. Phosphitylation of compounds **29b** and **29d** with 2-cyanoethyl-N,N,N',N'-tetraisopropyl-phosphorodiamidite in presence of tetrazole gave the respective phosphoramidite **30b** and **30d** monomers.¹⁹ These amidites were characterized by ³¹P NMR spectroscopy which showed two signals at 149.8 and 149.4

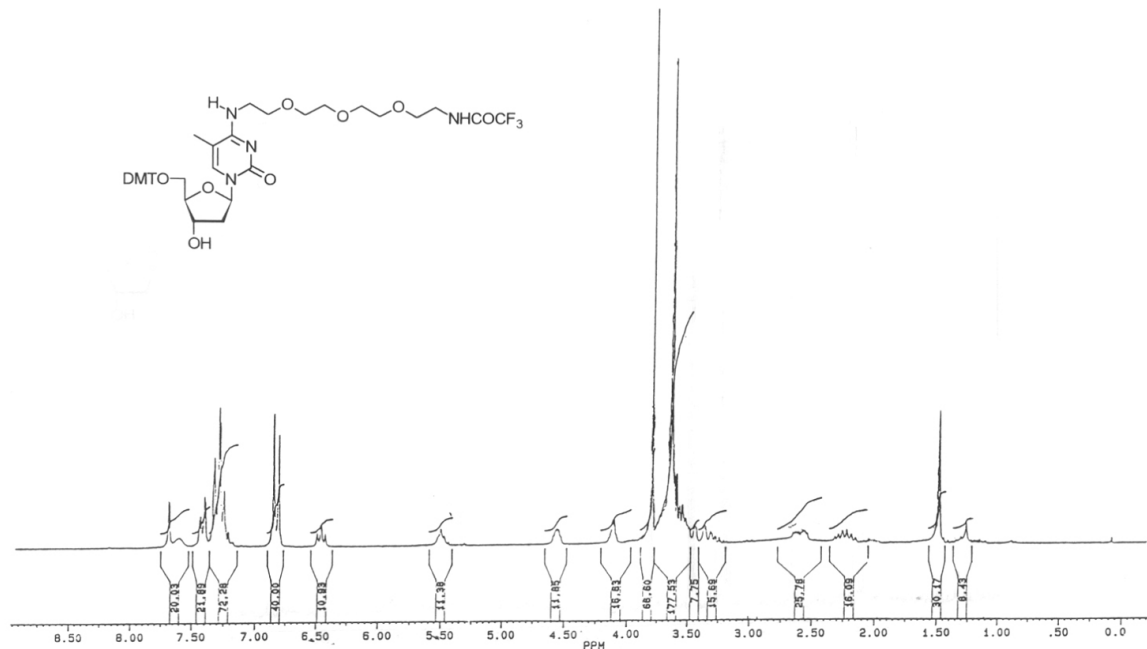


Figure 4. ^1H NMR spectrum of compound 29d in CDCl_3 .

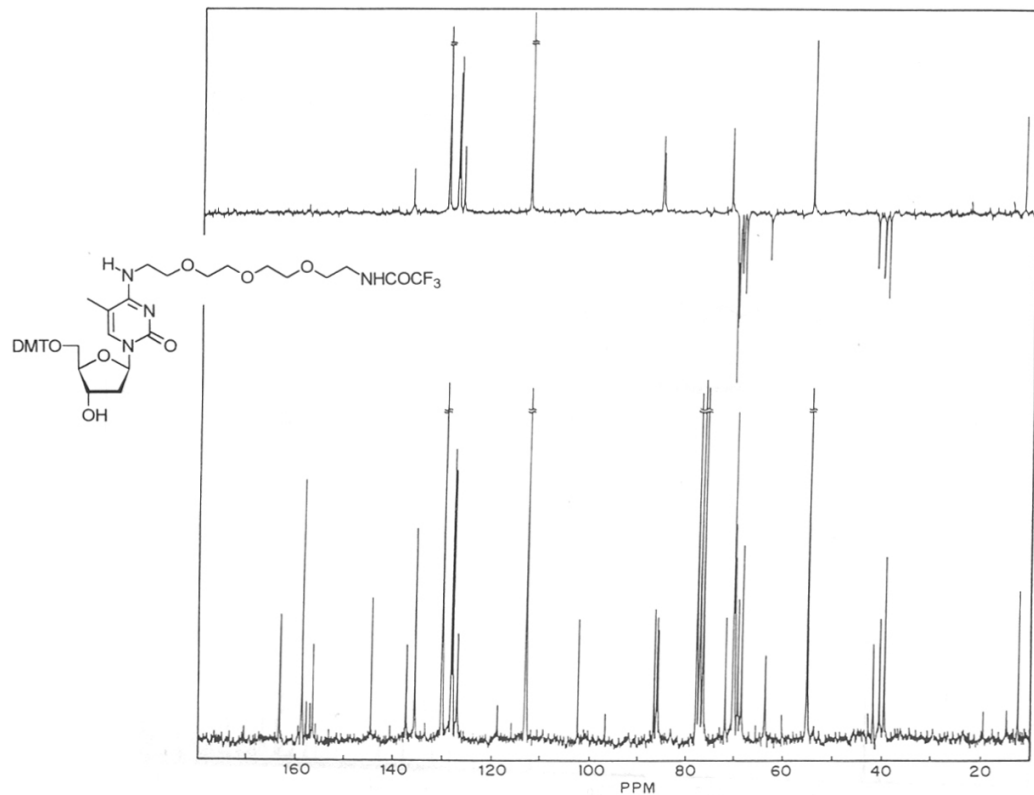


Figure 5. ^{13}C NMR spectrum of compound 29d in CDCl_3 .

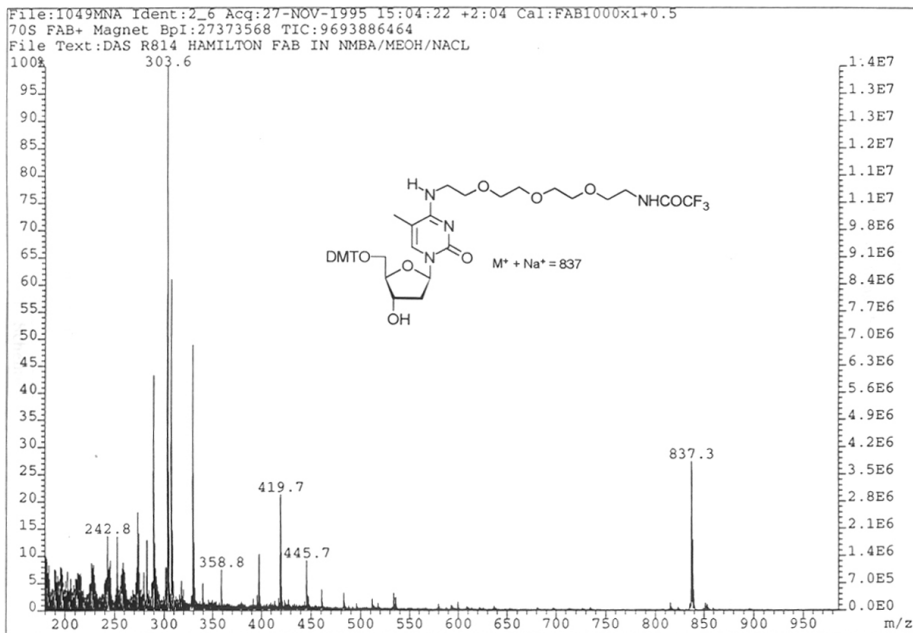
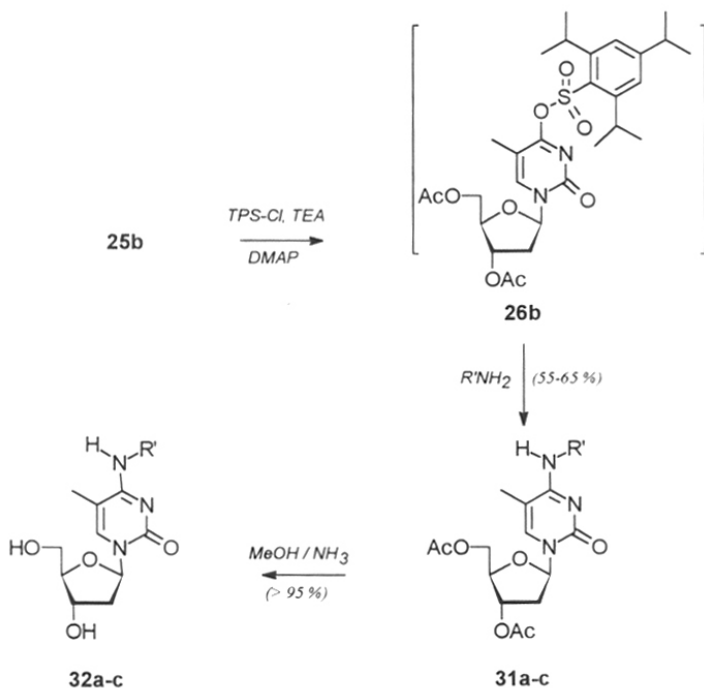


Figure 6. FAB MS of compound 29d in NMBA/MeOH/ NaCl matrix

ppm characteristic of amidite phosphorous and later incorporated into oligonucleotides for further studies (see *Chapter 3*).

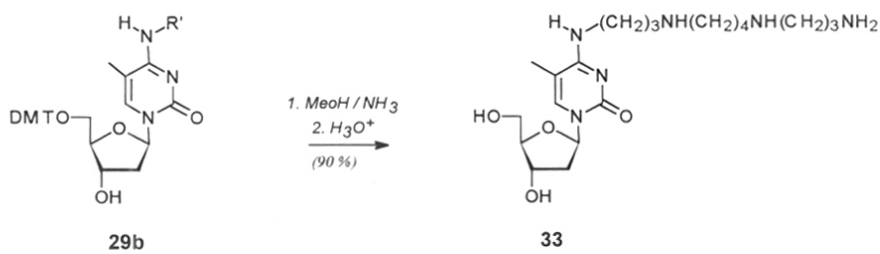
The amine tethered nucleobases could be obtained in moderate yield and in a lesser number of steps by slightly modifying the 'convertible nucleoside approach'¹¹ as shown in Scheme 6. The 3',5'-O-diacetate derivative **25b** was treated with 1.5 equivalent of TPS-Cl and TEA in dichloromethane in the presence of catalytic amount of DMAP. The formation of sulfonate intermediate **26b** was complete in 40h, (as evident from TLC) and this without isolation was directly treated with different amines to get the N⁴-substituted derivatives **31a-c** in moderate yield. It is pointed out that the earlier procedure¹⁶ required the use of large excess of TPS-Cl to get the intermediate **26b** and necessitated its conversion to the 2,6-dimethylphenol intermediate **27b** prior to reaction with amines to get **31a-c**. These are overcome by the present improved procedure.



Scheme 6

Reaction of the sulfonate **26b** with *n*-propylamine was complete in 10 min as evident from TLC and the excess amine present in the reaction mixture was immediately removed under vacuum followed by work-up and silica gel column chromatography giving N^4 -*n*-propyl derivative **31a**. The reaction of the intermediate **26b** with dodecyl amine and with 1-amino-11-O-*t*-butyldimethylsilyl-3,6,9-trioxaundecane (**23**) was complete in 0.5 h and 1 h respectively. All the three N^4 -substituted derivatives obtained were characterized by usual spectroscopic technique (1H and ^{13}C NMR spectra of the N^4 -alkoxy derivative **31c** are shown in Figure 7 and 8). As in the case of the N^4 -alkoxyamino derivative **29d**, the FAB MS of the compound **31c** gave peaks corresponds to $M^+ + 1$ and $M^+ + Na^+$ when the spectra were recorded in MNBA and MNBA/NaCl matrix respectively (Figure 9). This indicates the crown ether nature/behavior of the alkoxy substituent at N^4 . The treatment of the 3',5'-O-diacetyl derivatives with methanolic ammonia at ambient temperature for 1 h gave the free bases **32a-c** in quantitative yield. These free bases are used for determining the N_3 pK_a of various N^4 -substituted dC analogues for comparative analysis with behavior of dC as discussed in section 2.3.

The free base 5-methyl-2'-deoxy- N^4 -(spermine) (**33**) was obtained from the spermine conjugated derivative **29b** for pK_a determination as shown in Scheme 7. The trifluoroacetamide protection of compound **29b** was removed by methanolic ammonia²⁰ treatment and subsequent deprotection of the 5'-O-(4,4'-O-dimethoxy)trityl with acid²¹ gave the free base **33** in good yield.



Scheme 7

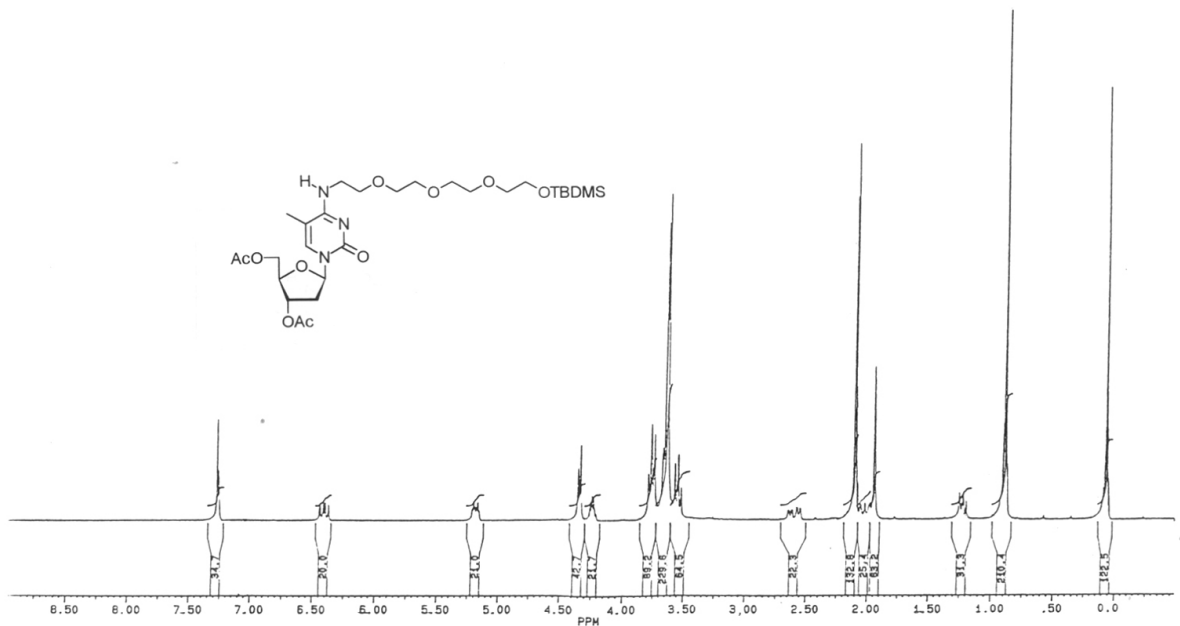


Figure 7. ^1H NMR spectrum of compound 31c in CDCl_3 after D_2O exchange.

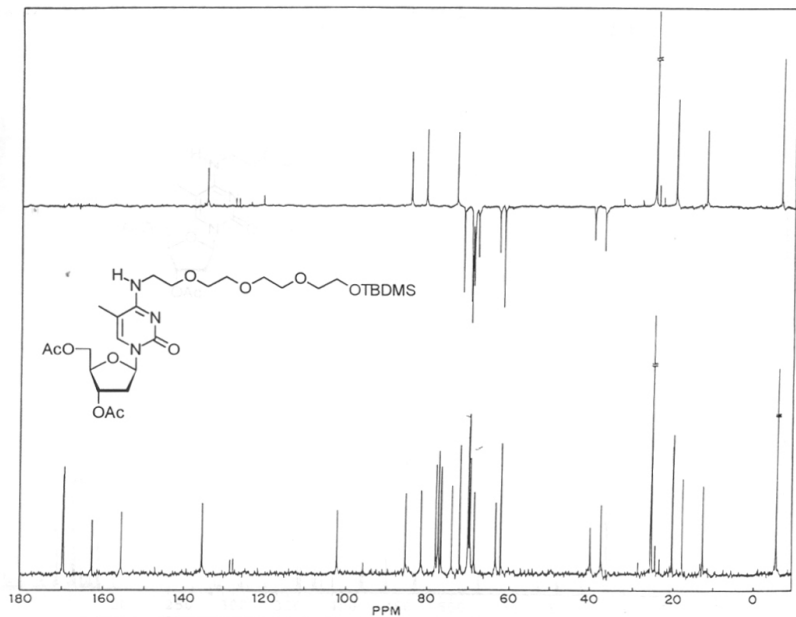


Figure 8. ^{13}C NMR spectrum of compound 31c in CDCl_3 .

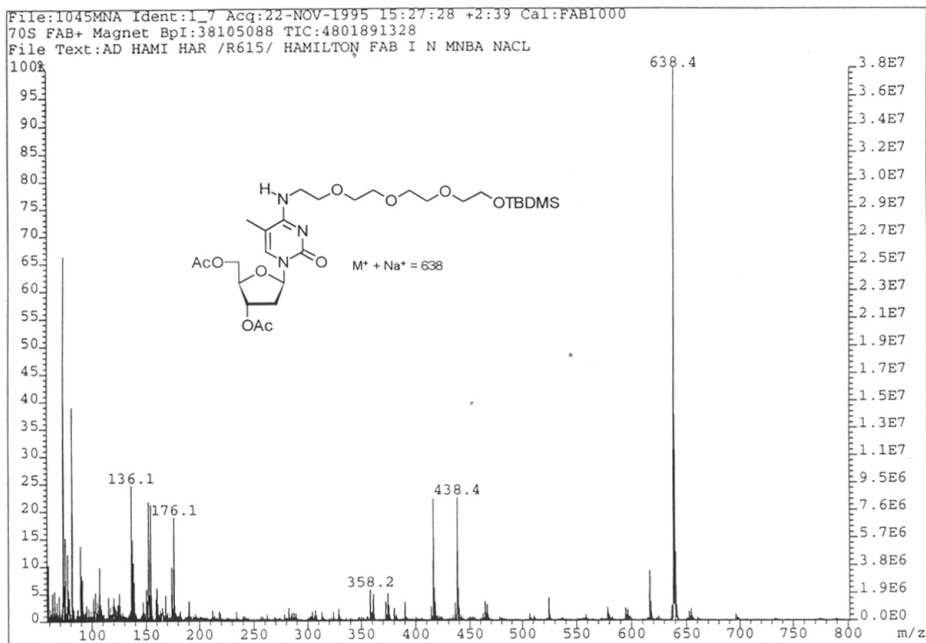
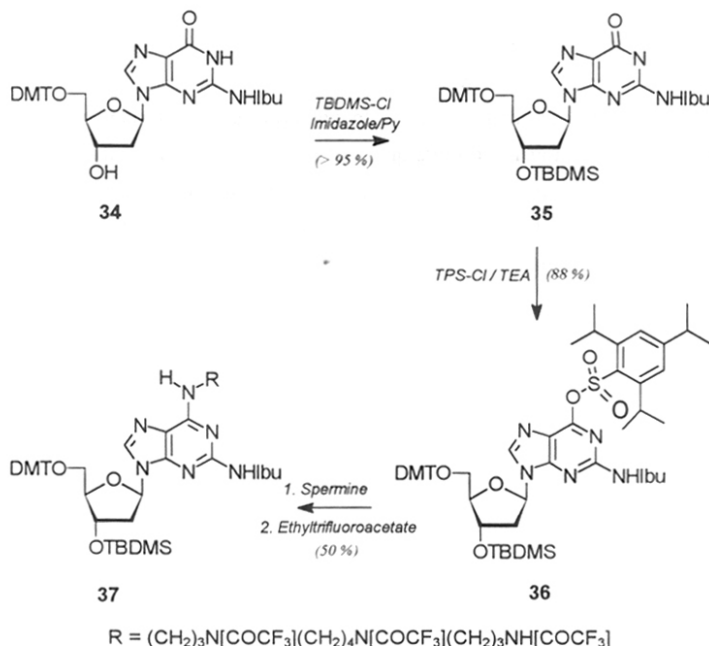


Figure 9. FAB MS of compound 31c in NMBA/NaCl matrix.

2.2.4 Synthesis of 5'-O-(4,4'-dimethoxy)trityl-3'-O-(tert-butyldimethyl)silyl-2-(isobutyroxy)amino-(N⁶-spermino)-2'-deoxy-adenosine

The synthesis of the target compound **37** is accomplished from 5'-DMT-(N²-isobutyryl)-2'-deoxyguanosine (**34**).¹⁷ The convertible nucleoside approach reported by Ferentz and Verdine¹² for C-6 substitution of dI has been modified to achieve spermine conjugation at C-6 of dG with lesser number of synthetic steps (**Scheme 8**). Unlike pyrimidine nucleosides, the C-6 sulfonate ester **36** of dG is stable and enables its isolation²² prior to treatment with spermine.



Scheme 8

The reaction of the compound **34** with 2 equivalents of TBDMSCl (*t*-butyldimethylsilylchloride) and imidazole in dry pyridine gave the 3'-O-TBDMS derivative **35** in quantitative yield.²² This on treatment with TPS-Cl (1.2 eq.) in the presence of TEA and catalytic amount of DMAP led to the formation of C-6 sulfonated derivative **36** in

good yield. The compound **36** on reaction with 5 equivalents of spermine in dry dichloromethane in the presence of TEA followed by protection of side chain amino functions with ethyltrifluoroacetate⁶ yielded the fully protected spermine conjugated derivative **37** of dA. The replacement of the sulfonate function with spermine in purine was complete after 4 h at ambient temperature whereas in the case of pyrimidines the replacement reaction of the corresponding sulfonate **26b** with amines was complete within 1 h under identical conditions. The isobutyryl protection of N² was found to be intact when treated with a large excess of spermine. The structure of **37** was unambiguously established by NMR and Mass spectrometry (see Figure 10a and 10b for ¹H NMR spectra of compounds **36** and **37**).

It is to be pointed out that the traditional isobutyryl group for guanosine is quite difficult to remove from the N²- position of 6-substituted dG.²² The isobutyryl protection of N² was therefore found intact after the treatment of **36** with a large excess of spermine. This may lead to incomplete deprotection of N² of 6-substituted dG when incorporated into oligonucleotides and may be forced to completion by prolonged ammonia treatment. The problem associated with such drastic deprotection procedure is the formation of side products^{23,24} when the C-6 substitution through O-aotm (O⁶-substitution) is not very stable to ammonia treatment and the major side product characterized is 2,6-diaminopurine. However, in the present system, the substitution at C-6 is by a N - atom and the C-N bond is very stable so that after incorporation into ODNs the probability of getting side products can be ruled out under prolonged ammonia treatment.

2.3 pK_a DETERMINATION OF MODIFIED dC ANALOGUES

The pK_a of the ring nitrogen (N3) is an important factor which determines the C*GC triplex stability²⁵ (see *Chapter 1* for details). To understand the effect of substituents at N⁴ of dC on N3 pK_a, the N3 pK_a of all the N⁴-substituted dC analogues prepared was determined by acid - base titration.²⁶ A titration curve (Figure 13) was generated by titration of aqueous solution of the base (1 mg/mL) under study with aqueous NaOH (2 mM) by incremental addition of aliquots of 40 µL at 25 °C under constant stirring. The pK_a of the base was obtained from the titration curve²⁷ and the results are summarised in the Table 1. The pK_a values show that in the case of amine conjugated dC, the N3 pK_a is shifted towards the acidic side as compared to the unmodified base dC having pK_a = 4.3.

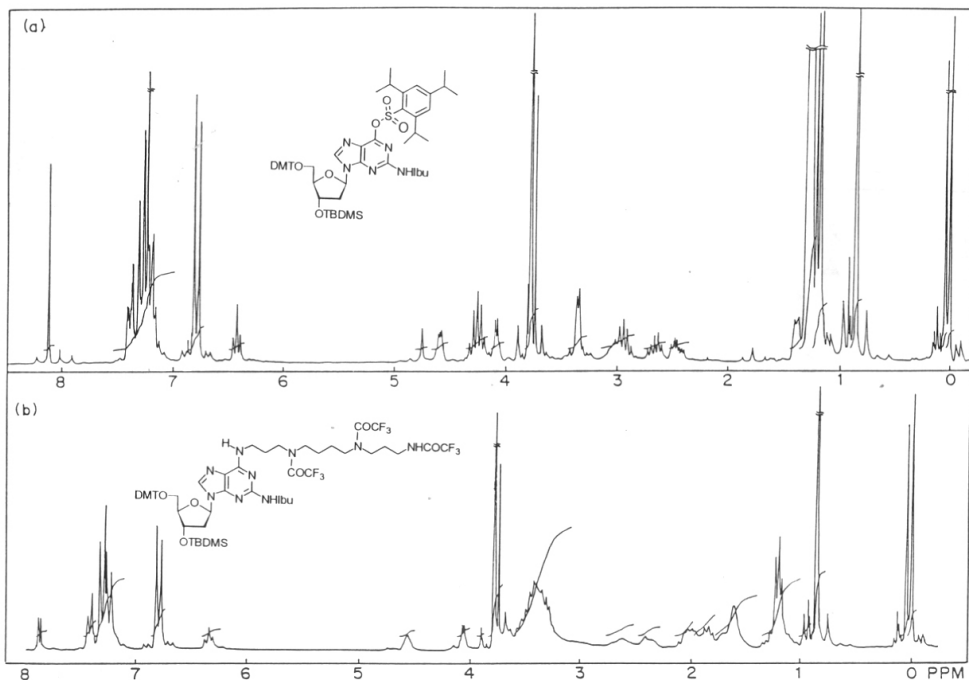


Figure 10. ^1H NMR spectra of compounds 36 and 37 in CDCl_3 .

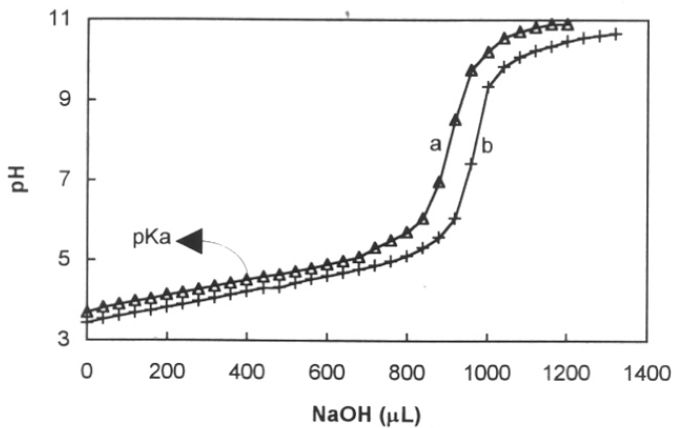


Figure 13. pH titration curve of (a) 5-Me-N⁴-(*n*-propyl)-dC (32a) and (b) dC

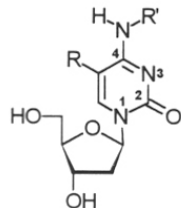


Table 1: pK_a of N⁴ - substituted dC Analogue

	R	R'	pK _a *
1	H	H	4.3
2	Me	H	4.4
3	Me	CH ₂ CH ₂ CH ₃	4.5
4	Me	CH ₂ CH ₂ CH ₂ NH ₂	3.8
5	Me	(CH ₂) ₃ NH(CH ₂) ₄ NH(CH ₂) ₃ NH ₂	3.7
6	Me	(CH ₂) ₂ O(CH ₂) ₂ O(CH ₂) ₂ O(CH ₂) ₂ OH	4.0

* Experimental error limit is ± 0.1

N⁴ substitution with a simple alkyl chain (*e.g.* *n*-propyl *entry 3*) does not seem to affect the pK_a of N3 while the presence of single amino function in the side chain lowers the pK_a by 0.5-0.6 U as seen for 5-Me-dC-N⁴-(*n*-butylamino)nucleoside (*entry 4*). Increasing the number of amino groups on the side chain as in 5-Me-dC-N⁴-(spermine) did not have any further progressive effect on N3 (*entry 5*). In dC nucleosides with N⁴ substituents carrying amino groups, the lower pK_a of N3 may arise due to the prior

existence of a positive charge on the side chain alkyl amino group (having higher pK_a) which may disfavor a second protonation at N3. When the side chain is devoid of amino groups (*entry 6*), but consists of ether/hydroxy functions, the pK_a is in between those of alkyl and alkylamino groups. These data indicate that the N3 pK_a of dC is considerably influenced by the nature of N⁴ substitution.

2.4. CONCLUSIONS

In summary, the syntheses of various N⁴- alkyl/alkylamino/alkoxy substituted analogues of 5-Me-dC were accomplished by following the known 'convertible nucleoside approach'¹¹ or by its modified version. Spermine, the naturally occurring polyamine of considerable biological significance, has been attached to the C-6 of suitably protected dG. pK_a determination of modified dC analogues was carried out in an attempt to understand the effect of substituent at N⁴ of dC on N3 pK_a . The present study shows that N3 pK_a of dC is lowered by the presence of a single amino function at N⁴ side chain though the same does not seem to be appreciably changed with the presence of a simple alkyl chain at N⁴.

2.5. EXPERIMENTAL SECTION

All the melting points are uncorrected and were recorded on electrothermal melting point apparatus. All the chemicals used were of reagent grades. All the solvents used were purified according to the literature procedure.²⁸ TLC was performed on Merck pre-coated 60 F₂₅₄ plates and the spots were rendered visible by UV lights and/or as dark spots after spray with perchloric acid in ethanol (60 %) followed by charring. Loba silica gel (100-200 mesh) was used for column chromatography. Infrared spectra were recorded on a Perkin Elmer 599B instrument. ¹H NMR (200 MHz) and ¹³C NMR (50 MHz) spectra were recorded on a Bruker ACF200 spectrometer fitted with an Aspect 3000 computer. All chemical shifts are referred to internal TMS unless otherwise mentioned and chemical shifts are expressed in d scale (ppm). ³¹P NMR spectra were recorded at 81 MHz with 85 % H₃PO₄ as external reference. Usual work-up implies sequential washing of the organic extract with water, brine, water followed by drying over anhydrous sodium sulfate and evaporation of the solvent under vacuum.

1,11-dichloro-3,6,9-trioxaundecane (14): Tetraethyleneglycol (5.0 g) was dried over toluene by azeotropic distillation and was taken in dry toluene (30 mL). Dry pyridine (5.0 mL, 61.9 mmol) was added into the mixture under reflux followed by drop-wise addition of freshly distilled thionylchloride (6.75 mL, 93.0 mmol). The addition was over in 30 min. and the reflux was continued for 6 h. The reaction mixture was cooled and the precipitated pyridine hydrochloride was filtered off. The filtrate was concentrated under reduced pressure, dissolved in dichloromethane (40 mL), washed with water (30 mL), brine (30 mL) and dried over anhydrous sodium sulfate. The solvent was removed under vacuum on a rotatory evaporator and the residue was purified by passing through a column of basic alumina (activated at 150 °C) and eluting with dichloromethane/methanol (9:1). Concentration of the solvent yielded 3.25 g (54.5 %) of the desired dichloride 14. ¹H NMR δ(CDCl₃): 3.58-3.80 (m, 16H)

1,11-diazido-3,6,9-trioxaundecane (15): Compound 14 (3.21 g, 13.9 mmol) was dissolved in dry DMF (30 mL) containing sodium azide (14.5 g, 230.2 mmol). The reaction mixture was stirred at 120 °C for 4 h, cooled, the residue filtered off under suction and washed with ethylacetate. The combined filtrates was evaporated under vacuum and the residue was repeatedly coevaporated with chloroform to get the diazide 15, 3.32 g (98 %).

IR: 2090 cm⁻¹. ¹H NMR d(CDCl₃): 3.69-3.64(m, 12H) and 3.45-3.42(t, 4H, N₃-CH₂). ¹³C NMR d(CDCl₃): 70.5 & 69.9(O-CH₂)and 50.6(N₃-CH₂).

1,11-diamino-3,6,9-trioxaundecane (16): Compound 15 (3.0 g, 12.3 mmol) was dissolved in absolute methanol (10 mL) containing 10 % Pd-C (0.4 g) and was hydrogenated in a Parr low pressure hydrogenation apparatus at 35 psa for 6 h. The catalyst was filtered off and removal of the solvent gave the diamino compound 16 (2.7 g, 98.0 %).

¹H NMR δ(CDCl₃): 4.05(bs, 4H, 2 x -NH₂, exchangeable with D₂O), 3.65-3.58(m, 12H) and 2.90(t, 4H, N-CH₂). ¹³C NMR δ(CDCl₃): 70.9, 70.0, 69.6 and 40.5(N-CH₂)

1-azido-11-O-tetrahydropyranyl-3,6,9-trioxaundecane (19): To a solution of dry tetraethyleneglycol (5.0 g, 25.8 mmol) in of dry toluene (30 mL) was added dry pyridine (2.5 mL, 31.0 mmol) and the reaction mixture was allowed to reflux. Freshly distilled thionylchloride (2.0 mL, 27.39 mmol) was added drop-wise while maintaining the reaction mixture under reflux. The addition was completed after 30 min. and the reflux was continued for 4 h. The reaction mixture was cooled, the precipitated pyridine hydrochloride was filtered off and washed with toluene. The residue obtained after evaporation of the filtrate was dissolved in dichloromethane (40 mL). 5 mL of DHP (5.0 mL, 4.61 g, 54.9 mmol) was added to the above solution and stirred at ambient temperature for 8 h. (The dissolved pyridineumhydrochloride [from the previous step] was sufficient to catalyse the DHP reaction). The reaction mixture was diluted to 100 mL with dichloromethane and subjected to usual work-up. The residue was dissolved in dichloromethane and then passed through a column of activated basic alumina (activated at 150 °C). The product was eluted from the column using dichloromethane containing 10 % methanol. The solvent was removed under low pressure and the residue was coevaporated with dry dichloromethane. The residue was redissolved in dry DMF (30 mL), to which sodium azide (12.8 g, 8 eq.) was added and the reaction mixture was stirred at 120 °C for 5 h. The reaction mixture was cooled, the solid residue was filtered off and the solvent DMF was removed under vacuum at 40 °C, the residue left was dissolved in ethylacetate (60 mL) and subjected to usual work-up. The product was purified by column chromatography over silica gel (60-120 mesh) as adsorbent and pet-ether/ethylacetate/pyridine: 5.8:4:0.2 as the eluent. The fraction having R_f value 0.5 corresponded to The desired product 19 (4.4 g, 56 %, overall yield, R_f = 0.5) was separated as a pale yellow liquid.

IR: 2120 cm⁻¹. ¹H NMR δ(CDCl₃): 4.20(t, 1H, -O-CH₂-O), 3.90-3.80(m, 2H), 3.80-3.38(m, 16H) and 1.90-1.48(m, 6H, 3 x CH₂ of THP). ¹³C NMR δ(CDCl₃): 98.7(-OCHO- of THP), 70.5, 70.4, 69.7, 66.5 & 61.9(O-CH₂s), 50.5(N3-CH₂) and 30.4, 25.3 & 19.3(CH₂s of THP).

The diazide **15** (0.9 g, $R_f = 0.4$) was also obtained as side product.

1-amino-11-O-tetrahydropyranyl-3,6,9-trioxaundecane (20): Compound **19** (3.07 g, 10.1 mmol) was hydrogenated in presence of 10 % Pd-C (0.3 g) as in the preparation of **15** to get **20** (2.64 g, 94 %) as a colorless liquid.

^1H NMR δ (CDCl₃ + D₂O): 4.20(t, 1H, OCHO of THP), 3.90-3.80(m, 2H), 3.75-3.45(m, 4H), 2.84-2.80(t, 2H, CH₂-NH₂) and 1.90-1.48(m, 6H, 3 x CH₂ of THP).

1-azido-11-O-(t-butyldimethylsilyl)-3,6,9-trioxaundecane (22): The monochlorination of tetraethyleneglycol (5.0 g, 25.8 mmol) was done as described before in the preparation of **19**. The crude monochloro-tetraethyleneglycol derivative was dissolved in dry DMF (20 mL) followed by the addition of sodium azide (10.0 g, 153.9 mmol). The reaction mixture was then stirred at 120 °C for 4 h. The solid residue was filtered off, washed with chloroform and the combined filtrates were evaporated under vacuum at 40 °C. The residue was redissolved in chloroform and passed through a column of activated basic alumina (activated at 150 °C). The eluent was concentrated to a viscous mass of 4.18 g. The residue obtained was redissolved in 20 mL of dry DMF and to this was added TBDMS-Cl (2.86 g, 19.0 mmol) and imidazole (2.6 g, 38.1 mmol). The mixture was allowed to stir at 35 °C for 24 h. DMF was removed under vacuum at 40 °C and the residue was dissolved in ethylacetate (60 mL) and subjected to usual work-up. TLC of the residue showed two spots (eluent ethylacetate/pet-ether, 2:3, R_f values 0.4 and 0.5) The two fraction were separated by column chromatography. The faster moving fraction was separated with 30 % ethylacetate in pet-ether to get **22** (5.0 g, 57.6 %) as a pale yellow liquid.

IR: 2920-2860, 2090 cm⁻¹. ^1H NMR δ (CDCl₃): 3.78-3.73(t, 2H, J = 5.8 Hz), 3.70-3.67(m, 10H), 3.65-3.55(t, 2H), 3.41-3.35(t, 2H, J = 5 Hz, N3-CH₂), 0.89(s, 9H, 3 x Si-C-CH₃) and 0.04(s, 6H, 2 x SiCH₃). ^{13}C NMR δ (CDCl₃): 72.5, 70.6, 69.9, 62.6, 50.5(N3-CH₂), 25.8(Si-C-CH₃), 18.2(Si-CMe₃) and -5.4(Si-CH₃).

The diazide **15** (0.95 g, $R_f = 0.4$) was also obtained as side product.

1-amino-11-O-(t-butyldimethylsilyl)-3,6,9-trioxaundecane (23): Compound **22** (2.0 g, 6.0 mmol) was hydrogenated using 10 % Pd-C (0.3 g) as in the preparation of **15** to get **23** (1.8 g, 98 %), as a colorless liquid.

IR: 3100-3050 cm⁻¹. ^1H NMR δ (CDCl₃): 6.13(bs, 2H, NH₂ exchangeable with D₂O), 3.78-3.73(m, 4H), 3.72-3.68(m, 8H), 3.61-3.58(t, 2H), 3.16-3.14(t, 2H, N-CH₂), 0.90(s, 9H) and 0.04(s, 6H). ^{13}C NMR δ (CDCl₃): 72.6, 70.6, 70.4, 67.3, 62.9, 39.8(H₂N-CH₂), 26.0, 18.4 and -5.2.

3',5'-O-diacetyl-2'-deoxyuridine (25a): A mixture of 2'-deoxyuridine, **24a** (2.0 g, 11.0 mmol) and acetic anhydride was stirred in dry pyridine (40 mL) at 15-20 °C overnight. Pyridine and excess acetic anhydride were removed under vacuum on a rotary evaporator. The residue was taken in chloroform (40 mL) and washed with 5 % aq. bicarbonate solution (30 mL) followed by usual work-up of the reaction mixture affording 3',5'-O-diacetate **25a** (2.6 g, 95 %) as a white solid. R_f ($\text{CH}_2\text{Cl}_2/\text{MeOH}$ 9:1) = 0.5. ^1H NMR δ (CDCl_3): 7.54-7.48(d, 1H, H6), 6.28-6.23(m, 1H, H1'), 5.84-5.78(d, 1H, H5), 5.27-5.21(m, 1H, H3'), 4.38-4.29(m, 3H, H4', H5' & H5''), 2.60-2.51(m, 1H, H2') and 2.23-2.10(m, 7H, H2'' & 2 x COCH_3).

3',5'-O-diacetylthymidine (25b): A mixture of thymidine (**24b**, 2.5g, 10.3 mmol) and acetic anhydride (4 equivalent) in pyridine were stirred at ambient temperature overnight. Usual work-up and purification yielded the 3',5'-O-diacetyl thymidine, **25b** (3.3 g, 97 %) as a white solid. R_f ($\text{CH}_2\text{Cl}_2/\text{MeOH}$ 9:1) = 0.5, mp. = 135 °C. ^1H NMR δ (CDCl_3): 9.5(bs, 1H, N3H), 7.28(s, 1H, H6), 6.33(dd, $J' = 5.4$ & $J'' = 8.1$ Hz, 1H, H1'), 5.30(m, 1H, H3'), 4.35(m, 2H, H4' & H5'), 4.24(m, 1H, H5''), 2.5(m, 1H, H2'), 2.2(m, 1H, H2''), 2.14(s, 6H, 2 x COCH_3), 1.85(s, 3H, 5CH₃).

3',5'-O-diacetyl-C4-(2,6-dimethyl)phenyl-thymidine (27b): Compound **25b** (3.26 g, 10.0 mmol), freshly crystallised TPS-Cl (8.6 g, 28.4 mmol), TEA (4 mL) and DMAP (0.3 g, 2.5 mmol) were taken in dry dichloromethane (80 mL) and the mixture was stirred at ambient temperature for 24 h. As monitored by TLC the formation of the sulfonate intermediate was complete after 24 h. 2,6-Dimethylphenol (4.4 g, 36.0 mmol), TEA (5.2 mL, 37.4 mmol) and a catalytic amount of DABCO (0.12 g, 1.1 mmol) were added into the reaction mixture and stirred for another 24 h. Removal of solvent and excess TEA from the reaction mixture under vacuum followed by usual work-up afforded a residue which was subjected to silica gel column chromatography (eluent: chloroform) to furnish the desired compound **27b** as a white foam, (3.0 g, 69.8 %).

^1H NMR δ (CDCl_3): 7.72(s, 1H, H6), 7.05(s, 3H, ArH), 6.33(dd, 1H, H1'), 5.30(m, 1H, H3'), 4.45-4.30(m, 3H, H4', H5' & H5''), 2.76-2.19(m, 1H, H2'), 2.21-2.07(m, 13H, H2', 2 x COCH_3 & 2 x Ar- CH_3) and 1.70(s, 3H, 5CH₃).

3',5'-O-diacetyl-C4-(2,6-dimethyl)phenyl-2'-deoxyuridine (27a): The same procedure for the synthesis of **27b** was adopted here using **25a** (1.3 g, 4.2 mmol), TPS-Cl (3.12 g, 10.3 mmol), TEA (1.5 g, 14.9 mmol), DMAP (0.1 g), 2,6-dimethylphenol (2.0 g, 16.4 mmol), TEA (2.0 g, 2.75 mL, 19.8 mmol) and DABCO (0.12 g) to obtain **27a** (1.5 g, 86.5 %).

¹H NMR δ(CDCl₃): 7.97-7.93(d, 1H, H6, J = 7.4 Hz), 7.06(s, 3H, ArHs), 6.330-6.24(dd, 1H, H1', J = 5.6, J" = 2.3), 6.17-6.14(d, 1H, H5, J = 7.4 Hz), 5.25-5.21(m, 1H, H3'), 4.39-4.31(m, 3H, H4', H5' & H5"), 2.85-2.73(m, 1H, H2') and 2.23-2.10(m, 13H, H2", 2 x COCH₃ & 2 x Ar-CH₃).

5'-O-DMT-C4-(2,6-dimethyl)phenyl-2'-deoxyuridine (28a): Compound 27a (1.3 g, 3.1 mmol) was stirred in saturated methanolic ammonia for 1 h at ambient temperature to effect hydrolysis of acetyl groups. The reaction was monitored by TLC. After completion of the reaction, methanol and ammonia were completely removed and the residue was coevaporated with dry pyridine. Finally the residue was dissolved in dry pyridine (40 mL) and DMT-Cl (1.2 g, 3.6 mmol) was added to the above solution over a period of 6 h under constant stirring at ambient temperature. The reaction mixture was stripped off the solvent, dissolved in dichloromethane (50 mL) and subjected to usual work-up to get a reddish mass. The compound 28a (1.52 g, 76.7 %) was obtained as a light yellowish foam after silica gel column chromatography (eluent: CH₂Cl₂/EtOAc/TEA 8:1.5:0.5, R_f = 0.4). mp 92-96 °C.

¹H NMR δ(CDCl₃): 8.28-8.24(d, 1H, H6), 7.45-7.20(m, 9H, Ar-H), 7.00(s, 3H, Ar-H), 6.82(d, 4H, Ar-H), 6.27-6.20(m, 1H, H1'), 5.81-5.78(d, 1H, H5), 4.55-4.48(m, 1H, H4'), 4.14-4.08(m, 1H, H3'), 3.82(s, 6H, 2 x OCH₃), 3.56-3.40(m, 2H, H5' & H5"), 2.67-2.56(m, 1H, H2') and 2.33-2.12(m, 7H, H2" & 2 x Ar-CH₃).

5'-O-DMT-C4-(2,6-dimethyl)phenyl-5-methyl-thymidine (28b): The same procedure as above was used to get 28b (1.9 g, 84 %) starting from 27b (1.5 g, 3.49 mmol).

mp 113-123 °C. ¹H NMR δ(CDCl₃): 8.00 (s, 1H, H6), 7.45-7.20(m, 9H, Ar-H), 7.00(s, 3H, Ar-H), 6.82(d, 4H, Ar-H), 6.30(t, 1H, H1'), 4.50(m, 1H, H4'), 4.08(m, 1H, H3'), 3.80(s, 6H, 2 x OCH₃), 3.40(m, 2H, H5' & H5"), 2.60(m, 1H, H2'), 2.20(m, 1H, H2"), 2.10(s, 3H, Ar-CH₃), 2.02(s, 3H, Ar-CH₃) and 1.70(s, 3H, 5CH₃).

5'-O-DMT-5-methyl-N⁴-(trifluoroacetamidospermine)-2'-deoxycytidine (29b):

Compound 28b (0.5 g, 0.8 mmol) was dissolved in dry pyridine (1 mL) and treated with spermine (0.8 g, 4.0 mmol, 5 eq.) at 60 °C for 36 h. The reaction mixture was concentrated to dryness and the residue was dissolved in dichloromethane (40 mL), washed with water (10 mL) and the organic layer was concentrated to a pasty mass. The residue was then coevaporated with ethanol, redissolved in ethanol (30 mL) followed by treatment with ethyltrifluoroacetate (1.5 mL, excess) in the presence of TEA for overnight at ambient temperature. The solvent and excess ethyltrifluoroacetate were removed under vacuum. Usual work-up followed by silica gel column chromatography (eluent: CH₂Cl₂/EtOAc 4:1, R_f = 0.6) afforded 29b (0.52 g, 66 %).

¹H NMR d(CDCl₃): 7.65(s, 1H, H6), 7.50-7.20(m, 9H, Ar-H), 6.85(d, 4H, Ar-H), 6.50(t, 1H, H1'), 4.55(bs, 1H, H4'), 4.10(bs, 1H, H3'), 3.80(s, 6H, 2 x OCH₃), 3.60-3.25(m, 14H, H5', H5" and N-CH₂s), 2.60-2.45(m, 1H, H2'), 2.3-2.15(m, 1H, H2"), 2.10-1.60(m, 8H, alkyl CH₂s of spermine side chain), 1.50(s, 3H, 5-CH₃). ¹³C NMR d(CDCl₃): 163.4(C4), 156.6(C2), 158.2, 157.8 & 157.2 (3 x COCF₃), 136.4(C6), 113.7(CF₃), 102.7(C5), 86.8(C1'), 86.3(C4'), 71.9(C3'), 63.8(C5'), 47.3, 46.5, 46.1, 45.4, 44.5, & 41.8 (spermine N-CH₂s), 37.1(C2'), 28.3, 26.4, 25.9 & 24.0 (spermine CH₂s) and 12.8(5CH₃).

FAB MS: M⁺ = 1017.1 (75 %, M⁺ Calculated for C₄₇H₅₄N₆O₉F₉: 1017.37).

5'-O-DMT-N⁴-(tirfluoroacetamido)spermine-2'-deoxycytidine (29a): The compound 29a (0.48 g, 56.2 %) was prepared from 28a (0.54 g, 0.8 mmol) and spermine (1.0 g, 5.0 mmol, 5 eq.) as above.

¹H NMR d(CDCl₃): 7.65(d, 1H, H6), 7.50-7.20(m, 9H, Ar-H), 6.85(d, 4H, Ar-H), 6.50(t, 1H, H1'), 5.44(d, 1H, H5), 4.55(bs, 1H, H4'), 4.10(bs, 1H, H3'), 3.80(s, 6H, 2 x OCH₃), 3.60-3.25(m, 14H, H5', H5" and N-CH₂s), 2.60-2.45(m, 1H, H2'), 2.30-2.15(m, 1H, H2"), 2.10-1.60(m, 8H, alkyl CH₂s of spermine side chain).

5'-O-DMT-4-N-(11-trifluoroacetamido-3,6-9-trioxaundecyl)-2'-deoxycytidine (29c): Compound 28a (0.23 g, 0.4 mmol) was coevaporated with pyridine and redissolved in dry pyridine (2 mL). To this was added compound 16 (0.6 g, 3.13 mmol, 8.5 eq.) and the reaction mixture was stirred at 65-70 °C for 48 h. The progress of the reaction was monitored by TLC (eluent: dichloromethane/ethylacetate 1:1). Pyridine was removed from the reaction mixture under vacuum and the residue was taken in dry methanol (10 mL). TEA (1 mL) was added to the above solution followed by drop-wise addition of ethyltrifluoroacetate (0.33 mL, 2.77 mmol) at 0 °C under constant stirring. The reaction mixture was slowly allowed to attain room temperature and the stirring was continued for 8 h at ambient temperature. The progress of the reaction was monitored by TLC (eluent: chloroform/methanol 4:1, R_f value, ~0.7). The reaction mixture was evaporated to dryness under vacuum and the residue was directly loaded on a column of silica gel (100-200 mesh). The column was packed in pet-ether-tether containing 1 % TEA. The product 29c (0.25 g, 77.6 %) was eluted out with chloroform/methanol/TEA 9:0.9:0.1 as a light yellow foam.

¹H NMR δ(CDCl₃): 7.80(d, 1H, H6), 7.62(bs, 1H, -NH, exchangeable with D₂O), 7.44-7.30(m, 2H, Ar-H), 7.33-7.21(m, 7H, Ar-H), 6.84-6.80(d, 4H, Ar-H), 6.32-6.30(m, 1H, H1', J = 6.5 Hz), 5.95(bs, 1H, -NH, exchangeable with D₂O), 5.44(d, 1H, H5), 4.52(m, 1H, H4'), 4.10(m, 1H, H3'), 3.79(s, 6H, 2 x -OCH₃), 3.78-3.30(bm, 18H, H5', H5", N-

CH₂s and O-CH₂s), 2.62-2.53(m, 1H, H2') and 2.20-2.12(m, 1H, H2''). ¹³C NMR δ(CDCl₃): 163.9(C4), 158.7(C2), 157.2(COCF₃), 144.7, 135.8(C6), 130.2, 128.3, 128.0, 127.0, 113.3, 95.2(C5), 86.7(CF₃), 86.1(C1'), 85.9(C4'), 71.2(C3'), 70.5, 70.3, 69.5 & 68.8(-OCH₂s), 63.3(C5'), 55.3(-OCH₃), 42.0(N-CH₂), 40.5(N-CH₂) and 39.8(C2').

FAB MS: 800 (M⁺, 70 %), 497 (M⁺ - DMT, 61 %). FAB mass on NMBA/MeOH matrix for C₄₀H₄₇N₄O₁₀F₃ 800.9 (M⁺), calculated 800.32 (M⁺) and on NMBA/MeOH/NaCl matrix, 822.9 (M⁺ + Na⁺), calculated 823.32 (M⁺ + Na⁺).

5'-O-DMT-4-N-(11-trifluoroacetamido-3,6-9-trioxaundecyl)-5-methyl-2'-deoxycytidine (29d): Compound **28b** (.45 g, 0.7 mmol) and **16** compound (1.0 g, 5.2 mmol, 7.5 eq.) were stirred at 70 °C in pyridine (2 mL) for 48 h. Trifluoroacetylation and purification of the compound **29d** (0.4 g, 70.7 %) was followed as in the preparation of **29c**.

¹H NMR δ(CDCl₃): 7.68(s, 1H, H6), 7.60(bs, 1H, NH, exchangeable with D₂O), 7.44-7.39(m, 2H, Ar-H), 7.33-7.21(m, 7H, Ar-H), 6.84-6.80(d, 4H, Ar-H), 6.48-6.42(t, 1H, H1', J = 6.5 Hz), 5.50(bs, 1H, NH, exchangeable with D₂O), 4.56(m, 1H, H4'), 4.10(m, 1H, H3'), 3.79(s, 6H, 2 x OCH₃), 3.75-3.31(m, 18H, H5', H5'', NCH₂s & OCH₂s), 2.64-2.53(m, 1H, H2'), 2.26-2.20(m, 1H, H2'') and 1.48(s, 3H, 5CH₃). ¹³C NMR δ(CDCl₃): 163.7(C4), 158.7(C2), 156.6(COCF₃), 144.7, 137.4(C6), 135.8, 130.2, 128.3, 128.0, 127.0, 113.3, 102.4(C5), 86.7, 86.1(C1'), 85.9(C4'), 72.0(C3'), 70.5, 70.3, 70.1, 69.5, 68.8(-OCH₂s), 63.8(C5'), 55.3(-OCH₃), 42.0(-NCH₂), 40.7(-NCH₂), 39.7(C2') and 12.4(5CH₃).

FAB MS: 815 (M⁺ + 1, 11 %), 512 ([M⁺ + 1] - DMT, 17 %), 392 (100 %). FAB mass on NMBA/MeOH matrix for C₄₁H₅₀N₄O₁₀F₃, 815.3 (M⁺ + 1), calculated 815.34 (M⁺ + 1) and on NMBA/MeOH/ NaCl matrix, 837.3 (M⁺ + Na⁺), calculated 837.34 (M⁺ + Na⁺).

3'-O-(2-cyanoethyl-N,N-diisopropylphosphoramido)-5'-O-(4',4'-dimethoxytrityl)-5-methyl-4-N-(N',N'',N'''-trifluoroacetamidospermine)-2'-deoxycytidine (30b):

Compound **29b** (0.3 g, 0.3 mmol) was dissolved in dry ethylenedichloride (5 mL) followed by the addition of tetrazole (21mg, 0.3 mmol) and 2-cyanoethyl-N,N,N',N'-tetraisopropylphosphorodiamidite (0.107 g, 0.4 mmol, 1.2 eq.) and the reaction mixture was stirred at ambient temperature for 3 h. It was then diluted with dichloromethane and washed with 10 % aq. sodium bicarbonate solution. The organic phase was dried over anhydrous sodium sulfate and concentrated to a foam. The residue was dissolved in minimum amount of dichloromethane and passed through a column of dry silica gel packed in dry dichloromethane. The product was eluted out using a mixture of ethylacetate/dichloromethane/TEA (1:1:0.01, R_f = 0.4, two close moving spots due to diastereomers) to get the amidite **28b** (0.35 g, 97 %) as a white foam.

³¹P NMR d(CDCl₃): 149.73, 149.33.

3'-O-(2-cyanoethyl-N,N-diisopropylphosphoramido)-5'-O-(4',4'-dimethoxytrityl)-5-methyl-4-N-(11-trifluoroacetamido-3,6,9-trioxaundecyl)-2'-deoxycytidine (30d): The phosphoramidite 30d (0.18 g, 85 %) was prepared from 29b (0.17 g, 0.2 mmol) as described above.

³¹P NMR d(CDCl₃): 149.80, 149.28.

3',5'-O-diacetyl-4-N-(n-propyl)-5-methyl-2'-deoxycytidine (31a): Compound 25b (0.3 g, 0.9 mmol), freshly crystallised TPS-Cl (0.4 g, 1.3 mmol, 1.4 eq.), TEA (0.16 g, 1.5 mmol) and DMAP (30 mg) were dissolved dry dichloromethane (8 mL) and stirred at ambient temperature. The formation of the intermediate 26b was complete after 36h. n-propylamine (1.0 mL, 12.2 mmol) was added into the above solution and the reaction mixture was stirred at ambient temperature for 10 min. The reaction mixture was evaporated to dryness under vacuum and the residue was taken in dichloromethane (15 mL) and subjected to usual work-up. The product 25b (0.2 g, 59 %) was purified by silica gel column chromatography (eluent: EtOAc/MeOH/ 9.9:0.1) to a white solid. A portion of this was crystallised from ethylacetate/pet-ether (40-60 °C) to get colorless needles of 31a. mp. 164 °C.

¹H NMR δ(CDCl₃): 7.28(s, 1H, H6), 6.45-6.38(m, 1H, H1', J = 5.5 Hz), 5.16-5.21(m, 1H, H3'), 4.35-4.34(d, 2H, H4' & H5', J = 3.9 Hz), 4.26-4.21(m, 1H, H5''), 3.56-3.46(m, 2H, -NCH₂), 2.67-2.56(m, 1H, H2'), 2.10(s, 6H, 2 x -COCH₃), 2.09-1.94(m, 1H, H2''), 1.92(s, 3H, C5-CH₃), 1.73-1.54(m, 2H, -N-C-CH₂) and 0.99-0.92(t, 3H, J = 7.4). ¹³C NMR δ(CDCl₃): 170.4 & 170.2(COCH₃), 163.1(C4), 156.1(C2), 135.6(C6), 102.5(C5), 85.7(C1'), 81.8(C3'), 74.4(C4'), 63.9(C5'), 42.7(-NCH₂), 38.1(C2'), 22.3(N-C-CH₂), 20.8 & 20.7(CO-CH₃), 13.3(C5-CH₃) and 11.3(N-C-C-CH₃).

FAB MS: 367 (M⁺, 16 %), 167 ([M⁺ + 1] - sugar, 51 %), 125 (5-Me-cytosine, 100 %).

3',5'-O-diacetyl-4-N-(11-O-[t-butyldimethylsilyl]-3,6,9-trioxaundecyl)-5-methyl-2'-deoxycytidine (31c): Compound 25b (0.5 g, 1.5 mmol), freshly crystallised TPS-Cl (0.8 g, 2.6 mmol), TEA (0.31 g, 3.0 mmol), DMAP (50 mg) and compound 23 (0.8 g, 2.6 mmol) were used to get 31c by following the procedure described for the synthesis of 31a. The product 31c (0.6 g, 63.6 %) was purified by silica gel (100-200 mesh) column chromatography (eluent: 6 % MeOH in ethylacetate) as a pasty mass.

¹H NMR δ(CDCl₃ + D₂O): 7.24(s, 1H, H6), 6.44-6.37(q, 1H, H1', J' = 5.5 & J'' = 3 Hz), 5.20-5.16(m, 1H, H3'), 4.36-4.34(d, 2H, H4' & H5', J = 3.9 Hz), 4.26-4.23(m, 1H, H5''), 3.79-3.52(m, 16H, N-CH₂ & O-CH₂s), 2.63-2.54(m, 1H, H2'), 2.10 & 2.09(s, 6H, 2 x CO-CH₃), 2.05-1.97(m, 1H, H2''), 1.93(s, 3H, C5-CH₃), 1.90(s, 9H, 3 x Si-C-CH₃) and

0.06(s, 6H, 2 x Si-CH₃). ¹³C NMR δ(CDCl₃): 169.7 & 169.6(2 x COCH₃), 162.7(C4), 155.5(C2), 135.5(C6), 102.2(C5), 85.3(C1'), 81.5(C3'), 74.0(C4'), 72.1, 70.1, 70.0, 69.6, 68.7 & 63.4(O-CH₂s), 62.2(C5'), 40.1(N-CH₂), 37.6(C2'), 25.4(2 x CO-CH₃), 20.3 & 20.2(Si-C-[CH₃]₃), 17.8(Si-C-Me₃), 12.6(C5-CH₃) and -5.6(Si-CH₃).

FAB MS: 616(M⁺ + 1, 21 %), 416([M⁺ + 1] - sugar, 38 %), 73(100 %). FAB mass on NMBA matrix for C₂₈H₄₉N₃O₁₀Si, 616.5 (M⁺ + 1), calculated: 616.42 (M⁺ + 1) and on NMBA/NaCl: 638.4 (M⁺ + Na⁺) and calculated 638.40 (M⁺ + Na⁺).

3',5'-O-diacetyl-4-N-(n-dodecyl)-5-methyl-2'-deoxycytidine (31b): Compound **25b** (0.5 g, 1.5 mmol), freshly crystallised TPS-Cl (0.95 g, 3.1 mmol), TEA (1 mL), DMAP (50 mg) and n-dodecylamine (0.6 g, 3.3 mmol) were used to get **31b** (0.6 g, 79 %) by employing procedure and worked-up as reported for **31a**. The product **31b** was purified by silica gel column chromatography (eluent: ethylacetate/pet-ether (60-80 °C) as a form. ¹H NMR δ(CDCl₃ + D₂O): 7.23(s, 1H, H6), 6.40-6.34(m, 1H, H1', J = 5.6 & J" = 2.7 Hz), 5.16-5.13(bd, 1H, H3', J = 6.3 Hz), 4.32-4.30(m, 2H, H4' & H5'), 4.21-4.19(m, 1H, H5"), 3.51-3.43(t, 2H, NCH₂, J = 7 Hz), 2.58-2.50(m, 1H, H2'), 2.06(s, 6H, 2 x COCH₃), 2.02-1.95(m, 1H, H2"), 1.89(s, 3H, C5-CH₃), 1.59-1.52(bm, 2H, CH₂ of alkyl), 1.21(bs, 18H, CH₂ of alkyl) and 0.86-0.80(t, 3H, alkyl-CH₃). ¹³C NMR δ(CDCl₃): 170.5 & 170.3(2 x COCH₃), 163.1(C4), 156.1(C2), 135.9(C6), 102.2(C5), 85.9(C1'), 82.0(C3'), 74.5(C4'), 64.0(C5'), 41.3(N-CH₂), 38.3(C2'), 32.0, 29.7, 29.4, 27.0 & 22.7(-CH₂s), 21.0 & 20.9(2 x CO-CH₃), 14.1(C5-CH₃) and 13.3(CH₃ of alkyl).

FAB MS: 493(M⁺, 37 %), 294([M⁺ + 1] - sugar, 59 %), 81(100 %).

4-N-(n-propyl)-5-methyl-2'-deoxycytidine (32a): Compound **31a** (0.14 g, 0.4 mmol) was stirred with methanolic ammonia at ambient temperature for 2 h. The reaction mixture was evaporated to dryness and the residue was directly loaded on a column of silica gel and the product **32a** (0.1 g, 93.6 %).was eluted out using dichloromethane and methanol in 2:1 ratio.

¹H NMR δ(D₂O): 7.48(s, 1H, H6), 6.29-6.21(t, 1H, H1', J = 7.5 Hz), 4.47-4.39(m, 1H, H4'), 4.04-3.98(m, 1H, H3'), 3.84-3.37(m, 2H, H5' & H5"), 3.37-3.30(t, 2H, -NH₂), 2.43-2.16(m, 2H, H2' & H2"), 1.89(s, 3H, C5-CH₃), 1.62-1.51(q, 2H, N-C-CH₂) and 0.93-0.85(t, 3H CH₃). ¹³C NMR δ(D₂O): 164.0(C4), 158.0(C2), 137.3(C6), 105.7(C5), 87.2(C1'), 86.4(C4'), 71.4(C3'), 62.1(C5'), 47.4(N-CH₂), 40.0(C2'), 22.4(N-C-CH₂), 13.1(C5-CH₂) and 10.9(N-C-C-CH₂).

HRMS: 284 (M⁺ + 1, 25 %), 168 ([M⁺ + 1] - sugar, 100 %). Analysis: calculated for C₁₃H₂₂N₃O₄, 284.16 and found 284.16.

4-N-(11-O-[*t*-butyldimethylsilyl]-3,6,9-trioxaundecyl)-5-methyl-2'-deoxycytidine (32c): Procedure and worked-up as above. Compound **32c** (0.18 g, 74 %) was obtained from **31c** (0.3 g) by following the procedure for the preparation of **32a**.

¹H NMR δ(CDCl₃): 7.55(s, 1H, H6), 6.14-6.12(bm, 1H, H1'), 5.85(bs, 1H, NH, exchangeable with D₂O), 4.51-4.48(bm, 1H, H4'), 4.00-3.95(bm, 1H, H3'), 3.80-3.50(m, 18H, H5', H5", NCH₂ & -OCH₂s), 2.38-2.18(bm, 2H, H2' & H2"), 1.92(s, 3H, C5-CH₃), 0.90(s, 9H, 3 x Si-C-CH₃) and 0.09(6H, Si-CH₃).

5-methyl-2'-deoxycytidine-N⁴-(spermine) (33): Compound **29b** (0.2 g) was suspended in saturated methanolic ammonia (2 mL) in a sealed vial and kept at 50 °C overnight. The reaction mixture was cooled, ammonia and methanol were removed under vacuum. The residue was treated with methanolic HCl (2 mL) for 5 min. Methanol and HCl were removed under vacuum and the residue was taken in water (2 mL). The aqueous layer, after repeated washing with benzene (4 x 5 mL) to remove 4,4'-dimethoxy-tritanol, was co-evaporated several times with ethanol to yield the hydrochloride salt of **33** (65 mg, 91.8 %) as a white hygroscopic solid.

¹H NMR δ(D₂O): 7.73(s, 1H, H6), 6.29-6.22(t, 1H, H1', J = 6.5 Hz), 4.48-4.41(m, 1H, H4'), 4.05-4.01(m, 1H, H3'), 3.89-3.69(m, 2H, H5' & H5"), 3.64-3.57(t, 2H, N-CH₂), 3.23-3.10(bm, 10H, 5 x NH₂), 2.41-2.32(m, 2H, H2' & H2"), 2.16-1.99(m, 7H, C5-CH₃ & 2 x CH₂ of spermine chain) and 1.80-1.76(bm, 4H, 2 x CH₂ of spermine chain). ¹³C NMR δ(D₂O): 160.8(C4), 152.7(C2), 139.7(C5), 106.5(C6), 87.6(C1'), 86.8(C4'), 71.1(C3'), 61.9(C5'), 47.8, 47.5, 45.3, 39.7 & 39.4(NCH₂s), 37.4(C2'), 25.7, 24.5 & 23.5(CH₂ of spermine chain) and 13.0(C5-CH₃).

HRMS: 427(M⁺ + 2, 68 %), 154(100 %). Analysis: calculated for C₂₀H₃₈N₆O₄, 427.30; found 427.30.

5'-O-DMT-3'-O-(*tert*-butyldimethylsilyl)-N²-isobutyryloxy-2'-deoxyguanosine (35): 5'-O-DMT-N²-isobutyryoxy-2'-deoxy-guanosine (1.2 g, 1.7 mmol) and imidazole (0.4 g, 5.9 mmol) were dried and dissolved in anhydrous pyridine (15 mL). TBDMS-Cl (0.5 g, 3.3 mmol) was added into the above solution and stirred for 10 h at room temperature. The progress of the reaction was monitored by TLC (eluent dichloromethane/ethylacetate 5:1 v/v). After removal of pyridine under vacuum the residue was taken in dichloromethane (40 mL) and subjected to usual work-up. The compound **35** (1.28 g, 98 %) was obtained in pure form by column chromatography of the residue using silica gel as adsorbent and dichloromethane/ethylacetate/TEA, 4:1:0.05 (R_f = 0.5) as eluent. mp 78-84 °C (dec)

¹H NMR δ(CDCl₃): 7.82(s, H8), 7.50-7.20(m, 9H Ar-H), 6.83-6.78(m, 4H ArH), 6.23-6.16(q, 1H, H1', J = 5.55 & J" = 2.36 Hz), 4.57-4.55(m, 1H, H3'), 4.05-4.02(m, 1H, H4'),

3.79(s, 6H, 2 x OCH₃ of DMT), 3.40-3.34(m, 1H, H5'), 3.20-3.12(m, 1H, H5''), 2.75-2.63(m, 1H, CH of N²-isobutyryl), 2.36-2.30(m, 1H, H2'), 2.16-2.09(m, 1H, H2''), 1.09-0.90(m, 6H), 0.85(s, 9H 3 x Si-CCH₃), 0.00(s, 3H Si-CH₃) and -0.01(s, 3H Si-CH₃). ¹³C NMR δ(CDCl₃): 179.6, 171.2, 158.6, 156.2, 148.5, 148.1, 144.6, 137.1, 135.7, 130.0, 128.1, 127.8, 126.9, 121.3, 113.2, 86.7(C1'), 86.4, 84.1(C4'), 72.1(C3'), 63.3(C5'), 60.4, 55.6, 46.0, 41.1(C2'), 35.9, 25.7, 21.0, 18.9, 18.8, 17.8, 14.2, 10.7, -4.8 and -4.9.

O⁶-(2,4,6-triisopropylbenzenesulfonyl)-5'-O-Dimethoxytrityl-3'-O-(tert-butyldimethylsilyl)-N²-isobutyryloxy-2'-deoxyguanosine (36): Compound 35 (1.2 g, 1.6 mmol) after drying was dissolved in dry dichloromethane (30 mL) followed by the addition of TEA (0.6 mL, 4.3 mmol) and DMAP (20 mg) constant stirring at ice bath temperature. Freshly recrystallised TPS-Cl (0.6 g, 2.0 mmol, 1.25 eq.) was added to the above solution and the stirring was continued for 8 h at temperature below 10 °C. The reaction mixture was diluted to 50 mL, washed with 5 % aq. solution of sodiumbicarbonate (30 mL) followed by usual work-up. The residue was purified on a column of silica gel using dichloromethane/TEA 99:1 as eluent to get the desired sulfonate 36 (1.44 g, 88 %) as a white foam. mp 85-95 °C (dec)

¹H NMR δ(CDCl₃): 8.13(s, 1H, H8), 7.41-7.16(m, 11H, Ar-H), 6.82-6.77(d, 4H, Ar-H), 6.46-6.40(t, 1H, H1', J = 6.5 Hz), 4.61-4.58(m, 1H, H3'), 4.30-4.21(m, 2H, 2 x o -CH₂ Me₂ of SO₂Ar), 4.10-4.08(m, 1H, H4'), 3.78(s, 6H, 2 x OCH₃ of DMT), 3.37-3.34(d, 2H, H5' & H5''), 3.01-2.90(m, 2H, CH of N²-isobutyryl & p -CH of SO₂Ar), 2.68-2.60(m, 1H, H2'), 2.50-2.40(m, 1H, H2''), 1.40-1.14(m, 24H), 0.87(s, 9H 3 x Si-CCH₃), 0.03(s, 3H Si-CH₃) and 0.01(s, 3H Si-CH₃).

5'-O-(4,4'-dimethoxy)trityl-3'-O-(tert-butyldimethylsilyl)-2-(isobutyroxy)amino-(N⁶-[trifluoroacetamido]spermino)-2'-deoxy-adenosine (37): The sulfonate derivative 36 (1.0 g, 1.0 mmol) was dissolved in dry dichloromethane (15 mL). TEA (2.5 mL) and spermine (1.0 g, 4.9 mmol, 5 eq.) were added to the above solution under constant stirring at ambient temperature for 4 h. The progress of the reaction was monitored by TLC (eluent dichloromethane/TEA 9.9 : 0.1). The reaction mixture was then concentrated to a pasty mass and redissolved in dichloromethane (60 mL). The dichloromethane solution was washed with water (20 mL) to remove unreacted spermine and dried over anhydrous sodium sulfate. The residue was dried by coevaporation with dry ethanol, redissolved in dry ethanol (20 mL), treated with ethyltrifluoroacetate (2 mL) containing TEA (1.0 mL, TEA was added to neutralize trifluoroacetic acid which is normally present in ethyltrifluoroacetate). The reaction mixture was stirred over night at room temperature. The progress of the reaction was monitored by TLC and ninhydrin spray. The residue

obtained after removal of methanol and excess ethyltrifluoroacetate at room temperature in vacuum was taken in dichloromethane (50 mL) and subjected to usual work-up. Silica gel column chromatography, using dichloromethane/ethylacetate/TEA (7:3:0.1, $R_f = 0.6$) as eluent, of the residue yielded the desired compound 37 (0.58 g, 49.5 %) as a pale yellow foam. mp 130-140 °C (dec).

¹H NMR δ(CDCl₃): 7.90-7.87(d, 1H, H8), 7.44-7.17(m, 9H Ar-H), 6.83-6.78(d, 4H Ar-H), 6.36-6.32(t, 1H, H1'), 4.57-4.55(m, 1H, H3'), 4.05-4.04(m, 1H, H4'), 3.77(s, 6H, 2 x OCH₃ of DMT), 3.70-2.90(bm, 15H, H5', H5'', 6 x NCH₂ & CH of N²-isobutyryl), 2.68-2.58(m, 1H, H2'), 2.44-2.40(m, 1H, H2''), 2.06-1.58(bm, 8H of spermine side chain), 1.24-1.14(bm, 6H of isobutyryl), 0.86(s, 9H 3 x Si-CCH₃), 0.05(s, 3H Si-CH₃) and 0.00(s, 3H Si-CH₃). ¹³C NMR δ(CDCl₃): 158.5, 155.0, 152.7, 144.5, 137.5, 135.6, 130.0, 128.1, 127.8, 126.8, 113.1, 86.7, 86.4, 72.6, 63.3, 55.1, 47.1, 45.8, 43.9, 40.9, 37.0, 36.6, 26.4, 25.7, 23.9, 19.2, 17.9, 8.6 and -4.8.

Determination of N3 pK_a of modified dC nucleosides: The N3 pK_a of dC, 32a, 32c, 33 and 5-methyl-C-4-N-(4-aminobutyl)-2'-deoxycytidine were determined by titration of their individual aqueous solution (1 mg/mL) with aqueous NaOH (2 mM) by incremental addition of aliquots of 40 μL, at 25 °C under constant stirring.^{26,27} After each addition the solution was allowed to equilibrate for 5 min followed by pH measurements using standard pH electrode. pK_a were determined from the plot of volume of NaOH used against corresponding pH of the solution.

2.6. REFERENCES:

1. Tung, C.; Breslauer, K.; Stein, S. *Nucleic Acids Res.*, **1993**, *21*, 5489.
2. Prakash, T. P.; Barawkar, D. A.; Kumar, V. A.; Ganesh, K. N. *Bioorg. Med. Chem. Lett.*, **1994**, *4*, 1733.
3. Schmid, N.; Behr, J. P. *Tetrahedron Lett.*, **1995**, *36*, 1447.
4. Bigey, P.; Pratveil, G.; Meunier, B. *J. Chem. Soc., Chem. Comm.*, **1995**, 181.
5. Sund, C.; Puri, N.; Chattopadhyaya, J. *Tetrahedron*, **1996**, *52*, 12275.
6. Barawkar, D. A.; Kumar, V. A.; Ganesh, K. N. *Biochem. Biophys. Res. Comm.* **1994**, *205*, 1665.
7. Nara, H.; One, A.; Matsuda, A.; *Bioconj. Chem.*, **1995**, *6*, 45.
8. Hanvey, J.; Williams, E.; Besterman, J. *Antisense Res. Development* **1991**, *1*, 307.
9. Thomas, T.; Thomas, T. *Biochemistry*, **1993**, *32*, 14068.
10. Tabor, C. W.; Tabor, H. *Annu. Rev. Biochem.* **1984**, *53*, 749.
11. MacMillan, A. M.; Verdine, G. L. *J. Org. Chem.* **1990**, *55*, 5931.
12. Ferentz, A. E.; Verdine, G. L. *Nucleosides, Nucleotides*, **1992**, *11*, 1703.
13. Zalipsky, S.; Gilon, C.; Zilkha, A. *Eur. polym. J.*, **1983**, *19*, 1177.
14. Miyashita, M.; Yoshikoshi, A.; Grieco, P. A. *J. Org. Chem.*, **1977**, *42*, 3772.
15. Corey, E. J.; Venkateswarlu, A. *J. Am. Chem. Soc.*, **1972**, *94*, 6190.
16. Zhou X. -X.; Chattopadhyaya, J. *Tetrahedron*, **1986**, *42*, 5149.
17. Jones, R. A. in *Oligonucleotide Synthesis a Practical Approach*, **1985**, p 23, Gaite, m. J. (ed.) IRL Press, Oxford, W. DC.
18. Markiewicz, W. T.; Groger, G.; Rosch, R.; Zebrowska, A.; Seliger, H. *Nucleosides, Nucleotides*, **1992**, *11*, 1703.
19. Sinha, N. D.; Biernat, J.; McManus, J.; Koster, H. *Nucleic Acids Res.* **1984**, *12*, 4539.
20. Imazava, M.; Eckstein, F. *J. Org. Chem.*, **1979**, *44*, 2039.
21. Choy, Y. M.; Unrau, A. M. *Carbohydr. res.*, **1971**, *17*, 349.
22. Raynaud, F.; Asseline, U.; Roig, V.; Thuong, N. T. *Tetrahedron*, **1996**, *52*, 2047.
23. Borowy-Borowski, H.; Chambers, R. *Biochemistry*, **1987**, *26*, 2465.
24. Gaffney, B. L.; Jones, R. A. *Biochemistry*, **1989**, *28*, 5881.
25. (a) Francois, J. C.; Saison-Behmoras, T.; Thuong, N. T.; Helene, C. *Biochemistry*, **1989**, *28*, 9617.
 (b) Rajagopal, P.; Feigon, J. *Biochemistry*, **1989**, *28*, 7859. (c) Singleton, S. F.; Dervan, P. B. *Biochemistry*, **1992**, *31*, 10995. (d) Thibaudeau, C.; Plavec, J.; Chattopadhyaya, J. *J. Org. Chem.*, **1996**, *61*, 266.
26. Froehler, B. C.; Ricca, D. *J. Am. Chem. Soc.*, **1992**, *114*, 8320.
27. Segal, I. H. in *Biochemical Calculations*, **1975**, 2nd edition., Wiley & Sons Inc.
28. Perrin, D. D.; Armarego, W. L. F.; *Purification of Laboratory Chemicals*. **1988** 2nd edition, Pergamon Press.

CHAPTER 3.

**BIOPHYSICAL STUDIES ON THE MOLECULAR ORIGIN OF
TRIPLEX STABILIZATION BY dC-N⁴-(SUBSTITUTED)
OLIGONUCLEOTIDES FORMING TRIPLEXES**

3.1. INTRODUCTION

Earlier studies on spermine conjugated oligodeoxynucleotides (sp-ODNs) revealed that spermine appended through C4 of pyrimidine [5-Me-dC-N⁴-(spermine)] destabilizes corresponding duplexes.¹ Most interestingly, these oligodeoxynucleotides (ODNs) were found to be better candidates for stabilizing **C⁺*GC** triplets at physiological conditions when they are employed as the third strand of the triplet. In contrast to the lower stability of the natural **C⁺*GC** triplets at neutral pH, sp-ODN triplets are stabilized at neutral pH and the stability decreases with lowering of pH. However, the contribution of appended spermine for stabilizing triplet at neutral pH and its effect on the N3 pK_a of the modified base in single strand ODN, duplexes and triplets remains to be established. The objective of the chapter are (i) to examine the effect of N⁴-substitution on N3 pK_a of dC in ODNs, (ii) the contribution of appended spermine to triplet stability, (iii) the role of appended spermine on the association and dissociation of triplets at neutral pH (hysteresis and salt effect on hysteresis) and (v) the molecular origin of triplet stabilization by sp-ODNs.

3.2. RESULTS

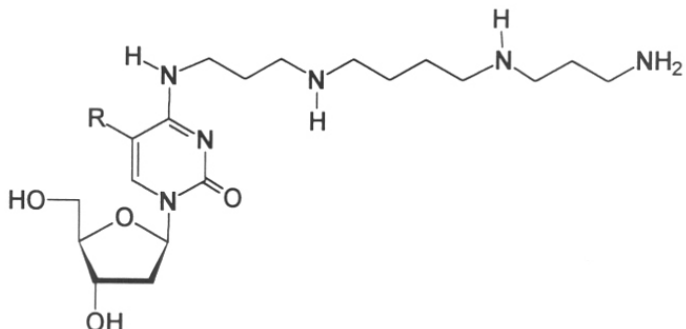
3.2.1 Synthesis and characterization of spermine-oligonucleotide (sp-ODN) conjugates

The phosphoramidite of 5-Me-dC-N⁴-(spermine) was synthesized as described earlier (see *Chapter 2, section 2.2.3*) and incorporated at desired sites of various oligodeoxynucleotides, (ODNs, 5-9) on an automated DNA synthesizer. The synthesis of unmodified ODNs 1-4 and 10 (see *section 3.7* for detail) were done by standard procedure.¹ The coupling efficiency of modified amidites were similar to that of the commercially available unmodified amidites. After completion of the oligonucleotide syntheses, final on-column detritylation was followed by aqueous ammonia treatment to yield the fully deprotected oligonucleotides 1-10. These were purified on FPLC using reverse phase column (RP 18) and the purity was rechecked by HPLC as described in *section 3.7*. Figure 1 shows HPLC chromatogram of some of the modified and

unmodified ODNs with corresponding retention times for comparison. Generally, the spermine conjugated ODNs eluted later compared to the corresponding unmodified one perhaps due to the net reduction of negative charge by the conjugated spermine which may make it more hydrophobic.

1	C G G T T C T T T T T C T T T T T C T G C G - d
2	d - G C C A A G A A A A A A G A A A A A A G A C G C
3	d - T T C T T T T T C T T T T T C T
4	d - <u>C</u> <u>C</u> <u>C</u>
5	d - X C C
6	d - C C X
7	d - C X C
8	d - X C X
9	d - X X X
10	A A G A A A A A A G A A A A A A G A - d

d - represents 5' terminus. C is 5-Me-dC



X = 5-Me-dC-N⁴-(spermine)

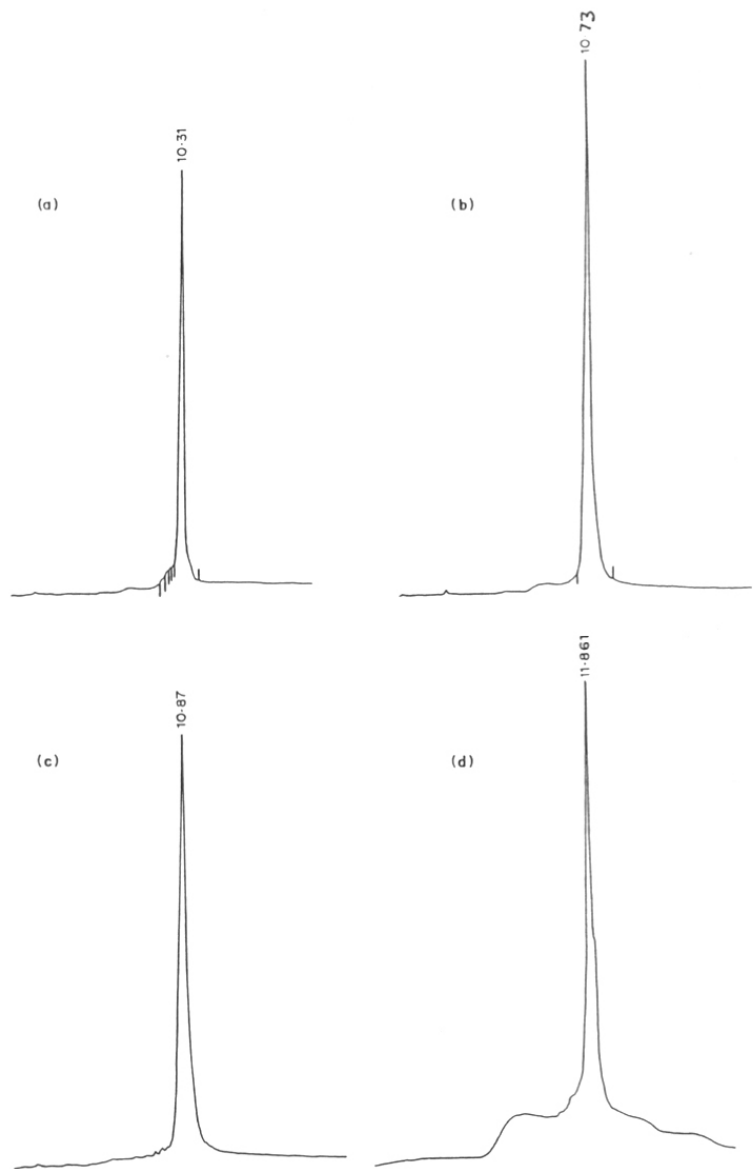


Figure 1. HPLC chromatogram of ODNs (a) 3, (b) 5, (c) 6 and (d) 12.

3.2.2. Triplex formation by *sp*-ODN

The triplexes bearing spermine on the third strand were generated by hybridization of unmodified ODNs **3-4** or *sp*-ODNs **5-9** with the duplex **1:2** constituted from unmodified 24-mer oligonucleotides containing polypurine and polypyrimidine stretches. The 5' and 3' ends in duplex **1:2** were designed to avoid concatenation and to resolve triplex-duplex transition from that of duplex-single strand. The thermal denaturation profiles of hybrids constituted from *sp*-ODNs with the control duplex **1:2** in Tris buffer (pH 7.3) containing NaCl (100 mM), showed a biphasic dissociation (Figure 2) characteristic of triplexes. The transition in the lower temperature range 25-40 °C corresponds to the melting of third strand and that in the range 62-67 °C arises from duplex denaturation (Table 1).¹ In order to rule out the formation of any secondary structures involving only *sp*-ODNs, control thermal denaturation experiments were performed on *sp*-ODNs in the absence of duplex. The resulting uneventful thermal denaturation curves indicated non-existence of any ordered structure in *sp*-ODNs alone.

Table 1:* UV-melting temperature (T_m) of *sp*-ODN triplexes¹ in the presence and absence of MgCl₂ (20 mM).

	Triplex	T_m with MgCl ₂ °C		T_m without MgCl ₂ °C	
		X*GC	First	Second	First
1	3*2:1		30.0	67.0	nd
2	4*2:1		46	68.0	nd
3	5*2:1		46.0	67.0	40.0
4	6*2:1		45.0	67.0	40.0
5	7*2:1		41.0	67.0	32.0
6	8*2:1		40.0	67.0	32.0
7	9*2:1		31.0	67.0	25.0

* All T_m were obtained from melting experiments of the corresponding triads in TRIS buffer containing NaCl (100 mM) at pH 7.3. nd: not detected

The ODNs **3** and **4** containing dC or 5-Me-dC respectively, which are devoid of conjugated spermine showed no triple helix formation under above conditions.¹ The triplexes from these were obtained at pH 7.3 only in the presence of either 100 mM NaCl

containing 20 mM MgCl₂ or high NaCl (800 mM) concentration. The stabilities of triplexes from *sp*-ODNs **5-9** measured with added MgCl₂ (20 mM) showed an enhancement of melting temperature (T_m) by 6-7 °C (Table 1). Significantly, triplexes derived from mono *sp*-ODNs **5** and **6** (Table 1, entry 3 and 4) were as stable as that from ODN with three 5-Me-dC (**4**, Table 1, entry 2) in presence of MgCl₂. The formation of the unmodified triplex (**3*2:1**) was also examined in presence of externally added spermine (1 mM). A T_m of 33 °C obtained with 1 mM extraneous spermine is similar to that from *sp*-ODN **9**, in which the concentration of appended spermine (equivalent to [ODN]) is only ~1 μM.

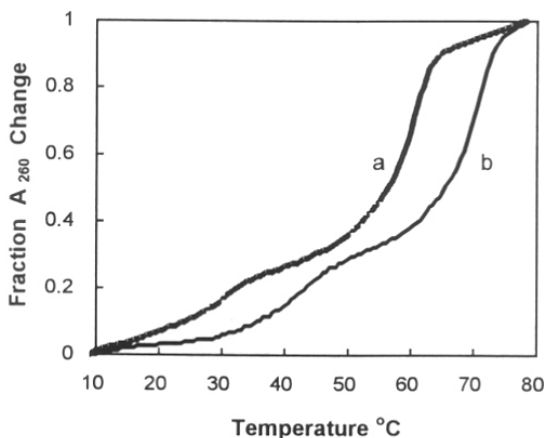


Figure 2: UV-melting profile of triplex **7*2:3** in TRIS buffer at pH 7.3 (a) in 100 mM NaCl and (b) in 800 mM NaCl

3.2.3 pH dependence of *sp*-ODN triplexes

The pK_a of N3 in dC was considered to be one of the critical factors in determining the stability of triplexes.² Earlier studies indicated that sp-ODN triplex stability decreases at lower pH.¹ The appended spermine may influence the pK_a of the modified base which results in stabilization of the triplex at physiological pH. In order to understand the effect of spermine linked at C4 of dC on N3 pK_a, a series of N⁴-substituted dC analogues were prepared and the pK_a of each modified base was determined (see Chapter 2, Section 2.3).

It was observed that substitution at N⁴ with an aminoalkyl chain considerably decreases the pK_a of N3. The N3 pK_a of dC in monomer is known to increase slightly upon incorporation into ODN and this aspect of spermine conjugated dC needs to be explained. The N3 pK_a of dC and 5-Me-dC-N⁴-(spermine) after incorporation into ODNs were determined by UV-titration (Figure 3). Upon incorporation into oligonucleotides, the pK_a value for N3 of dC³ was 4.6 and that of 5-Me-dC-N⁴-(spermine) was 4.2 which are enhanced relative to the corresponding monomers by 0.3 to 0.5 unit respectively. The four pK_a values of spermine (10.97, 10.27, 9.04 and 8.03) as reported in the literature⁴ are distinctly much higher than N3 pK_a of dC or its analogs and hence the interaction of the spermine side chain in the N3 pK_a measurements is negligible.

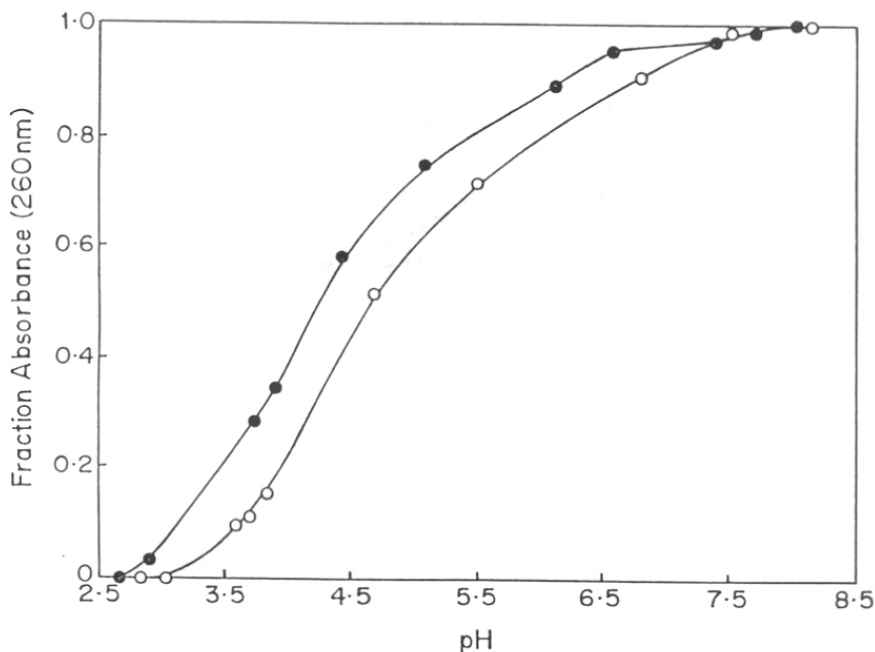


Figure 3: Protonation curves for ODNs 3 (○) and 9 (●) as a function of pH at 45 °C.

The pH dependence of triplex stability is critical for in vivo applications and hence the effect of pH on triplex formation from ODNs **5-9** in presence of Mg^{2+} was examined. The unmodified triplex (**3*2:1**) exhibited a large increase in T_m towards the acidic pH with a plateau around pH 5.6-5.8, while 5-Me-dC containing triplex (**4*2:1**) showed only a marginal increase in T_m at lower pH. On the other hand, in case of sp-ODNs, T_m was maximum in the pH range 7.1 to 7.4 and displayed moderate destabilization at acidic pH (Figure 4).⁵ Even in the absence of Mg^{2+} , this stability pattern was retained in *sp*-ODN triplexes. To understand this behavior, the pH dependent stabilities of triplexes (**3*2:1** and **7*2:1**) were determined by UV titration³ at 4 °C and monitored at 260 nm. The titration curves (Figure 5) indicated improved stability of *sp*-ODN triplex at neutral pH as compared to the unmodified triplex. The most significant and useful result is that *sp*-ODNs have optimum triplex stability at physiological conditions.

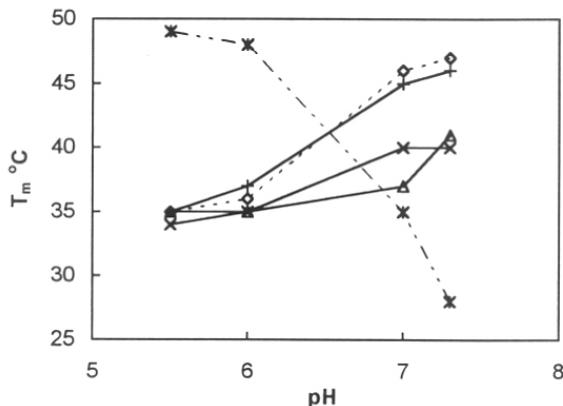


Figure 4: pH dependent of T_m of triplexes constituted from the duplex 1:2 and 3 ($\cdots X \cdots$), 5 ($\cdots \diamond \cdots$), 6 ($- + -$), 7 ($- \Delta -$) and 8 ($- X -$).

3.2.4 Protonation status of N3: UV-spectral study

Among the four nucleobases, only dC shows significant near UV spectral changes which are pH dependent.⁶ Upon N3 protonation of dC, a characteristic shoulder between 270-295 nm range is observed in the UV spectrum as compared to the spectrum at neutral pH where there is no N3 protonation. This new band can be delineated from the major

band only by difference spectroscopy and appearance of such a band is a reasonable certainty for N3 protonation. Such a spectral shift, although characteristic, is small in magnitude and can be unambiguously identified by difference UV-spectroscopy. Figure 6 shows the UV spectra of dC recorded at pH 3.0, 5.3 and 7.3 and Figure 7a shows the corresponding UV-difference spectrum (dotted line) of dC between the pH 7.3 and 3.0 { Δ_{UV} pH(7.3 - 3.0)}.

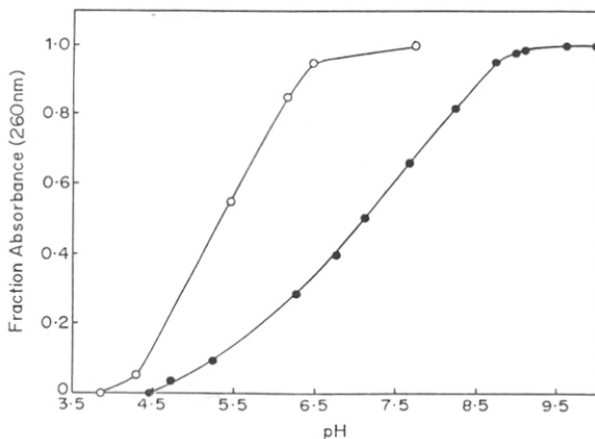


Figure 5: Stability of triplets 3*2:1 (○) and 7*2:1 (●) as a function of pH at 5 °C.

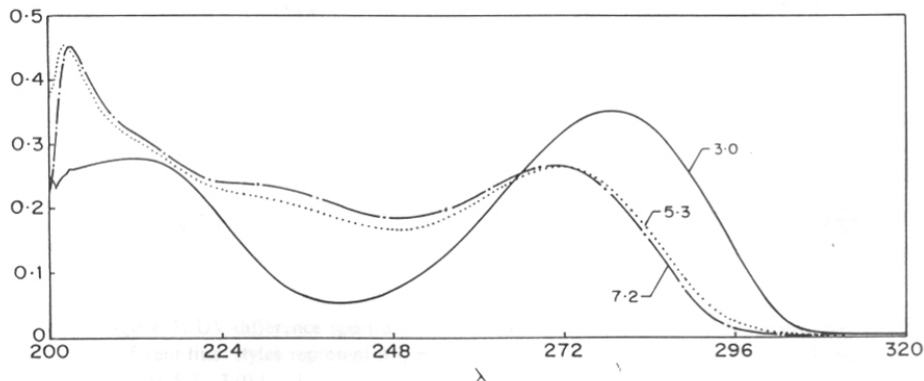


Figure 6: UV spectra of dC at different pHs: Different styles represent (i) — at pH 3.0, (ii) at pH 5.3 and (iii) - - - at pH 7.3.

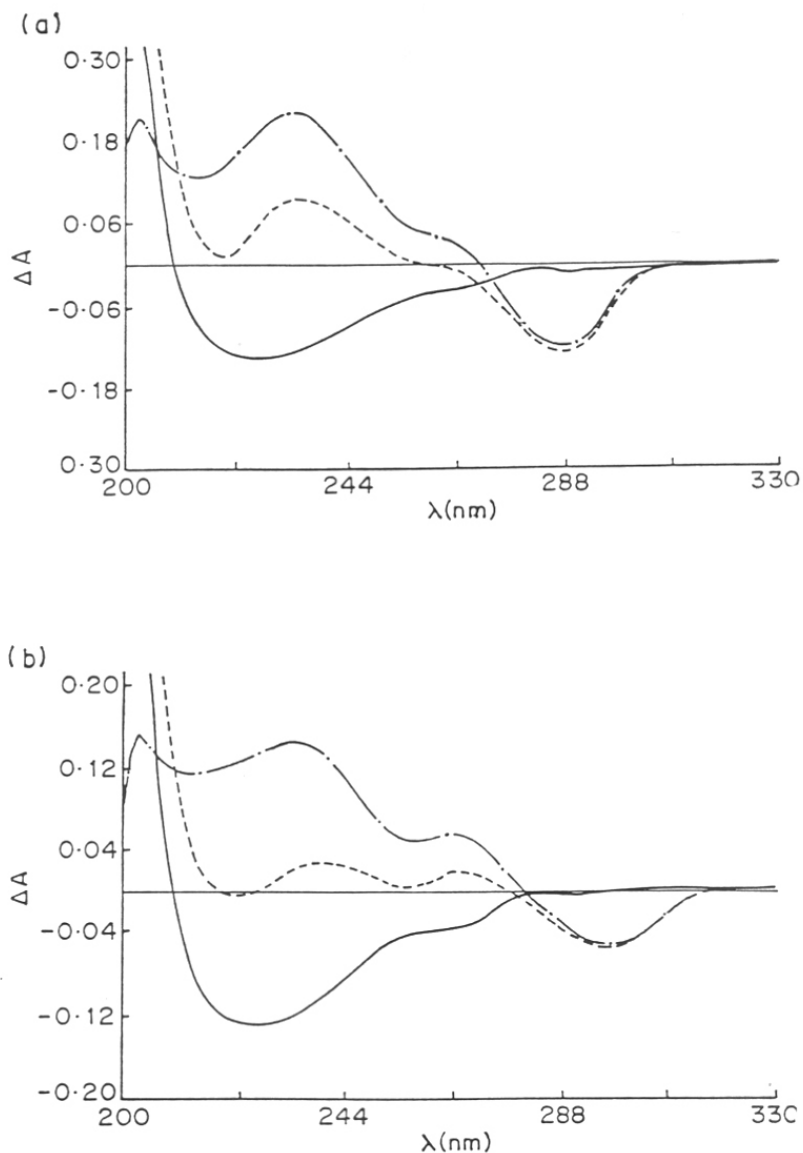


Figure 7: UV-difference spectra at 5 °C of (a) dC and (b) 5-Me-dC-N⁴-(spermamine). Different line styles represent $\Delta_{UV} \text{ pH}(7.3 - 5.3)$ [—], $\Delta_{UV} \text{ pH}(7.3 - 3.0)$ [- -] and $\Delta_{UV} \text{ pH}(5.3 - 3.0)$ [- · -].

The appearance of the characteristic negative band with a λ_{\min} at 288 nm in the difference spectrum is indicative of protonation of dC at pH 3.0, much below its pK_a(4.3). A weak negative band at 288 nm was observed in the difference spectrum between pH 7.3 and 5.3 { Δ_{UV} pH(7.3 - 5.3), solid line in Figure 7a}, the pH above its N3 pK_a value, indicating minor protonation of dC at pH 5.3. The effect of spermine conjugation at N⁴ of 5-Me-dC on N3 protonation can be similarly characterized by UV-difference spectral data (Figure 7b). The protonation of N3 in 5-Me-dC-N⁴-(spermine) is also accompanied by a negative band in the difference spectra Δ_{UV} pH(7.3 - 3.0) (Figure 7b, dotted line) but interestingly, the λ_{\min} is shifted to 298 nm. This behavior persisted even upon incorporation of dC into oligonucleotide since N3 pK_a does not change appreciably. The UV-difference spectra of ODNs 3 and 9, containing dC and 5-Me-dC-N⁴-(spermine) respectively, were recorded at different pH to ascertain the degree of protonation in the ODN level. The UV - difference spectra of ODN 3, that contains three dC residues, between the pH 7.3 and 2.3 showed characteristic negative band with λ_{\min} at 292 nm similar to that in dC monomer (Figure 8a). In comparison, the UV-difference spectrum of ODN 9 (Figure 8b), where all the cytosine are replaced by 5-Me-dC-N⁴-(spermine), showed a protonation (negative) band in which the λ_{\min} was shifted to 300 nm. This property has been used to investigate the N3 protonation status of dC in triplex⁷ and tetraplexes.⁸ In view of the above characteristic observation, we examined the UV-difference spectra of triplexes from *sp*-ODN constituted at different pHs, to determine the protonation status of N3. The validity of this approach is substantiated by a recent report⁷ which demonstrated that in unmodified triplexes, third strand dC residues are slightly protonated even at pH 7.0, far above its intrinsic pK_a. In unmodified triplex 3*2:1, Δ_{UV} pH(7.3 - 5.3) spectral pattern with a negative band at 292 nm confirmed that N3 of dC is appreciably protonated even above pH 5.3 and much more below pH 5.3 (Figure 9a). *In contrast to this, in sp-ODN triplex 9*2:1, N3 of 5-Me-dC-N⁴-(spermine) residues are negligibly protonated in the pH range 7.3 - 5.3 as seen by lack of negative band at 294 nm (Figure 9b).* The origin of negative band in the difference spectrum of triplex 3*2:1 [Δ_{UV} pH(7.3 - 5.3)] is from dC protonation in third strand rather than those in duplex. This

was confirmed by lack of any negative band characteristic of protonation in UV-difference spectrum of duplex 2:1 in the pH range 7.3-5.3 (Figure 10).

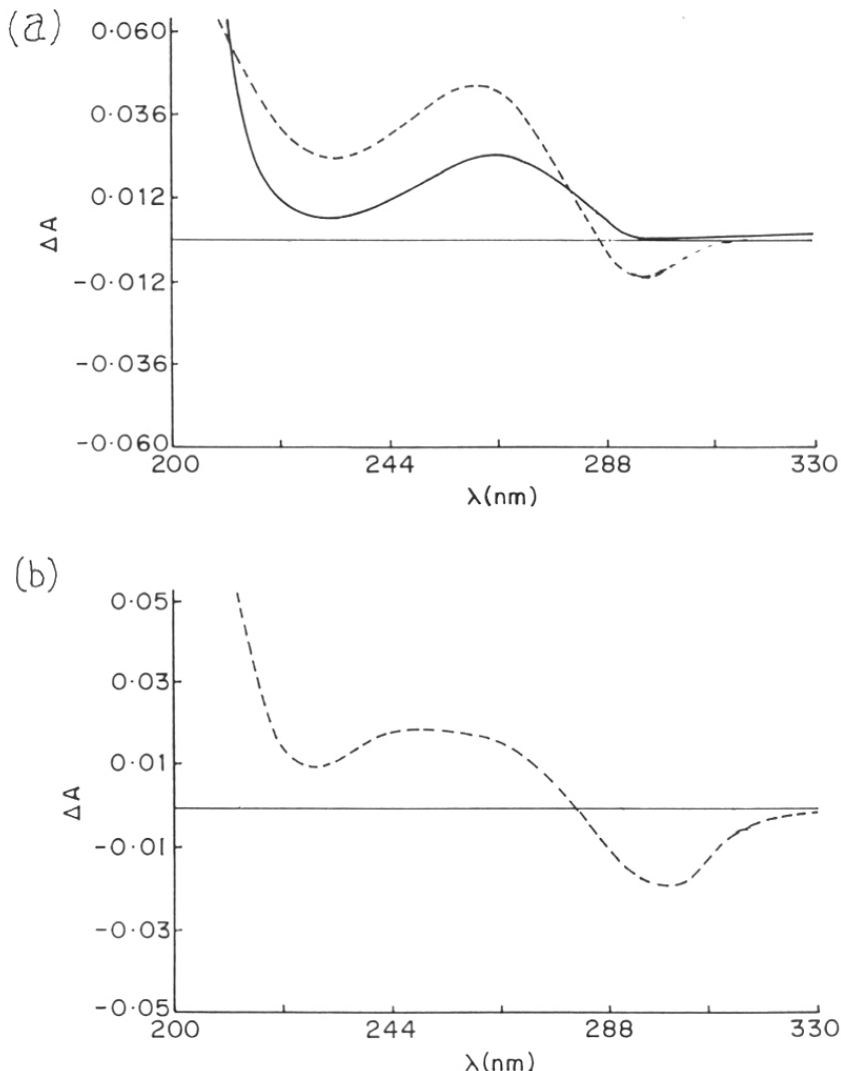


Figure 8: UV-difference spectra at 5 °C of ODNs (a) 3 and (b) 9. Different line styles represent $\Delta_{\text{UV}} \text{pH}(7.3 - 5.3)$ [——] and $\Delta_{\text{UV}} \text{pH}(7.3 - 2.3)$ [- - -].

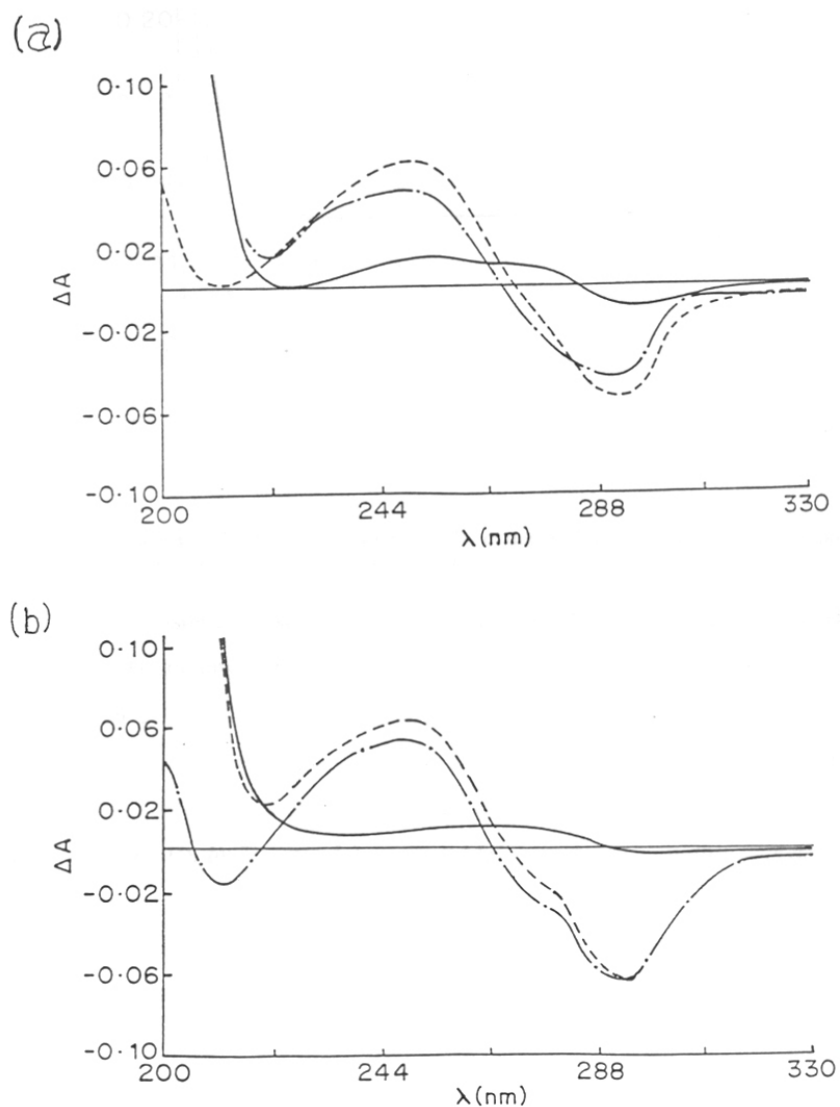


Figure 9: UV-difference spectra at 5 °C of (a) 3*2:1 and (b) 9*2:1. Different line styles represent $\Delta_{\text{UV}} \text{pH}(7.3 - 5.3)$ [—], $\Delta_{\text{UV}} \text{pH}(7.3 - 3.0)$ [- -] and $\Delta_{\text{UV}} \text{pH}(5.3 - 3.0)$ [---]

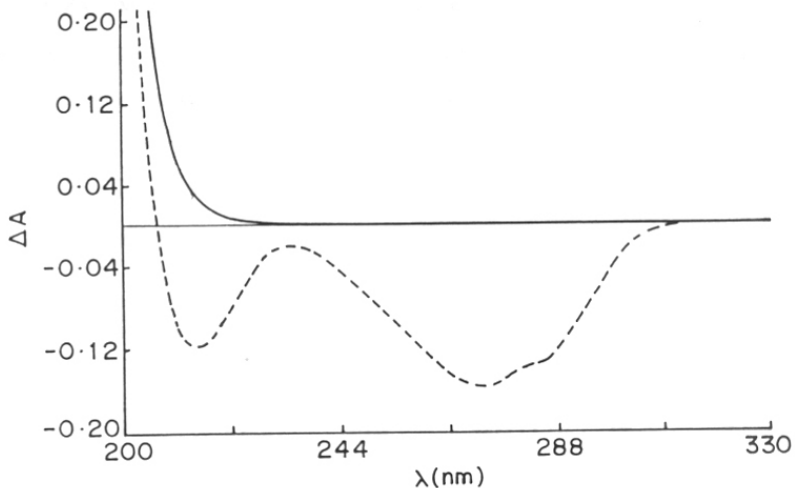


Figure 10: UV-difference spectra at 5 °C of duplex 2:1. Different line styles represent Δ_{UV} pH(7.3 - 5.3) [—], Δ_{UV} pH(7.3 - 3.0) [- -]

The existence of stable triplexes from *sp*-ODN in this pH range was shown by T_m data and pH stability curve. N3 protonation of 5-Me-dC-N⁴-(spermamine) occurred at pH lower than 5.3 as observed in the difference spectrum Δ_{UV} pH(5.3 - 2.3) in which the characteristic negative band appeared at 294 nm. The *sp*-ODN triplexes in this pH range have lower stability than at pH 7.0. *Thus, conditions under which most stable sp-ODN triplexes are seen by Tm (pH 7.3, without Mg²⁺), no N3 protonation was detected by UV-difference spectral data.* Similar UV-difference spectra were also obtained for unmodified and *sp*-ODN triplexes at different temperatures, with and without MgCl₂ and the result was in agreement with above observations.

3.2.5. Sequence specificity

To study the stringency of triplex formation by *sp*-ODNs (**5-9**), triplexes were constituted with duplexes containing all the four Watson-Crick (W-C) base pairs at position complementary to 5-Me-dC-N⁴-(spermamine) of third strand and also by introducing Hoogsteen mismatches at neighboring W-C base pairs of the **X*GC** triad. Apart from **X*GC**, the other triplexes (**X*CG**, **X*AT** and **X*TA**) contain mismatched Hoogsteen

base pairing of **X** with duplexes. Amongst them, a decreased triplex stability was observed in the following order: **X*GC** ~ **X*AT** > **X*CG** > **X*TA** (Table 2), which is similar to that reported for unmodified base triad by affinity cleavage method.⁹ However, this order differed slightly from that obtained from thermal denaturation studies by Helene *et. al.*¹⁰ All the ODN sequences used for mismatch studies (Figure 11) were synthesized and purified as described in *section 3.2.1*.

Table 2: Mismatch specificity.*

	Triplex	T_m with $MgCl_2$ °C		T_m without $MgCl_2$ °C	
		First	Second	First	Second
1	X*YZ				
1	C*GC	30.0	67.0	nd	---
2	X*GC	41.0	67.0	32.0	62.0
3	X*CG	36.0	69.0	29.0	62.0
4	X*AT	40.0	67.0	27.0	60.0
5	X*TA	nd	---	nd	---
6	5'T*GC ↑ C*GC 3'T*AT	nd	--	nd	---
7	5'T*AT ↑ C*GC 3'T*GC	nd	---	nd	---
8	5'T*GC ↑ X*GC 3'T*A:T	nd	nd	nd	---
9	5'T*AT ↑ X*GC 3'T*GC	16	69	nd	---

*All T_m were obtained from melting experiments of the corresponding triads.

'First' refers to triplex ↔ duplex and 'second' refers to duplex ↔ single strand meltings. nd: not determined.

When triplexes were constituted with a 3' **T*GC** Hoogsteen mismatch with respect to **X/C*GC** triad, the unmodified dC sequence did not show any triplex transition during UV-melting in the presence of $MgCl_2$ (20 mM), however the corresponding spermine conjugated sequence showed triplex transition at 16 °C (entry 9, Table 2) approximately 14 °C lower than the perfectly matched control **C*GC** triplex. On the other hand 5'**T*GC** Hoogsteen mismatch failed to show any triplex transition during UV-

melting in the case of unmodified and spermine conjugated ODNs. These results suggest that the conjugated spermine perhaps interacts not only with the same triplex triad but with the neighboring triad also, preferably towards its 3' side.

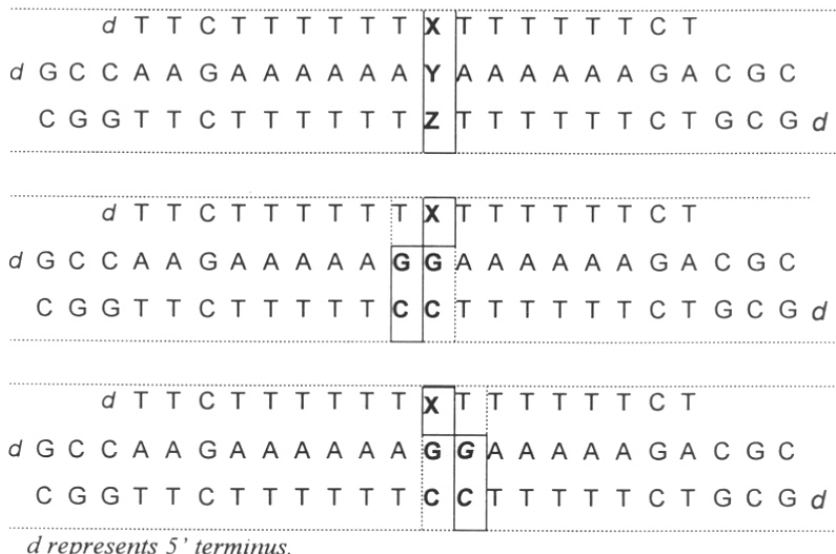


Figure 11. Triplex sequences with various mismatches.

3.2.6 Hysteresis in triplex transitions and effect of ionic strength

It is known from literature¹¹ that association constant K_a for triplex formation is about 1000 times lower than that for duplex and the rate of third strand hybridization with the duplex is about 100 times slower than association of duplex from single strands. As a consequence, hysteresis is observed for normal triplex association-dissociation which is dependent on both pH and ionic strength.¹² At neutral pH and 100 mM NaCl, the association rates are much slower than the dissociation while at lower pH (5.8) where triplex stability is higher, the heating and cooling curves tend to merge. To understand the role of appended spermine in triplex stabilization through strand dissociation and association events, relative profiles of heating and cooling curves were examined for both control (3*2:1) and modified (7*2:1) triplexes under identical conditions. This is also necessary in view of the gel retardation results⁵ that indicated an intramolecular charge

neutralization which may significantly influence the triplex association-dissociation equilibrium.

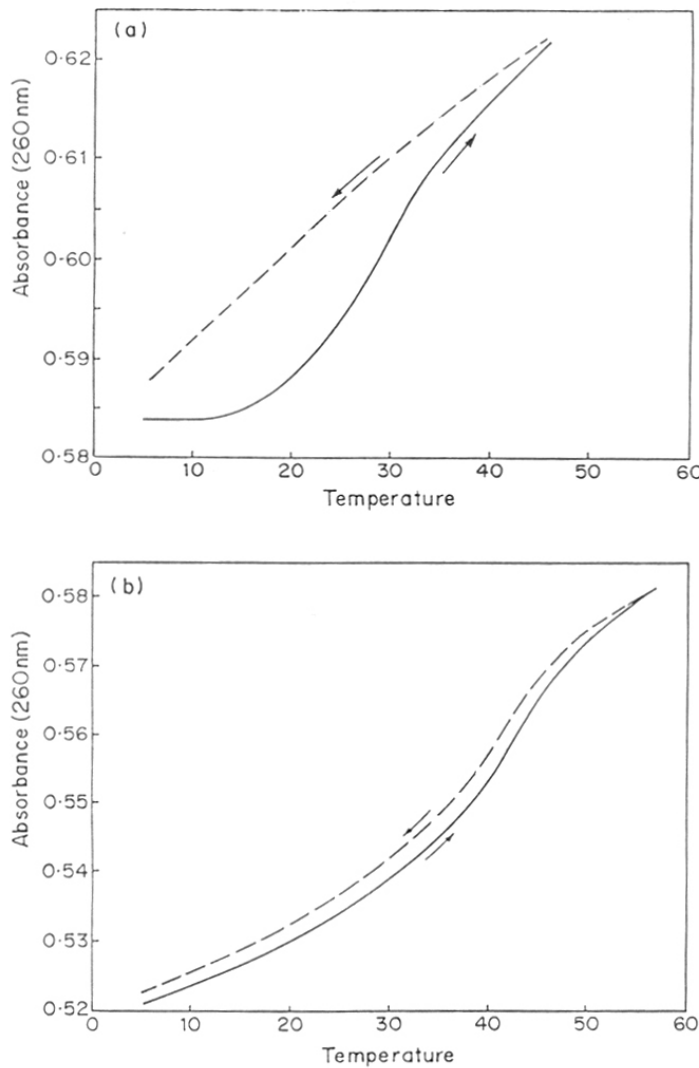


Figure 12: Hysteresis curve for triplexes (a) 3*2:1 and (b) 7*2:1 at pH 7.3 in TRIS buffer containing NaCl (800 mM), solid line represents heating curve and dashed line represents cooling curve at a heating or cooling rate of 5 °C/min.

The unmodified hybrid (**3*2:1**) formed triplex at neutral pH only in the presence of 800 mM NaCl and upon cooling from 46 °C to 5 °C, no detectable duplex-triplex transition was noticed (Figure 12a). This indicated an incomplete association of triplex even at 5 °C in the cooling experiment. The heating/cooling rates were slow enough (0.5 °C/min) to ensure an equilibrium attainment. A similar hysteresis was observed when unmodified triplex was constituted in 100 mM NaCl in presence of either divalent cation (20 mM Mg²⁺) or externally added polycation (1 mM spermine). In contrast to this, under identical conditions of pH and ionic strength (100 mM NaCl with 20 mM MgCl₂ or 800 mM NaCl alone, pH 7.2), triplex from *sp*-ODN exhibited nearly superimposable heating-cooling curves with well defined triplex-duplex transitions (Figure 12b). This implies that appended spermine favors the association process in triplex formation by increasing the third strand affinity to duplex.

Since ionic strength has critical effects on association-dissociation rates,^{11b,13} the hysteresis experiments on *sp*-ODN containing triplexes were carried out at varying salt concentrations. T_m s calculated from both heating and cooling curves shifted to higher values with an increase in ionic strength and showed a linear dependence in the range 100 mM - 800 mM NaCl (Figure 13). The magnitude of hysteresis (ΔT_m 1-3 °C) although small, was enhanced at higher salt concentration suggesting a slightly retarded association of *sp*-ODN with complementary duplex at higher ionic strength.

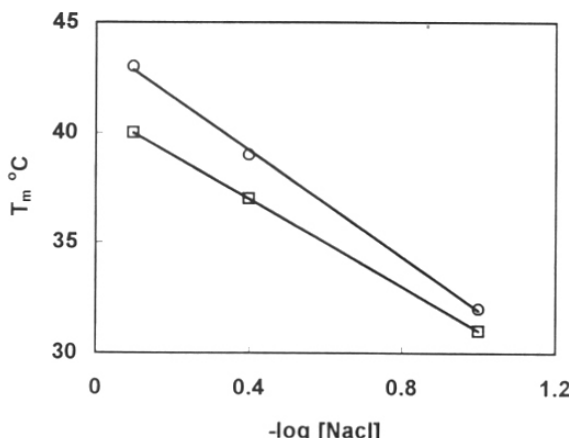


Figure 13: Heating (o) and cooling (□) T_m of triplex **7*2:1** as a function of salt concentration.

It was also very interesting to see that the *sp*-ODN stabilizes triplex 7*2:1 between the salt range 0.1 M to 3 M. The change in T_m with salt concentration between 0.1 M and 0.8 M was marginal (10 °C), however, beyond 0.8 M and up to 3 M salt concentration, the change in T_m was negligible (3 °C). As mentioned above the unmodified third strand ODN gave a triplex transition in 0.8 - 1.0 M salt concentration range, but at 2 - 3 M range it did not show triplex formation.

3.3. DISCUSSION

The rationale for covalent conjugation of spermine to 5-Me-dC present in Hoogsteen strand of triplex to enhance the triplex stability is well supported by the UV T_m results. The higher stability of *sp*-ODN containing triplex is perhaps due to the extra binding energy resulting from interaction of duplex with the polyamine appended to the third strand.

The factors leading to triplex stability from the appended polyamine may arise due to a combined consequence of several effects: (a) altered pK_a of N3 of 5-Me-2'-dC by N⁴-(spermine) substitution (b) stabilization by additional hydrogen bonding interactions of spermine with complementary or adjacent base pair¹⁴ (c) intra/inter strand electrostatic phosphate neutralization imparted by polycationic appendage¹⁵ (d) entropic changes from counter-ion effects during melting as predicted from polyelectrolyte theory¹⁶ and (e) favored association/dissociation equilibrium.

3.3.1. Effect of pK_a

From a study of triplexes containing 5-substituted dC, pK_a of N3 was postulated to be a major determinant of triplex stability, with a higher pK_a leading to more stable triplex at physiological pH.^{2d} In this context, it is interesting to see from present results that although pK_a of N3 in 5-Me-dC-N⁴-(spermine) monomer is lower than that of dC by 0.7 units (see *Chapter 2 section 2.3*), its incorporation leads to stable triplex formation under conditions where corresponding unmodified ODN analogue fails to form triplex. On the basis of monomer pK_a, the optimal stability of *sp*-ODN triplexes should shift to lower pH

side (acidic) while the experimentally observed results indicate a shift to higher pH side (neutral). The N3 pK_a factor is therefore highly unlikely to be the cause for improved stability of *sp*-ODN containing triplexes. A pK_a shift of 0.3 to 0.5 units to higher values upon incorporation of monomer into oligonucleotide is consistent with earlier observations.^{3b}

The pH dependent UV-difference spectral studies show that N3 protonation is not necessary for triplex formation by sp-ODN at physiological pH. N3 protonation which occurs at acidic pH (< 5.3) as seen from UV-difference spectra actually destabilizes the *sp*-ODN triplex (Figure 9b). This is a remarkable result which suggests that at neutral pH, where *sp*-ODN triplex stability is maximal, in the triad **X*GC**, **X** is held by only one Hoogsteen hydrogen bond possible between N⁴-H of **X** and O₆ of **G**. The observed additional stability must therefore arise from interaction of spermine side chain with the phosphate backbone and/or neighboring base pair of the duplex (Figure 14). Thus the loss in triplex stability arising from absence of the second Hoogsteen hydrogen bond due to non protonation of N3 is probably more than compensated by interaction of appended spermine chain with the duplex.

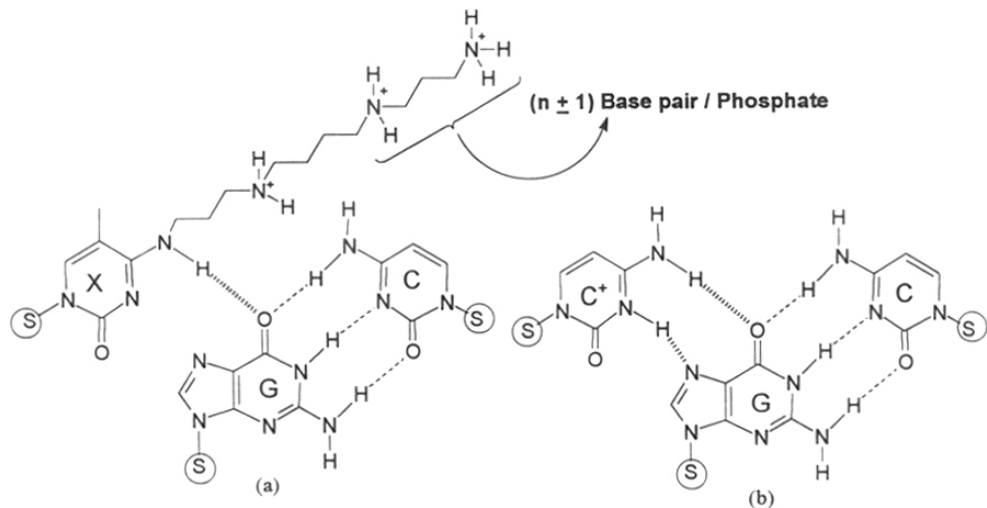


Figure 14. (a) **X*GC** and (b) **C*GC** triads

Interestingly, in the present study on *sp*-ODNs **5-9**, a decrease of triplex stability was noticed upon lowering the pH, in reverse trend to that seen with unmodified oligonucleotides (Figure 4). This may arise perhaps as a consequence of pH induced change in conformation of appended spermine chain, which at low pH, may assume orientations unfavorable for specific interactions with the backbone or the base pairs. The orientation change may also occur from the imino tautomer of 5-Me-dC-N⁴-(spermine) due to partial double bond character of exocyclic C4-N bond.¹⁷ This is less likely to occur at physiological pH since the N3 pK_a for 5-Me-dC-N⁴-(spermine) is very low (3.70) but may become reasonable at acidic pH (5.5). The fact that increasing the degree of spermine substitution also lowers triplex stability suggests electrostatic repulsion, either among the spermine chains or between spermine and protonated C⁺, as a major causant of low pH destabilization of *sp*-ODN triplexes.

3.3.2. Effect of mismatches

Thermal denaturation studies of triplexes containing a single Hoogsteen mismatched triad of 5-Me-dC-N⁴-(spermine) with Watson-Crick doublets CG, TA and AT showed that the inverted doublet CG also formed triplex, although less effective than the original GC (Table 2). Of the other pairs, AT and TA, only the former exhibited any detectable triplex transition. With both CG and AT doublets, a carbonyl group (O⁶ of G and O⁴ T) is available in the first base of the triad as a hydrogen bond acceptor in major groove.¹⁸ It is possible that the N⁴-spermine side chain from the third strand can span across the major groove to form additional hydrogen bonds from its imino/amino group with the O⁶/O⁴ carbonyls of G and T (Figure 15). Thus C and A are well tolerated in the central purine position of the triad, with protonation requirement of C in the third strand assuming less significance and hence favoring triplex even at neutral pH. This may have utility for employing 5-Me-dC-N⁴-(spermine) as a Hoogsteen mismatch tolerator, without loss of stability.

Hoogsteen mismatch studies on the neighboring/adjacent base triad of the modified base have shown that the appended spermine extends its interaction to neighboring base

triad at the 3' side of the underlying triplex. Thus spermine chain probably participates in hydrogen bonding with WC base pair of adjacent triads. It may also interact with the phosphate backbone of the duplex resulting in the stabilization of triplex even in the presence of a Hoogsteen mismatch at the 3' side.

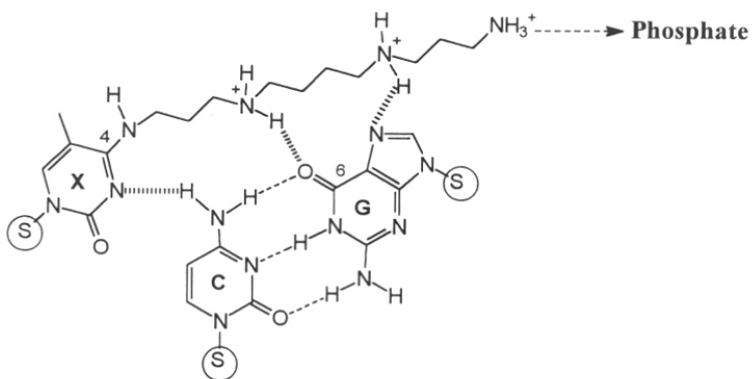


Figure 15. Schematic representation of the possible H-bonding between the protonated spermine side chain of 5-Me-dC-N⁴-(spermine) (X) and the O⁶ of dG in the triad X*CG.

3.3.3. Counter-ion effects

In a recent study of intramolecular triplexes,¹⁹ it was observed that electrostatic interactions between protonated C (C⁺) of third strand and phosphate backbone offer considerable stabilization in a global, sequence independent manner. However, repulsion between adjacent C⁺ can cause successful negation of the above electrostatic advantage, thereby imparting local sequence dependent effects. Application of polyelectrolyte theory to DNA suggests that DNA melting is accompanied by release of a part of counter-ions from DNA bound state to bulk as the condensed charge density is reduced in the melting process. In zwitterionic DNA such as that from *sp*-ODNs, 5-9 described here or 5-hexylamino-2'-dC incorporated DNA reported earlier,^{15b} the high charge density in triplex/duplex form is partially balanced by the covalently bound, non diffusible cations, offering a unique stabilization effect.

3.3.4. Electrostatic neutrality

The intramolecular phosphate neutralization by polycationic spermine leading to a net diminished charge for *sp*-ODNs 5-9 is clearly apparent from mobility retardation seen for them in gel electrophoresis and better association of *sp*-ODN in triplex formation.⁵ Mono spermine 18-mer ODN 5 migrates equal to an unsubstituted 24-mer 1 and the migration is systematically retarded as a function of degree of spermine substitution. Such a correspondence illustrates the zwitterionic character of *sp*-ODNs 5-9 similar to those reported by Switzer *et. al.*^{15b} An analogous effect of interstrand phosphate charge neutralization is possible in triplex. Such charge neutralization effects by externally added cations are known to lead to electrophoretic retardation of high molecular weight (1-5kb) linear/plasmid DNA due to counter-ion condensation effects.²⁰ The third strand of DNA asymmetrically partitions the major groove²¹ and the N⁴-linked spermine chain may position itself across the major groove accessing the phosphate backbone of either of WC duplex strands.

3.3.5. Effect of spermine on dissociation/association equilibrium

The nature of the observed hysteresis (Figure 12b) and its salt dependence (Figure 13) indicated that the appended spermine may assist association of third strand with complementary duplex. Normally, hysteresis in triplex melting as seen with 3*2:1 arises from a slower association of third strand with duplex during cooling as compared to dissociation rates during heating.¹² The insignificant hysteresis phenomena seen in *sp*-ODN triplex (100 mM NaCl) suggests that the association rate is comparable to that of dissociation rate, i.e., the association is enhanced relative to that seen in unmodified triplex. In presence of higher salt concentration (800 mM NaCl or 100 mM NaCl with 20 mM MgCl₂), the hysteresis is marginally increased ($\Delta T_m \sim 3$ °C) due to a slower association. This perhaps arises from accumulated salt cations on duplex surface which electrostatically disfavors the approach of cationic spermine chain. Thus, stable triplex formation by *sp*-ODNs at physiological pH may be a combined consequence of

intermolecular hydrogen bonding and electrostatic stabilization leading to a favored association event.

The overall experimental results presented here suggest that when spermine molecule is covalently attached to the third strand, it may still be accommodated in the deep major groove of the duplex DNA along with the third strand, yielding a stable triple helix.

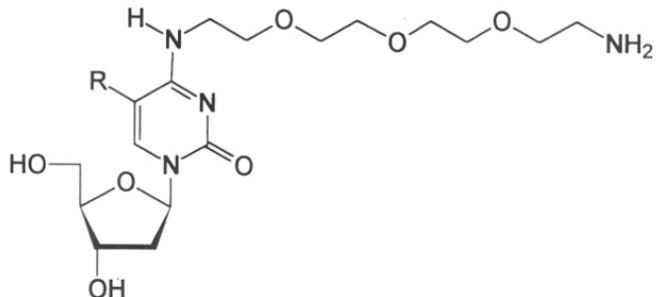
3.4. STABILIZATION OF TRIPLEX BY *teg*-ODN: A COMPARATIVE STUDY WITH *sp*-ODN TRIPLEXES

The above studies demonstrated that ODNs with spermine conjugation at C4 of 5-Me-dC (*sp*-ODN) exhibit triple helix formation with complementary duplex, with foremost stability at low salt, neutral pH 7.3 where the corresponding unmodified ODNs do not form triplexes. Further, N3 protonation of C in third strand was not observed in *sp*-ODN triplexes and the loss in stability thereby due to the absence of (C)^{N4-H--N7(G)} Hoogsteen bond is compensated by favorable electrostatic interactions of sperminyl side chain with DNA, leading to an enhanced association with duplex. To gain further insights into factors that contribute to enhancement of triplex stability and for engineering better triplex systems, similar studies were conducted on ODNs having ω,ω' -dideoxydiaminotetraethyleneglycol in place of spermine conjugation (*teg*-ODNs 11-15). As described in *Chapter 2 (section 2.2.3)* both spermine and ω,ω' -dideoxydiaminotetraethyleneglycol have very close molecular mass and atom chain length and hence provide a close comparison between *sp*-ODN and *teg*-ODN triplexes. Towards understanding the role of tetraprotonated spermine side chain in causing the triplex stability, this appendage at C4 of 5-Me-dC was replaced with ω,ω' -dideoxydiaminotetraethyleneglycol that has only a single protonation site, to obtain *teg*-ODNs for constituting triplexes. A comparative biophysical study presented here employs measurements of thermal stability, hysteresis and the effect of salts on thermal transitions of *sp*-ODN and *teg*-ODN triplexes.

The incorporation of 5-Me-dC-N⁴-(ω,ω' -dideoxydiaminotetraethyleneglycol) monomer into desired sites of ODNs (**11-15**) and their purification were successfully carried out as in the case of *sp*-ODNs (see section 3.7 for details).

1	C G G T T C T T T T T T C T T T T T C T G C G - d
2 d -	G C C A A G A A A A A G A A A A A G A C G C
3 d -	T T C T T T T T T C T T T T T T C T
11 d -	Y C C
12 d -	C C Y
13 d -	C Y C
14 d -	Y C Y
15 d -	Y Y Y
10	A A G A A A A A G A A A A A G A - d

d represents 5' terminus.



Y = 5-Me-dC-N⁴-(ω,ω' -dideoxydiaminotetraethyleneglycol)

3.4.1. Thermal stability of *teg*-ODN duplexes and triplexes

Figure 16 and Table 3 documents UV- T_m results on duplexes derived from *teg*-ODNs. The duplexes from *teg*-ODN containing different degrees of substitutions (**10:12**, **10:13**, **10:14** and **10:15**) exhibited lower T_m s compared to the control unmodified duplex **10:3**, similar to the behavior of *sp*-ODN duplexes;¹ the destabilizing order being control **10:3** ≈ 3'10:12 < M 10:13 < 3'5'10:14 < 3'5'M 10:15. *teg*-ODNs as third strand, formed triplexes with the complementary 24-mer duplex **2:1** (Figure 17, Table 2), even in the absence of Mg⁺⁺, in contrast to the control **3*2:1** where triplex was not observed. In

presence of Mg^{++} , T_m s of triplexes were enhanced by $\sim 12\text{-}19$ °C; the 3'5'-disubstituted *teg*-ODN had the highest ΔT_m (≈ 19 °C). The trisubstituted *teg*-ODN 15*2:1 was less stable than the control 3*2:1. The decrease in triplex T_m of *teg*-ODNs upon lowering of pH, though qualitatively similar, the magnitude was less than that seen with *sp*-ODN triplexes under identical conditions. Thus the enhanced stability of *teg*-ODNs over unmodified triplex and the pH-dependence of T_m parallels the behavior of *sp*-ODNs. No change in T_m of unmodified triplex 3*2:1 was observed upon external addition of 1 mM ω,ω' -dideoxydiaminotetraethyleneglycol, unlike that seen from addition of external spermine which increased T_m .

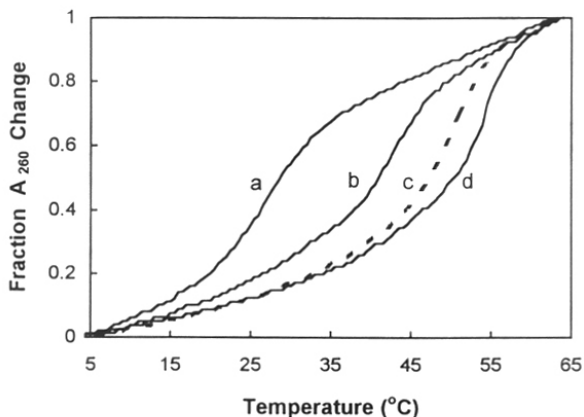


Figure 16: UV-melting profiles of duplexes constituted from *teg*-ODNs in TRIS buffer containing NaCl (100 mM) and MgCl₂ (20 mM) at pH 7.3. (a) 10:15 (b) 10:14 (c) 10:13 and (d) 10:3

Table 3: Melting data for *teg*-ODN duplexes and triplexes*

Duplex	T_m °C	Triplex	Triplex T_m °C		Duplex T_m in Triplex ^b
			-Mg ⁺⁺	+Mg ⁺⁺	
10:3	50	3*2:1	nd	30	68
10:12	50	12*2:1	34	47	67
10:13	47	13*2:1	nd	41	67
10:14	42	14*2:1	23	42	68
10:15	29	15*2:1	12	24	68

* nd, not detected; b, duplex T_m in triplex with MgCl₂

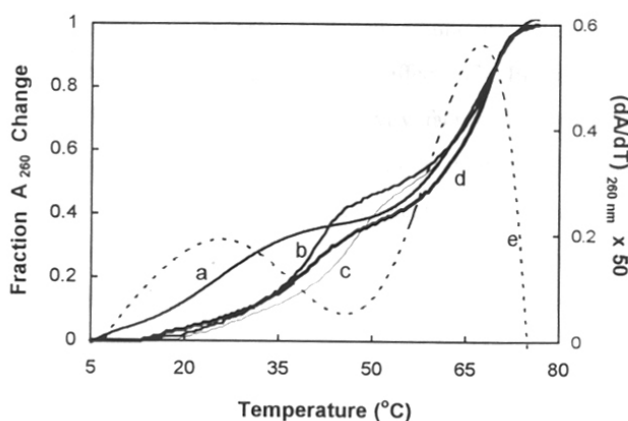


Figure 17: UV-melting profiles of *teg*-ODN triplexes in TRIS buffer at pH 7.3 containing NaCl (100 mM) and MgCl₂ (20 mM). (a) 15*2:1, (b) 14*2:1, (c) 12*2:1, (d) 13*2:1 and (d) first derivative of (a).

3.4.2. Effect of PEG on macromolecular physical properties

Polyethyleneglycols (PEG) have been increasingly used in biomedical applications such as separation of biological materials.²² These biological functions of PEG are largely due to its ability to control the solubilities and the molecular dimensions of other biological molecules. The distribution coefficient of a series of proteins in a PEG/phosphate two-phase system were earlier shown to reflect the unoccupied volumes in the two phases (“available volume model”); this behavior provided a means of estimating the effective volumes of the proteins in excluded volume interactions.²³

The application of this technique to molecules of very different geometry, like single- and double-stranded ODNs, provides a further test of the validity of the available volume model to this system.²⁴ Later on it has been found²⁵ that external addition of polyethylene glycols (PEG) induces dramatic change in melting temperature of duplex and triplex with increasing concentration and molecular weight of polymer, studied in the range PEG 400 - 3400. By steric exclusion of volume, the neutral polymers such as PEG effect both condensation and increase of the effective concentration of DNA random

coil.²⁶ The presence of low molecular weight PEG leads to dissociation of DNA apparently by reducing water activity. On the other hand, addition of high molecular weight PEGs favors association of DNA due its larger excluded volume effect in aqueous medium than the water activity change. Thus the observed effect of PEGs was attributed to a composite of excluded volume and water activity factors operating together. Triplex stability is a complex function of multiple factors, including salt concentration, water activity and presence of crowding-agent namely neutral polymers like PEG. Hence, to understand the role of conjugated polyoxy ethyleneamino chain in *teg*-ODN in inducing stable triplexes, the differential behavior of heating and cooling curves (hysteresis) and salt effects on T_m were examined.

3.4.3. Hysteresis in *teg*-ODN triplexes

As described in *sections 3.2.6 and 3.3.5*, absence of hysteresis seen for *sp*-ODN triplexes may be attributed to its better association with complementary duplex through polycationic spermine chain, as compared to the unmodified ODN. On the other hand, triplexes constituted from *teg*-ODN having only one amino group in the side chain, may show considerable hysteresis. To examine this effect, heating and cooling curves were recorded for triplex transitions in *teg*-ODN triplexes (see *section 3.7* for details), both in the absence and presence of Mg^{++} and the results are shown in Figure 18. No significant hysteresis (~15 %) for triplex ⇔ duplex transition was noticed with triplexes in presence of Mg^{++} upon cooling (Figure 18a). However, in the absence of Mg^{++} , *teg*-ODN exhibited a strong hysteresis (~50 %) with non-superimposable heating and cooling curves as shown in Figure 18b.

The results indicate that the stability of *sp*-ODN triplexes is primarily derived from the protonated side chain, which is capable of establishing interstrand electrostatic contacts with phosphate backbone and/or hydrogen bonding with nucleobases, thereby enhancing the reassociation rate. In case of *teg*-ODN, which has polyether functions that are non-protonated under the experimental conditions, the observed triplex stability must be derived from factors other than charge effects, for eg., hydrophobic desolvation of

major groove of duplex by the appended polyethylene glycol side chain of third strand. This induces changes in hydration network in the vicinity of polyether side chain, improving its association via hydrophobic and hydrogen bonding interactions with neighboring DNA strands. Externally added polyethylene glycols are known to selectively stabilize triplex DNA due to multiple factors including salt concentration, water activity and solution crowding.²²

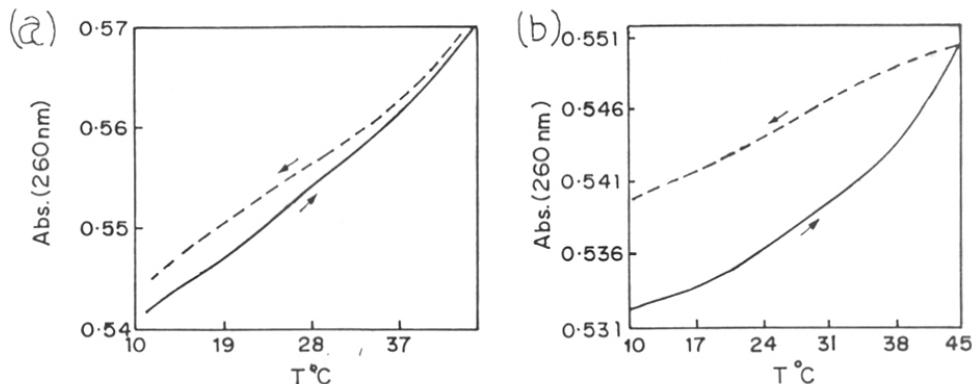


Figure 18: Hysteresis curves of triplex 14*2:1 at pH 7.3 in TRIS buffer containing NaCl (100 mM). (a) in the presence of MgCl₂ (20 mM) and (b) in the absence of MgCl₂.

3.4.4. Effect of salts on teg-ODN triplex stability

The stabilities of triplex DNA are strongly influenced by the presence of salt and are more cation specific as compared to duplex and single stranded DNA.^{11b} For monocations, increasing the sodium ion concentration typically increases the stabilities of triplexes in solution. Triplex formed by T-rich third strands show a markedly greater salt sensitivity than those containing C⁺ in the third strand.²⁷ In contrast to the situation in solutions containing a single cationic species, the stabilization of triplex in mixed valence salt solutions is cation specific. In the presence of millimolar concentration of spermine and magnesium, increasing the concentration of a monovalent cation decreases the triplex

stability.²⁸ In general, the effect of salts on biopolymers has been found to be complex even in the absence of specific ion effects.

In addition to the electrostatic interaction, salt can also influence/affect hydrophobic interaction in condensation and precipitation of biopolymers.²⁹ Strongly hydrated anion such as SO_4^{2-} has most stabilizing effect on proteins in solution whereas weakly hydrated anions such as ClO_4^- and CNS^- are known to destabilize with Cl^- and Br^- in between. These salt effects on protein stability are generally taken as empirical evidence for hydrophobic interactions.³⁰ This property of salts has been employed successfully to study the hydrophobic interaction of calicheamicin with DNA.³¹ The presence of strongly hydrated sodium sulfate (antichaotropic agent) increased hydrophobic association of calicheamicin with DNA which resulted in an increase in the rate of cleavage of DNA by the drug. On the other hand, sodium perchlorate (chaotropic agent), a weakly hydrated polar salt, increased the solubility of calicheamicin in water by readily adsorbing to the lipophilic surfaces of the drug and that caused a reduction in the rate of binding/cleavage of the DNA by the drug. In view of these facts, the effect of salts on *sp*-ODN and *teg*-ODN triplex were studied to understand the nature of interaction of spermine conjugated ODN and that of ω,ω' -didehydroxydiaminotetraethyleneglycol conjugated ODN with the WC duplex.

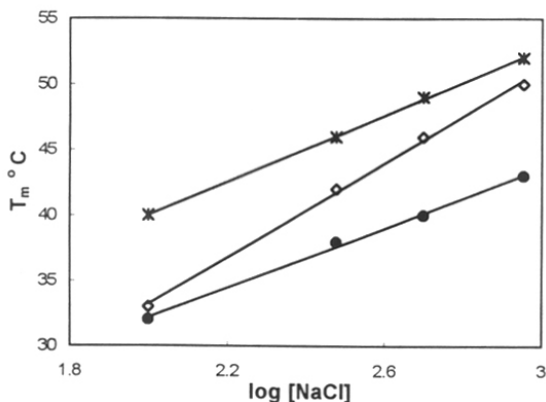


Figure 19: Salt dependence of *sp*-ODN and *teg*-ODN triplexes. Line —*— stands for 6*2:1, line —●— stands for 7*2:1 and line —◇— stands for 12*2:1 triplexes.

3.4.4a. Effect of salt on *sp*-ODN and *teg*-ODN triplex stabilities

Both *sp*-ODN and *teg*-ODN triplexes showed enhancement of T_m upon increasing NaCl concentration from 100 mM to 900 mM. The melting of *teg*-ODN triplexes were more salt dependent than that of *sp*-ODN triplexes, as is evident from a higher slope for *teg*-ODN triplex in salt concentration- T_m plot (Figure 19). Comparative UV- T_m data for triplexes containing either *sp*-ODN or *teg*-ODN recorded in Tris buffer containing salts of different compositions are indicated in Figure 20. The addition of 100 mM Na₂SO₄ to the buffer instead of 100 mM NaCl had no effect on the T_m of *sp*-ODN triplexes irrespective of the position and degree of substitution (**A, B, C**) with a slight destabilization in case of trisubstituted *sp*-ODN triplex. On the other hand, 100 mM Na₂SO₄ induced a significant raise in T_m for *teg*-ODN triplexes with a higher magnitude of induced stability accompanying an increasing degree of substitution (**D, E, F**).

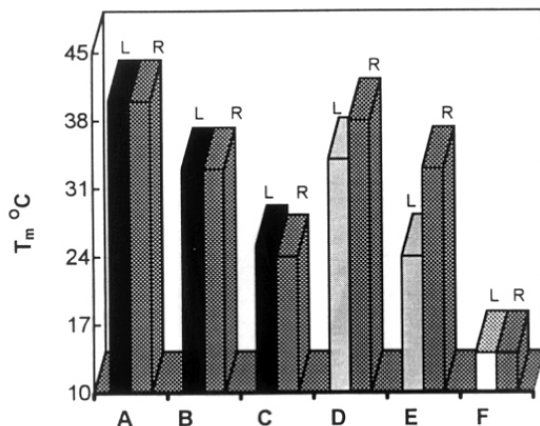


Figure 20: Bar diagram shows anion dependence of *sp*-ODN and *teg*-ODN triplexes in TRIS buffer at pH 7.3. L stands for buffer containing NaCl (100 mM) and R stands for buffer containing Na₂SO₄ (100 mM). A (6*2:1), B (8*2:1) and C (9*2:1) represent *sp*-ODN triplexes with 1, 2 & 3 modifications respectively. D (12*2:1), E (14*2:1) and F (15*2:1) represent *teg*-ODN triplexes with 1, 2 & 3 modifications respectively.

In case of trisubstituted *teg*-ODN (**E**), triplex formation which was undetectable with 100 mM NaCl, was observed only in presence of 100 mM Na₂SO₄. The observed raise in T_m of *teg*-ODN triplets in presence of 100 mM Na₂SO₄, could be either due to increased cation concentration (Na⁺) or anion (SO₄²⁻) effects. Hence, a set of UV- T_m experiments on 3'-monosubstituted triplets **6*7:9** (*sp*-ODN) and **14*19:20** (*teg*-ODN) were carried out at different compositions of NaCl and Na₂SO₄, keeping the total cation concentration constant and the results are depicted in Figure 21. Increasing [Na⁺] from 500 mM (a) to 900 mM (c) enhanced T_m of both *sp*-ODN and *teg*-ODN triplets. In presence of 100 mM NaCl with 400 mM Na₂SO₄ (total [Na⁺] = 900 mM) (b), *sp*-ODN showed a lower T_m compared to that at 900 mM NaCl alone (c). This is unlike that seen for *teg*-ODN triplet, which was equally stable in both salt compositions. Thus salts effects seem to be more pronounced in stabilizing *teg*-ODN triplets than *sp*-ODN triplets and the observed order of induced stability by the anions SO₄²⁻ > Cl⁻ > ClO₄⁻ suggesting that hydrophobic interaction³¹ from the polyethylenoxy side chain contribute significantly to the stability of *teg*-ODN triplet.

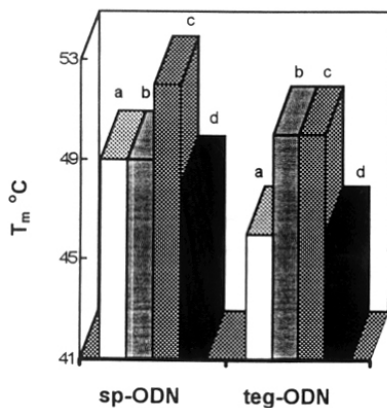


Figure 21: Bar diagram shows salt dependence of *sp*-ODN (**6*2:1**) and *teg*-ODN (**12*2:1**) triplets in TRIS buffer at pH:3 having different salt composition. (a) NaCl : 500 mM, (b) NaCl : 100 mM and Na₂SO₄ : 400 mM, (c) NaCl : 800 mM and (d) NaCl : 100 mM and LiClO₄ : 400 mM

3.4.5. Gel Electrophoresis Behavior of *sp*-ODN and *teg*-ODN

The relative cationic charge contributions to the properties of *sp*-ODN and *teg*-ODN can also be probed by their electrophoretic behavior. It has been shown that *sp*-ODNs were considerably retarded in gel mobility on polyacrylamide gel electrophoresis (PAGE),⁵ compared to the unmodified parent ODN and the retardation increases with the degree of substitution. The retardation in electrophoretic mobility arises from the positive charges of conjugated spermine chain and experiments were done to examine this effect in *teg*-ODNs that have only terminal amino group in its side chain. Similar to *sp*-ODNs, the 5'-end ³²P labeled *teg*-ODNs showed retardation on gel compared to unmodified ODNs, but with a lesser magnitude compared to that of *sp*-ODN. As seen in the Figure 22, mono-, di- and trisubstituted *sp*-ODNs (Lane 3, 5 and 7, respectively) were found to retard more compared to their mono-, di- and trisubstituted *teg*-ODNs (Lane 4, 6 and 8, respectively) counterparts. Since the molecular weight difference between the two types of modifications is insignificant (~10), the observed retardation differences among *sp* and *teg*-ODNs must arise due to charge effects, the higher positive charge in *sp*-ODN leading to a relatively greater retardation. The retardation increased with the degree of substitution and interestingly, showed dependence on the position of the modification on the sequence (Table 4). The terminally modified monosubstituted ODNs (3'/5') in each class had not only closer R_f values, but retarded slightly more than the centrally modified ODNs.

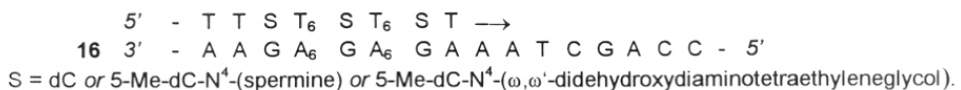
Table 4: Gel retardation data on *sp*-ODNs and *teg*-ODNs*

<i>sp</i> -/ <i>teg</i> -ODN	Site of Modification	R _f values	
		<i>sp</i> -ODN	<i>teg</i> -ODN
5 / 11	5' ^a	0.76	0.83
6 / 12	3' ^b	0.76	0.84
7 / 13	M ^c	0.84	0.89
8 / 14	5', 3'	0.56	0.70
9 / 15	5', 3, M	0.34	0.60

*R_f value for unsubstituted ODN, 1.0. ^a Modification towards 5' end of ODN, ^b modification towards 3' end of ODN and ^c modification in the middle of ODN

3.4.6. Primer Extension Reactions with *sp*-ODNs and *teg*-ODNs

It would be interesting to see the effect of conjugation of polyamine and polyether functions to nucleobases in oligonucleotides on their ability to act as substrates in biological reactions. To examine this, template directed DNA polymerase (Klenow Poll)³² catalysed chain extension reactions were carried out using 18-mer *sp*-ODNs **5-9** and *teg*-ODNs **11-15** as primers with a 25-mer complementary ODN **16** as the template (see section 3.7 for details).



The results shown in Figure 23 indicate that both classes of modified oligomers act as efficient primers in the primer extension reaction, regardless of the position and degree of modification to yield 25-mer products as analysed by gel electrophoresis under denaturing conditions. All modified ODNs were also found to be efficient substrates in 5'-end phosphorylation reactions by T4 polynucleotide kinase. These results suggest that spermine or ω,ω' -dideoxydiaminotetraethyleneglycol conjugations on ODNs do not interfere in their ability to act as substrates by enzymes like polymerase and kinase. The characteristic gel mobility retardation seen for the modified primers was also evident in their corresponding 25-mer extended products (Figure 23).

3.5. ORIGIN OF TRIPLEX STABILITY: *sp*-ODN versus *teg*-ODN

The experimental data presented in this chapter clearly demonstrate that oligonucleotides with a spermine or a tetraethyleneoxy amine side chain appended at C4 of 5-Me-dC form stable triplexes under low salt conditions. Triplex formation by *sp*-ODN is most stable at neutral pH. UV difference spectra and pK_a measurements indicate that N3 of *sp*-ODN is predominantly non-protonated at pH 7.0 and hence handicapped by loss of one HG hydrogen bond with N7 of dG in central strand. The stability of *sp*-ODN triplex under low salt conditions (100 mM NaCl) is mostly due to enhanced reassociation of duplex and third strand, accelerated by ionic interaction of conjugated cationic spermine with anionic phosphate backbone and possible hydrogen bonding interaction with bases in

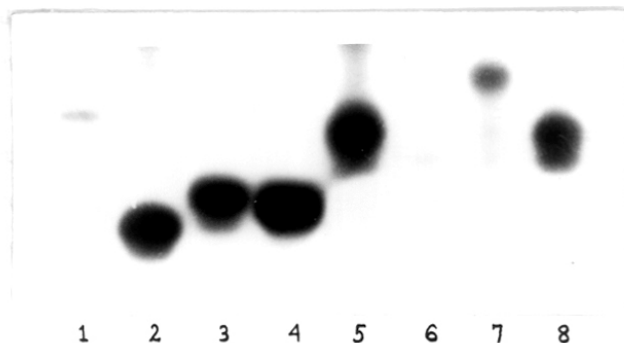


Figure 22. Comparative gel electrophoretic pattern of *sp*-ODNs and *teg*-ODNs. Lane 1: 24-mer ODN (1), Lane 2: 18-mer ODN (3), Lane 3: *sp*-ODN (6), Lane 4: *teg*-ODN (12), Lane 5: *sp*-ODN (8), Lane 6: *teg*-ODN (14), Lane 7: *sp*-ODN (9) and Lane 8: *teg*-ODN (15). ODNs 6, 8, 9 (*sp*-ODNs) and 12, 14, 15 (*teg*-ODNs) correspond to mono-, di- and trisubstitutions respectively.

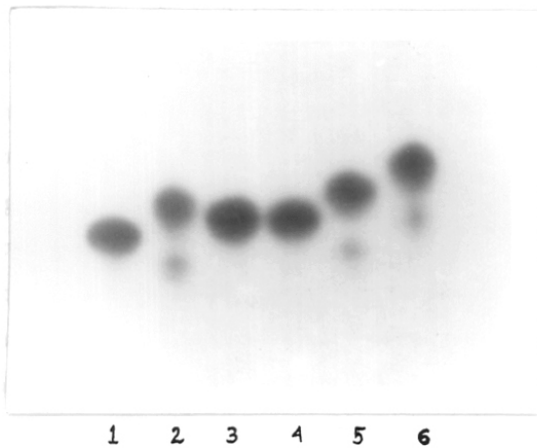


Figure 23. Denaturing PAGE analysis of primer extension reactions using *sp*-ODNs as primer and ODN 16 as template. Lanes 2-6 contain the extended products of primer extension reactions obtained using different *sp*-ODNs. Lane 1: 25-mer template 16, Lane 2: *sp*-ODN 5, Lane 3: *sp*-ODN 6, Lane 4: *sp*-ODN 7, Lane 5: *sp*-ODN 8 and Lane 6: *sp*-ODN 9.

adjacent strand. These stabilizing effects of *sp*-ODN triplexes were evident from absence of hysteresis in melting and cooling cycle and weak stabilizing influence on *sp*-ODN triplex by added salts.

Substitutions/modifications in the interior of ODNs (in the case of *sp*-ODN and *teg*-ODN) are less stabilizing than substitutions towards the 3'/5' terminii. This is in agreement with nucleation-zipping model for association-dissociation of duplex,³³ also valid for triplexes¹² with nucleation involving 3-5 base triplets which governs the rate determining step for association of third strand with duplex. The formation of triplex structures by association of a homopurine -homopyrimidine duplex with a third strand resembles in many aspects the formation of a duplex by association of two complementary single strand. According to the nucleation-zipping model the double-helix formation begins with two or three bases pairing to form a critical intermediate and unpairing in rapid but unfavorable equilibrium. The so-called nucleation can take-place anywhere in the sequence provided the bases are in the proper alignment.³⁴ Since nucleation phase is the rate-limiting step in the association reaction, mismatch/modification in the interior of the triplex does not affect the rate of association but it increases the dissociation rate of the triplex.¹² The decrease in T_m of triplexes, **7*2:1** and **13*2:1**, having modifications at the middle of the third strand is therefore due to an enhancement in the dissociation rate when compared to the corresponding terminal modified triplexes.

In case of *teg*-ODN triplexes lacking a polycationic side chain, the triplex stability arises from a fine tuning of microenvironment by the polyether side chain in terms of desolvation, facilitating a hydrophobic interaction. This is based on the effect of strongly hydrated, antichaotropic agent Na₂SO₄ which enhanced T_m of *teg*-ODN triplexes in contrast to the weakly hydrated chaotropic agent such as NaClO₄ which destabilized the *teg*-ODN triplex. The result is consistent with a hydrophobic nature of interaction of *teg* side chain with DNA duplex.³¹ In contrast to the ionic interaction of *sp*-ODN, hydrophobic binding in *teg*-ODN is weaker as realized from a lower stabilizing and a greater hysteresis effect, but nevertheless significantly exists since *teg*-ODNs form triplexes with a better stability compared to unmodified controls.

3.6. CONCLUSIONS

In summary, the present studies on triple helices employing spermine and ω,ω' -dideoxydiaminotetraethyleneglycol conjugated ODNs as third strand showed remarkable stabilization at physiological pH, the conditions under which ODNs containing dC and 5-Me-dC fail to show triplex formation. Site-specific conjugation of spermine in ODNs permits introduction of polycations at desired sites in ODN sequences, thereby imparting significant zwitterionic character to DNA. N3 protonation does not seem to be a requirement for triplex formation by *sp*-ODNs since the corresponding loss in stability is more than compensated for by spermine's favorable interactions with duplex DNA. The increased stability of *sp*-ODN triplets is also a consequence of favored association of third strand with the duplex. A lower net negative charge arising from multiple substitution may assist the cellular uptake of ODNs. The observed mismatch tolerance may also enlarge the scope of *sp*-ODN's applications in triplets.

The stability of *sp*-ODN triplets under low salt concentrations is mostly due to enhanced reassociation of duplex and third strand, accelerated by ionic interaction of conjugated cationic spermine with anionic phosphate backbone of the duplex and possible H-bonding interaction with bases in the adjacent strand. On the other hand, *teg*-ODNs stabilize triplets through hydrophobic desolvation. In contrast to the ionic interactions of *sp*-ODN, hydrophobic binding in *teg*-ODN is weaker as realized from a lower stabilizing and greater hysteresis effect. These results suggest that factors other than base stacking/interstrand H-bonding effects are significantly involved in triplex formation and stabilization.

3.7. MATERIALS AND METHODS

All chemicals used were of reagent quality or better grade. Base protected standard nucleoside phosphoramidites and 5'-O-DMT-nucleoside derivatised controlled pore glass supports (CPG) were purchased from Cruachem UK. T4 polynucleotide kinase from Boehringer Mannheim and 5'-[γ -³²P]ATP from Bhabha Atomic Research Center, Bombay were used for radiolabelling of oligonucleotides. All melting experiments were performed on a Perkin Elmer Lambda 15 UV/VIS spectrophotometer between the temperature range 5-80 °C.

3.7.1. Oligonucleotide synthesis, purification and labeling

All oligodeoxynucleotides (ODNs) were synthesized on 0.2/1.3 μ mol scale on a Pharmacia GA plus DNA synthesizer using CPG and nucleobase (A, G, C and T) protected 5'-O-(4,4'-dimethoxytrityl)deoxyribonucleoside-3'-O-[(N,N-diisopropylamino)- β -cyanoethyl-phosphoramidite] monomers. The solid phase synthesis protocol of ODNs is summarised in **Scheme 1**. The protected 5-Me-dC-N⁴-(spermine), dC-N⁴-(spermine) and 5-Me-dC-N⁴-(ω -aminotetraethyleneglycol) phosphoramidites (see *Chapter 2, section 2.2.3*, for the preparation) were incorporated at desired sites of ODN by following custom methods on the Pharmacia GA plus DNA synthesizer.

The synthesis report of ODN 8 is given below (Table 6) as a representative example. All oligonucleotides were purified by reversed phase FPLC on C18 column and purities rechecked on reverse phase HPLC using the buffer systems A: 5 % CH₃CN in 0.1 M triethylammoniumacetate (TEAA) and B: 30 % CH₃CN in 0.1 M TEAA using a gradient A to B of 1.5 %/min at a flow rate of 1.5 mL/min. The HPLC retention time for all the modified ODNs are given in Table 5 along with the unmodified counter part for comparison.

The purified oligonucleotides were labeled at the 5'-end with T4 polynucleotide kinase and 5'-[γ -³²P]ATP according to standard procedures.³⁵ The radiolabeled oligonucleotide samples were run on a 20 % polyacrylamide gel containing 7 M urea and

with Tris-borate-EDTA (pH 8.3) as buffer. Samples were mixed in formamide, heated to 70 °C for 5 min and then cooled on ice bath before loading on the gel. Autoradiograms were developed after 1 h exposure using an intensifying screen.

Table 5. HPLC Retention Time of ODNs

	ODN	Retention Time (min.)
1	3	10.31
2	5	10.87
3	6	10.73
4	7	10.82
5	8	11.38
6	9	11.57
7	11	11.86
8	12	11.65
9	13	11.84
10	14	12.08
11	15	12.22

3.7.2. Melting experiments

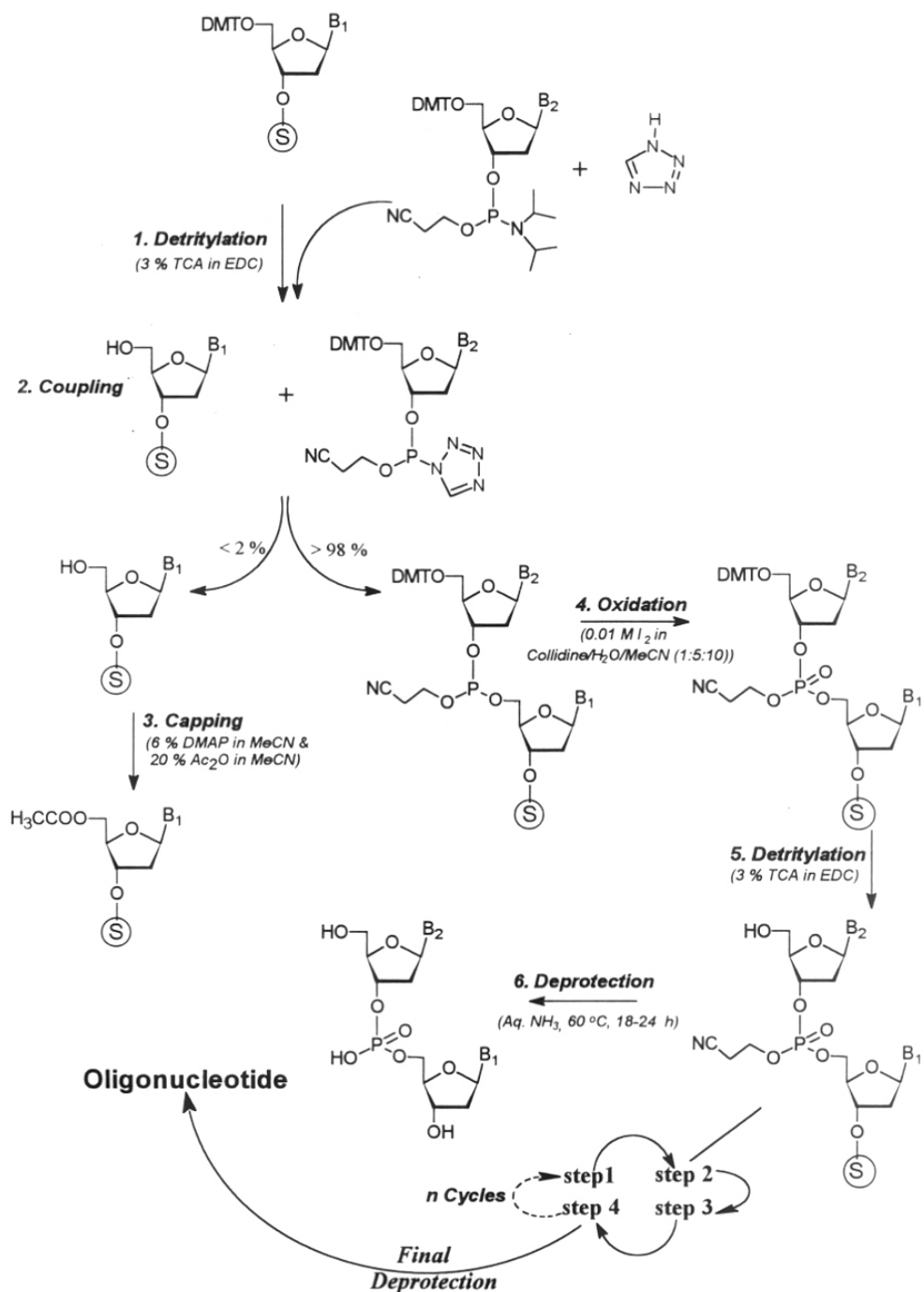
Duplex and triplex melting experiments were carried out in the buffer 25 mM Tris, pH 7.0-7.3, containing varying amounts of salts NaCl, Na₂SO₄, NaClO₄ in the presence or absence of MgCl₂ as mentioned in each case. 50 mM NaOAc, pH 5.5; 10 mM PIPES [piperazine-N-N'-bis(2-ethanesulphonic acid)], pH 6.0; and 25 mM Tris [2-Amino-2-hydroxymethylpropane-1,3-diol], pH 7.0 - 7.3 were used for pH dependent studies of triplexes. Appropriate oligonucleotides, each at a strand concentration of 1 μM based on UV absorbance of 260 nm calculated using molar extinction coefficients of dA = 15.4, dC = 7.3, dG = 11.7, T = 8.8 cm²/mmol were mixed and heated at 70 °C for 3 min, cooled to room temperature followed by overnight storage at 4 °C. The A₂₆₀ at various temperatures were recorded using Perkin Elmer Lambda 15 UV/VIS spectrophotometer, fitted with a water jacketed 5-cell holder and a Julabo temperature programmer with a heating rate of 0.5 °C/min over the range of 5-75 °C. Dry nitrogen gas was flushed in the spectrophotometer chamber to prevent moisture condensation at temperatures below 15 °C. The triplex dissociation temperature (T_m) was determined from the midpoint of the

first transition in the plots of fraction absorbance change versus temperature and were further confirmed by differential (dA/dT vs T) curves. The T_m values are accurate to ± 0.5 °C over the reported values. The reassociation of third strand with complementary duplex were studied by hysteresis experiments in which the samples were heated (0.5 °C/min) and maintained above triplex-duplex transition temperature for 10 min to achieve constant absorbance, followed by cooling (0.5 °C/min). The T_m of triplexes containing mismatches were similarly determined under identical conditions.

The UV-difference spectra were obtained using graphic software of Perkin Elmer Lambda 15 UV/VIS spectrophotometer by subtracting individual spectra of corresponding triplexes at pH 2.3, 5.3 and 7.3. All spectra were recorded at constant temperature (5 °C) in buffer containing Tris (25 mM) and NaCl (100 mM) with or without MgCl₂ (20 mM).

3.7.3. pH titrations

The pK_a of nucleosides dC and 5-Me-dC-N⁴-(spermine) incorporated into the oligonucleotides (**6** and **5**) were determined by UV titration of their aqueous solutions (1 mM) with aq. NaOH at 45 °C and the titration was monitored at 260 nm³ (see *Chapter 2, Section*). The pH stability curves of triple helices (**6*8:9**) and (**3*8:9**) were obtained at 4 °C by similar UV titration monitored at 260 nm.^{3a} All oligonucleotide samples for titration were prepared in aq. solutions containing 100 mM NaCl and 20 mM MgCl₂.



Scheme 1: Solid phase oligodeoxynucleotide synthesis.

DNA C-PAT

Gene Assembler Plus

Date : 2/07/1995
 Sequence : RAJ4
 Synthesis : RAJ4
 Scale : 1.3 micromole
 Sequence Length : 18
 Column : 1
 Final Detritylation : Yes
 Coupling Efficiency Threshold : 20 %

Pos	Base	Retention mins	Duration mins	Peak ht %FS	Acc Area %min	Last eff %	Ave eff %
18	T	0.62	1.00	3001	583.54	-	-
17	X	0.60	1.00	2962	591.78	-	-
16	T	0.59	1.00	2989	562.44	-	-
15	T	0.59	1.00	3001	564.07	100.3	100.0
14	T	0.60	1.00	3001	561.69	99.6	99.9
13	T	0.59	1.00	3001	550.21	98.0	99.3
12	T	0.59	1.00	3001	548.45	99.7	99.4
11	T	0.59	1.00	3001	549.87	100.3	99.6
10	C	0.55	1.00	3001	541.29	-	99.6
9	T	0.58	1.00	3002	541.12	99.2	99.5
8	T	0.61	1.00	3002	541.66	100.1	99.6
7	T	0.60	1.00	3001	537.93	99.3	99.5
6	T	0.59	1.00	3000	541.26	100.6	99.7
5	T	0.60	1.00	2892	532.89	98.5	99.5
4	T	0.60	1.00	2854	529.09	99.3	99.5
3	X	0.61	1.00	2445	473.22	-	-
2	T	0.61	1.00	2406	450.02	92.2	98.9
1	T	0.60	1.65	2373	485.72	107.9	99.6

Total synthesis yield from start = 93.5 %

Table 6. Solid-phase synthesis report of *sp*-ODN 8 on Pharmacia GA plus DNA synthesizer. X = 5-Me-dC-N¹-(spermine).

3.8. REFERENCES

1. Barawkar, D. A.; Kumar V. A.; Ganesh, K. N. *Biochem. Biophys. Res. Comm.* **1994**, *205*, 1665.
2. (a) Francois, J. C.; Saison-Behmoras, T.; Thuong, N. T.; Helene, C. *Biochemistry*, **1989**, *28*, 9617.
(b) Rajagopal, P.; Feigon, J. *Biochemistry*, **1989**, *28*, 7859. (c) Singleton, S. F.; Dervan, P. B. *Biochemistry*, **1992**, *31*, 10995. (d) Plum, G. E.; Park, Y. W.; Singleton, S. F.; Dervan, P. B.; Breslauer, K. J. *Proc. Natl. Acad. Sci. USA*, **1990**, *87*, 9436.
3. (a) Xodo, E. L.; Mazini, G.; Quadrifoglio, F.; Van der Marel, G. A.; van Boom, J. H. *Nucleic Acids Res.*, **1991**, *19*, 5625. (b) Manzini, G.; Xodo, L. E.; Gasparotto, D.; Quadrifoglio, F.; Gijs, A.; Van der Marel, van Boom, J. H. *J. Mol. Biol.* **1990**, *213*, 833.
4. Takeda, Y.; Samesima, K.; Nagano, K.; Watanabe, M.; Sugeta, H.; Kyogoko, Y. *Eur. J. Biochem.* **1983**, *130*, 383.
5. Barawkar, D. A. *Ph. D. thesis* titled “*Designer Oligonucleotides with Nucleobase Modification: Synthesis and Applications for Studying Molecular Recognition of Nucleic Acids*” submitted to the University of Poona, April, **1995**.
6. Inman, R. B. *J. Mol. Biol.* **1964**, *9*, 624.
7. Lavalle, L.; Fresco, J. R. *Nucleic Acids Research*, **1995**, *23*, 2692.
8. Mergny, J.-L.; Lacroix, L.; Han, X.; Leroy, J.-L.; Helene, C. *J. Am. Chem. Soc.* **1995**, *117*, 8887.
9. Greenberg, W. A.; Dervan, P. B. *J. Am. Chem. Soc.* **1995**, *117*, 5016.
10. Mergny, J. -L.; Sun, J. -S.; Rougee, M.; Garestier, T.; Barcelo, F.; Chomilier, J.; Helene, C. *Biochemistry*, **1991**, *30*, 9791.
11. (a) Fox, K. R.; Polucci, P.; Jenkins, T. C.; Neidle, S. *Proc. Natl. Acad. Sci. USA*, **1995**, *92*, 7887.
(b) Plum, G. E.; Pilch, D. S.; Singleton, S. F.; Breslauer, K. J. *Annu. Rev. Biophys. Biomol. Struct.* **1995**, *24*, 319.
12. Rougee, M.; Faucon, B.; Mergny, J. L.; Barcelo, F.; Givannangeli, C.; Garestier, T.; Helene, C. *Biochemistry*, **1992**, *31*, 9269.
13. Anderson, C. F.; Record Jr., M. T. *Ann. Rev. Phys. Chem.*, **1995**, *46*, 657.
14. (a) Feurstein, B. G.; Pattabiraman, N.; Marton, L. J. *Nucleic Acids Research*, **1990**, *18*, 1271. (b) Jain, S.; Zon, G.; Sunderalingam, M. *Biochemistry*, **1989**, *28*, 2360. (c) Haworth, I. S.; Rodger, A.; Richards, W. G. *Proc. Royal. Soc. Lon.*, **1991**, *244*, 107. (d) Hashimoto, H.; Nelson, M. G.; Switzer, C. *J. Org. Chem.*, **1993**, *58*, 4194. (e) Hashimoto, H.; Nelson, M. G.; Switzer, C. *J. Am. Chem. Soc.*, **1993**, *115*, 7128.
15. Tung, C. H.; Breslauer, K. J.; Stein, S. *Nucleic Acids Res.*, **1993**, *21*, 5489.

16. Manning, G. S. *Acc. Chem. Res.*, **1979**, *12*, 443.
17. Huang, C. Y.; Miller, P. S. *J. Am. Chem. Soc.*, **1993**, *115*, 10456. (b) Xiang, H.; Soussou, W.; McLaughlin, L. W. *J. Am. Chem. Soc.*, **1994**, *116*, 11155.
18. Huang, C. Y.; Cushman, C. D.; Miller, P. S. *J. Org. Chem.* **1993**, *58*, 5048.
19. Volker, J.; Klump, H. H. *Biochemistry*, **1994**, *33*, 13502.
20. Ma, C.; Bloomfield, V. A. *Biopolymers*, **1995**, *35*, 211.
21. Radhakrishnan, I.; Patel, D. J. *Biochemistry*, **1994**, *33*, 11405.
22. Tasaki, K. *J. Am. Chem. Soc.* **1996**, *118*, 8459.
23. Zimmerman, S. B.; Trach, S. O. *Biopolymers* **1990**, *30*, 703.
24. Zimmerman, S. B.; Murphy, L. D. *Biopolymers* **1992**, *32*, 1365.
25. Spink, C. H.; Chaires, J. B. *J. Am. Chem. Soc.* **1996**, *117*, 12887.
26. Louie, D.; Serwer, P. *J. Mol. Biol.* **1994**, *242*, 547.
27. (a) Volker, J.; Botes, D. P.; Lindsey, G. G.; Klump, H. H. *J. Mol. Biol.* **1993**, *230*, 1278. (b) Wilson, W. D.; Hopkins, H. P.; Mizan, S.; Hamilton, D. D.; Zon, G. *J. Am. Chem. Soc.* **1994**, *116*, 3607.
28. Maher, L. J. III; Dervan, P. B.; Wold, B. J. *Biochemistry* **1990**, *29*, 8820. (b) Singleton, S. F.; Dervan, P. B. *Biochemistry* **1993**, *32*, 13171.
29. (a) Bloomfield, V. A. *Current Opinion in Structural Biology* **1996**, *6*, 334, (b) Melander, W.; Horvath, C. *Arch. Biochem. Biophys.* **1977**, *183*, 200.
30. Muller, N. *Acc. Chem. Res.* **1990**, *23*, 23.
31. Ding, W.; Ellestad, G. A. *J. Am. Chem. Soc.* **1991**, *113*, 6617.
32. Joyce, C. M.; Grindley, N. D. F. *Proc. Natl. Acad. Sci. USA.* **1983**, *80*, 1830.
33. Porschke, D.; Eigen, M. *J. Mol. Biol.* **1971**, *62*, 361.
34. Craig, M. E.; Crothers, D. M.; Doty, P. *J. Mol. Biol.* **1971**, *62*, 383.
35. (a) Sambrook, J.; Fritsch, E. F.; Maniatis, T. in *Molecular Cloning: a Laboratory Manual*. **1989**, Cold Spring Harbor, NY. (b) Koh, J. S.; Dervan, P. B. *J. Am. Chem. Soc.* **1992**, *114*, 1470.

CHAPTER 4.

**CONFORMATIONALLY RESTRAINED CHIRAL ANALOGUES OF
SPERMINE: CHEMICAL SYNTHESIS AND
IMPROVEMENTS IN DNA TRIPLEX STABILITY**

4.1. INTRODUCTION:

The linear polyamines - putrescine, spermidine and spermine (**1**) are biological cations ubiquitously found in all cells with a diverse role in physiological processes.¹ These range from stabilization/modulation of membrane function and mitochondria,¹ facilitation of DNA transfection by phage,² to regulation of cell growth and differentiation.³ They play an important role in proliferative processes, in particular, neoplastic growth and chemical carcinogenesis.⁴ *In vitro*, polyamines affect many enzymatic systems such as phosphatidylinositol-G and adenylate cyclase-G protein pathways, post translational modification of proteins by transglutaminases⁵ and inhibit voltage activated ion channels.⁶ The high level of polyamines noticed in transformed cells has led to design of their analogues as inhibitors of polyamine biosynthesis enzymes such as ornithine decarboxylase and S-adenosylmethionine decarboxylase.⁷ The modulatory activity of spermine on N-methyl-D-glutamate (NMDA) receptor has potential for application of polyamine analogues in therapy of neurological diseases such as epilepsy.⁸ Polyamine analogues are also emerging as serious therapeutic options for development of potent new antidiarrheals, in particular, AIDS related diarrhea.⁹ The wide therapeutic potential of polyamines has led to design, synthesis and biological evaluation of a large number of their analogues towards understanding structure-activity relationships.¹⁰ These studies have pointed out that polyamine analogues at tetramine level must be charged to be recognized by the cell and analogues with low pK_as that are poorly protonated at pH 7.0 do not compete efficiently with biogenic amines for uptake.

4.1.1. Polyamine-DNA interaction

The detailed mechanisms by which polyamines bind to DNA are far from clear, but it is known that they bind to B-DNA and produce a conformational change.¹¹ Spermine at physiological pH induces helical bending and leading ultimately to DNA condensation into toroidal particles.¹¹ Polyamine induces B-Z transition and stabilize Z-DNA.¹² Two distinct

modes of spermine complexation to Z-DNA hexamer d(CGCGCG)₂ have been observed in crystal structure: one type interacts with phosphate backbone and the other depending on spermine-base pair interactions.¹³ Another X-ray structure of d(GTGTACAC)₂ in A form of DNA has spermine bound deep in the major groove of the helix.¹⁴ In solution, spermine bind more strongly to poly(dG-dC) than to the equivalent poly(dA-dT) helix.¹⁵ Electric dichroism measurements have indicated that spermine induces a bend in poly(dA-dT) while a stiffening of helix axis in poly(dG-dC)¹⁶ and such a model is supported by hydrogen-deuterium exchange rate measurements upon spermine complexation.¹⁷ Molecular mechanics calculations of spermine binds to a number of solvated DNA helices suggests a model in which spermine remains in a cross-major groove binding mode for AT-sequences (Figure 1a) while for CG-sequences binding is via specific ligand-base pair hydrogen bond formation along the major groove (Figure 1b).¹⁸

Spermine is known to promote triplex stability when externally added¹⁹ in millimolar concentration as well as upon covalent conjugation to sugar²⁰ or nucleobase residues.²¹ In eukaryotes, spermidine and spermine are present in millimolar concentration and may be as high as 5 mM in nucleus.²² Exogenous polyamines and their analogues are readily transported into the cell.²³ Natural polyamines favor triplex DNA formation in neutral pH and it was suggested that polyamines could be important in stabilizing triplex DNA in chromosomal structures.^{19a} Since the negative charge density of a triplex is higher than that of a duplex, polyamine should bind more tightly to the former and shift the equilibrium in favor of triplex formation. In a series of putrescine homologues, H₂N(CH₂)_nNH₂ where n = 2-6 (n = 4 for putrescine), H₂N(CH₂)₃NH₂ was the most effective diamine to stabilize poly (dA).2poly(dT) triplex.^{19b} Among a series of triamines H₂N(CH₂)₃NH(CH₂)_nNH₂ (where n = 2-8), spermidine (n = 4) was the most effective triplex stabilizing agent. In contrast, effect of these compounds on duplex DNA stabilization were relatively insensitive to change in length of the methylene bridging region. Chemical structural effects play an important role in stabilizing the poly(dA).2poly(dT) triplex, whereas poly(dA).poly(dT) duplex stabilization is largely governed by the number of positive charges on the polyamine.^{19b} The stabilization

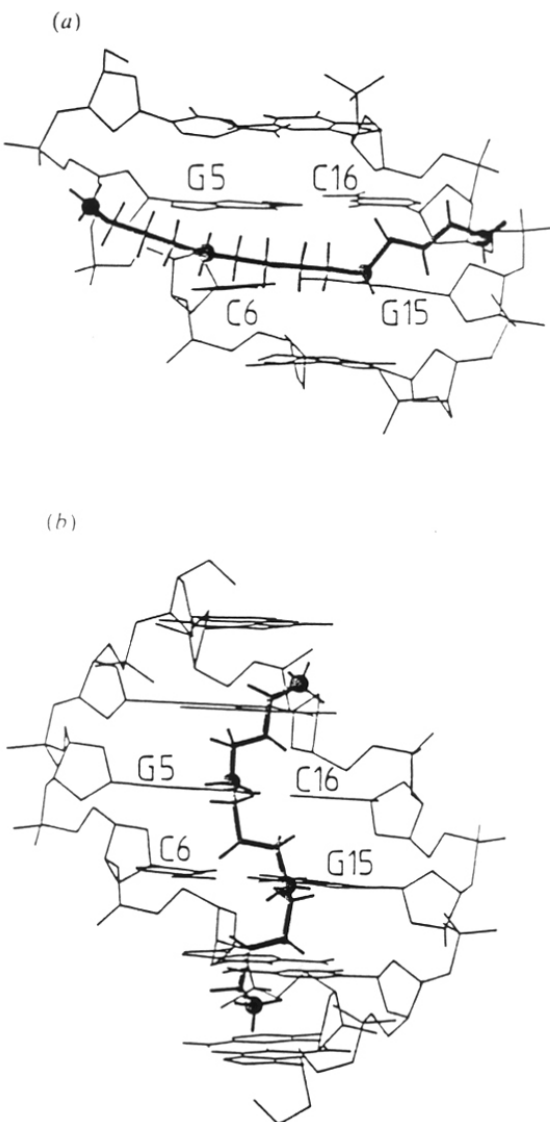


Figure 1. Minimized structures showing the complexation of spermine to the major groove of d(CGCGCGCG)₂ in the cross-groove (a) and down-groove (b) binding sites. The spermine molecule is represented by thickened lines with circles indicating N atoms of the protonated amine groups.

of DNA triplex by polyamines is particularly important because of the ubiquitous presence of these molecules and the feasibility of modifying their structural features to provide efficient ligands to interact with and stabilize unusual structures of DNA.

4.1.2. Structurally modified polyamine analogues

Several structural modifications made to the polyamine backbone include variation in the number and distance between nitrogens²⁴ (Figure 2, **a - c**), terminal N-substitutions of varying sizes⁹ (Figure 2, **d - i**), and rigidification via interconnection of secondary amines (cyclopolyamines) based on cyclopentrescine core²⁵ (Figure 2, **k - m**) or by introducing aromatic moiety into the polyamine backbone¹⁵ (Figure 2, **n**). Bisguanidine analogues of spermine have also been reported²⁶ (Figure 2, **p, q**) as better DNA duplex and triplex stabilizing candidates compared to spermine. Most of these chemical modifications are through N-substitutions and are achiral (except, **j** in Figure 2). Since many of the polyamine receptor sites (nucleic acids, membranes) are chiral in nature, it was reasoned that introduction of asymmetry into polyamine backbone may be beneficial to their activity. This and previous studies on stabilization of DNA triplexes at physiological conditions through covalent linking of spermine (*Chapter 3*) to oligonucleotides prompted synthesis of chiral spermine analogues and study their interaction with nucleic acids.

4.1.3 Design of pyrrolidyl polyamines: A rationale

These analogues are derived from spermine **1** by introducing a bridge of CH₂-NH between the carbon atoms 1 and 3 of the central tetramethylene fragment as shown in **Scheme 1** to generate a five membered pyrrolidine ring (**2**). This makes the molecule chiral with creation of two asymmetric centers (C2 and C4) and hence 2 pairs of diastereomers (*cis* 2*S*,4*S*; 2*R*,4*R* and *trans* 2*S*,4*R*; 2*R*,4*S*) with a simultaneous introduction of one additional nitrogen atom.

A retrosynthetic analysis reveals that the four possible isomers can be derived from commercially available *trans*-4-hydroxy-L-proline²⁷ (**3**, **Scheme 1**). In addition to the interaction with DNA, these newer analogues of spermine with an additional N atom may find potential applications as drugs and/or drug delivery agents.

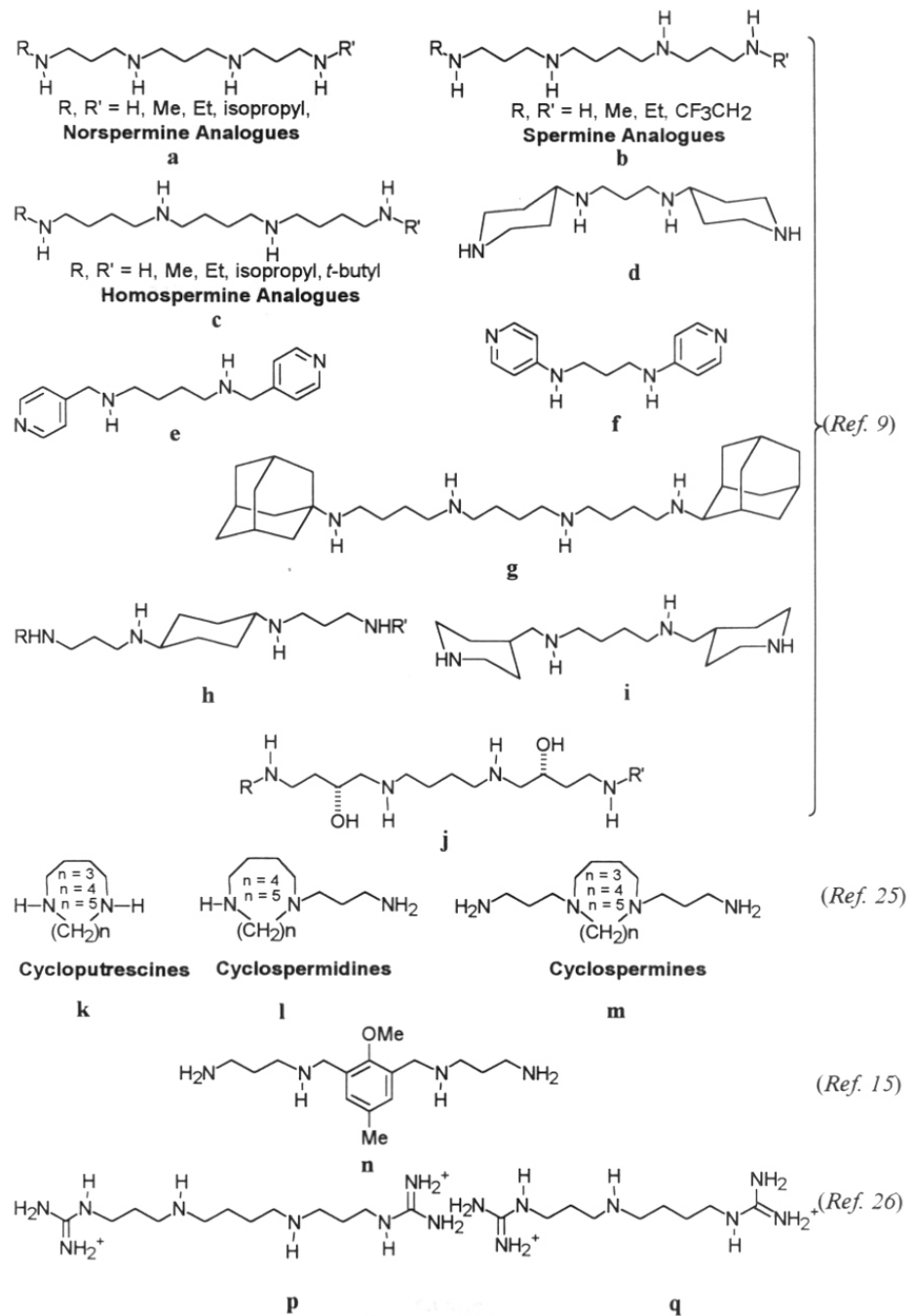
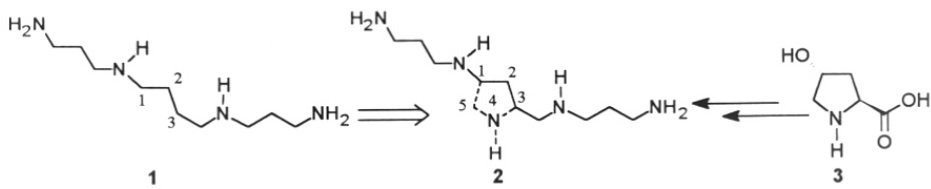
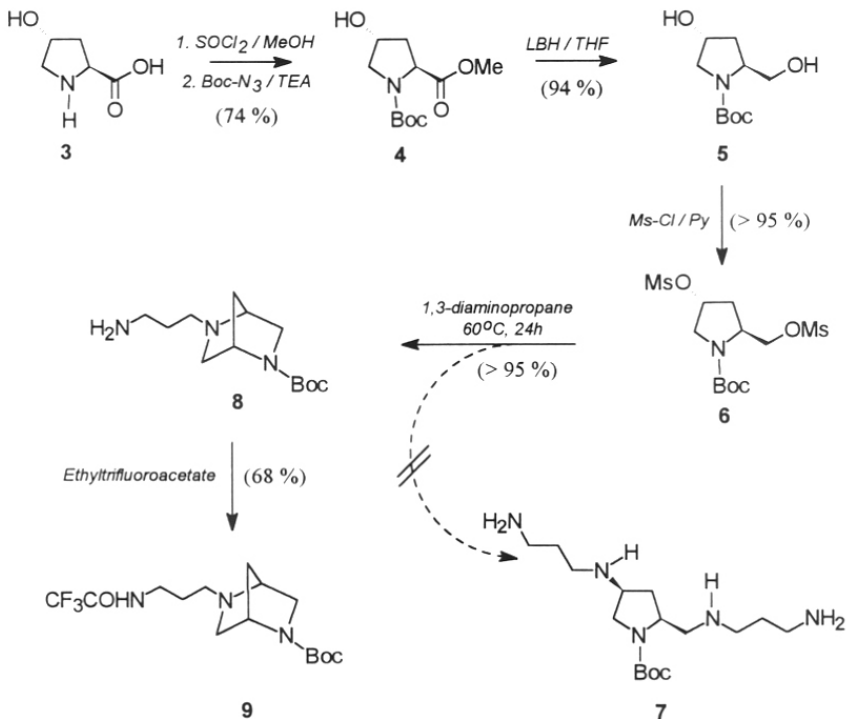


Figure 2

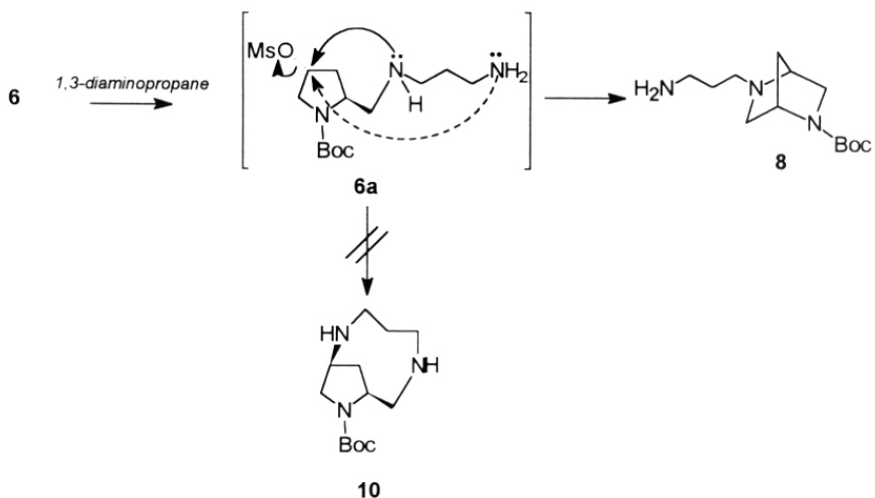
**Scheme 1**

4.2. SYNTHESIS OF PYRROLIDYL POLYAMINES

trans-4-Hydroxy-L-proline (**3**) on treatment with thionylchloride (1.2 eq.) in methanol followed by protection of the ring nitrogen as *t*-Boc through reaction with *t*-butoxycarbazine, furnished *trans*-4-hydroxy-N-(*t*-butoxycarbonyl)-L-proline methyl ester (**4**, Scheme 2).²⁸

**Scheme 2**

The reduction of this methyl ester with lithiumborohydride (LBH) in THF gave *trans*-4-hydroxy-L-prolinol (**5**) in quantitative yield.²⁹ This upon mesylation afforded the dimesylate **6** which was subsequently treated with neat 1,3-diaminopropane at ambient temperature for 4 h and then at 60 °C for 24 h. Surprisingly the resulting product was not the expected polyamine **7** but instead, it was identified as the bicyclic compound, *1S,4S*-5-(3-aminopropyl)-2-*tert*-butoxycarbonyl-2,5-diazabicyclo-[2.2.1]-heptane (**8**). A plausible mechanism for the formation³⁰ of the bicyclic compound is shown in Scheme 3.



Scheme 3

The initial reaction of 1,3-diaminopropane with the more reactive primary mesylate in **6** leads to the intermediate **6a**, which undergoes an intramolecular cyclization to form **8**. In the intermediate **6a**, the leaving group (4-O-mesylate) and the newly formed secondary N-atom are *trans* to each other and consequently the mesylate function is easily displaced in an S_N2 fashion resulting in the formation of **8**. The intermediate **6a** can also in principle lead to the formation of the macrocyclic analogue **10** which however was not observed in this case. A possible explanation for the exclusive formation of **8** could be that the

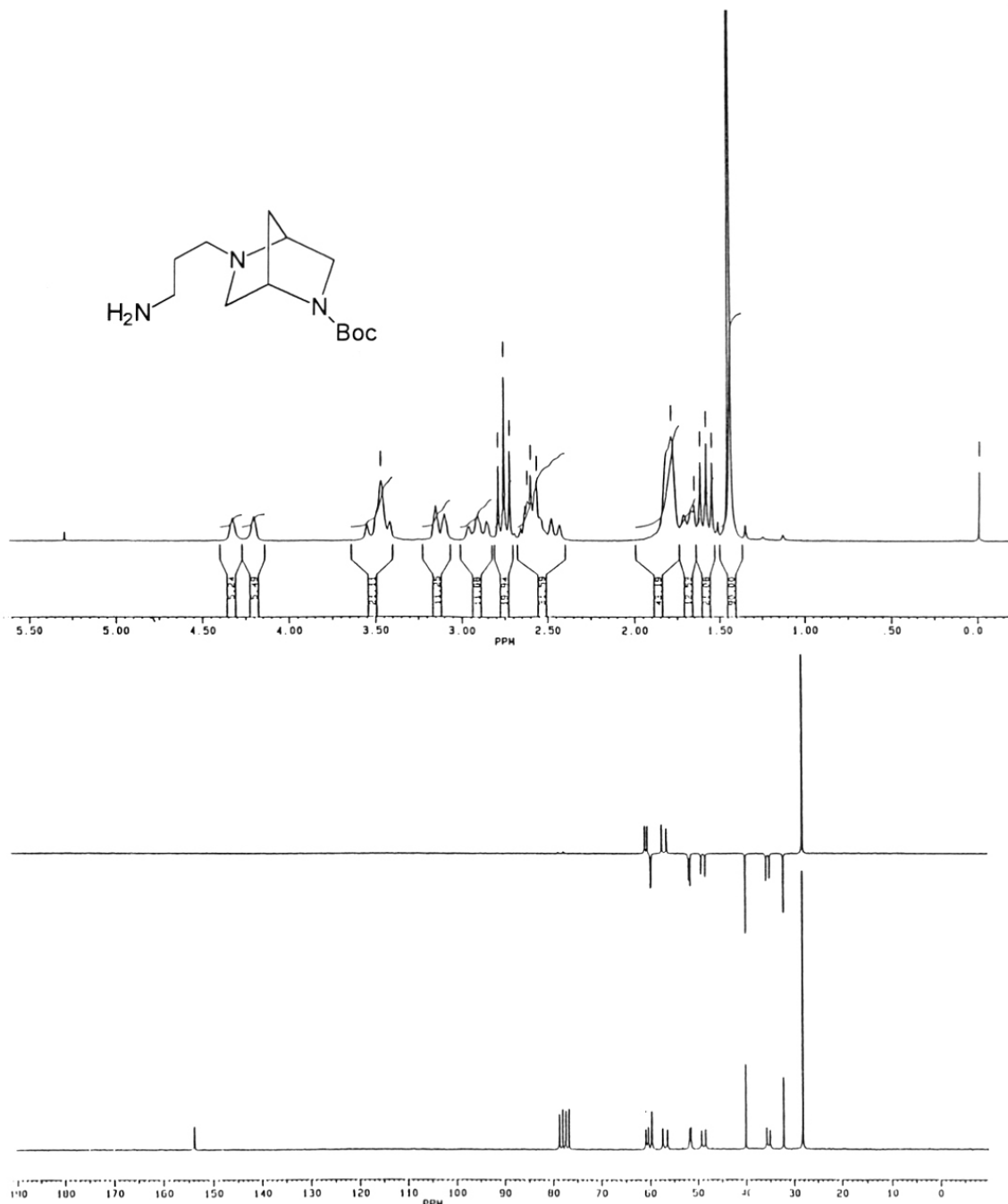


Figure 3. ¹H ($\text{CDCl}_3 + \text{D}_2\text{O}$) and ¹³C NMR (CDCl_3) spectra of the bicyclic compound 8

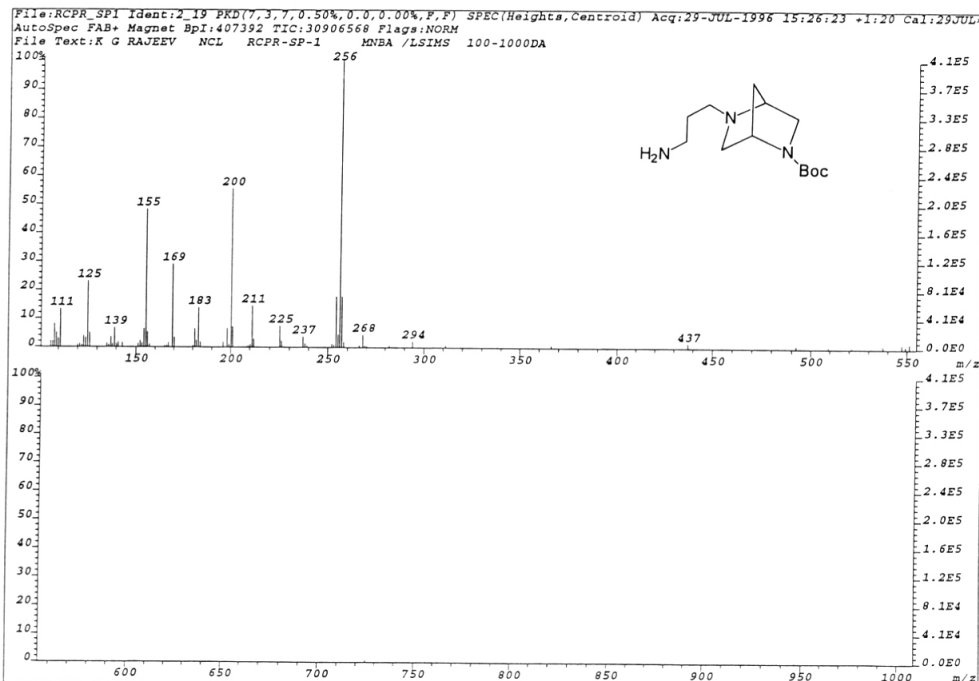


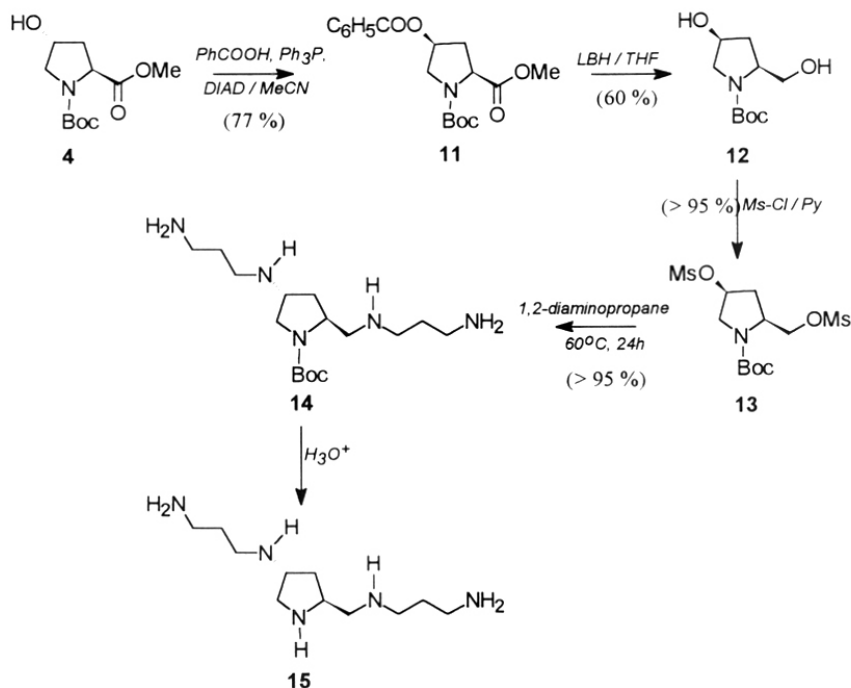
Figure 4. FAB Mass spectrum of the bicyclic compound 8.

secondary N-atom being in close proximity and in a favorable *trans* orientation with respect to the leaving group triggers a rapid S_N2 displacement before the remote primary amine function could take part in the reaction. The ¹H NMR spectrum (Figure 3a) in CDCl₃ (after D₂O exchange) shows a distinct triplet of the H₂N-CH₂ of the side chain of 8. The appearance of such a triplet in the ¹H NMR spectrum of 10 is impossible which supports the formation of 8 instead of 10 and additional evidence was sought from mass spectrum (Figure 4). The reaction of 8 with ethyltrifluoroacetate in methanol gave the monotrifluoroacetamide 9 in moderate yield. ¹H and ¹³C NMR spectra of 9 further confirmed the structure of the bicyclic compound 8. The FAB mass of compound 9 gave the expected molecular ion peak at 352 (M⁺ + 1) for the monotrifluoroacetamide which unambiguously proved the formation of the bicyclic compound.

The synthesis of two of the four stereo isomers (**15** and **21**) of polyamine **2** could be achieved by inversion of configuration at C4 or C2 of **3**. The inversion of configuration at the asymmetric center C4 (**Scheme 4**) or C2 (**Scheme 5**) in **3** results in *cis* isomers of 4-hydroxyproline. The reduction of the carboxy group as described above, after inversion, leads to *cis*-4-hydroxy-L-prolinol (**12**) or *cis*-4-hydroxy-D-prolinol (**18**). These diols on mesylation and subsequent treatment with neat 1,3-diaminopropane gave the desired polyamines **15** and **21** as shown in **Scheme 4** and **Scheme 5**. As in the case of the *trans*-mesylate **6**, the amine first replaces primary mesylate but the *cis* - configuration of the resulting secondary mesylate disfavors intramolecular substitution. Consequently, intermolecular substitution at C4 follows eventually by another incoming nucleophile (1,3-diaminopropane) which is present in large excess.

The successful purification of the highly water soluble amines **14** and **20** was achieved under non-aqueous conditions. After reaction of the *cis*-dimesylates **13** and **19** with neat 1,3-diaminopropane the excess diamine was removed from the reaction mixture under vacuum. Anhydrous sodium sulfate was added to the residue and the mixture was washed several time with small amount of dry ethylacetate. The ethylacetate extracts were combined and concentrated to a pale yellow oil in good yield. The structure and purity of the polyamines **14** and **20** were confirmed by NMR and Mass spectrometry. The 2*S*,4*R*

isomer, 14 gave an optical rotation of $-45.9 \pm 0.5^\circ$ ($[\alpha]_D^{25}$, $c = 0.64$) in methanol and that of its enantiomer 20 (*2R,4S* isomer) was $+45.3 \pm 0.5^\circ$ ($[\alpha]_D^{25}$, $c = 0.64$) in methanol. The complete displacement of the mesylates were confirmed by absence of signals due to the methyl group of mesylate in the ^1H NMR spectrum (Figure 5) of the amine recorded after anhydrous sodium sulfate treatment and subsequent washing with dry ethylacetate.



Scheme 4

The reaction of **4** with benzoic acid under Mitsunobu condition³¹ (benzoic acid, triphenylphosphine and diisopropylazodicarboxylate, DIAD) gave the *cis*-4-O-benzoyl-N-(*t*-butoxycarbonyl)-L-proline methyl ester (**11**, **Scheme 4**) which on treatment with LBH in dry THF gave the *cis*-diol **12** in moderate yield. The mesylation of the diol **12** in pyridine gave the dimesylate **13** which was reacted with neat 1,3-diaminopropane to yield the polyamine **14**. This was characterized by NMR and Mass spectroscopy (Figure 5 and Figure 6). The removal of *t*-Boc protection of the ring N-atom in **14** to get the free amine

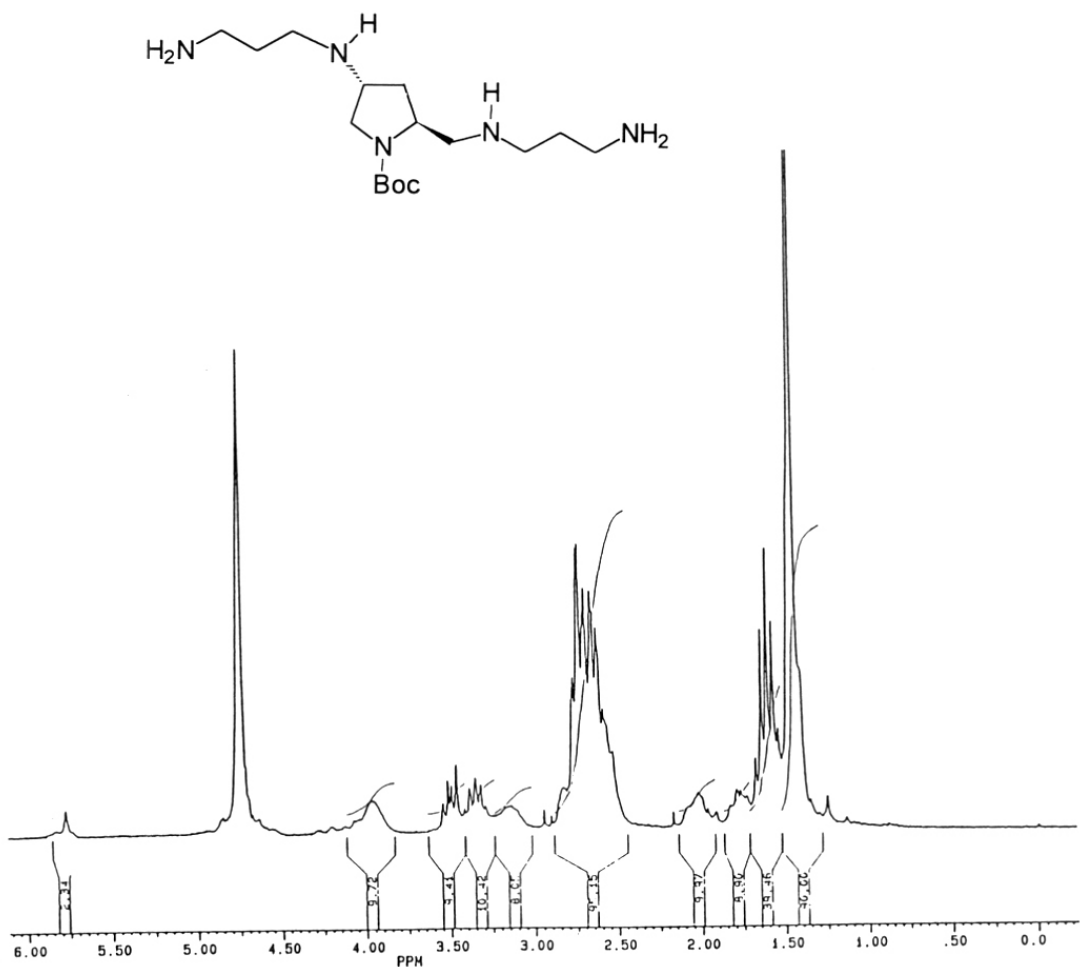


Figure 5. ^1H NMR spectrum of the amine 14 in CDCl_3 after D_2O exchange.

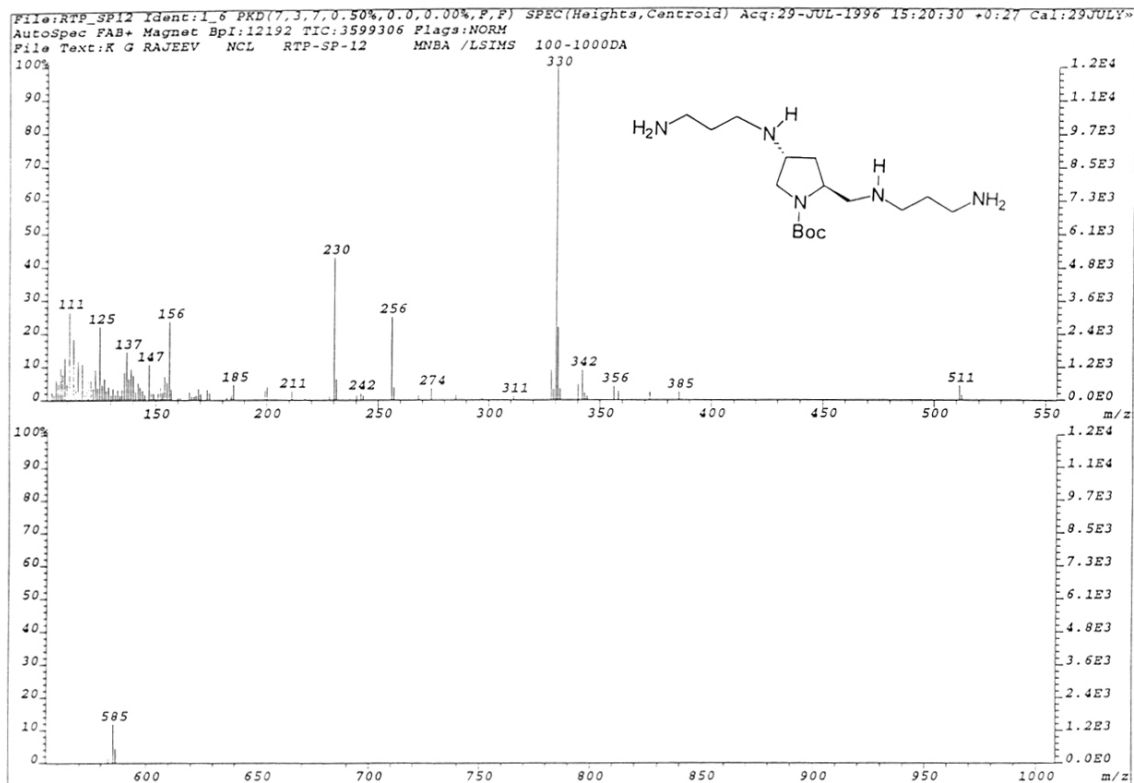


Figure 6. FAB Mass spectrum of amine 14.

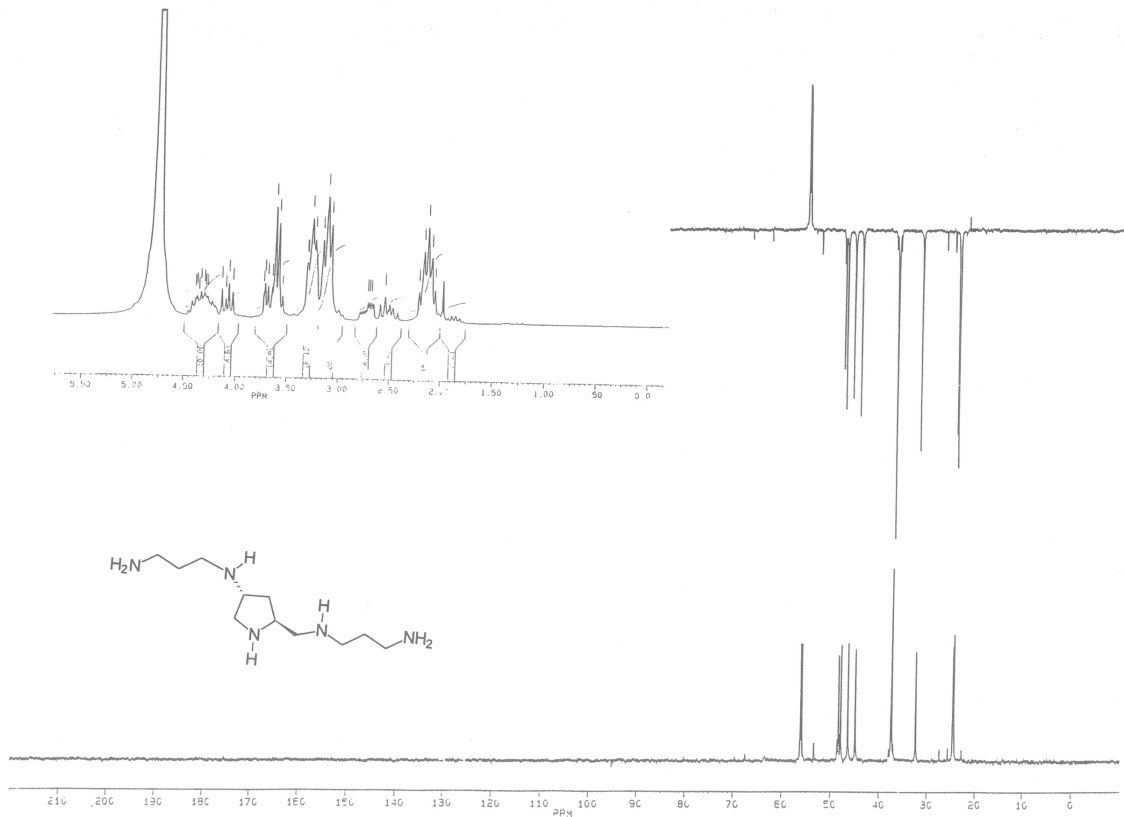
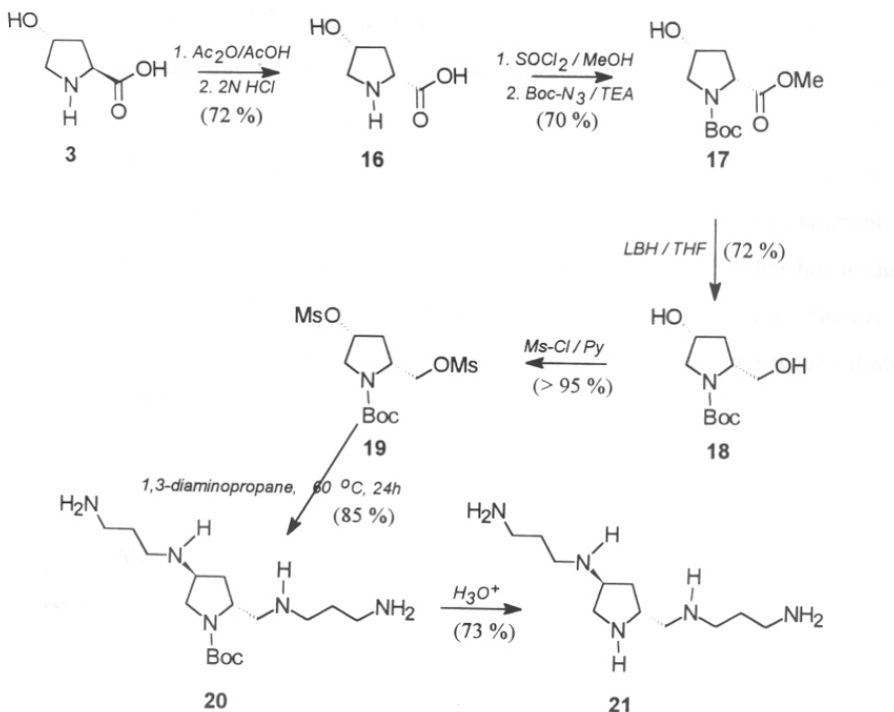


Figure 7. ¹H and ¹³C NMR spectra of pentahydrochloride salt of the amine 15.

15 (as its pentahydrochloride salt) was achieved by treatment with 5N HCl and was characterized by usual spectroscopic technique (Figure 7). Attempts to completely deblock the ring N-atom of the Boc protected amine, 14, under non-aqueous conditions by passing dry HCl gas through a solution of 14 in dry dioxane was unsuccessful. The free amines present in the compound formed hydrochloride salt which immediately precipitated from the reaction mixture with partial deprotection of the *t*-Boc function.

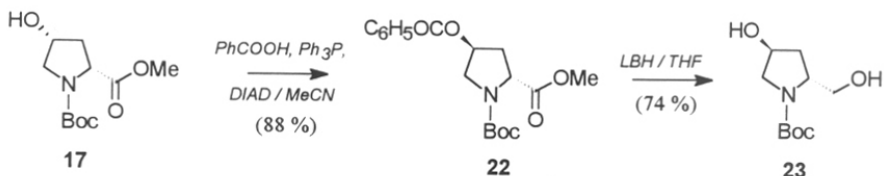


Scheme 5

The epimerization²⁹ of *trans*-4-hydroxyproline (**3**) by acetic anhydride/acetic acid treatment followed by reflux in 2N HCl gave *cis*-4-hydroxy-D-proline (**16**) in high optical purity (Scheme 5) as confirmed by ¹³C NMR spectrum which showed single peaks for each C-atom and by optical rotation. The synthesis of polyamine **20** and its

pentahydrochloride salt **21** were accomplished from *cis*-4-hydroxy-D-proline (**16**) as described above.

To check the optical purity of the C4 inverted L-proline derivative 11, the same inversion reaction³¹ on the methyl ester of *cis*-4-hydroxy-D-proline derivative 17 was carried out under identical conditions to get *trans*-4-O-benzoyl-N-(*t*-butoxycarbonyl)-D-proline (22) as shown in **Scheme 6**. The ¹H NMR spectra of 4-O-benzoates, 11 and 22, (Figure 8) showed distinct differences in position and pattern of the C3-protons but the ¹³C NMR spectra did not show any noticeable difference (Figure 9), except slight variations in their rotameric population. The reduction of the benzoate 22 with LBH in dry THF gave *trans*-4-hydroxy-D-prolinol (23). The optical rotation of the diol as compared with the diols 5, 12 and 18 exhibited a good correlation in terms of sign and magnitude. The ¹H NMR spectra (Figure 10) of diasteromeric diols differ from each other but in the ¹³C NMR spectra only a minor variation of the rotameric population was seen. The *cis* - diols were isolated as solids having melting points close to 90 °C whereas the *trans* - diols were isolated as viscous liquids.



Scheme 6

An attempt was made to convert the *trans*-mesylate 6 into the *cis*-diiodide 24 by refluxing 6 and sodium iodide (10 times excess) in dry acetone.^{30,32} The reaction was complete after 24h of reflux as evident from TLC. However, the reaction proceeded with racemization. It is likely that iodide ion being both a good leaving group and a good nucleophile may displace the initially formed iodide by a second iodide ion during the course of the reaction (Scheme 7).

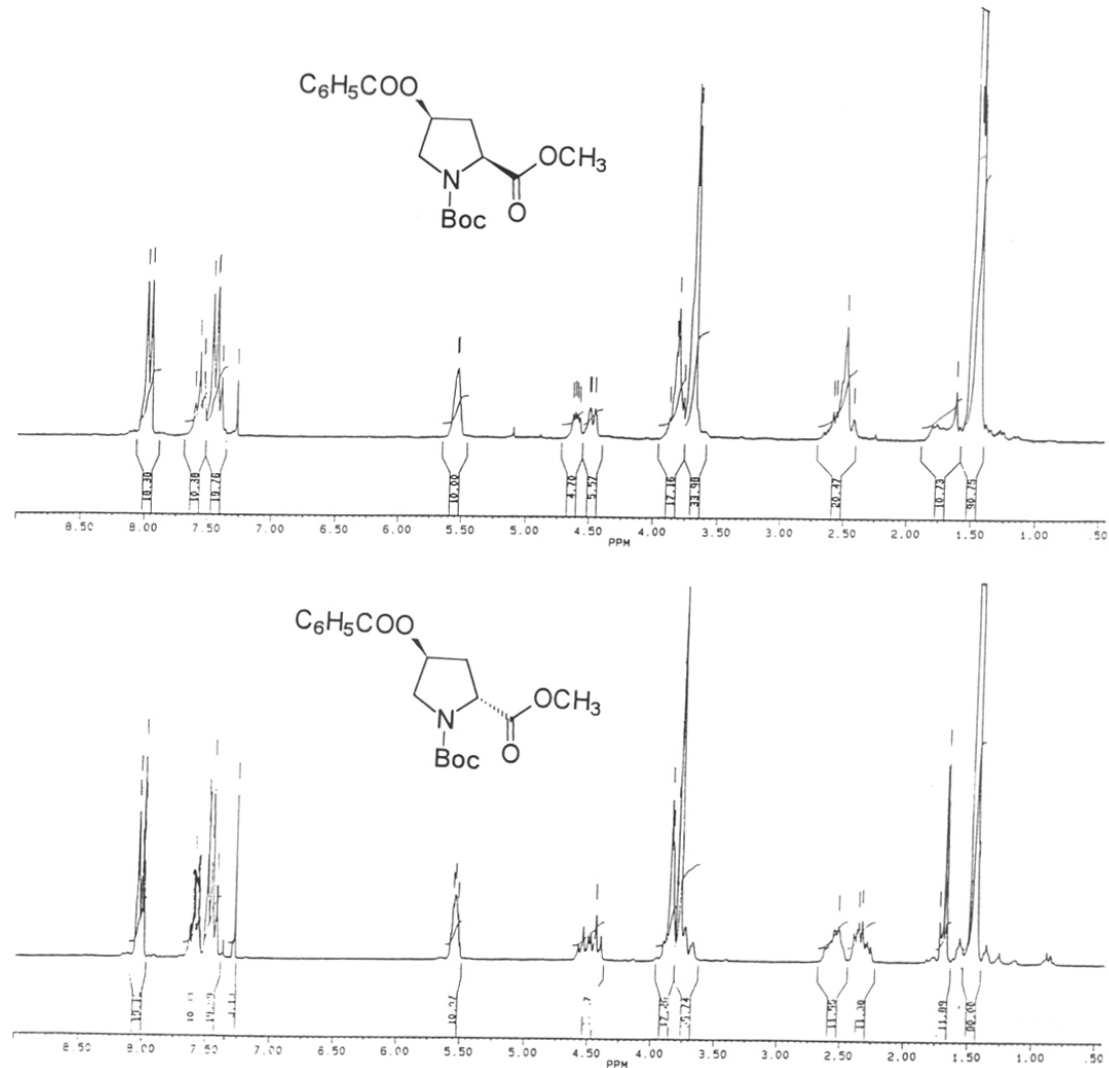


Figure 8. ^1H NMR spectra of 4-O-benzoates, **11** (a) and **22** (b) in CDCl_3 .

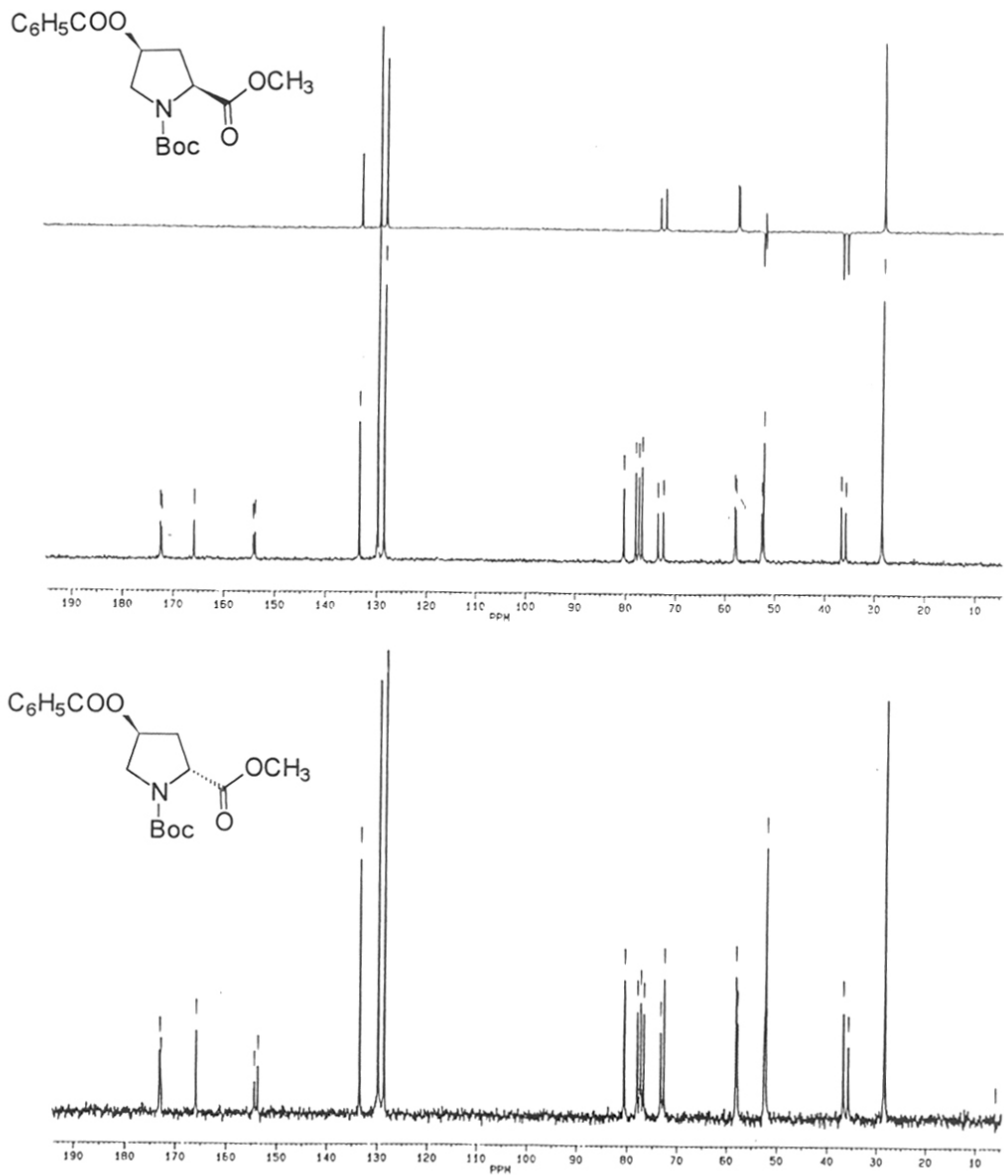


Figure 9. ^{13}C NMR spectra of 4-O-banzoates, 11 (a) and 22 (b) in CDCl_3 .

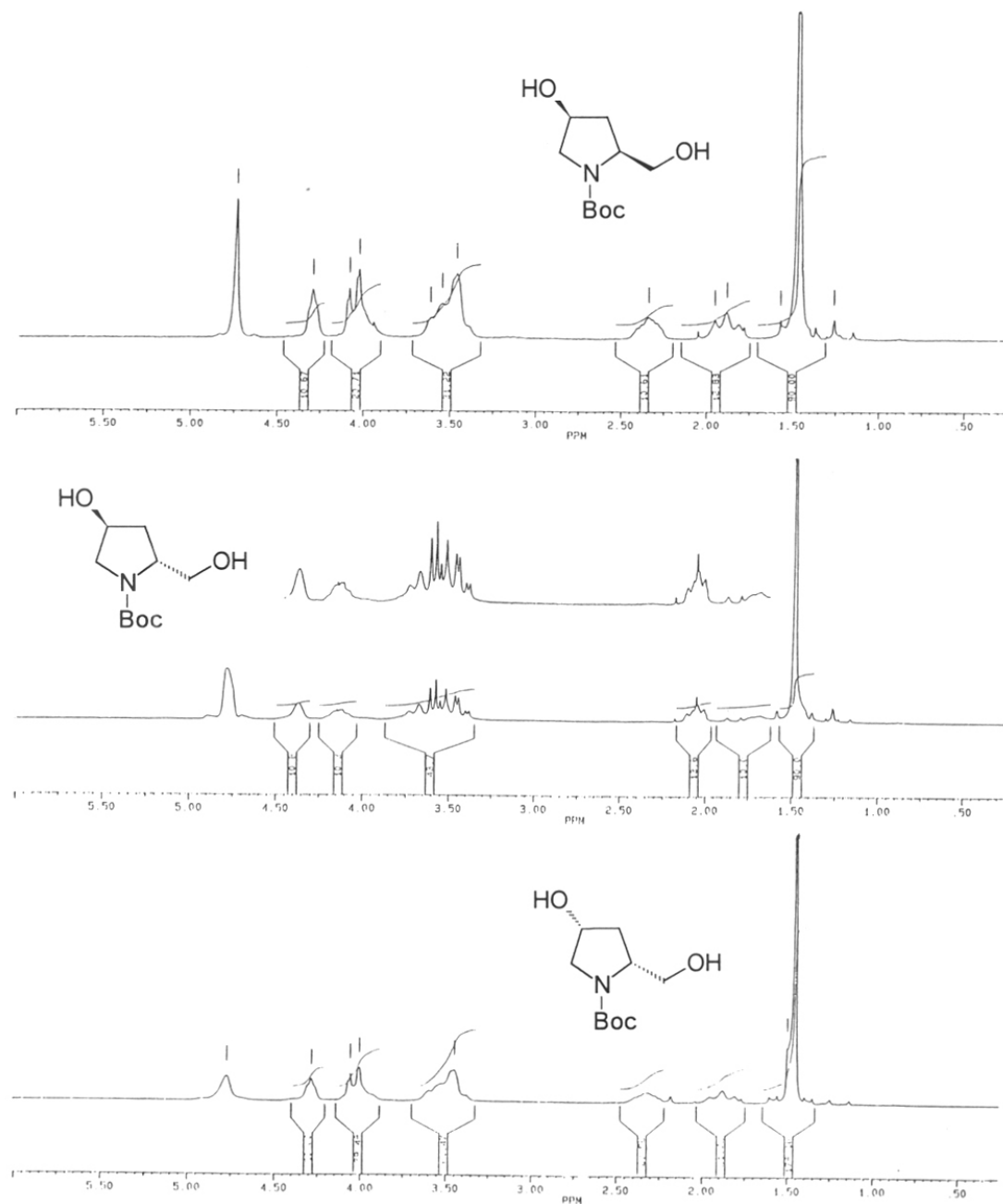
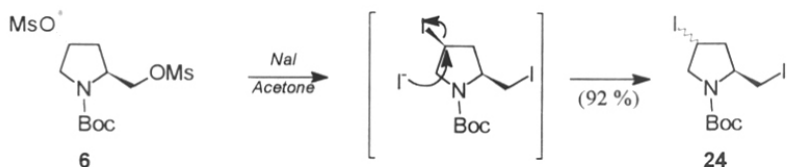


Figure 10. ^1H NMR spectra of diols 12 (a), 23 (b) and 18 (c) in CDCl_3 after D_2O exchange.

This cascade of bimolecular substitution reactions by iodide ions might have led to racemization at C4. S_N1 mode of substitution can also in principle lead to racemization at C4. The ¹H NMR spectrum of **24** showed two separate peaks (in the ratio 7:3) for one of the C3-hydrogens (see Figure 11) which indicates racemization at C4. The racemization at C4 was further confirmed by ¹³C NMR spectroscopy. Due to the existence of rotameric structures, most of the optically pure hydroxy-proline derivatives give two sets of peaks for the ring carbons in their ¹³C NMR spectra and the relative intensity of these peaks depends on the population of rotamers present. In the ¹³C NMR spectrum of **24**, the ring carbons appeared as multiplets which again clearly shows the racemization at C4.



Scheme 7

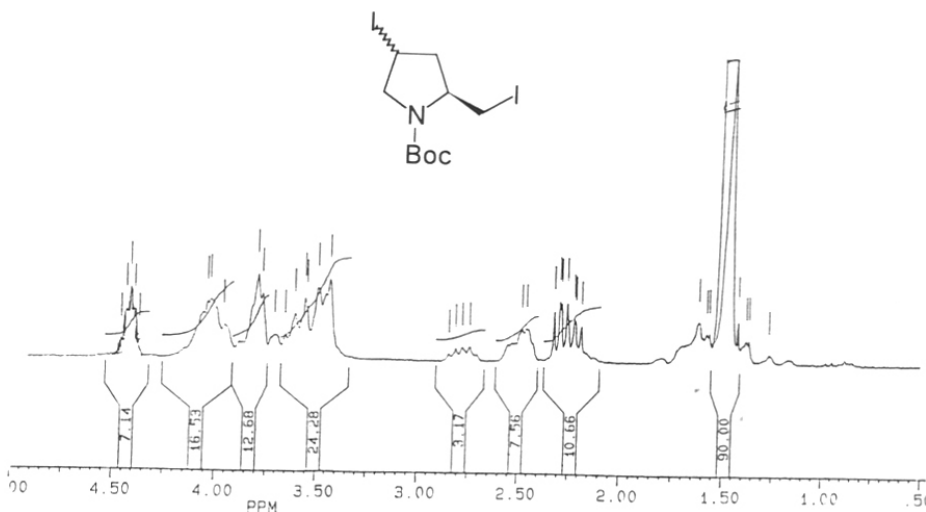


Figure 11. ¹H NMR spectrum of diiodide **24** in CDCl₃.

Thus, starting from *trans*-4-hydroxy-L-proline, successful syntheses of the chiral polyamines, **15** and **21**, were achieved and these products were well characterized for both structural and optical integrity. These were used for studying DNA duplex/triplex stability as described in the next section.

4.3 DNA DUPLEX AND TRIPLEX STABILIZATION WITH SPERMINE ANALOGUES 15 AND 21

4.3.1 Interaction of spermine with DNA

Spermine is well known to stabilize DNA duplexes and triplexes,^{18,19,33} although the exact molecular details are not yet clear (see *section 4.1.1* for detail). In case of triplexes, stabilization by cationic polyamines is ascribed to proceed via electrostatic neutralization of large negative charge density on triplexes.^{19c} Spermine, a linear aliphatic chain, enjoys enormous conformational freedom and theoretical calculations have suggested a preferential occurrence of *trans/gauche* conformations at C-N and N-C bonds.³⁴ In the presently designed analogues, conformational constrain imposed by the 5-membered chiral pyrrolidine ring (*2R,4S* and *2S,4R*) on spermine backbone may influence its interaction with DNA and to examine such structural effects, we carried out *UV-T_m* DNA melting studies of DNA duplexes and triplexes in presence of these analogues.

4.3.2 Present results

The DNA binding studies with **15** and **21** were done at 1 mM concentration of the amine in the experimental buffer solution and the results are presented in Table-1. Since Mg²⁺ is well known to stabilize duplexes and triplexes, experiments were carried out both in the presence and absence of Mg²⁺.

It is seen from the experimental data that the self complementary CG rich Dickerson 12-mer duplex **25** is stabilised by spermine **1** ($\Delta T_m \approx +6^\circ\text{C}$), as well as the free amine analogues (**15**) and (**21**) ($\Delta T_m \approx +7\text{--}8^\circ\text{C}$) compared to the control (Table 1, entry 1). Although no significant differences were noticed among the free amines, the N-Boc derivatives **14** and **20**, exhibited a relatively lower stabilizing effect ($\Delta T_m \approx +3\text{--}5^\circ\text{C}$). This may arise from

25 d C G C G A A T T C G C G
 26 A A G A A A A A A G A A A A A A G A d
 27 d T T C T T T T T C T T T T T C T
 28 d G C C A A G A A A A A A G A A A A A A G A C G C
 29 C G G T T C T T T T T C T T T T T C T G C G d

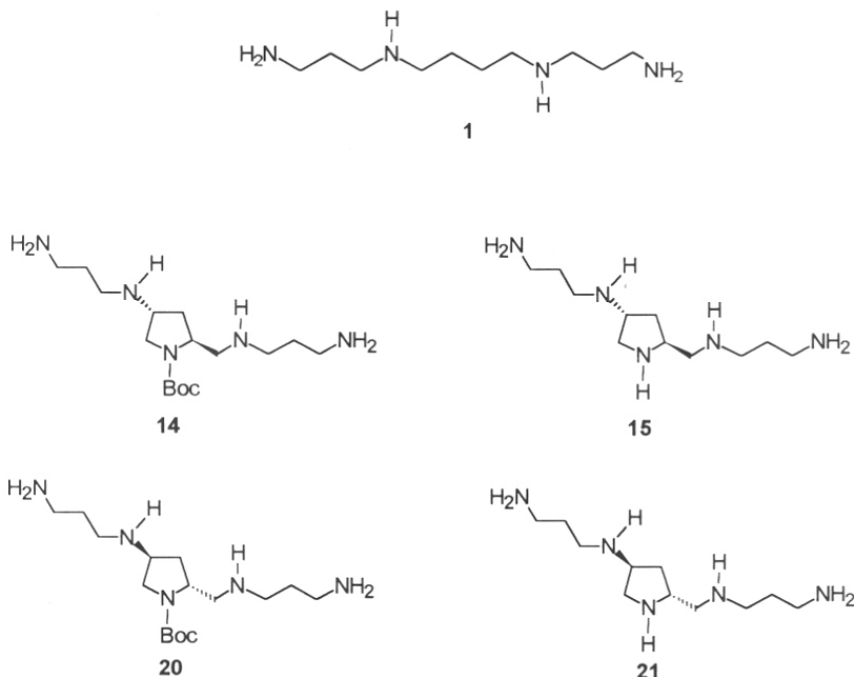


Table 1: UV- T_m ($^{\circ}$ C) of DNA duplexes and triplex with spermine analogues^a

No	Duplex/Triplex	Control	1	14	15	20	21
1	25	50	56	53.0	58.0	55.0	57.0
2	26:27	43	50	49.5	51.5	48.5	51.0
3	27*28:29	nd ^b	30	nd ^b	42.0	nd ^b	45.0

a: For conditions, see experimental. Concentration of amine, 1 mM, No Mg⁺⁺

b: not detected

either a steric interference by Boc group or a lack of protonation on ring N atom. The addition of 20 mM MgCl₂ raised the T_m by 3-5 °C, in case of control and duplex containing Boc derivatives **14** and **20** as expected, but with spermine **1** or its analogues **15** and **21**, the increase was not appreciable. The non self complementary AT rich duplex (26:27) showed a similar trend of stabilization with spermine and its analogues (Figure 12, Table 1, entry 2). Thus the constrained spermine analogues are as good as spermine in effecting duplex stability of both AT and CG rich sequences and structural specificity effects are minimal on duplex stabilization which is largely governed by the number of positive charges.

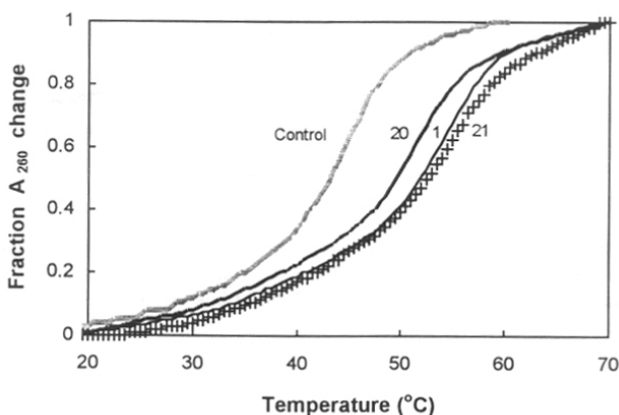


Figure 12. UV-melting profiles, at 260 nm, of duplex 26:27 in TRIS buffer containing NaCl (100 mM) at pH 7.3, in the absence (control) and in the presence of 1 mM of **1**, **20** and **21**.

In comparison, considerable specificity differences were noticed among spermine and its constrained analogues in their interaction with the triplex (27*28:29). In the absence of Mg²⁺, while no triplex was detected with the control (Table 1, entry 3), spermine and its analogues **15/21** exhibited well recognizable triplex formation (Figure 13) with the lower transition corresponding to triplex ⇌ duplex and higher one to duplex melting. Further, the analogues showed remarkably improved stabilization of triplexes ($\Delta T_m \approx +12\text{--}15$ °C), over that by spermine with 2S,4R isomer **15** being slightly better than

2R,4S isomer **21**. Interestingly, the N-Boc analogues **14/20** failed to promote triplexation in the absence of Mg^{2+} . As expected, all including control and Boc derivatives, showed triplex formation in the presence of Mg^{2+} .

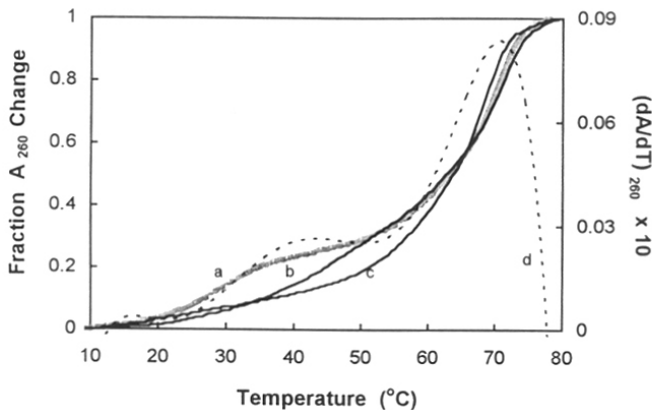


Figure 13. UV-melting profile, monitored at 260 nm, of triplex **27*28:29** in TRIS buffer containing NaCl (100 mM) at pH 7.3 in the presence 1 mM of spermine, **1** (a), **15** (b) and **14** (c). The curve (d) is the first derivative of (b)

These results indicate that the constrained spermine analogues **15** and **21**, while stabilizing duplexes as effectively as spermine, are significantly better than spermine in selectively stabilizing DNA triplexes. The topology of polyamine-DNA interactions in duplexes differ considerably from that in triplexes where polyamine structural effects (number and distribution of positive charges) have profound consequences on stability.^{19b} The magnitude of observed triplex stability with **15** and **21** cannot be solely attributed to the effect of an additional positive charge in them as compared to spermine. It is more likely that the rigid conformations of the constrained analogues **15** and **21** are more suitable for triplex binding than the flexible conformation of spermine.²³

4.4 CONCLUSIONS:

In summary, novel chiral analogues of spermine, incorporating a pyrrolidine ring on its backbone with consequential conformational restraintment have been synthesized from *trans*-4-hydroxy-L-proline. These are shown to substantially improve DNA triplex stability over that by spermine. These studies suggest that rational fine tuning of stereochemistry in the polyamine analogues may lead to improvement in DNA duplex/triplex binding/stability and such approaches have potential to design/develop more efficient and selective DNA binding agents. The newer spermine analogues reported here have features for extension to branched structures through ring N and such new entities add to an expanding library of polyamines required for drug and novel material designs.

4.5. EXPERIMENTAL SECTION:

For general procedure and protocol see *Chapter 2, section 2.5* TLC was performed on Merck pre-coated 60 F₂₅₄ plates and the spots were developed using the standard ninhydrin spray. Optical rotations were measured on JASCO DIP-181 polarimeter.

Oligodeoxynucleotide synthesis and UV-Melting Experiments: All oligonucleotides were synthesized on 1.3 μMol scale on a Pharmacia GA Plus DNA synthesiser and purified as described in *Chapter 3, Section 3.7* Duplex and triplex melting experiments were carried out in TRIS (25 mM) buffer at pH 7.3, containing NaCl (100 mM) and amine (1, 14, 15, 20 or 21 in 1 mM concentration) in the presence or absence of MgCl₂ (20 mM). For detailed procedure see *Chapter 3, section 3.7*.

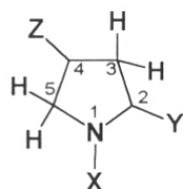


Figure 14. 2,4-disubstituted pyrrolidine. NMR peaks are assigned according to the numbering of pyrrolidine ring as shown in the figure.

***trans*-4-Hydroxy-N-(tert-Butoxycarbonyl)-L-proline methyl ester (4):** A slurry of *trans*-4-hydroxy-L-proline, 3, (10.0 g, 76.3 mmol) in absolute methanol (60 mL) was stirred at 0 °C. To this was added thionylchloride (6.1 mL, 10.0 g, 83.6 mmol, 1.1 eq.) drop-wise in 10 min. The stirring was continued at 0 °C for 4 h and then at ambient temperature until the reaction mixture became homogeneous (6 h). Removal of methanol under vacuum and washing the precipitate with ethylacetate and then with diethylether followed by drying under vacuum over phosphorous pentoxide yielded 13.5g (97.4 %) of methyl ester hydrochloride of 3 as a white solid. (The solid was used for the following experiment without further purification).

A mixture of the ester (8.0 g, 44.0 mmol), *tert*-butoxycarbonylazide (8.0 g, 55.9 mmol), TEA (20 mL), water (20 mL) and dioxane (20 mL) was stirred under argon atmosphere at 40-45 °C for 24 h. The mixture was concentrated to a pasty mass on a rotary evaporator, dissolved in ethylacetate (50 mL) and subjected to the usual work-up to obtain an yellow oil. The oil obtained was purified by silica gel column chromatography using 20 % ethylacetate in dichloromethane containing 0.05 % TEA as eluent ($R_f = 0.5$) yielding **4** (8.0 g, 74 %) as a pale yellow oil.

IR (neat): 3400, 2980-2900, 1735 and 1670 cm^{-1} . ^1H NMR δ ($\text{CDCl}_3 + \text{D}_2\text{O}$): 4.48-4.40(m, 2H, H2 & H4), 3.72(s, 3H, COOCH_3), 3.60-3.44(m, 2H, H5A & H5B), 2.32-2.40 (bm, 1H, H3A), 2.08-2.00(m, 1H, H3B) and 1.45-1.40(d, 9H, 3 x CH_3 of Boc).

$[\alpha]_D^{25} = -62.0 \pm 0.5^\circ$ ($c = 0.42$, CHCl_3).

trans-4-hydroxy-*N*-(*tert*-Butoxycarbonyl)-*L*-prolinol (**5**): To an ice cold solution of **4** (1.2 g, 4.9 mmol) in THF (20 mL) was added LBH (0.45 g, 20.7 mmol) in one portion. The mixture was stirred at 5-10 °C for 4 h and then at ambient temperature for 36 h. Saturated ammoniumchloride solution (10 mL) was added to the reaction mixture at 0 °C and stirred for further 2 h. The reaction mixture was concentrated to a pasty mass under reduced pressure and the residue was subjected to usual work-up to get a colorless viscous liquid which was then purified by column chromatography on silica gel (eluent: dichloromethane/EtOAc 1:1) to yield the diol **5** as a colorless oil (1g, 94 %).

IR (CHCl_3): 3500-3300, 1670 cm^{-1} . ^1H NMR δ ($\text{CDCl}_3 + \text{D}_2\text{O}$): 4.33(bs, 1H), 4.12-4.05(m, 1H), 3.62-3.35(m, 4H), 2.08-1.99(bm, 1H, H3A), 1.75-1.59(bs, 1H, H3B) and 1.45(s, 9H, 3 x CH_3 of Boc).

$[\alpha]_D^{25} = -56.2 \pm 0.5^\circ$ ($c = 0.56$, CHCl_3 lit.³⁵ $[\alpha]_D^{20} = -58.87$ $c = 1.01$, EtOH)

trans-4-hydroxy-*N*-(*tert*-Butoxycarbonyl)-*L*-prolinoldimethanesulfonate (**6**): To a stirred and precooled solution of diol **5** (0.95 g, 4.4 mmol) in pyridine (10 mL) under nitrogen was added methanesulfonylchloride (1 mL, 12.9 mmol) drop-wise. The stirring was continued at 0 °C for 4 h. Progress of the reaction was followed by TLC. The solvent was removed under vacuum at 30 °C, the residue left was taken in ethylacetate (20 mL)

and subjected to usual work-up to get a yellowish solid (1.5 g, 91 %). This solid was used for the following experiment without further purification.

¹H NMR δ(CDCl₃): 5.29-5.26(m, 1H, H4), 4.70-4.55(bm, 1H), 4.40-4.28(m, 2H), 3.88-3.76(m, 1H), 3.62-3.48(bm, 1H), 3.08(s, 3H, SO₂-CH₃), 3.05(s, 3H, SO₂-CH₃), 2.47-2.28(m, 2H, H3A & H3B) and 1.48(s, 9H, 3 x CH₃ of Boc).

(1S, 4S)-5-(3-aminopropyl)-2-t-butoxycarbonyl-2,5-diazabicyclo[2.2.1]-heptane (8):

Procedure 1: The dimesylate 6 (0.8 g, 2.1 mmol) was stirred in neat 1,3-diaminopropane (5 mL) at ambient temperature for 4 h followed by stirring at 60 °C for another 24 h. The excess amine was removed under reduced pressure at 50 °C. The residue was taken in dichloromethane (30 mL) and washed with water (20 mL). The aqueous layer was re-extracted with dichloromethane (10 mL x 4), dried over anhydrous sodium sulfate and concentrated to yield a pale yellow oil of 8 (0.45 g, 40 %)

Procedure 2: The dimesylate 6 (0.95 g, 2.5 mmol) was stirred in neat diaminopropane (6 mL) under argon atmosphere at ambient temperature for 4 h and then at 60 °C for 8 h. Excess amine was removed under low pressure at 40 °C. To the residue left was added anhydrous sodium sulfate (10g) and the product was extracted into ethylacetate (3 x 10 mL) and filtered. Evaporation of ethylacetate under vacuum gave 8 as a pale yellow oil (0.9 g, 100 %).

¹H NMR δ(CDCl₃ + D₂O): 4.34(bs, 0.5H), 4.21(bs, 0.5H), 3.55-3.43(bt, 2H), 3.16-3.11(bd, 1H), 2.95-2.86(t, 1H), 2.79-2.73(t, 2H, N-CH₂ of side chain), 2.64-2.43(m, 3H), 1.79-1.52(bm, 4H, H3A, H3B & middle CH₂ of the side chain) and 1.45(s, 9H, 3 x CH₃ of Boc). ¹³C NMR δ(CDCl₃): 153.7(CO of Boc), 78.6(O-CMe₃), 60.9, 60.3, 59.6, 57.3, 56.3, 51.8, 51.4, 49.2, 48.4, 40.0, 35.7, 35.0, 32.1 and 28.1(CH₃ of Boc).

[α]_D²⁵ = -47.5 ± 0.5° (c = 0.64, MeOH).

FAB Mass: 256(M⁺ + 1, 100 %), 155(M⁺ - COOCMe₃, 50 %).

(1S, 4S)-5-(3-trifluoroacetamidopropyl)-2-t-butoxycarbonyl-2,5-diazabicyclo[2.2.1]-heptane (9): Compound 8 (0.75 g) was trifluoroacetylated using ethyltrifluoroacetate (0.5 mL) in ethanol (10 mL). Standard work up followed by column chromatography on silica

gel (dichloromethane/ethylacetate 4:1) yielded the trifluoroacetamide derivative **9** as an yellow oil (1.1 g, 67.6 %).

¹H NMR δ(CDCl₃): 9. 67-9.58(bd, 1H, NHCOCF₃), 4.39(bs, 0.6H), 4.25(bs, 0.4H), 3.58-3.35(bm, 4H), 3.21(d, 0.6H, J = 2.0 Hz), 3.16(d, 0.4H, J = 2.0 Hz), 2.95-2.79(m, 3.5H), 2.52-2.47(bd, 0.5H), 1.76-1.65(m, 4H, H₃A, H₃B and middle CH₂ of the side chain) and 1.46(s, 9H, 3 x CH₃ of Boc). ¹³C NMR δ(CDCl₃): 157.4, 156.9 & 156.5(COCF₃), 154.0(CO of Boc), 121.7, 117.9 & 114.1(CF₃), 79.4(O-CMe₃), 61.7, 61.2, 59.6, 57.3, 56.3, 54.5, 53.6, 53.3, 49.9, 48.4, 40.8, 36.4, 35.9, 34.7 and 28.2(CH₃ of Boc).

[α]_D²⁵ = -28.8 ± 0.5° (c = 0.84, MeOH).

FAB Mass: 352(M⁺, 100 %).

cis-4-O-Benzoyl-1-(tert-Butoxycarbonyl)-L-proline methyl ester (11): To a solution of **4** (2.0 g, 8.2 mmol), triphenylphosphine (2.8g, 10.7 mmol) and benzoic acid (1.3 g, 10.6 mmol) in acetonitrile (30 mL) at 0 °C was added diisopropylazodicarboxylate (2.15 g, 10.6 mmol) as a neat liquid. The reaction mixture was stirred at 0 °C for 2 h and then at ambient temperature for 24 h. Methanol was added into the reaction mixture and was concentrated to a pasty mass. The residue was dissolved in minimum amount of diethylether followed by addition of pet-ether (40-60 °C) until the reaction mixture became turbid and then kept at 5 °C overnight. Triphenylphosphineoxide formed during the course of the reaction was crystallised out and was filtered off. The residue was washed with diethylether/pet-ether mixture (2:3) and the filtrate was concentrated to dryness. The residue was taken in dichloromethane (30 mL) and subjected to usual work-up. The product **11** (2.2 g, 77 %) was obtained as a white solid after silica gel column chromatography using pet-ether/dichloromethane (2:3, R_f = 0.4) as eluent. A portion of it was crystallised from EtOAc/pet-ether (40-60 °C) solvent system.

mp. 85-88 °C.

IR (nujol): 2950-2850, 1745, 1710, 1690 cm⁻¹. ¹H NMR δ(CDCl₃): 7.98(d, 2H, ArH), 7.61-7.40(m, 3H, ArH), 5.54(bm, 1H, H₄), 4.64-4.58(m, 0.5H, H₂), 4.51-4.46(m, 0.5H, H₂), 3.87-3.68(m, 5H, H₅A, H₅B & COOCH₃), 2.59-2.42(m, 2H, H₃A & H₃B), 1.47(d, 9H, 3 x CH₃ of Boc). ¹³C NMR δ(CDCl₃): 172.4 & 172.1(COOMe), 165.7(COPh), 154.1

& 153.7(CO of Boc), 133.3, 129.7, 128.4, 80.3(OCMe₃ of Boc), 73.5 & 72.4(C2), 57.9 & 57.6(C5), 52.5(OCH₃), 52.1(C4), 36.6 & 35.7(C3), 28.3(CH₃ of Boc).

$[\alpha]_D^{25} = -28.0 \pm 0.5$ (c = 0.5, CHCl₃).

Analysis for C₁₈H₂₃NO₆: Calc. C 61.86, H 6.64, N 4.01 %; Found C 61.78, H 6.76, N 4.01 %. FAB Mass: 350 (M⁺ + 1, 18 %), 250([M⁺ + 2] - COOCMe₃, 100 %)

cis-4-hydroxy-N-(t-butoxycarbonyl)-L-prolinol (12): Reduction of 11 (1.8g, 5.2 mmol) with LBH (0.75 g, 34.4 mmol) in THF (25 mL) followed by silica gel column chromatography as in the case of 5 yielded 12 (0.65 g, 58 %) as a white solid.

mp. = 88-90 °C.

IR (nujol): 3300-3200, 2920-2860, 1685 cm⁻¹. ¹H NMR δ(CDCl₃ + D₂O): 4.29(bs, 1H), 4.08-4.01(bm, 2H), 3.61-3.45(bm, 3H), 2.37-2.26(bm, 1H, H3A), 1.95-1.75(bm, 1H, H3B) and 1.46(s, 9H, 3 x CH₃). ¹³C NMR δ(CDCl₃): 155.7 & 154.9(CO of Boc), 80.0(OCMe₃ of Boc), 69.6 & 68.9(C2), 64.0 & 63.4(C5), 58.5(C4), 56.6, 38.0 & 37.3(C3) and 28.5(CH₃ of Boc).

$[\alpha]_D^{25} = -44.6 \pm 0.5^\circ$ (c = 0.4, CHCl₃).

Anal. for C₁₀H₁₉NO₄: Calc. C 55.29, H 8.75, N 6.45 %; Found: C 55.53, H 8.51, N 6.47 %. FAB Mass: 218(M⁺ + 1, 32 %), 188([M⁺ + 1] - COOCMe₃, 100 %).

cis-4-hydroxy-N-(t-butoxycarbonyl)-L-prolinoldimethanesulfonate (13): Compound 12 (0.55 g, 2.5 mmol) was mesylated using mesylchloride (0.6 mL, 7.8 mmol) in dry pyridine (5 mL) to yield 13 (0.94 g, 99 %). This dimesylate was used directly for the following experiment with out further purification.

¹H NMR δ(CDCl₃): 5.31-5.26(m, 1H, H4), 4.47-4.43(bm, 1H), 4.36-4.14(bm, 2H), 3.70(bs, 2H), 3.08(s, 3H, SO₂CH₃), 3.04(s, 3H, SO₂CH₃), 2.41-2.31(bm, 2H, H3A & H3B) and 1.48(s, 9H, 3 x CH₃ of Boc).

(2S,4R)-2-([N-3-aminopropyl]amino)-methyl-4-(N-3-aminopropyl)amino-1-t-butoxycarbonyl-pyrrolidine (14): Compound 13 (0.9 g, 2.4 mmol) was treated with neat 1,3-diaminopropane (6 mL) at 60 °C for 24 h and followed procedure 2 for the preparation of 8 to get 14 (0.66 g, 83 %) as a pale yellow oil.

¹H NMR δ(CDCl₃ + D₂O): 3.95(bs, 1H), 3.55-3.48(m, 1H), 3.38-3.10(bm, 2H), 2.81-2.50(m, 10H), 2.1-1.99(bm, 1H, H3A), 1.83-1.57(m, 5H, H3B and middle [CH₂]₂ of the two side chains) and 1.46(s, 9H 3 x CH₃ of Boc). ¹³C NMR δ(CDCl₃): 154.4, 78.7, 77.6, 55.9, 55.5, 52.9, 52.0, 47.3, 45.7, 39.8, 39.2, 36.1, 33.1, 33.0 and 28.0.
 $[\alpha]_D^{25} = -45.9 \pm 0.5^\circ$ (c = 0.64, MeOH).

FAB Mass: 330(M⁺ + 1, 100 %), 230([M⁺ + 1] - COOCMe₃, 50 %).

(2S,4R)-2-([N-3-aminopropyl]-amino)-methyl-4-(N-3-aminopropyl)aminopyrrolidine pentahydrochloride (15): Compound 14 (0.2 g, 0.6 mmol) was treated with 5N HCl (10 mL) at ambient temperature for 8 h. Water and HCl were removed under vacuum and the residue left was dried over P₂O₅ under vacuum. The pentahydrochloride salt 15 (0.2 g, 80 %) was obtained as a white hygroscopic solid.

¹H NMR δ(D₂O): 4.44-4.18(m, 2H), 4.13-4.02(m, 1H), 3.70-3.53(m, 3H), 3.30-2.96(m, 8H), 2.74-2.64(m, 1H, H3A), 2.58-2.45(m, 1H, H3B) and 2.20-2.05(m, 4H, middle [CH₂]₂ of the side chains). ¹³C NMR δ(D₂O): 56.1, 55.9, 48.3, 47.9, 46.4, 44.9, 37.4, 32.3, 24.6 and 24.4.

cis-4-hydroxy-D-proline (16): A solution of acetic anhydride (25g, 244.9 mmol) in 50 mL acetic acid was heated to 50 °C and compound 3 (6.0 g, 45.8 mmol) was added in one portion. The reaction mixture was refluxed for 10 h. Excess acetic anhydride and acetic acid were removed under vacuum and the residue was refluxed in 2N HCl (50 mL) for 4h. The reaction mixture was concentrated until crystallization began. The crystals were filtered under suction, washed with dioxane and dried over P₂O₅ in a vacuum desicator. Yield 5.5g (71.67 %), mp. = 145 °C (lit.²⁹ 153-153.5 °C).

¹³C NMR δ(D₂O): 172.6, 69.7, 59.1, 54.3 and 37.6.

cis-4-Hydroxy-N-(tert-Butoxycarbonyl)-D-proline methyl ester (17): The compound 17 (4.1g, 70 %) was obtained as a solid from 16 (4.0 g, 23.9 mmol), thionylchloride (3.4 g, 28.6 mmol), MeOH (40 mL), *t*-butylcarbazide 4.5g (31.5 mmol) and TEA 10 mL. Procedure, work-up and purification are same as in the preparation of 4. mp. = 79-80 °C (lit.³⁶ mp. = 82.5-83 °C).

IR (nujol): 3450, 2950-2860, 1730, 1660 cm^{-1} . ^1H NMR $\delta(\text{CDCl}_3)$: 4.39-4.26(m, 2H), 3.79(d, 3H, COOCH₃), 3.66-3.49(m, 2H), 2.37-2.25(m, 1H, H3A), 2.12-2.04(m, 1H, H3B) and 1.46-1.43(d, 9H, 3 x CH₃ of Boc). ^{13}C NMR $\delta(\text{CDCl}_3)$: 174.4(COOMe), 154.4 & 153.7(CO of Boc), 80.1(OCMe₃ of Boc), 70.4, 69.4, 57.8, 57.5, 55.1, 54.6, 52.3, 52.1, 38.5, 37.8, 28.2 and 28.1.

$[\alpha]_D^{25} = +19.0 \pm 0.5^\circ$ (c = 0.5, CHCl₃, lit³⁶ $[\alpha]_D^{22} = +26.6^\circ$, MeOH).

cis-4-Hydroxy-N-(tert-Butoxycarbonyl)-D-prolinol (18): Reduction of **17** (1.25 g, 5.1 mmol) using LBH (0.8 g, 36.7 mmol) in THF (20 mL) afforded **18** (0.8 g, 72 %) as a white solid. Procedure, work-up and purification are same as in the preparation of **5**. mp. = 91-93 °C.

IR (nujol): 3300-3100, 2920-2850, 1670 cm^{-1} . ^1H NMR $\delta(\text{CDCl}_3 + \text{D}_2\text{O})$: 4.28(bt, 1H), 4.05-3.99(bm, 2H), 3.55-3.44(bm, 3H), 2.37-2.26(bm, 1H, H3A), 1.94-1.80(bm, 1H, H3B) and 1.46(s, 9H, 3 x CH₃ of Boc). ^{13}C NMR $\delta(\text{CDCl}_3)$: 155.5 & 154.7(CO of Boc), 79.8(OCMe₃ of Boc), 69.4 & 68.7(C2), 63.7 & 63.2(C5), 58.3(C4), 56.3, 37.7 & 37.0(C3) and 28.3(CH₃ of Boc).

$[\alpha]_D^{25} = +46.3 \pm 0.5^\circ$ (c = 0.16, CHCl₃).

Anal. for C₁₀H₁₉NO₄: Calc. C 55.29, H 8.75, N 6.45 %; Found: C 55.65, H 8.39, N 6.77 %.

cis-4-Hydroxy-N-(tert-Butoxycarbonyl)-D-prolinoldimethanesulfonate (19): Reaction of compound **18** (0.5 g, 2.3 mmol) with mesylchloride (0.6 mL, 7.8 mmol) in pyridine (5 mL) gave **19** (0.85 g, 99 %) as a pale yellow solid. Procedure and work-up are same as in the preparation of **6**. The compound **19** was used for the following experiment without further purification.

^1H NMR $\delta(\text{CDCl}_3)$: 5.32-5.28(m, 1H, H4), 4.46-4.44(m, 1H), 4.42-4.16(bm, 2H), 3.71-3.69(m, 2H), 3.10(s, 3H, SO₂CH₃), 3.06(s, 3H, SO₂CH₃), 2.47-2.37(bm, 2H, H3A & H3B) and 1.48(s, 9H, 3 x CH₃ of Boc).

(2R,4S)-2-((N-3-aminopropyl)amino)-methyl-4-(N-3-aminopropyl)amino-1-t-butoxy-carbonyl-pyrrolidine (20): Compound **19** (0.8 g, 2.1 mmol) was treated with neat 1,3-

diaminopropane (6 mL) at 60 °C for 24 h and worked-up according to procedure 2 for the preparation of **8** to get **20** (0.6 g, 85 %) as a pale yellow oil.

¹H NMR δ(CDCl₃ + D₂O): 3.97(bs, 1H), 3.53-3.48(m, 1H), 3.47-3.06(bm, 2H), 2.79-2.58(m, 10H), 2.09-1.99(bm, 1H, H3A), 1.80-1.47(m, 5H, H3B & middle [CH₂]₂ of the two side chains) and 1.46(s, 9H, 3 x CH₃ of Boc). ¹³C NMR δ(CDCl₃): 154.3, 78.6, 77.5, 55.8, 55.5, 52.7, 51.8, 47.2, 45.6, 39.7, 39.1, 36.4, 36.3, 33.1, 32.1 and 27.9.

[α]_D²⁵ = +45.3 ± 0.5° (c = 0.64, MeOH).

(2R,4S)-2-((N-3-aminopropyl)-amino)-methyl-4-(N-3-aminopropyl)aminopyrrolidine pentahydrochloride (21): Compound **20** (0.2 g, 0.6 mmol) was treated with 5N HCl at ambient temperature for 8 h. Water and HCl were removed under vacuum and the residue left was dried over P₂O₅ in a vacuum desicator overnight. The pentahydrochloride salt **21** (0.18 g, 73 %) was obtained as a white hygroscopic solid.

¹H NMR δ(D₂O): 4.40-4.25(m, 2H), 4.14-4.03(m, 1H), 3.73-3.55(m, 3H), 3.31-3.08(m, 8H), 2.73-2.68(m, 1H, H3A), 2.59-2.48(m, 1H, H3B) and 2.21-2.06(m, 4H, middle [CH₂]₂ of the two side chains). ¹³C NMR δ(D₂O): 56.4, 56.2, 48.6, 48.2, 46.7, 45.2, 37.6, 32.5, 24.8 and 24.6.

trans-4-O-Benzoyl-N-(tert-butoxycarbonyl)-D-proline methyl ester (22): Compound **17** (2.0 g, 8.2 mmol) was treated with triphenylphosphine (2.8 g, 10.7 mmol, 1.3 eq.), DIAD (2.15 g, 10.6 mmol, 1.3 eq.) and benzoic acid (1.3 g, 10.6 mmol) and worked-up according to the procedure given for the synthesis of **11** to get **22** (2.5 g, 87.7 %) as a white solid. A portion of it was crystallised from EtOAc/pet-ether (40-60 °C) solvent system.

mp. = 90-91 °C.

IR (nujol): 2950-2850, 1745, 1715, 1670 cm⁻¹. ¹H NMR δ(CDCl₃): 8.04-8.00(m, 2H, ArH), 7.61-7.41(m, 3H, ArH), 5.54(bm, 1H, H4), 4.58-4.42(m, 1H, H2), 3.85-3.68(m, 5H, H5a, H5B & OC₂H₅), 2.61-2.50(bm, 1H, H3A), 2.38-3.26(m, 1H, H3B), 1.17(s, 1H, exchangeable with D₂O) and 1.46(d, 9H, 3 x CH₃ of Boc). ¹³C NMR δ(CDCl₃): 173.1 & 172.8(COOMe), 165.9(COPh), 154.4 & 153.6(CO of Boc), 133.4, 129.7, 128.5,

80.5(OCMe₃ of Boc), 73.3 & 72.6(C2), 58.1 57.7(C5), 52.4(COOCH₃), 52.2(C3), 36.7 & 35.7(C3) and 28.3(CH₃ of Boc).

[α]_D²⁵ = +49.5 ± 0.5° (c = 0.44, CHCl₃).

Analysis for C₁₈H₂₃NO₆: Calc. C 61.86, H 6.64, N 4.01 %;

Found C 61.92, H 6.31, N 3.89 %.

trans-4-Hydroxy-N-(tert-Butoxycarbonyl)-D-prolinol (23): Compound 22 (1.2 g, 3.4 mmol) was reduced with LBH (0.5 g, 23.0 mmol) in THF (25 mL) affording 23 (0.55 g, 73.7 %). Procedure and work-up are same as in the preparation of 5.

IR (CHCl₃): 3420-3300, 3010-2960, 1660 cm⁻¹. ¹H NMR δ(CDCl₃): 4.38(bs, 1H), 4.16-4.11(bm, 1H), 3.73-3.38(m, 4H), 2.11-2.00(bm, 1H, H3A), 1.73-1.62(bs, 1H, H3B) and 1.48(s, 9H, 3 x CH₃ of Boc). ¹³C NMR δ(CDCl₃): 156.9, 80.5(OCMe₃), 68.9(C2), 66.1(C5), 58.6(C4), 55.6, 37.3(C3) and 28.5(CH₃ of Boc).

[α]_D²⁵ = +56.0 ± 0.5° (c = 0.16, CHCl₃, lit³⁶ [α]_D²² = +53.6°, abs. EtOH)

2-(iodomethyl)-4-iodo-1-(t-butoxycarbonyl)-pyrrolidine (24): Compound 6 (0.8 g, 2.1 mmol) and sodium iodide (3.2g, 21.3 mmol) were refluxed in dry acetone (20 mL) for 24 h. The progress of the reaction was monitored by TLC (eluent CH₂Cl₂/EtOAc, 1:1, R_f = 0.5 for 6 and R_f = 0.8 for 24). The reaction mixture was stripped off the solvent and the residue was taken in ethylacetate (20 mL) followed by usual work-up. The product 24 (0.86 g, 92%) was purified by silica gel column chromatography using pet-ether (60-80 °C)/CH₂Cl₂, (1:1 R_f = 0.4) as eluent.

IR (neat): 2950-2850, 1690 cm⁻¹. ¹H NMR δ(CDCl₃): 4.44-4.37(m, 1H), 4.08-3.96(bm, 2H), 3.92-3.77(bm, 1H), 3.61-3.44(m, 2H), 2.85-2.74(m, 0.3H of H3A), 2.55-2.46(bm, 0.7H of H3A), 2.33-2.19(m, 1H, H3B), 1.47(d, 9H, 3 x CH₃ of Boc).

¹³C NMR δ(CDCl₃): 154.0, 153.0, 80.3, 63.5, 58.7, 58.2, 57.7, 57.2, 56.7, 45.1, 44.8, 44.3, 28.3, 18.7, 13.1, 11.3.

4.6. REFERENCES:

1. (a) Tabor, C. W.; Tabor, H. *Ann. Rev. Biochem.*, **1984**, *53*, 749. (b) Schuber, F., *Biochem. J.*, **1989**, *260*, 1.
2. Henner, W. D.; Kleber, I.; Benzinger, R. *J. Virol.*, **1973**, *12*, 741.
3. (a) Pegg, A. E. *Cancer Res.*, **1988**, *48*, 759. (b) Pegg, A. E. *Biochem. J.*, **1986**, *234*, 249.
4. (a) Heby, O.; Janne, J. in *Polyamines in Biology and Medicine*, D. R. Morris, L. J. Morton, eds. Dekker NY, 1981. (b) Behr, J. P. *Acc. Chem. Res.*, **1993**, *26*, 274.
5. (a) Seiler, N. *Prog. Drug Res.*, **1991**, *37*, 107. (b) Cordella-Miele, E.; Miele, L.; Beninati, S.; Mukherjee, A. *J. Biochem.*, **1993**, 164.
6. Scott, R. H.; Sutton, K. G.; Dolphin, A. C. *Trends Neurosci.*, **1993**, *16*, 153.
7. Flink, I.; Pettijohn, D. E. *Nature* **1975**, *253*, 62.
8. (a) Williams, K. *Neurosci. Lett.*, **1995**, *184*, 181. 14 (b) Bergeron, R. J.; Weimar, W. R.; Wu, Q.; Austin Jr., J. K.; McManis, J. S. *J. Med. Chem.*, **1995**, *38*, 425.
9. Bergeron, R. J.; Yao, G. W.; Yao, H.; Weimar, W. R.; Sninsky, R. B.; Feng, Y.; Wu, Q.; Gao, F. *J. Med. Chem.*, **1996**, *39*, 2461.
10. Bergeron, R. J.; McManis, J.; Weimar, W. R.; Schreier, S.; Gao, F.; Wu, Q.; Ortiz-Ocasio, J.; Luchetta, G. R.; Porter, J. R.; Vinson, T. *J. Med. Chem.*, **1995**, *38*, 2278.
11. Marquet, R.; Houssier, C.; Fredericq, E. *Biochem. Biophys. Acta.*, **1985**, *825*, 365.
12. (a) Chen, H. H.; Behe, M. J.; Rau, D. C. *Nucleic Acids Res.*, **1984**, *12*, 2381. (b) Thomas, T. J.; Messner, R. P. *J. Mol. Biol.*, **1988**, *201*, 463. (c) Vertino, P. M.; Bergeron, R. J.; Cavanaugh, P. F.; Porter, C. W. *Biopolymers*, **1987**, *26*, 691.
13. Gessner, R. V.; Frederick, C. A.; Quigley, G. J.; Rich, A.; Wang, A. H.-J. *J. Biol. Chem.*, **1989**, *264*, 7921.
14. Jain, S.; Zon, G.; Sundaralingam, M. *Biochemistry*, **1989**, *28*, 2360.
15. Stewart, K. D. *Biochem. Biophys. Res. Commun.*, **1988**, *152*, 1441.
16. Marquet, R.; Houssier, C. *J. Biomolec. Struct. Dyn.*, **1988**, *6*, 235.
17. Basu, H. S.; Shafer, R. H.; Marton, L. J. *Nucleic Acids Res.*, **1987**, *15*, 5873.
18. Haworth, I. S.; Rodger, A.; Richards, W. G. *Proc. R. Soc. Lond. B*, **1994**, *244*, 107.
19. (a) Hampel, K. J.; Crosson, P.; Lee, J. S. *Biochemistry*, **1991**, *30*, 4455. (b) Thomas, T.; Thomas, T. J. *Biochemistry*, **1993**, *32*, 14068. (c) Volker, J.; Klump, H. H. *Biochemistry*, **1994**, *33*, 13502.

20. (a) Tung, C. H.; Breslauer, K. J.; Stein, S. *Nucleic Acids Res.*, **1993**, *21*, 5489. (b) Bigey, P.; Prativel, G.; Meunier, B. *J. Chem. Soc. Chem. Comm.*, **1995**, 181. (c) Sund, C.; Puri, N.; Chattopadhyaya, J. *Tetrahedron*, **1996**, *52*, 12275.
21. (a) Nara, H.; One, A.; Matsuda, A. *Bioconjugate Chem.*, **1995**, *6*, 54. (b) Prakash, T. P.; Barawkar, D. A.; Kumar, V. A.; Ganesh, K. N. *BioMed. Chem. Lett.*, **1994**, *4*, 1733. (c) Barawkar, D. A.; Kumar, V. A.; Ganesh, K. N. *Biochem. Biophys. Res. Commun.*, **1994**, *205*, 1665. (d) Barawkar, D. A.; Rajeev, K. G.; Kumar, V. A.; Ganesh, K. N. *Nucleic Acids Res.*, **1996**, *24*, 1229.
22. Sarhan, S.; Seiler, N. *Biol. Chem. Hoppe-Seyler*, **1989**, *370*, 1279.
23. Feuerstein, B. G.; Szollsi, J.; Basu, H. S.; Marton, L. J. *Cancer Res.*, **1992**, *52*, 6782.
24. (a) Ganem, B. *Acc. Chem. Res.*, **1982**, *15*, 290. (b) Bergeron, R. J. *Acc. Chem. Res.*, **1986**, *19*, 105.
25. Brand, G.; Hosseini, M. W.; Ruppert, R. *Tetrahedron*, **1994**, *50*, 8609.
26. Pallan, P. S.; Ganesh, K. N. *Biochem. Biophys. Res. Commun.*, **1996**, *222*, 416.
27. Remuzon, P. *Tetrahedron*, **1996**, *52*, 13803.
28. Kaname, M.; Yoshifuji, S. *Tetrahedron Lett.*, **1992**, *33*, 8103.
29. Baker, G. L.; Fritschel, S. J.; Stille, J. R.; Stille, J. K. *J. Org. Chem.*, **1981**, *46*, 2954.
30. Jordis, U.; Sauter, F.; Siddiqi, S. M.; Kuenburg, B.; Bhattacharya, K. *Synthesis*, **1990**, 925.
31. (a) Mitsunobu, O. *Synthesis*, **1981**, 1. (b) Williams, M. A.; Rapoport, H. *J. Org. Chem.*, **1994**, *59*, 3616.
32. Codington, J. F.; Fecher, R.; Fox, J. J. *J. Am. Chem. Soc.*, **1960**, *82*, 2794.
33. (a) Feuerstein, B. G.; Pattibhiraman, N.; Marton, L. J. *Proc. Natl. Acad. Sci. USA*, **1986**, *83*, 5948. (b) Feuerstein, B. G.; Pattibhiraman, N.; Marton, L. J. *Nucleic Acids Res.*, **1989**, *17*, 6883. (c) Feuerstein, B. G.; Pattibhiraman, N.; Marton, L. J. *Nucleic Acids Res.*, **1990**, *18*, 1271. (d) Delcros, J.-G.; Strukenboom, C. J. M.; Basu, H. S.; Shafer, R. H.; Szollosi, J.; Feuerstein, B. G.; Marton, L. J. *Biochem. J.*, **1993**, *291*, 269.
34. Laquori, A. M.; Constantino, L.; Crescenzi, V.; *J. Mol. Biol.*, **1967**, *24*, 113.
35. Ojima, I.; Kogure, T.; Yoda, N. *J. Org. Chem.*, **1980**, *45*, 4728.
36. Peterson, M. L.; Vince, R. *J. Med. Chem.*, **1991**, *34*, 2787.

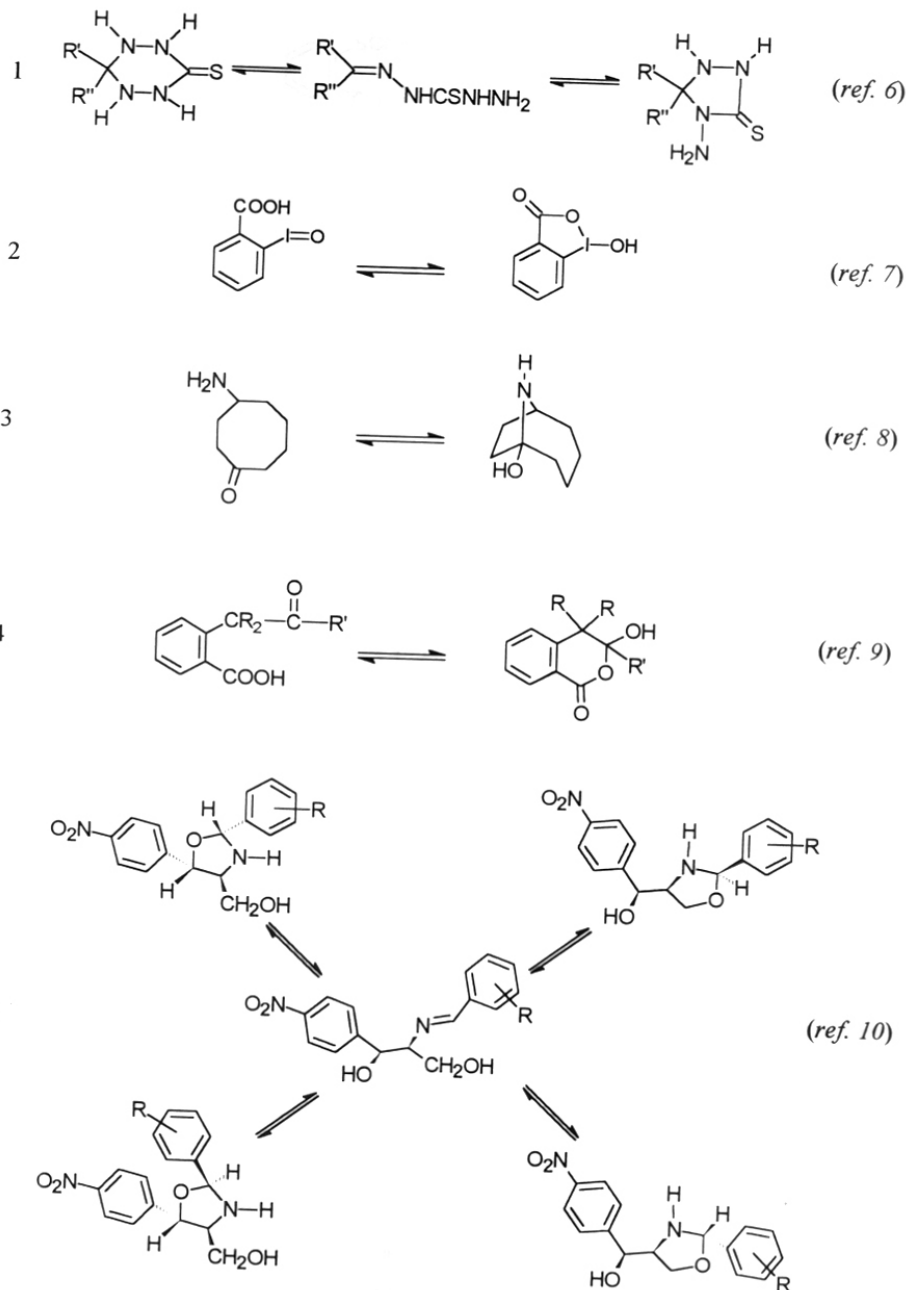
CHAPTER 5.

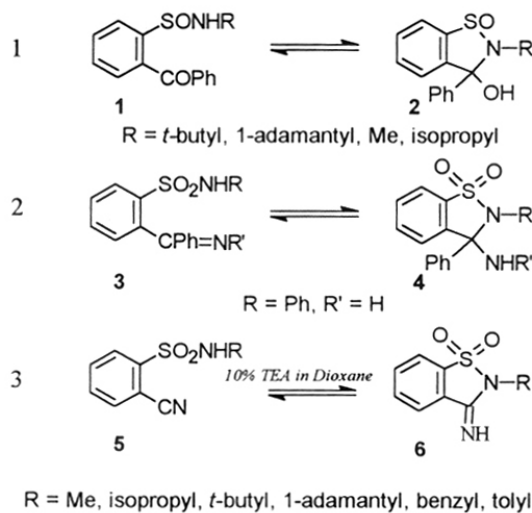
**RING-CHAIN TAUTOMERISM OF
2-FORMYLBENZENESULFONAMIDES:
THEIR STRUCTURE IN SOLID, SOLUTION AND GAS PHASES**

5.1. INTRODUCTION

Influence of one functional group on the reactions of another in the same molecule is well documented in the literature. Such effects have been categorized as electronic, steric, field and proximity effects. There are a large number of reports on the intramolecular catalytic reactions^{1,2} and ring-chain tautomerism in small organic molecules.³ These studies fall into the purview of proximity effects. Most of these studies concern the effect of a carbonyl or a hydroxy group on the behavior of a neighboring carboxylic acid or its derivative.^{1,4,5} However, there are few systematic studies of ring-chain tautomerism involving functional groups other than carboxylic acid derivatives.⁶⁻¹⁵

Some of the molecules that exhibit ring chain tautomerism involving different functional groups are summarised in **Scheme 1**. Ring-chain tautomerism of γ - and δ -ketocarboxylic³ acids and their derivatives have been extensively studied and the factors that affect this equilibrium have been well characterized. But systematic studies with ketosulfonic acids and their derivatives are scarce. Balode and Valters¹¹ studied the tautomerism of ketosulfinamides and found that the equilibrium lies towards the cyclic tautomer since sulfinamides have greater tendency towards intramolecular nucleophilic addition at the carbonyl carbon (**Scheme 2**, entry 1). Extent of formation of the ring tautomer depended on the alkyl substituent on the nitrogen atom, bulkier substituent like *t*-butyl group favored the open form 1 whereas the substituent like methyl group favored the cyclic tautomer 2. Benzene sulfonamides having imino or nitrile functions at the ortho position are known to exhibit ring-chain tautomerism.^{12,13} Sulfonamide 3 (**Scheme 2**, entry 2) undergoes intramolecular nucleophilic addition of the sulfonamide nitrogen at the imino carbon to form the cyclic tautomer 4.¹² *o*-Cyano-benzenesulfonamide 7 (**Scheme 2**, entry 3) exhibit ring-chain tautomerism in dioxane containing 10 % triethylamine.¹³ In this system, the equilibrium is attained more rapidly with N-aryl substituent than with N-alkyl substituents.

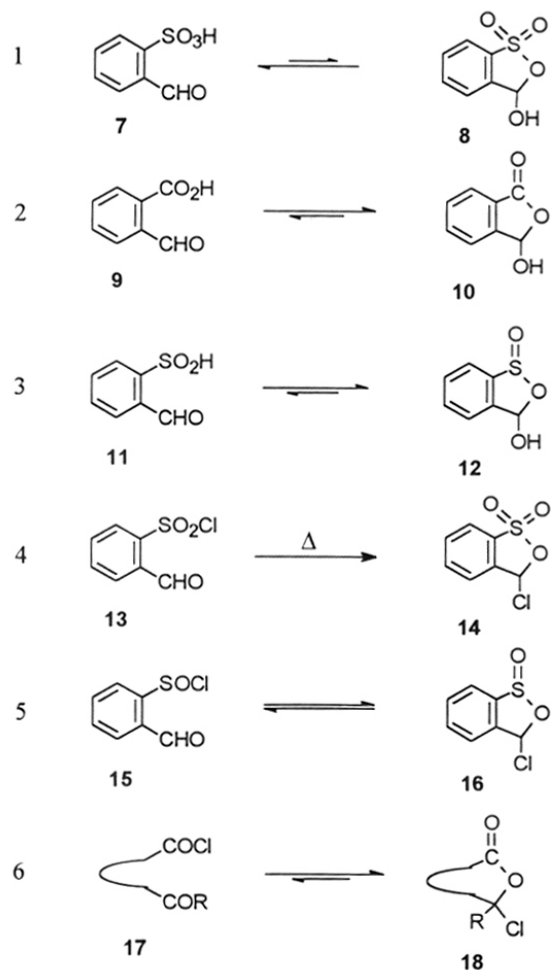
**Scheme 1**

**Scheme 2**

In all the examples mentioned above, the steric effects of the substituents on the hetero atom involved and the acidity of the proton are the two important factors that influence the tautomeric equilibrium. The electrophilicity of the carbonyl/imino carbon also plays a role in the ring-chain tautomeric equilibrium. Ring-chain tautoemric systems are therefore often convenient systems for the determination of electronic and steric affects associated with ring-forming reactions.³ Also it is often possible to glean valuable information about intermolecular reactions, even for intermediates that are not very stable, such as hemiacetal¹⁴ and hemiaminal¹⁵ species.

2-Formylbenzenesulfonic acid (**7**) is known to exist completely in the open form,¹⁶ (**Scheme 3**, entry 1) unlike its carboxylic acid analogue **9** which exists completely as the hydroxy lactone¹⁷ (**Scheme 3**, entry 2). In contrast, 2-formylbenzenesulfinic acid (**11**) is known to exist completely in the cyclic form (**Scheme 3**, entry 3). 2-formylbenzenesulfonylchloride on the other hand is known to exist both in open (**13**) and cyclic (**14**) forms, which can be separated by standard procedures.^{16,18} There is no equilibrium between the two forms. However, the normal sulfonylchloride **13** can be converted to the cyclic form **14** by heating. Similarly, 2-formylbenzenesulfinic acid

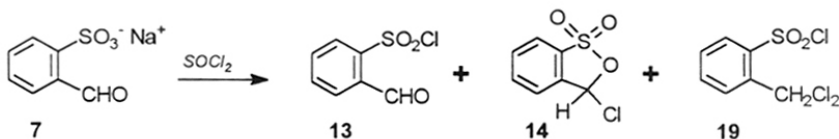
chloride also exists in both open and ring forms (**Scheme 3**, entry 5).¹⁸ However, this system has not been investigated in detail. γ -Keto carboxylic acid chlorides **17**, on the other hand, are known to exist as corresponding acyloxy alkyl halides **18** exclusively.



Scheme 3

The objectives of the present work are to study (i) reaction of amines with normal and pseudo 2-formylbenzenesulfonylchlorides and (ii) ring-chain tautomerism in 2-formylbenzenesulfonamides and the corresponding Schiff bases.

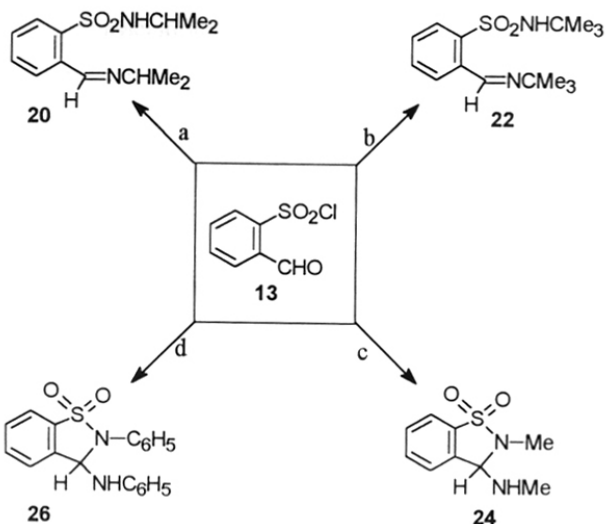
The sulfonylchlorides, normal 13 and pseudo 14 were prepared by the reaction of sodium salt of 2-formylbenzene sulfonic acid (7) with thionylchloride as reported earlier (Scheme 4).^{18,19} Normal and pseudo sulfonylchlorides 13 and 14 on treatment with primary amines gave the corresponding sulfonamide Schiff bases or the corresponding 2-formylbenzenesulfonamides depending on the condition and nature of the amine used.²⁰ Reaction of 13 and 14 with secondary amines gave the corresponding 2-formylbenzenesulfonamides in good yield irrespective of the amine used.



Scheme 4

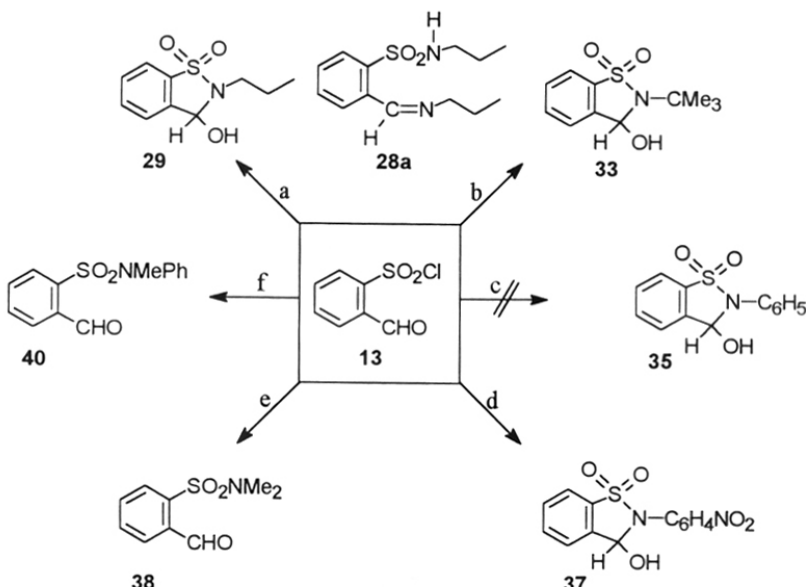
5.2 REACTION OF 2-FORMYLBENZENSULFONYLCHLORIDES WITH AMINES: PREPARATION OF 2-FORMYLBENZENESULFONAMIDES

Reaction of the normal sulfonylchloride 13 with excess of isopropyl and *t*-butyl amines resulted in the formation of the corresponding iminosulfonamides, 20 and 22 respectively (Scheme 5), which exist in equilibrium with their ring forms. Amounts of the ring and chain tautomers present depended on the nature of the alkyl substituent on the nitrogen atom (see section 5.4 for details). Reaction of normal sulfonylchloride 13 with excess of methylamine or aniline yielded the corresponding 3-amino benzisothiazole-1,1-dioxides, 24 and 26 respectively (Scheme 5). However, the reaction of the sulfonylchloride 13 with excess of *n*-propylamine gave the corresponding 2-formylbenzenesulfonamide majority of which exists as 3-hydroxy-benzisothiazole-1,1-dioxide, 29 (Scheme 6). The iminosulfonamide 28a could not be isolated.



a. isopropylamine, 1 h.; b. t-butylamine, 1 h.; c. methylamine, 1 h., d. aniline, 1 h

Scheme 5



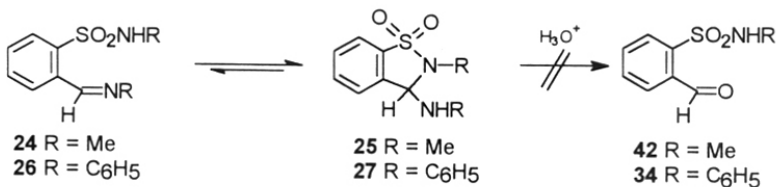
a. *n*-propylamine, b. *t*-butylamine (1 eq.)/TEA, c. aniline (1 eq.)/TEA, d. *p*-NO₂-aniline,
e. dimethylamine, f. N-methylaniline.

Scheme 6

Reaction of sulfonylchloride **13** with *p*-nitroaniline gave a mixture of products from which 2-formyl-benzenesulfonanilid **37** could be isolated by preperative TLC in 38% yield. Secondary amines, dimethylamine and N-methylaniline, reacted with the normal sulfonylchloride **13** to yield the corresponding sulfonamides **38** and **40** respectively.

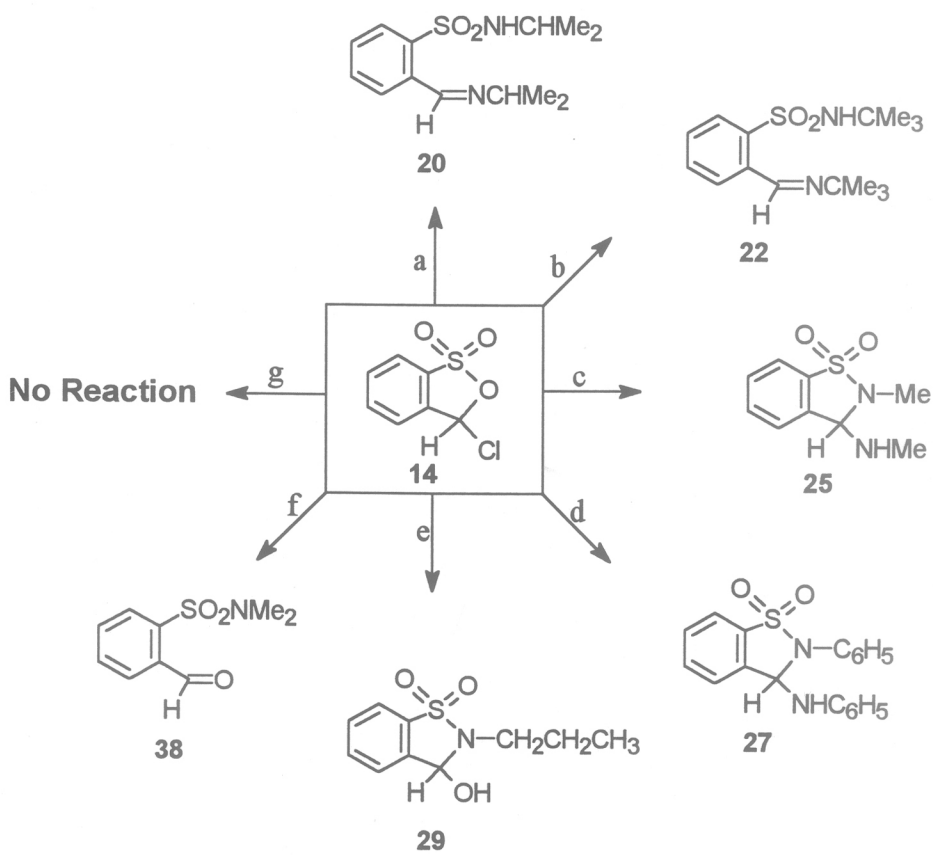


Schiff bases **20** and **22** on treatment with aqueous acetic acid at ambient temperature gave the corresponding benzothiazoles **31** and **33** in good yield (Scheme 7). On the other hand, products obtained from the reaction of normal sulfonylchloride **13** with methylamine and aniline did not undergo hydrolysis even under reflux in acetic acid methanol-water and were recovered unchanged (Scheme 8). These experiments suggested the possibility of existence of Schiff bases **24** and **26** in the cyclic form **25** and **27** which was confirmed by spectroscopic studies (see section 5.3). 2-formylbenzenesulfonamide **32** could also be obtained by the reaction of the normal sulfonylchloride **13** with one equivalent of the corresponding primary amine, in the presence of triethylamine, in a single step. The corresponding Schiff base was not formed.



Scheme 8

2-Formylbenzenesulfonamides and the corresponding Schiff bases (imino derivatives) could also be obtained by the reaction of amines with the pseudo sulfonylchloride **14**.²⁰ But the reaction of amines with pseudo sulfonylchloride **14** (Scheme 9) was very sluggish. When pseudo sulfonylchloride **14** was treated with an aqueous solution of methylamine, a very low yield of the benzisothiazole-1,1-dioxide **25** was obtained. Most of the sulfonyl chloride **14**, presumably underwent base catalyzed hydrolysis to 2-formylbenzenesulfonic acid.²⁰ However, a good yield of the benzisothiazole-1,1-dioxide **25** was obtained on using methylamine in non aqueous medium. Isopropylamine, aniline, *n*-propylamine and dimethylamine reacted with pseudo sulfonylchloride **14** at ambient temperature to give sulfonamides/benzisothiazole-1,1-dioxides **20**, **27**, **29**, and **38** in moderate to good yields.

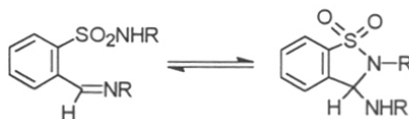


- a. isopropylamine, b. *t*-butylamine, c. methylamine, d. aniline, e. *n*-propylamine,
- f. dimethylamine, g. N-methylaniline.

Scheme 9

5.3 STRUCTURE AND CHARACTERIZATION OF 2-(N-ALKYL/ARYLIMINO)METHYLBENZENE-SULFONAMIDES

¹H and ¹³C NMR spectra of the Schiff bases (Table 1) showed that the methylamino derivative **24** exists completely in the cyclic form (Figure 1) and the *t*-butylamino derivative **22** completely in the open form (Figure 2), in solution (Scheme 10). ¹H NMR spectrum of the N-methylamino derivative showed signals characteristic only of the cyclic isomer **25** in which the benzylic hydrogen appeared at 5.22 ppm. But no signal characteristic of the imino proton was observed.



20	R = CHMe ₂	21
22	R = CMe ₃	23
24	R = Me	25
26	R = C ₆ H ₅	27

Scheme 10

Table 1: Amount of cyclic and open forms of Schiff bases present in solution.^a

Compound #	δ Open	% Open	δ Cyclic	% Cyclic
20 \leftrightarrow 21	08.47	93.0	5.48	07.0
22 \leftrightarrow 23	08.53	100.0	---	00.0
24 \leftrightarrow 25	---	00.0	5.22	100.0
26 \leftrightarrow 27	08.85	05.0	6.44	95.0

a: Determined by ¹H-NMR spectroscopy at ambient temperature in CDCl₃. Concentration of the compounds was about 0.08M and the percentage of the open and cyclic form were calculated from peak integrals.

Mass spectra of the Schiff bases **24** and **26** also supports the cyclic structure (see Table 8 and section 5.4.4 for details). ¹H NMR spectrum of the Schiff base obtained from *t*-butylamine showed signals characteristic of the open form **22**, in which the imino proton appeared at 8.53 ppm as a singlet (Figure 2). However, the isopropyl derivative showed signals characteristic of both the open and cyclic forms. In the ¹H NMR spectrum of the

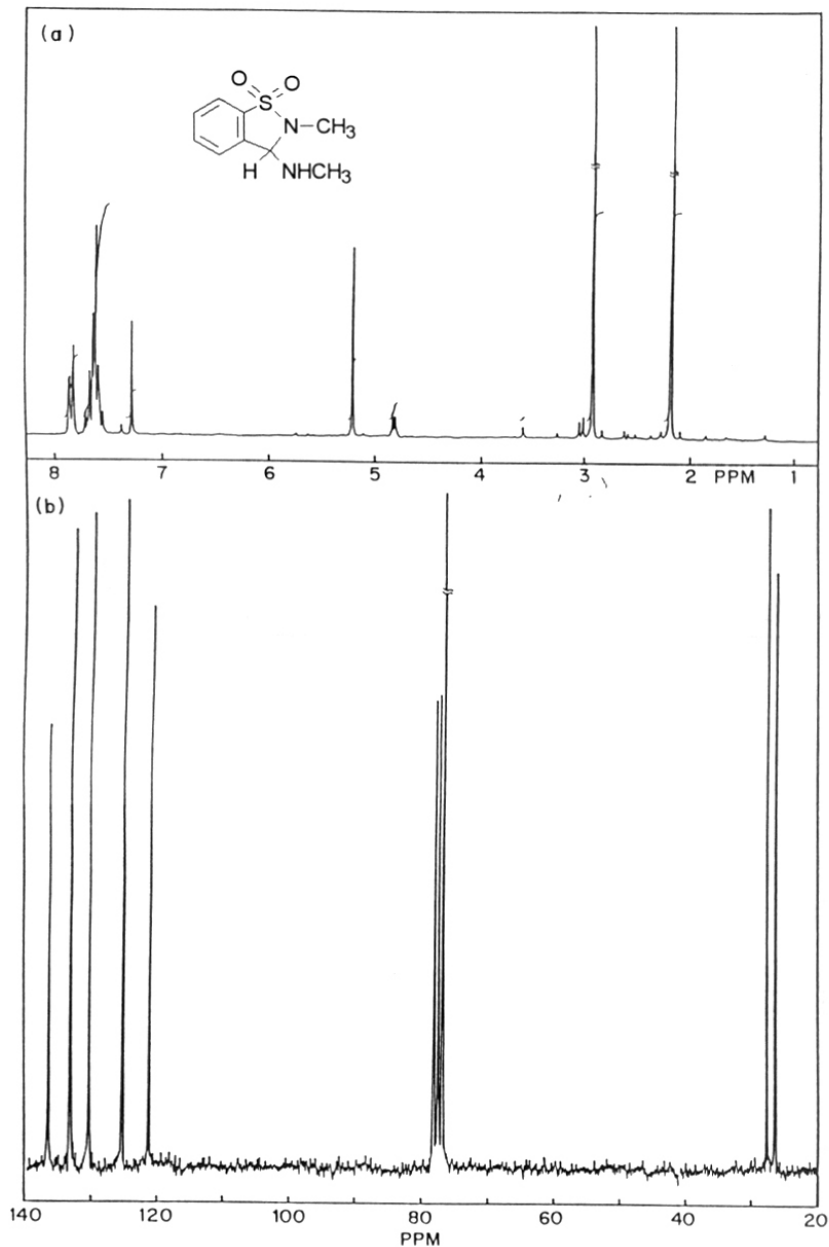


Figure 1. ¹H and ¹³C NMR spectra of compound 25 in CDCl₃.

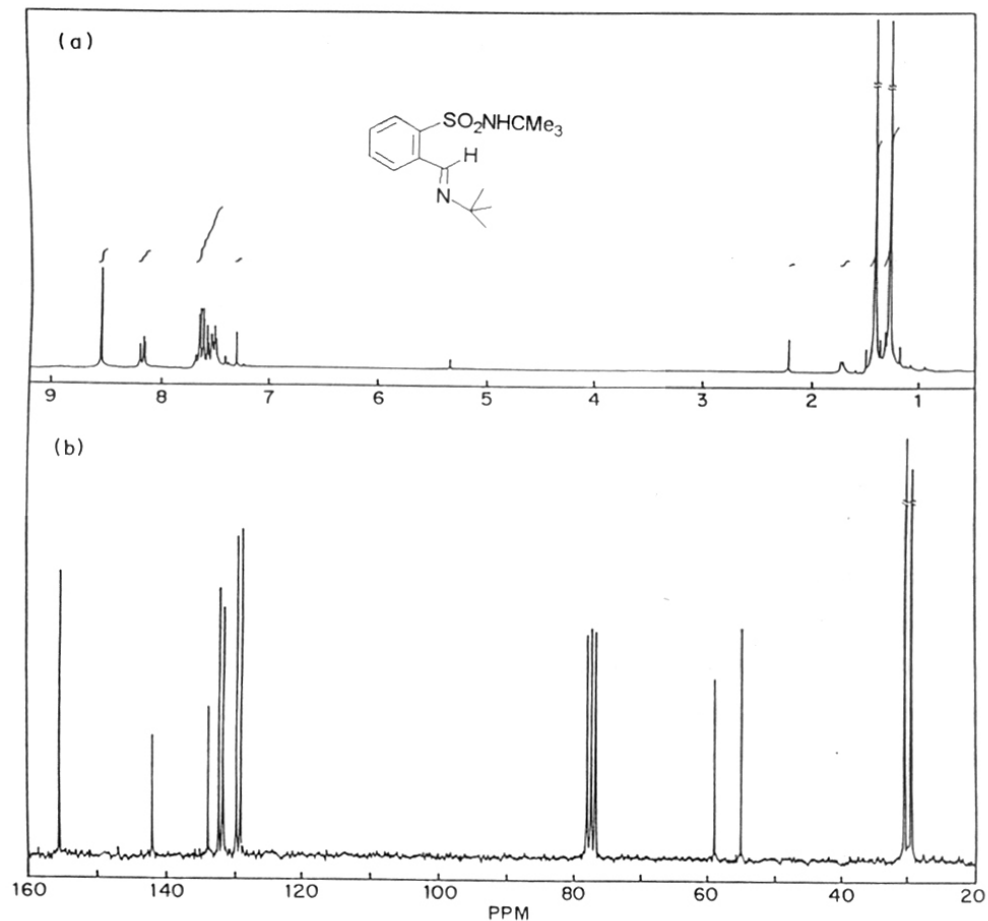


Figure 2. ¹H and ¹³C NMR spectra of compound 22 in CDCl₃.

isopropyl derivative the benzylic hydrogen of the cyclic isomer **21** appeared at 5.47 ppm and the imino proton of the open form **20** appeared at 8.48 ppm (Table 1). These results show that, in solution, the imino (open) form is favored as the steric bulk of the substituent on the nitrogen increases. Similar results have been reported in the case of the Schiff bases obtained from 2-benzoylbenzenesulfonic acid derivatives.¹² The IR spectra and mass spectra of the isopropyl and *t*-butyl derivatives **20** and **22** are more complex and definitive conclusions regarding their structure in the solid phase and the gas phase could not be arrived at.

5.4. STRUCTURE AND CHARACTERIZATION OF 2-FORMYLBENZENE-SULFONAMIDES

5.4.1. IR Spectra

The IR spectra of the N,N-disubstituted sulfonamide **40** (nujol mull and KBr disc) showed a strong peak at 1700 cm⁻¹ as expected for the aldehyde carbonyl group. The infrared spectra as nujol mull and KBr disc of the sulfonamides **28**, **30** and **32** did not show any absorption around 1700 cm⁻¹ indicating the absence of the carbonyl group. But, when the IR spectra of the same samples were recorded in chloroform solution, a relatively strong peak around 1695 cm⁻¹ was observed which suggested the existence of a carbonyl group. In the case of the n-propylamino derivative, a very weak peak was observed at 1699 cm⁻¹ in chloroform solution. The IR spectra of compound **30** as KBr disc and in chloroform solution are shown in Figure 3. A relatively strong carbonyl stretching band at 1695 cm⁻¹ was seen in the IR spectrum of **30** in chloroform (Figure 3b) but the same peak was absent in KBr disc (Figure 3a). The IR spectrum of sulfonamide **40** (KBr disc, Figure 3c) which has a strong carbonyl stretching band at 1700 cm⁻¹ and that of the isothiazole **24** (KBr disc, Figure 3d) which shows no carbonyl stretching are also shown for comparison. These results suggested the possibility of N-substituted 2-formylbenzenesulfonamides under study to be existing in the cyclic form in the solid state and possibly as a mixture of open and cyclic forms in solution, in varying amounts (Scheme 11)

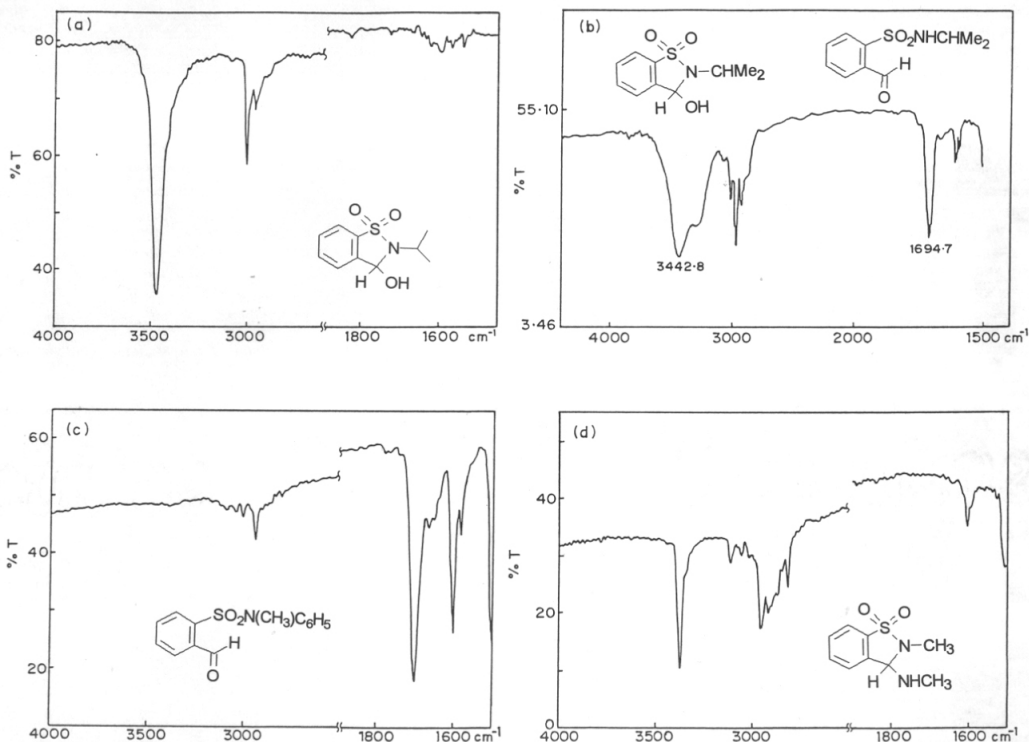
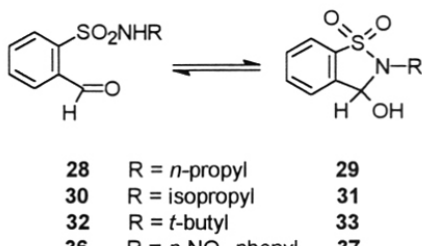


Figure 3. IR spectra of (a) compound 30/31 (KBr disc), (b) compound 30/31 (in chloroform), (c) compound 40 (KBr disc) and compound 25 (KBr disc).

**Scheme 11**

5.4.2. NMR Spectra

The ¹H NMR spectra (in CDCl₃) of N-substituted 2-formylbenzenesulfonamides showed signals characteristic of 2-formylbenzenesulfonamides as well as the corresponding 3-hydroxybenzisothiazole-1,1-dioxides. The benzylic hydrogen (of the cyclic form) appeared between 5.7 and 6.4 ppm and the aldehydic hydrogen (of the open form) appeared at about 10.3 ppm. In the case of *n*-propyl 28 ↔ 29, isopropyl 30 ↔ 31 and *t*-butyl 32 ↔ 33 (Figure 4) derivatives two sets of signals were observed for alkyl hydrogens (see section 5.6 for details) in their ¹H NMR spectra. The ¹³C NMR spectra (in CDCl₃ solution) of these derivatives also showed carbons characteristic of both the open and cyclic forms. The benzylic carbon of the cyclic form appeared at about 80 ppm and the aldehydic carbon appeared at 191 ppm. The signals due to the alkyl carbons could be assigned to the open and cyclic forms based on the relative intensities of the respective peaks (see Table 3). Signals due to aromatic carbons could not be assigned based on the relative intensities of the peaks due to the small differences in chemical shifts observed. However, the ¹³C NMR spectra (CP/MAS) of the same samples in the solid state showed signals characteristic of only the cyclic form (29, 31 and 33) and no peak due to the aldehydic carbon was observed. ¹³C NMR spectrum of the sodium salt of 2-formylbenzenesulfonic acid was recorded in solid state for comparison in which the carbonyl carbon appeared at 194 ppm. Also, only one set of signals, arising due to the cyclic form, was observed for the alkyl carbons of 29 and 33. But two signals were observed for the isopropyl methyl groups of 31 probably due to the nonequivalence of the

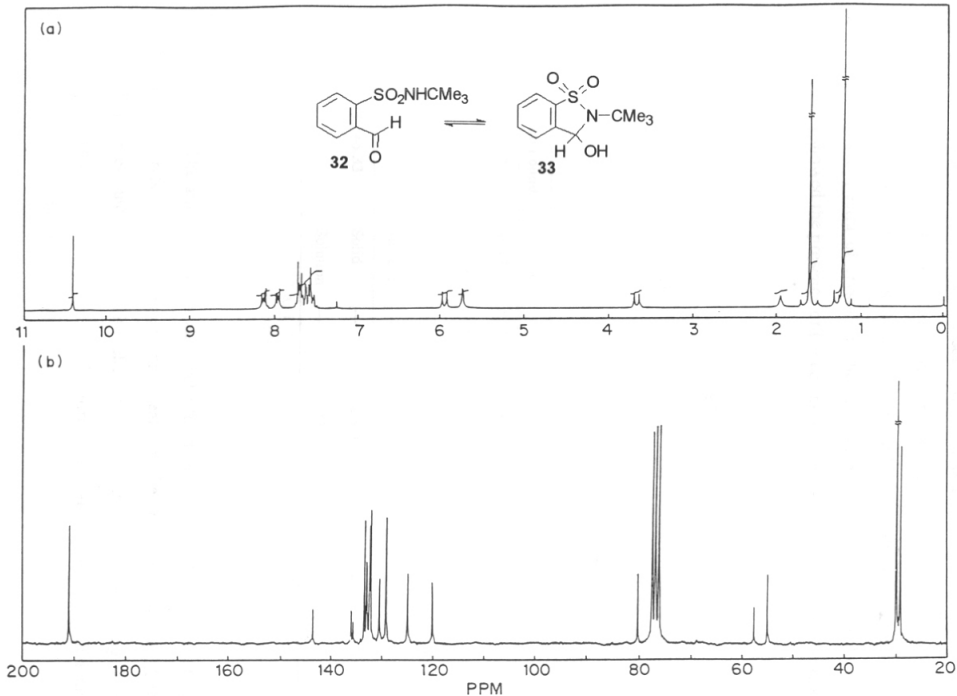


Figure 4. ^1H and ^{13}C NMR spectra of compound $32 \leftrightarrow 33$ in CDCl_3 at room temperature.

two methyl groups in the cyclic form (see section 5.4.2a for a detailed discussion of the ^1H NMR spectrum of 30). All the observed chemical shifts in the solid state are in close agreement with those in solution. These results showed that 2-formylbenzenesulfonamides exist in the cyclic form in the solid state and as a mixture of the open and cyclic forms in solution. The existence of 2-formylbenzenesulfonamides as corresponding benzisothiazole-1,1-dioxides in the solid state was confirmed by X-ray crystallography (see section 5.4.3). ^1H NMR spectra of crystals of benzisothiazole-1,1-dioxides, dissolved in CDCl_3 , once again showed the presence of the corresponding 2-formylbenzenesulfonamides.

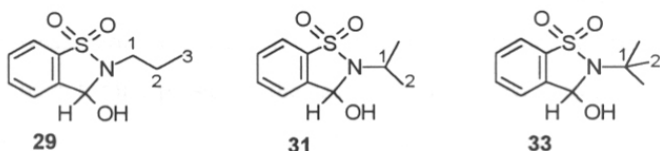


Table 2: ^{13}C NMR chemicalshifts of 2-formylbenzenesulfonamides in solid and solution^a states

Compound #	State	$\delta \text{ C}_3^{\text{b}}$	$\delta \text{ C}_2^{\text{b}}$	$\delta \text{ C}_1^{\text{b}}$	$\delta \text{ C(OH)}$	$\delta \text{ CHO}$
$28 \leftrightarrow 29$	Solid	11.0	22.0	43.0	84.0	---
	Solution	10.8 ^c , 11.2	21.5, 22.8 ^c	42.9, 44.9 ^c	81.7	191.0 ^c
$30 \leftrightarrow 31$	Solid	---	21.0, 23.0	46.0	80.0	---
	Solution	---	20.5, 23.1, 23.8 ^c	45.9, 46.4 ^c	79.6	191.0 ^c
$32 \leftrightarrow 33$	Solid	---	28.0	57.0	80.0	---
	Solution	---	29.2, 30.0 ^c	55.0 ^c , 57.7	80.3	191.0 ^c

a: In CDCl_3 . b: C1, C2 and C3 as shown in the structures above. c: Peaks arising from the open form, assigned on the basis of relative intensities of the signals.

The amount of open and cyclic forms present in solution could be estimated from the integrals of the corresponding peaks in the ^1H NMR spectra of the sulfonamide derivatives under study. The chemical shift values, corresponding integrals and the amounts of the open and cyclic forms of 2-formylbenzenesulfonamides present in solution are tabulated in Table 3.

Table 3: Amount of cyclic and open forms of 2-formyl-benzenesulfonamides in solution.^a

Compound #	δ Open	Integral of CHO	% Open	δ Cyclic	Integral of CHOH	% Cyclic
28 \leftrightarrow 29	10.38	3.7	04.0	5.71	80.7	96.0
30 \leftrightarrow 31	10.39	20.0	27.0	5.94	53.2	73.0
32 \leftrightarrow 33	10.45	20.0	63.0	6.02	11.6	37.0
36 \leftrightarrow 37	---	---	---	6.34	20.0	100.0

a: Determined by $^1\text{H-NMR}$ spectroscopy at ambient temperature in CDCl_3 . Concentration of the compounds was about 0.08M.

The n-propyl derivative $28 \leftrightarrow 29$ exists mainly as benzisothiazole-1,1-dioxide (hence a very weak carbonyl peak in the IR solution spectrum), whereas, an appreciable amount of the open form is present in the case of the isopropyl derivative $30 \leftrightarrow 31$. The *t*-butylamine derivative $32 \leftrightarrow 33$ exists largely in the open form (hence a strong carbonyl peak in the IR solution spectrum). The amount of the open and cyclic forms present in solution was independent of the concentration of the compound being examined in the range 0.04M to 0.18M.

Next, the *t*-butylamine derivative $32 \leftrightarrow 33$ was chosen to examine the effect of solvent on the ring-chain equilibrium, as appreciable amounts of both open and cyclic forms are present in solution, in this case. ^1H NMR spectra of $32 \leftrightarrow 33$ were recorded in various solvents and the amount of the open and cyclic forms present in solution was determined by peak integrals. From the results tabulated in Table 4, it is clear that the equilibrium $32 \leftrightarrow 33$ shifts towards the cyclic isomer 33 as the polarity of the solvent increases. Similar results were obtained in the case of isopropylamine and n-propylamine derivatives. For instance, isopropylamine derivatives $30 \leftrightarrow 31$ existed in the ratio 3:7 in chloroform-d and about 1:99 in acetone-d₆. The n-propyl derivative $28 \leftrightarrow 29$ consisted of about 95 % of the cyclic form in chloroform and it was completely cyclic in acetone-d₆. It is likely that water being a protic solvent favours the cyclization of 2-formylbenzenesulfonamides to the corresponding 3-hydroxy-benzisothiazole-1,1-dioxides, through the protonation of the carbonyl oxygen. This facilitates the nucleophilic addition of the sulfonamide nitrogen to the aldehydic carbonyl group.

Table 4: Effect of solvent^a on the equilibrium $32 \leftrightarrow 33$.

Solvent	δ Open	Integral of CHO	% Open	δ Cyclic	Integral of CHOH	% Cyclic
Chloroform	10.45	20.00	63.0	6.02	11.60	37.0
Acetone	10.76	04.05	43.0	6.12	05.49	57.0
Acetone-water 9:1	10.78	03.39	26.0	6.14	09.57	74.0
DMSO	10.74	04.05	22.0	6.05	14.19	78.0
Acetone-water 7:3	10.78	02.15	19.0	6.14	08.99	81.0
Acetone-water 1:1	10.57	04.70	08.0	6.08	51.60	92.0

a:Determined by $^1\text{H-NMR}$ spectroscopy at ambient temperature. Concentration of 32 was about 0.08M.

The effect of temperature on the sulfonamide \leftrightarrow benzisothiazole-1,1-dioxide equilibrium in solution (DMSO-d₆) was examined by VT-NMR. The isopropylamine derivative $30 \leftrightarrow 31$ consisted of about 2 % of 30 at 30 °C which increased to about 11 % on raising the temperature to 80 °C. Similarly, in the case of the *t*-butylamine derivative $32 \leftrightarrow 33$ the amount of the open form increased with temperature. However, the effect of temperature on the sulfonamide \leftrightarrow benzisothiazole equilibrium is not profound, as an increase of about 50 °C only increases the open form by about 10 %.

due to the *t*-butyl group with increasing temperature.

4.4.2a. Molecular Association of 2,3-Dihydro-2-alkyl-3-hydroxybenzisothiazole-1,1-dioxides: A detailed investigation of the ^1H NMR spectrum of the isopropyl derivative 31 under a variety of conditions showed that its ^1H NMR spectrum was concentration dependent. The $^1\text{H-NMR}$ spectrum of an equilibrium mixture of isopropyl derivatives $30 \leftrightarrow 31$ (at 298 °K, 10-20 mg/ml in CDCl₃) showed two doublets for the isopropyl methyl groups of 30 and 31 at 1.1 ppm and 1.5 ppm respectively indicating the equivalence of two methyl groups in both the isomers. But the $^1\text{H-NMR}$ spectrum of the same compound at a higher concentration (>24 mg/ml in CDCl₃) showed a doublet for the isopropyl methyl groups of 30, whereas two doublets for the isopropyl methyl groups of

31. The ^{13}C NMR spectrum of an equilibrium mixture of $30 \leftrightarrow 31$ showed three peaks at 20.5 and 23.1 ppm (due to 31) and 23.8 ppm (due to 30) for the isopropyl methyl groups irrespective of the concentration (Figure 5). These results suggested that the chemical shift of isopropyl methyl hydrogens of 31 are concentration dependent whereas the chemical shift of the isopropyl methyl carbons are independent of concentration. Hence we examined the ^1H NMR spectra of sulfonamides 28, 30 and 32 under various conditions and the results are described below.

^1H NMR spectra of $30 \leftrightarrow 31$ at different concentrations (in CDCl_3 , at 298 °K) is shown in Figure 6. The difference in chemical shift of the gem dimethyl group of cyclic isomer 31 increased with increase in concentration. The lowest concentration at which the isopropylmethyl hydrogens of the isothiazole 31 exhibit non equivalence and appear as a pair of doublets is 24 mg/mL (0.028 M of 30 and 0.078 M of 31 calculated based on the peak integrals) in CDCl_3 .

The chemical shift of the OH proton increased with increase in concentration (Figure 7). The increase in the chemical shift of NH proton of open form 30 with concentration was marginal. Variation of chemical shifts for the OH proton of the *t*-butyl derivative 33 with concentration was similar to that of the isopropyl derivative 31 (Figure 7). As in the case of isopropyl open form 30 the change in chemical shift of the NH proton of sulfonamide derivative 32 was minimal and unlike in the case of isopropyl derivative 31, the ^1H NMR spectra of *t*-butyl derivative 33 showed no change in the signal due to the *t*-butyl group with increase in concentration in solution. A considerable change in the chemical shift (~1ppm) for the OH proton was also observed in the ^1H NMR spectra of the *n*-propyl derivative 29 on changing the concentration from 2 mg/mL to 40 mg/mL. But the exact chemical shift of the OH proton could not be obtained at intermediate concentrations due to the overlap of the OH peak with other peaks in the ^1H NMR spectra.

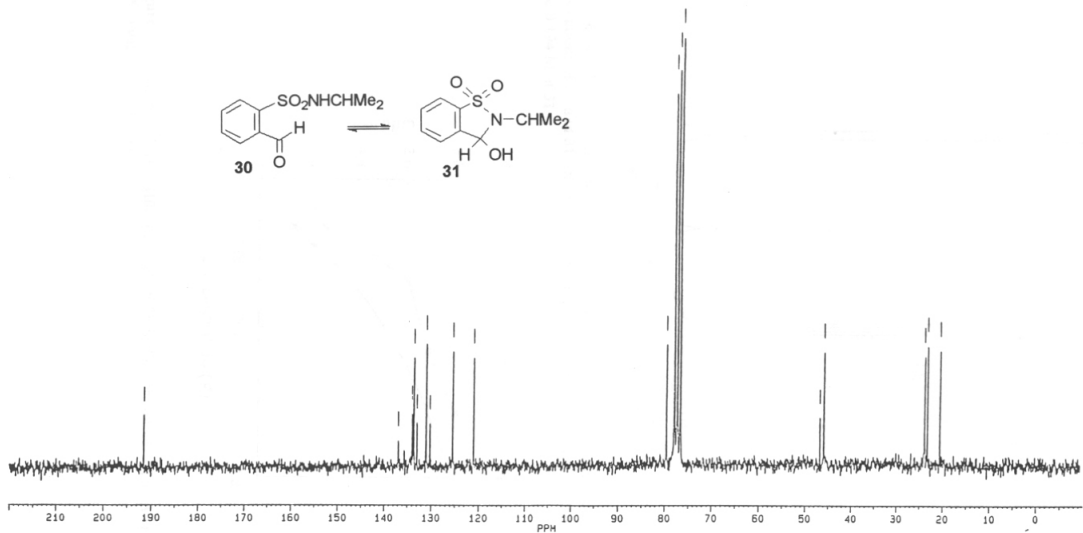


Figure 5. Low concentration (16 mg/mL) ¹³C NMR spectrum of compound 30 \leftrightarrow 31 in CDCl₃.

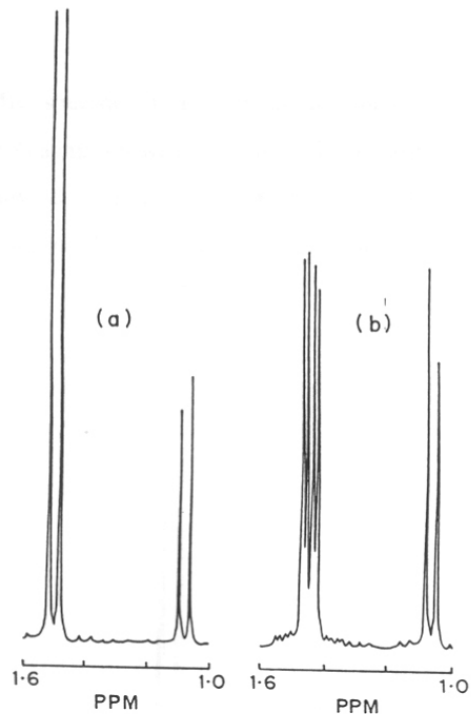


Figure 6. ^1H NMR spectral regions corresponding to the isopropyl methyl groups absorptions of 30 and 31: (a) 0.016 M of 30 and 0.045 M of 31 and (b) 0.070 M of 30 and 0.194 M of 31.

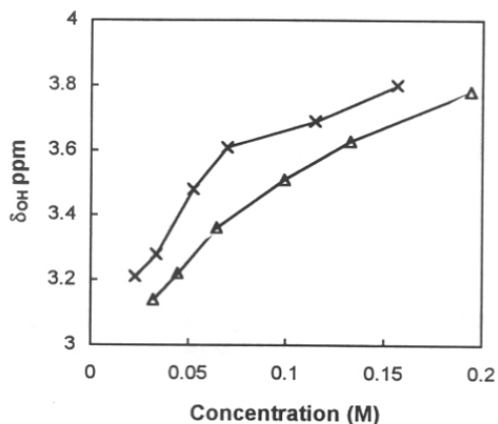


Figure 7. Variation of ^1H NMR chemical shifts of OH proton of 31 ($-\Delta-$) and 32 ($-X-$) with concentration.

The ^1H NMR spectra of an equilibrium mixture of $30 \leftrightarrow 31$ at various temperatures (Figure 8) again showed splitting of the isopropyl methyl signal of 31 . Figure 9 and Figure 10 show the variation of OH proton chemical shift and the change in chemical shift of the isopropyl methyl groups of 31 with temperature, respectively.

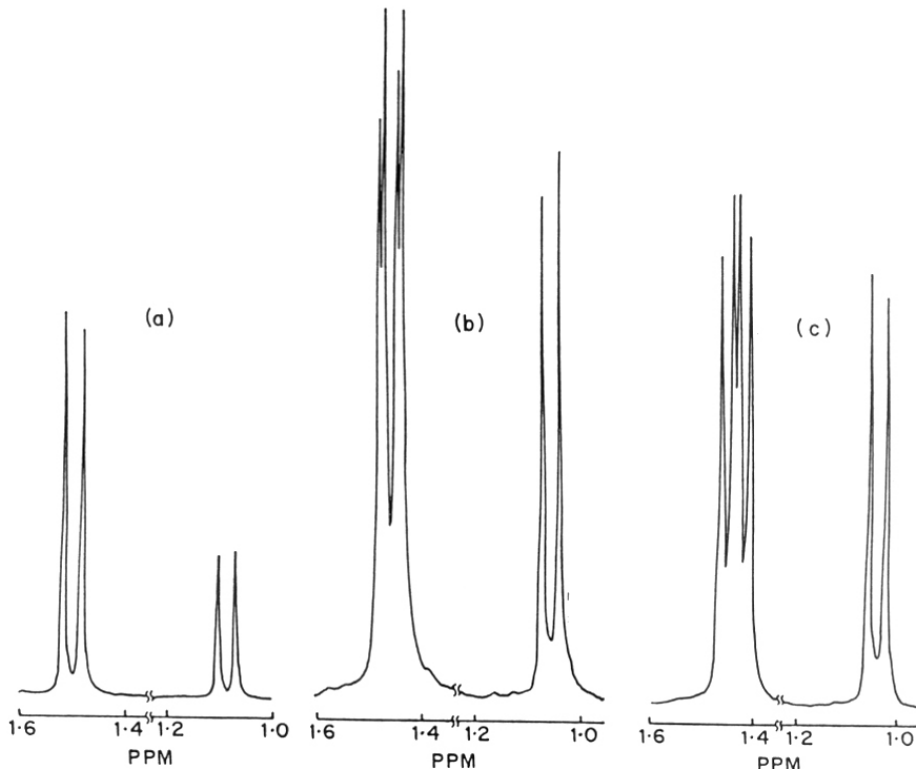


Figure 8. ^1H NMR spectral regions corresponding to the isopropyl methylgroups of 31 (0.052M) at different temperautres: (a) 298 °K, (b) 268 °K and (c) 248 °K.

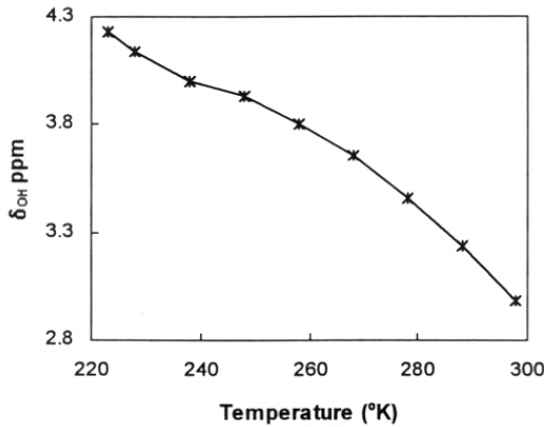


Figure 9. Variation of ^1H NMR chemical shifts of OH proton of **26** (0.052M) with temperature.

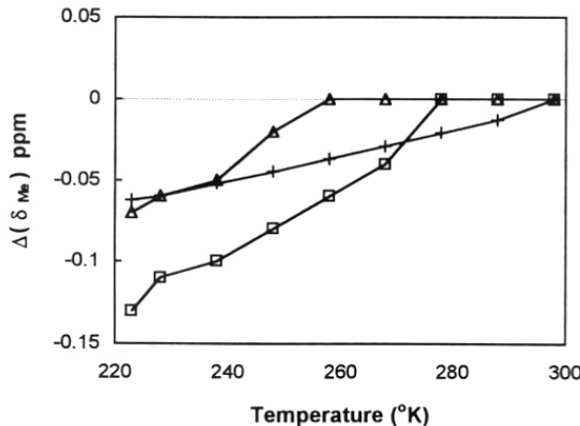


Figure 10. Plot of $(\delta_{\text{Me}, 298\text{°K}} - \delta_{\text{Me}, T\text{°K}})$ ppm for isopropyl groups of **30** and **31**: Line styles: —Δ— for one of the methyl groups of **31**, —□— for the second methyl group of **31** and —+— for methyl groups of **30**.

The difference in chemical shift ($\delta_{\text{Me}, 298\text{°K}} - \delta_{\text{Me}, T\text{°K}}$) of the isopropyl methyl groups of the cyclic isomer **31** (when plotted separately) with temperature (Figure 10) showed a greater shielding of one of the isopropyl methyl groups compared to the other. A plot of difference in chemical shifts ($\delta_{\text{Me}, 298\text{°K}} - \delta_{\text{Me}, T\text{°K}}$) of the isopropyl methyl groups of the open form **30** with temperature is shown for comparison. It is important to note that changes in

the NMR spectra of the cyclic tautomer **31** due to variation of temperature is similar (but with a larger magnitude) to the changes observed on varying the concentration. Again change in the chemical shift of the NH proton of the open form **30** with temperature was marginal.

The results presented above indicate association of 2-alkyl-3-hydroxy-benzisothiazoles under study in solution through hydrogen bonding at low temperatures (< 273 °K for isopropyl derivative **31**) or at high concentrations (>0.079 M for **31** and >0.070 M °K for *t*-butyl derivative **33**) at 298 °K. Nature of the aggregates of **31** or **33** present in solution is not obvious since hydroxy benzisothiazole dioxides have one hydrogen bond donor viz., the hydroxy group but two types of hydrogen bond acceptors viz., the ring nitrogen and sulfonyl oxygens. Intramolecular hydrogen bonding (between OH and SO₂) can however be ruled out since this would require OH chemical shift to be independent of concentration. Structure of the hydrogen bonded dimers were revealed by X-ray crystallography (see below) which clearly showed the formation of dimers through S=O.....HO interactions in the case of isopropyl derivative **31** and *t*-butyl derivative **33** (see Figure 14 and Table 7). Each hydrogen bonded dimer comprises of one pair of enantiomers, since benzylic carbon of one of the molecule in the dimer has the *R* configuration while that of the other has the *S* configuration (Figure 11).

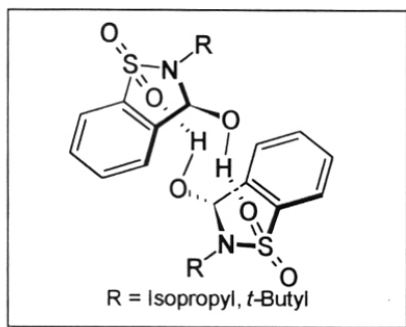


Figure 11

A discussion on the factors that could contribute to the changes observed in the ^1H NMR spectra of cyclic tautomer **31**, due to variation in temperature, solvent or concentration is given below. It is reasonable to expect non equivalence of the isopropyl methyl groups of **31** (in ^1H and ^{13}C NMR spectra), since 2,3-dihydro-2-isopropyl-3-hydroxybenzisothiazole-1,1-dioxide (**31**) has a chiral center at the benzylic position. This makes the isopropyl methyl groups of **31** diastereotopic which should have resulted in different chemical shifts for them (and hence they should have appeared as two doublets in ^1H NMR spectra, irrespective of the concentration of **31** in solution). However, accidental equivalence of diastereotopic groups is not uncommon.²¹ The ^{13}C NMR spectrum of the cyclic tautomer **31** showed two peaks due to diastereotopic methyl groups irrespective of its concentration in solution, as expected. Hence it is clear that the two methyl groups in **31** are equivalent (in ^1H NMR spectra) by accident.

The observed changes in the ^1H NMR spectra of **31** with variation of solvent and temperature can be accounted (based on accidental equivalence) since the chemical shift of diastereotopic groups is known to depend on various factors including solvent and temperature, but the sign and magnitude of these changes cannot be predicted with ease.²¹ Since diastereotropicity is inherent to the structure of a molecule, the chemical shifts of such groups may not be expected to depend on their concentration in solution. However, molecular association might have an effect on the chemical shifts of diastereotopic methyl groups and result in changes observed in the NMR spectra of **31** with variation in concentration. This is supported by the fact that one of the isopropyl methyl groups (of **31**) is in close contact (Table 7) with the aromatic ring of the other molecule of the hydrogen bonded dimer (see Figures 11 and 14). This could result in larger shielding of one of the isopropyl methyl groups of **31** due to the ring current effect²² of the benzene ring. In the case of *t*-butyl derivative **33** (which does not show any change in the methyl group signal with change in concentration), none of the methyl groups is at a distance lesser than 4 Å (Table 7).

5.4.3. X-ray Crystallographic Analysis

The solid state structures of benzene sulfonamides derived from *n*-propylamine, isopropylamine and *t*-butylamine as revealed through crystallography (Table 5), are shown in Figure 12. The hydroxyl group (O1 and O1') in both the molecules in the asymmetric unit of 29 occupy two disordered positions (in the ratio 8:2 and 6:4), and the *n*-propyl group has very high temperature factors. The disorder is caused by both the enantiomeric forms of the molecule occurring at the same position in the crystal, resulting in the hydroxyl group to appear at two places and the alkyl chain to have a diffused electron density. Because of the lesser accuracy of the structure it is not further included in the discussion.

The conformation of the isopropyl group in 31 is such that one of the methyl groups essentially eclipses the hydroxyl group, making the C8-H bond lie between the two sulfonyl oxygens. The eclipsing may be the reason for the widening of the C1-N-C8 angle (Figure 13). The conformation of the *t*-butyl group in 33 is different from that of the isopropyl group by a rotation of 42°, such that one C8-CH₃ bond is nearly perpendicular (78°) to the ring (and on the side opposite to the OH group). Because of the more steric crowding due to the *t*-butyl group in 33, the S-N, N-C8 and C8-CH₃ distances are 0.02 to 0.03 Å longer than those of 31 (Figure 13).

Table 6: Geometry of the Hydrogen Bond Interactions in the Crystal of 31 and 33

compound	atoms involved D-H...A	distance (Å) D...A	angle (°) D-H...A
31	O(1)-H(O1)...O(2) ^a	2.806	164.18
33	O(1)-H(O1)...O(2) ^b	2.802	163.75
	O(1')-H(O1')...O(2') ^c	2.809	169.77

Symmetry: (a) -x, 2-y, -z; (b) 1-x, 1-y, 1-z; (c) 1-x, 2-y, -z.

In the crystal, molecules of 31 and 33 form compact dimers related by crystallographic center of inversion (Figure 14). The dimers are held together by hydrogen bonding (Table 6); as the C1-O1 and S=O2 in the donor and acceptor sites have very

Table 5. Summary of Crystal Data, Data Collection, Structure Solution, and Refinement Details

	29	31	33
(a) Crystal Data			
formula	C ₁₀ H ₁₃ NO ₃ S	C ₁₀ H ₁₃ NO ₃ S	C ₁₂ H ₁₅ NO ₃ S
molar mass	227.27	227.27	241.30
color, habit	colorless, plate	colorless, plate	colorless, plate
crystal size, mm	0.60 x 0.50 x 0.40	0.40 x 0.40 x 0.30	0.60 x 0.50 x 0.40
crystal system	monoclinic	monoclinic	triclinic
<i>a</i> , Å	16.071(5)	8.003(2)	9.485(3)
<i>b</i> , Å	8.490(2)	15.894(2)	10.388(4)
<i>c</i> , Å	17.078(4)	9.127(3)	12.363(4)
α , deg	90	90	89.83(3)
β , deg	104.70(2)	109.51(2)	106.78(2)
γ , deg	90	90	90.26(3)
<i>V</i> , Å ³	2254.0(10)	1094.2(5)	1166.2(7)
space group	<i>P</i> 2 ₁ / <i>c</i>	<i>P</i> 2 ₁ / <i>c</i>	\overline{P} 1
<i>Z</i>	8	4	4
<i>F</i> (000)	960	480	512
<i>d</i> _{calcd} , g cm ⁻³	1.339	1.380	1.374
μ , mm ⁻¹	0.274	0.282	0.269
(b) Data Acquisition			
temp, K	293(2)	293(2)	293(2)
unit-cell reflcns	25 (8.6 16.7)	25 (9.2 23.2)	25 (13.4 23.19)
(θ range, deg)			
max θ (deg) for reflcns	23.5	23.4	23.5
<i>hkl</i> range of reflcns	-17 17; 0 9; 0 19	-8 8; 0 17; 0 10	-10 10; 0 11; -13 13
variation in three standrd reflcns	1.5%	1%	1%
reflcnns measd	3337	1602	3440
unique reflcns	3337	1602	3440
reflcnns with <i>I</i> > 2 σ (<i>I</i>)	1179	1439	2704
(c) Structure Solution and Refinement			
refinement on	<i>F</i> ²	<i>F</i> ²	<i>F</i> ²
solution method	NRCVAX	NRCVAX	NRCVAX
H-atom treatment	calculated, not refined	from Δ -map, not refined	from Δ -map, not refined
no. variables in L.S.			
<i>k</i> in $w = 1/(\sigma^2 F_o^2 + k)$ [$P = (F_o^2 + 2F_c^2)/3$]	290	136	290
<i>R</i> , <i>R</i> _w , gof	6.2427 <i>P</i>	(0.0539 <i>P</i>) ² + 0.8081 <i>P</i>	(0.1246 <i>P</i>) ² + 0.8885 <i>P</i>
density range in final Δ -map, eÅ ⁻³	0.091, 0.143, 0.811 -0.286, 0.253	0.047, 0.128, 1.285 -0.443, 0.249	0.057, 0.175, 1.040 -0.496, 0.478
final shift, error ratio	0.001	0.001	0.001
sec. extnct type	SHELXL	none	SHELXL
sec. extnct corrctn	0.0019(1)	---	0.023(4)

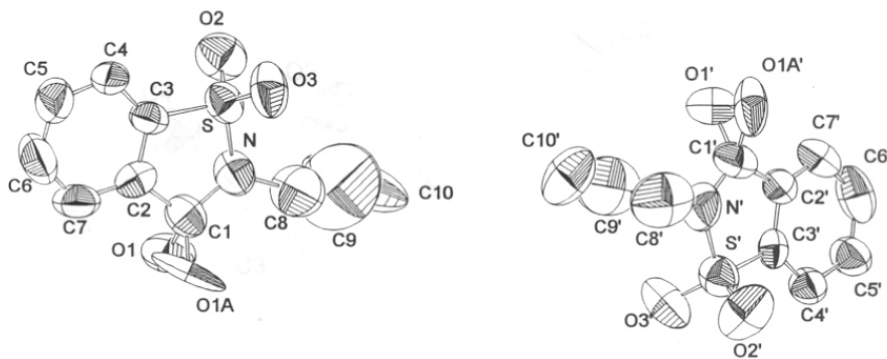


Figure 12a. ORTEP Representation of **29**.

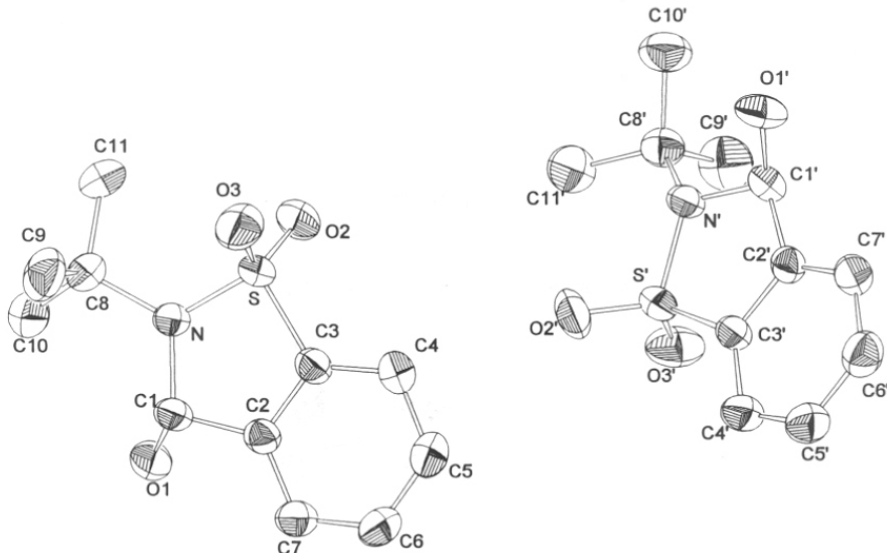


Figure 12b. ORTEP Representation of **32**

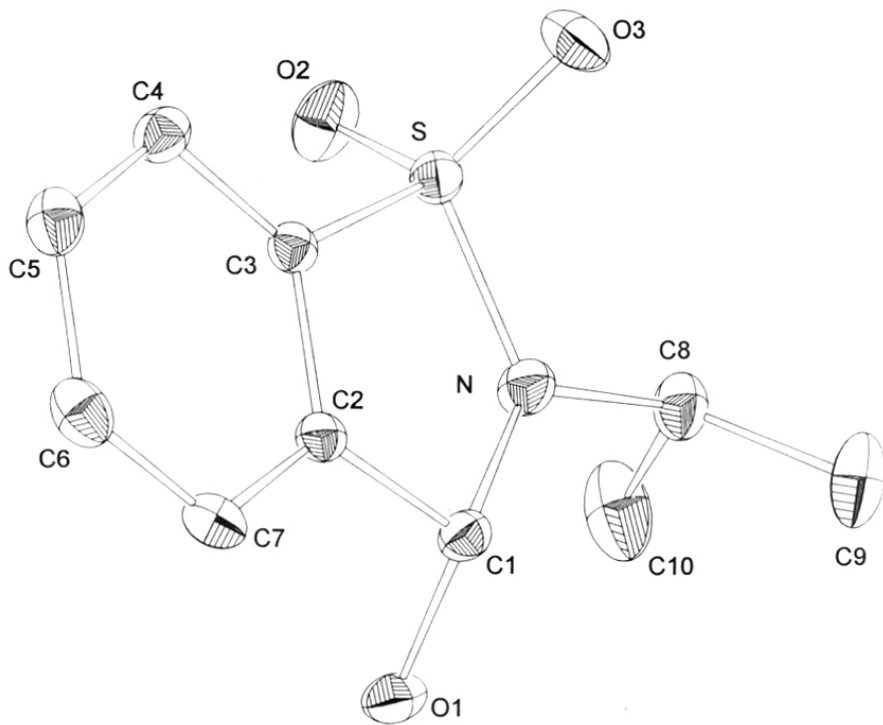


Figure 12c. ORTEP Representation of 31

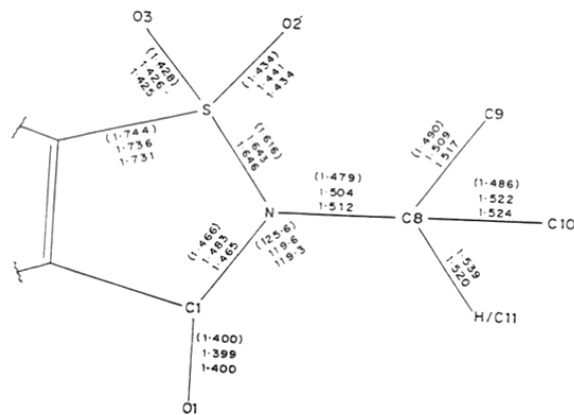


Figure 13. Selected bond lengths (Å) and angles (°) shown against the molecular diagram (the upper value, in parentheses, is for 31 and the lower ones are for the two molecules of 33). The standard deviations are in the range 0.002 to 0.006 Å and 0.3°, respectively.

comparable lengths the hydrogen bonded ring structure is quite symmetric. However, other forces like the CH/π interaction²³ can also provide stability, especially for 31. As can be seen from Table 8 a methyl group comes very close to the face of the benzene ring of the partner. The two groups do not show such close contact in 33, and there could be two reasons for this. Firstly, because of the increase in a few bond lengths, as discussed above, the methyl groups in 33 go out of the periphery of the benzene ring of the centrosymmetrically related partner. Secondly, the conformation of the *t*-butyl group is such that the methyl group which is nearly perpendicular to the ring and which could have the closest contact with the aromatic face of the partner is pointing in the opposite direction. The head-on orientation of a C-CH₃ group relative to the benzene ring in 31, in contrast to the rather inclined positioning of two such groups in 33 causes the two aromatic planes in the dimer to come closer (4.43 Å) in the latter than the former (5.02 Å).

Table 7: Geometric Parameters for the Alkyl Group Juxtaposed over the Benzene Ring within a Dimer.

Compound	Methyl C	Distance (Å) between the methyl C and the benzene		
		plane	centroid	C (nearest atom)
31	C(10)	3.665	3.932	3.676(C4)
33	C(10)	4.000	4.749	4.223(C4)
	C(11)	4.212	4.376	4.250(C6)
	C(10')	4.000	4.761	4.230(C4')
	C(11')	4.215	4.385	4.256(C6')

For compound 33 values for both the molecules in the asymmetric unit are given. Although not within the dimer, C(9) and C(9') of 33 have comparable close contact with symmetry related benzene rings.

The hydrogen bonded ring in the crystal of 31 and 33 is 12- or 14-membered depending on whether one traverses N or C3 and C2 while going from S to C1 along the cyclic hydrogen bond motif. Another unique feature of this dimeric structure is the additional involvement of the CH/π interaction which can play an important role in molecular association.²⁴ The hydrogen-bonded aromatic systems, like the DNA bases, usually form planar structures; but in system under investigation the hydrogen bonding is

in a direction normal to the two rings arranged in a parallel fashion. A 16-membered hydrogen bonded dimeric structure has been reported recently.²⁵

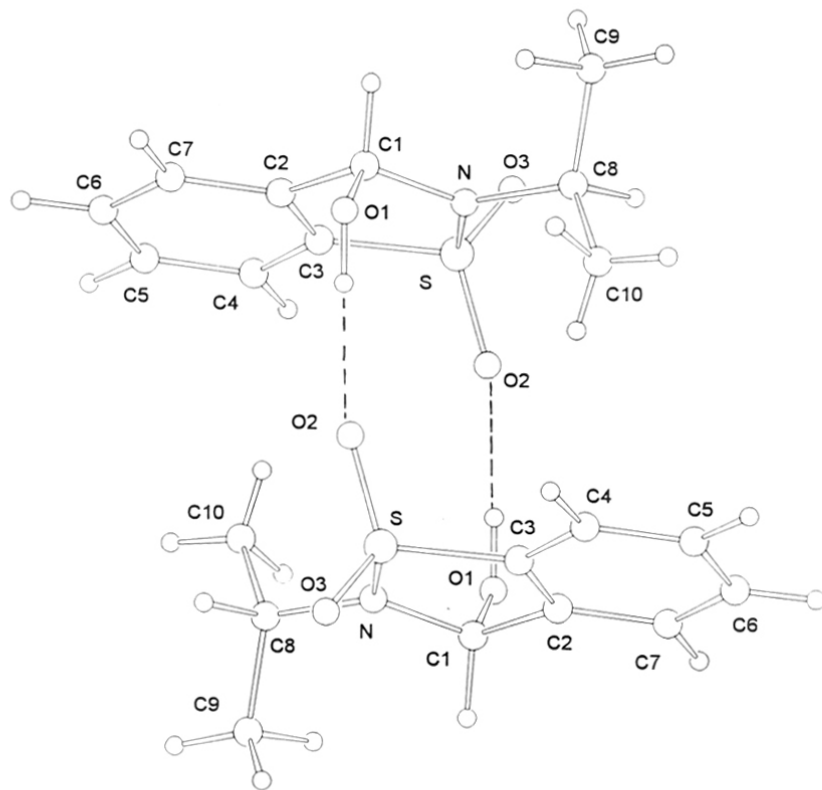


Figure 14a. H-bonded dimer of 31: Pair of molecules related by inversion center and connected by hydrogen bonds (shown in dashed line).

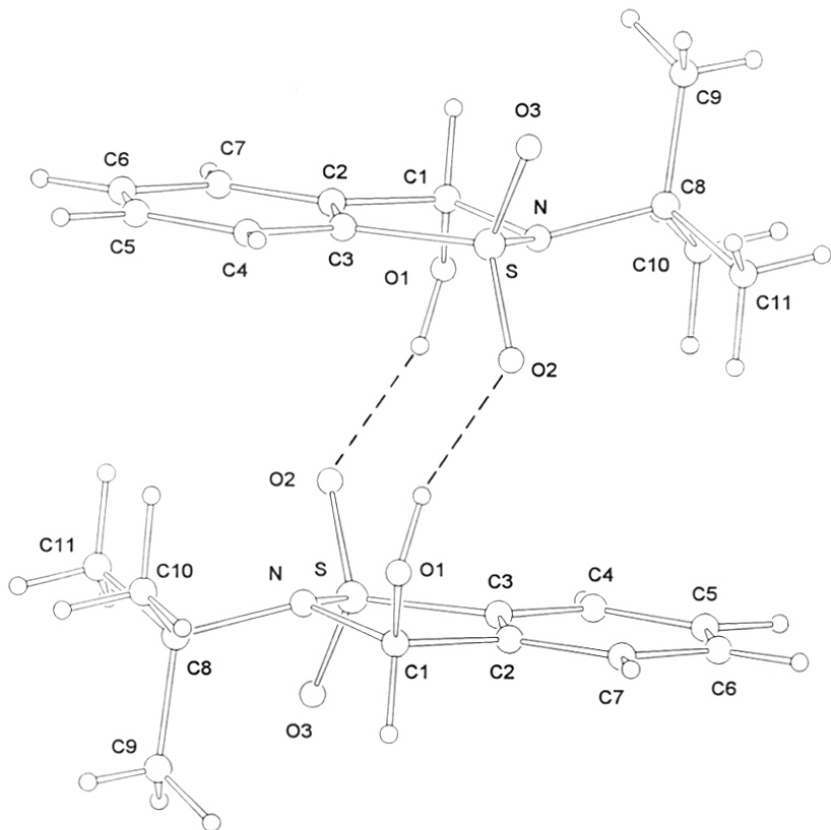
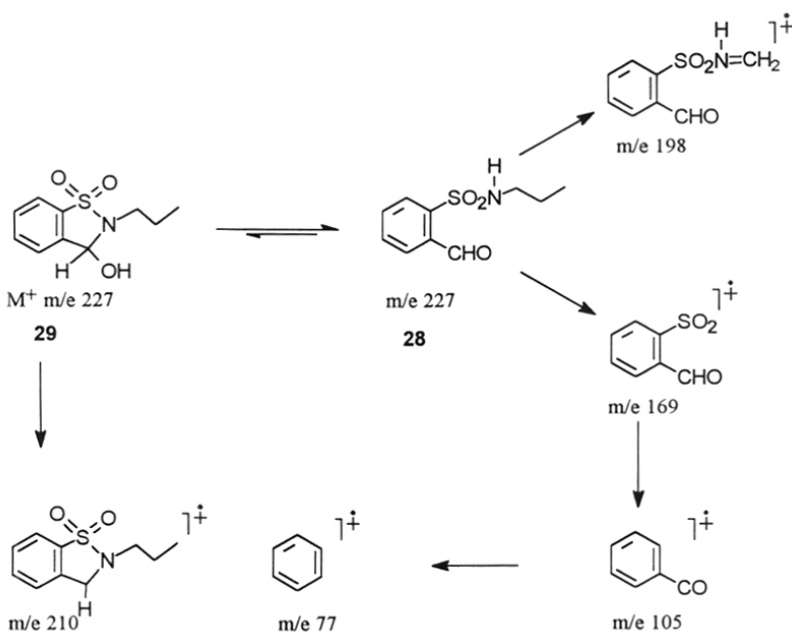


Figure 14b. H-bonded dimer of 33: Pair of molecules related by inversion center and connected by hydrogen bonds (shown in dashed line).

5.4.4. Mass Spectra

The major peaks observed in EI-MS of benzisothiazole-1,1-dioxides **25**, **27**, **29**, **31**, **33** and **37**, Schiff bases **20** and **22** as well as N-phenyl-N-methyl-2-formylbenzenesulfonamide (**40**) are shown in Table 8. To analyze the mass spectra of 2-formylbenzenesulfonamides, we used the mass spectra of the sulfonamide **40** and Schiff bases **24** and **26** as standards. Since **40** is completely open under all conditions its mass spectrum is characteristic of 2-formylbenzenesulfonamides and since **25** and **27** are completely cyclic under all conditions, their mass spectra are characteristic of benzisothiazole-1,1-dioxides. We were forced to use **25** and **27** as standards as none of the 2-formylbenzenesulfonamides under study is completely cyclic under all conditions used. The fragmentation pattern of the n-propyl derivative **28** ↔ **29** is shown in Scheme 12 as an example. Mass spectra of **29**, **31**, **33** and **37** show S-N bond cleavage to yield m/z 169 as the base peak. The ion with m/z 169 further undergoes loss of sulfur dioxide and carbon monoxide consecutively giving rise to peaks at m/z 105 and 77. The mass spectra of sulfonamides **32** and **40** are shown in Figure 15. Mass spectra of 2-formylbenzenesulfonamides **28**, **30** and **32** resemble that of the sulfonamide **40** (Figure 15). These findings are in agreement with *p*-substituted benzenesulfonamide derivatives which show similar mass spectral fragmentation pattern.²⁶ If the sulfonamides **30** and **32** existed as 3-hydroxy-benzisothiazole-1,1-dioxides in the gas phase (*i.e.*, under mass spectral conditions), it would be reasonable to expect the loss of the benzylic hydroxy group from the molecular ion and their mass spectra should have resembled those of benzisothiazole-1,1-dioxides **25** and **27** (see Figure 16) which show base peaks at m/z 182 and 244 respectively, due to the loss of the 3-amino group. However, no such prominent peak at m/z 289, 210 or 224 (due to loss of OH group) was observed in the mass spectra of isothiazole derivative **31**, **33** or **37** respectively. The mass spectrum of the n-propyl derivative **29** does show a very small peak (about 5%) at m/z 210. This indicates the presence of a small fraction of the cyclic isomer under mass spectral conditions.

**Scheme 12****Table 4:** EI-MS Fragmentation of benzisothiazole-1,1-dioxides

Compound #	m/z (Relative intensity)
20 ↔ 21	253(40), 210(20), 168(100), 146(5). 145(55), 104(35), 103(85), 77(55).
22 ↔ 23	281(12), 224(2), 168(100), 159(40), 104(15), 57(15).
24 ↔ 25	M ⁺ 212(<2), 182(100), 118(20), 117(25), 91(15).
26 ↔ 27	M ⁺ 336(<2), 244(100), 180(35), 179(20), 178(15), 153(15), 152(50), 151(15).
28 ↔ 29	M ⁺ 227(6), 210(5), 198(46), 169(100), 168(71), 105(30), 77(44).
30 ↔ 31	M ⁺ 227(1), 21(43), 169(100), 105(17), 77(8).
32 ↔ 33	M ⁺ 241(<1), 226(63), 169(100), 168(43), 105(60), 77(38).
36 ↔ 37	M ⁺ 306(9), 169(100), 138(46), 105(58), 77(69).
40	M ⁺ 275(4), 169(14), 107(100), 106(56), 105(19), 104(22), 77(12).

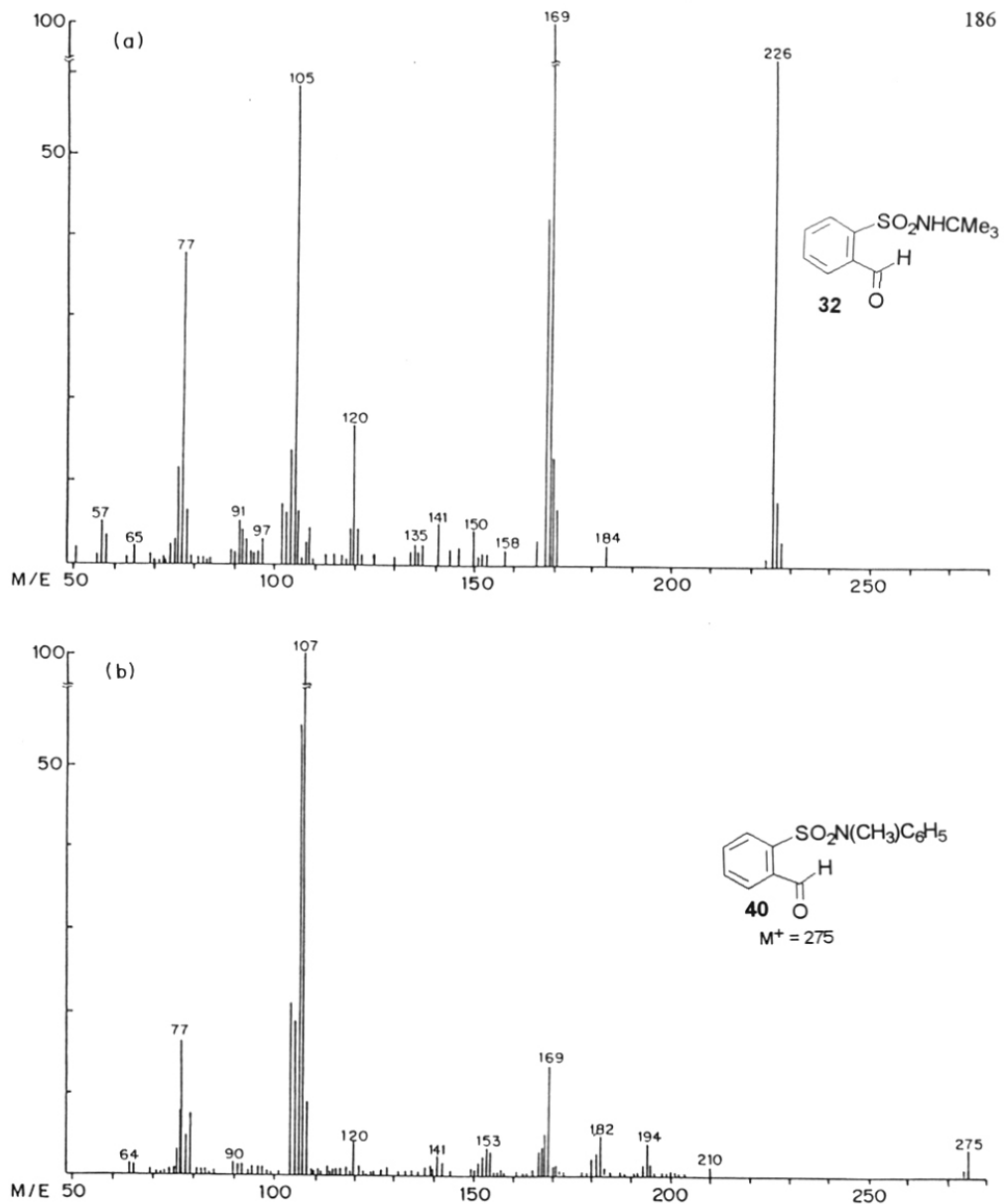


Figure 15. EI MS of compounds (a) 32 and (b) 40.

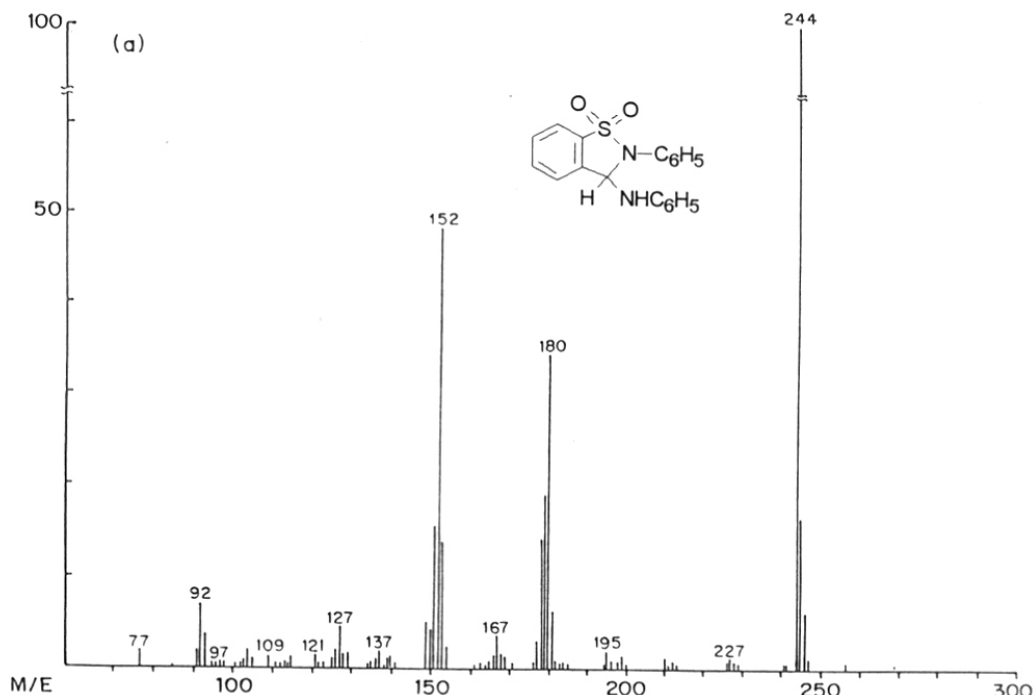
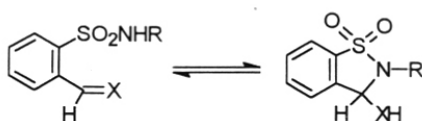


Figure 15. EI MS of compounds 27.

Thus, these results indicate that sulfonamides **29**, **31**, **33** and **37** exist more or less completely in the open form in the gas phase. This is in contrast to the corresponding carboxylic acid derivatives viz., 2-formylbenzoic acid amides, which are completely cyclic (*i.e.*, exist as 3-hydroxy-iso-indolenones) in solid, solution and gas phases.^{27,28} It is not surprising to see that benzisothiazole-1,1-dioxide \leftrightarrow 2-formylbenzenesulfonamide equilibrium is shifted completely towards the open form in the gas phase, as the polarity (dielectric constant) of the medium is very low. Furthermore, benzisothiazole-1,1-dioxides lack additional stabilization due to intermolecular hydrogen bonding or hydrogen bonding with the solvent molecules (see Tables 3 and 4) when present in the gas phase. However, preferential evaporation of one of the tautomers (open form) due to melting of the sample on the heated probe cannot be ruled out.



28	$X = O, R = n\text{-propyl}$	29
30	$X = O, R = \text{isopropyl}$	31
32	$X = O, R = t\text{-butyl}$	33
34	$X = O, R = \text{phenyl}$	35
42	$X = O, R = \text{Me}$	43
44	$X = \text{NH}, R = \text{Me}$	45
46	$X = \text{NH}, R = \text{phenyl}$	47

Scheme 13

A theoretical approach to the study of equilibrium involving tautomeric systems of the type discussed in the present work would serve to complement as well as supplement the experimental methods. The semi-empirical SCF-MO method²⁹ AM1 has been used in the present investigation to obtain the standard heats of formation of model systems. It is reasonable to assume that **42** (**Scheme 13**) would serve as a model for the systems **28**, **30** and **32**. The model system employed for the cyclic counterparts of these three species is **43**. Calculations have also been carried out on the species **34** and **35** in order to model the phenyl derivatives. Similarly to obtain the relative stabilities of Schiff bases like **24** and their cyclic analogs **25**, the heats of formation of model systems **44** \leftrightarrow **45** and **46** \leftrightarrow **47** have been computed (**Scheme 13**). The AM1 heats of formation values of all these species (in kcal/mol) are as follows: **34** (110.4), **35** (113.8), **42** (76.9), **43** (77.5), **44** (127.8), **45** (123.9), **46** (163.5), and **47** (160.2),

Computational studies with AM1 method reveal that **42** is more stable than the heterocyclic system **43** by 0.6 kcal/mol. Similarly the phenyl derivative **34** is computed to be less stable than its acyclic counterpart **35** by 3.4 kcal/mol. In the case of Schiff bases the acyclic form **44** is less stable than its cyclic tautomer **45** by 3.9 kcal/mol. The phenyl derivatives too follow the same trend; the cyclic tautomer **47** is computed to be more stable than **46** by 3.3 kcal/mol. Thus, the present investigation leads to the suggestion that an acyclic sulfonamide structure is intrinsically preferable to its isomeric 3-hydroxy isothiazole structure. These results are in close agreement with the experimental studies in

the gas phase. The reversal of the order of stability on going from the gas phase to the condensed phases is probably due to intermolecular interactions and medium effects. The present calculations do not include intermolecular or solvent interactions and hence the results are not valid in solution.

5.5 CONCLUSIONS

From the results discussed above, we can conclude that 2-formylbenzenesulfonamides exist (a) in the cyclic form in solid state, (b) as a mixture of open and cyclic forms in solution (c) more or less completely in the open form in the gas phase and (d) under a given set of conditions (solvent, temperature etc.) in solution the open form is favored as the steric bulk on the nitrogen increases or as polarity of the solvent decreases.

3-hydroxy-benzisothiazole-1,1-dioxides constitute a self-complementary hydrogen bonding donor - acceptor system that dimerize in the solid state as well as in solution through S=O \cdots HO H-bonding. Perhaps, this is the first report on hydrogen bonding interactions between a sulfonyl group and a hydroxy group resulting in the formation of a 12/14 membered ring. Delineation of these interactions could help design and synthesis of supramolecular structures with interesting properties.

5.6 EXPERIMENTAL

For general procedure and protocol see *Chapter 2, section 2.5.* Preparative TLC was performed using Merck Kieselgel 60 F₂₅₄ plates. Infrared spectra were recorded on a Perkin Elmer 599B or model 1620 instruments. Solutions for the recording of NMR spectra at various concentrations were prepared by directly weighing the appropriate compound in the NMR tube and dissolved in 0.5 ml of deuteriochloroform. The spectra were recorded at 298 °K unless otherwise stated. For VT-NMR experiments, 31 (8 mg) was dissolved in deuteriochloroform (0.5ml) and ¹H NMR spectra were recorded between 223 °K and 298 °K by decreasing the temperature in steps of 10 °K. The molar concentrations of cyclic and open forms given were calculated based on the integrals from the ¹H NMR spectra of compounds under discussion.

Solid state ¹³C NMR spectra (CP/MAS) were recorded on a Brucker MSL 300 spectrometer, operating at 75.476 MHz. Recording conditions were: spectral width, 400 ppm; pulse angle, 90°; width, 5.3 µs; repetition time, 4 sec; CP-contact time, 1 msec; spinning frequency, 2-3.5 kHz. Electron impact mass spectra were recorded on an automated Finnigan MAT 1020 mass spectrometer. The source conditions were as follows: temperature range, 150-200 °C; ionizing energy, 70 ev; pressure, 10⁻⁶ mm Hg (1mm Hg = 133.3 Pa). Samples were introduced into the source by direct insertion probe. Normal and pseudo 2-formylbenzenesulfonyl chlorides were prepared as reported earlier.^{18,19} Usual "work-up" implies washing of the organic extract with water followed by brine, drying over anhydrous sodium sulfate and evaporation of the solvent in vacuum.

X-Ray crystallography: Details of the crystal parameters, intensity data measurement, refinement and the solution of the structures are given in Table 1. Data were collected on an Enraf Nonius CAD4 diffractometer with graphite-monochromatized Mo K_α radiation ($\lambda = 0.7093 \text{ \AA}$). Data reduction and the structure solution were carried out with the PC-version of the NRCVAX system of programs.³⁰ The refinement was done with all data on F^2 with SHELXL-93.³¹

Reaction of normal 2-formylbenzenesulfonyl chloride (1) with excess of amines

Methylamine: The sulfonyl chloride **13** (0.205 g, 1 mmol) was dissolved in dichloromethane (10 mL) and dry methylamine gas was passed for 30 min. under ice cold condition and then worked-up as usual. The product was recrystallized from benzene-petroleum ether (40-60 °C) to obtain 2,3-dihydro-2-methyl-3-methylamino-benzisothiazole-1,1-dioxide (**25**) as a colorless solid (0.19 g, 90.0 %), m.p. 89-90 °C (lit.¹⁹ mp. 80 °C). IR (Nujol): 3300-3400 cm⁻¹. IR (KBr disc): 3390 cm⁻¹. ¹H-NMR, δ(CDCl₃): 7.86-7.62(m, 4H), 5.22(s, 1H), 4.84-4.81(d, 1H, exchangeable with D₂O), 2.94(s, 3H) and 2.20(s, 3H). ¹³C₆ δ(CDCl₃): 136.4, 133.2, 130.3, 125.3, 121.2, 76.8, 27.7 and 26.5. HRMS. Calcd. for C₈H₈NO₂S (M⁺-CH₃NH) = 182.0276; Found, M⁺-CH₃NH = 182.0275. For EI-MS data see Table 8.

Treatment of pseudosulfonylchloride **14** (0.41 g, 2.0 mmol) with methyl amine as above gave the isothiazole **25** (0.37 g, 87.0%).

n-Propylamine: The sulfonyl chloride **13**, (0.103 g, 0.5 mmol) was dissolved in dry dichloromethane (2 mL), n-propylamine (1 mL) was added and stirred at ambient temperature for 3 h. Solvent and excess of the amine were removed in vacuum. The residue was taken in dichloromethane (6 mL) and worked-up as usual. 2,3-Dihydro-2-n-propyl-3-hydroxy-benzisothiazole-1,1-dioxide (**29**) was purified by column chromatography; eluent: 10% ethylacetate-petroleum ether (0.080 g, 72 %), mp. 99-100 °C (lit.¹⁹ mp. 98-99 °C). IR (Nujol): 3550-3300 cm⁻¹. IR (KBr disc): 3550-3350 cm⁻¹. IR (CHCl₃): 3440, 1699(w) cm⁻¹. ¹H-NMR, δ(CDCl₃): 10.38(s, 1H, CHO of **28**), 8.12-7.58(m, 4H, open and cyclic), 5.70(s, 1H, CHOH of **29**), 3.49-3.20(m, 3H, NCH₂ of **29** and OH), 3.01-2.91(q, 2H, NCH₂ of **28**), 1.91-1.73(m, 2H, CH₂ of **29**), 1.55-1.45(m, 2H, CH₂ of **28**), 1.05-0.99(t, 3H, CH₃ of **29**) and 0.90-0.83(t, 3H, CH₃ of **28**). ¹³C-NMR, δ(CDCl₃): 191.0, 136.6, 134.9, 133.4, 133.1, 132.5, 132.3, 130.6, 129.7, 125.1, 121.0, 120.7, 81.7, 44.9, 42.9, 22.8, 21.5, 11.2 and 10.8. ¹³C NMR, δ(solid): 138.0, 134.0, 131.0, 120.0, 84.0, 43.0, 22.0 and 11. MS: M⁺ = 227 (for EI-MS data see Table 8).

Reaction of pseudo sulfonylchloride **14** (0.205 g, 1 mmol) with n-propylamine yielded the isothiazole **29** (0.136 g, 60.0 %).

Isopropylamine: The sulfonyl chloride **13** (0.30 g, 1.47 mmol) and isopropylamine (1 mL) were used and the reaction was carried out as above to obtain N-isopropyl-2-[(isopropylimino)methyl]-benzenesulfonamide (**20**) as a viscous liquid, (0.36 g, 53 %). IR (Neat): 3200-3400, 1630 cm^{-1} . $^1\text{H-NMR}$, $\delta(\text{CDCl}_3)$: 8.47(s, 1H of **20**), 8.05-8.02(m, 1H, ArH of **20**), 7.80-7.60(m, 3H, ArH of **21**), 7.56-7.41(m, 3H ArH of **20**), 7.23(s, 1H, -NH-exchangeable with D_2O), 5.48(s, 1H, benzylic H of **16**), 4.00-3.92(m, 1H of **21**), 3.59-3.47(m, 1H of **20**), 3.40-3.27(m, 1H of **20**), 3.08-3.00(m, 1H of **21**), 1.25(d, 6H of **20**), 1.01(d, 6H) and 0.88(d, 6H of **21**). $^{13}\text{C-NMR}$, $\delta(\text{CDCl}_3)$: 157.8, 139.9, 133.7, 132.3, 130.0, 129.9, 62.1, 46.6, 24.0 and 23.8.

Pseudo sulfonylchloride **14** (0.308 g, 1.5 mmol) on treatment with isopropylamine for 4 h gave the sulfonamide **20** (0.29 g, 74.0 %).

t-Butylamine: The sulfonylchloride **13** (0.25 g, 1.2 mmol) was reacted with *t*-butylamine (1 mL) as above. The product was crystallized from benzene-petroleum ether mixture to obtain N-*t*-butyl-2-[(t-butylimino)-methyl]benzenesulfonamide (**22**) (0.27 g, 75 %), mp. 131-132 °C. IR (Nujol): 2500-3250, 1620 cm^{-1} . $^1\text{H-NMR}$, $\delta(\text{CDCl}_3)$: 8.53(s, 1H), 8.15(d, 1H), 7.65-7.52(m, 4H, ArH and -NH), 1.35(s, 9H) and 1.23(s, 9H). $^{13}\text{C-NMR}$, $\delta(\text{CDCl}_3)$: 155.6, 142.2, 134.1, 132.5, 131.9, 130.0, 129.3, 58.9, 54.9, 30.5 and 29.6. MS: $\text{M}^+ = 296$.

Aniline: The reaction was carried out as above, using normal sulfonyl chloride **13** (0.55 g, 2.68 mmol) and aniline (1.2 mL). The reaction mixture was worked up as usual (except that dilute HCl wash was included to remove aniline). The product, 2,3-dihydro-2-phenyl-3-phenylamino-benzisothiazole-1,1-dioxide (**27**) was crystallized from benzene-petroleum ether, (0.54 g, 60 %), mp. 135 °C (lit¹⁹ mp. 135 °C). IR (Nujol): 3380, 1600 cm^{-1} . IR (KBr disc): 3380, 1610 cm^{-1} . $^1\text{H-NMR}$, $\delta(\text{CDCl}_3 + \text{D}_2\text{O})$: 8.85(s, 1H, CH=NC₆H₅ of **26**), 7.94-7.67(m, 3H), 7.50-7.35(m, 5H), 7.30-7.09(m, 2H), 6.77-6.57(m, 1H), 6.54-6.53(q, 2H) and 6.44(s, 1H, CHNHC₆H₅ of **27**). $^{13}\text{C-NMR}$ $\delta(\text{CDCl}_3)$: 144.1, 136.4, 135.6, 134.0,

133.5, 132.8, 130.8, 129.7, 129.4, 128.5, 128.3, 125.8, 125.1, 122.8, 121.6, 121.3, 120.0
115.3 and 72.5. MS: $M^+ = 336$ (for EI MS data see Table 8).

p-Nitroaniline: The sulfonyl chloride **13** (0.31 g, 1.5 mmol) was dissolved in dry dichloromethane (3 mL) and a solution of p-nitroaniline (0.09 g, 0.65 mmol) and pyridine (two drops) in dichloromethane (5 mL) was added and the mixture was stirred at ambient temperature for 12 h. The reaction mixture was evaporated to dryness in vacuum. Residue was chromatographic over a column of silica gel; eluent: dichloromethane. The solid obtained was further purified by preparative TLC (dichloromethane, three elution's). The fraction with R_f value 0.4 was collected. 2,3-Dihydro-2-p-nitrophenyl-3-hydroxy benzisothiazole-1,1-dioxide (**37**) was obtained as a yellow solid (0.075 g, 38 %), mp. 182 °C (dec). IR (Nujol): 3200-3500, 1590 cm⁻¹. IR (KBr disc): 3450, 1610 cm⁻¹. ¹H-NMR, δ(DMSO-d₆ + D₂O): 8.37-8.33(d, 2H), 8.04-8.00(d, 1H), 7.87-7.67(m, 5H), and 6.78(s, 1H). ¹³C-NMR, δ(DMSO-d₆): 143.2, 142.3, 135.8, 135.0, 133.5, 131.9, 126.4, 125.7, 121.1, 119.1 and 80.6. MS: $M^+ = 306$ (for EI-MS data see Table 8).

Dimethylamine: The reaction was carried out as in the case of methylamine, using **13** (0.204 g, 1 mmol) and 40% aqueous dimethylamine (1 mL). N,N-dimethyl 2-formylbenzenesulfonamide (**38**) was obtained as a viscous liquid. It was purified by filtering through a short column of silica gel, eluent: chloroform, (0.165 g, 77 %). IR (Neat): 1690, 1580 cm⁻¹. ¹H-NMR, δ(CDCl₃): 10.86(s, 1H), 8.14-8.09(m, 1H), 7.99-7.95(m, 1H), 7.82-7.74(m, 2H) and 2.81(s, 6H). ¹³C-NMR, δ(CDCl₃): 190.7, 138.7, 135.4, 133.3, 133.2, 129.9, 129.4 and 37.3.

N-Methylaniline: The sulfonyl chloride **13** (1.3 g, 6.36 mmol) was reacted with N-methylaniline (2 mL) as in the case of aniline. N-Methyl-N-phenyl-2-formylbenzenesulfonamide (**40**) (1.3 g, 74 %) was obtained as colorless needles mp. 67-68 °C (lit¹⁹ mp. 67-68 °C) IR (Nujol): 1700, 1600 cm⁻¹. IR (KBr disc) 1700, 1600 cm⁻¹. ¹H-NMR δ(CDCl₃): 9.86(s, 1H), 8.07-7.97(m, 2H), 7.81-7.73(m, 2H), 7.37-7.18(m, 2H), 7.15-7.07(m, 2H) and 3.24(s, 3H). ¹³C-NMR δ(CDCl₃): 189.8, 140.3, 137.3, 135.0,

133.3, 130.5, 129.5, 129.2, 128.5, 127.4 and 38.5. HRMS: Calcd. for $C_{14}H_{13}NO_3S$, $M^+ = 275.0616$; Found, $M^+ = 275.0641$. For EI-MS data see Table 8.

4.5.3 Hydrolysis of Schiff bases

Hydrolysis of the Schiff base 20: The Schiff base **20** (0.18 g, 0.67 mmol) was dissolved in dichloromethane (2 mL), a mixture of water and acetic acid (2:1, 1 mL) was added and the reaction mixture was stirred at ambient temperature for 4 h. The reaction mixture was diluted with dichloromethane (12 mL), washed with sodium bicarbonate solution and worked up as usual. The solid obtained was crystallized from benzene-petroleum ether (40–60 °C) mixture to obtain 2,3-dihydro-2-isopropyl-3-hydroxy-benzisothiazole-1,1-dioxide (**31**) as colorless crystals, (0.15 g, 98 %), mp. 85–86 °C. IR (Nujol): 3400–3500 cm^{-1} . IR (KBr disc): 3510–3480 cm^{-1} . IR (CHCl_3): 3440, 3320, 1695 cm^{-1} . $^1\text{H-NMR}$, $\delta(\text{CDCl}_3)$: 10.39(s, 1H, CHO of **30**), 8.18–7.62(m, 4H, ArH of **30** and **31**), 5.94(d, 1H, CHOH of **31**, collapses to singlet on D_2O exchange), 5.56(d, 1H, -NH of **30**, exchangeable with D_2O), 4.23–4.09(m, 1H, CH[Me]₂ of **31**), 3.60–3.50(m, 1H, CH[Me]₂ of **30**), 3.00–2.94(d, 1H, -OH, exchangeable with D_2O), 1.51–1.50(d, 6H, 2 x CH₃ of **31**) and 1.12–1.09(d, 6H, 2 x CH₃ of **30**). $^{13}\text{C-NMR}$, $\delta(\text{CDCl}_3)$: 191.0, 136.9, 135.5, 133.8, 133.5, 132.8, 130.9, 129.2, 125.4, 120.9, 79.6, 46.4, 45.9, 23.8, 23.1 and 20.5. $^{13}\text{C NMR}$, $\delta(\text{solid})$: 138.0, 135.0, 132.0, 131.0, 125.0, 120.0, 78.0, 43.0, 24 and 20. HRMS: Calcd. for $C_9H_{10}NO_3S$ ($M^+-\text{CH}_3$) = 212.0381; found, ($M^+-\text{CH}_3$) = 212.0358. For EI-MS data see Table 8.

Hydrolysis of the Schiff base 22: The Schiff base **22** (0.13 g, 0.44 mmol) was hydrolyzed as above, to obtain 2,3-dihydro-2-t-butyl-3-hydroxybenzisothiazole-1,1-dioxide (**33**) as white crystals (0.10 g, 94 %), mp. 120–121 °C (lit.¹⁹ mp. 105–106 °C). IR (Nujol): 3370–3500 cm^{-1} . IR (KBr disc): 3510–3360 cm^{-1} . IR (CHCl_3): 3440, 3285, 1695 cm^{-1} . $^1\text{H-NMR}$, $\delta(\text{CDCl}_3)$: 10.45(s, 1H, CHO of **32**), 8.26–8.21(m, 1H), 8.08–8.01(m, 1H), 7.80–7.62(m, 2H), 6.02(d, 1H, CHOH of **33**, collapses to singlet on D_2O exchange), 5.67(s, 1H, -NH of **32**, exchangeable with D_2O), 3.04–2.96(d, 1H, -OH of **33** exchangeable with D_2O), 1.66(s, 9H, 3 x CH₃ of **33**) and 1.23(s, 9H, 3 x CH₃ of **32**). $^{13}\text{C-NMR}$, $\delta(\text{CDCl}_3)$:

191.0, 143.6, 136.1, 135.7, 133.5, 133.0, 132.4, 132.2, 130.5, 129.2, 124.9, 120.2, 80.3, 57.7, 55.0, 30.0 and 29.0. ^{13}C NMR, δ (solid): 136.0, 134.0, 131.0, 126.0, 121.0, 80.0, 57.0 and 28.0. HRMS: Calcd. for $\text{C}_{10}\text{H}_{12}\text{NO}_3\text{S} (\text{M}^+ \text{-CH}_3)$ = 226.0538; Found, $\text{M}^+ \text{-CH}_3$ = 226.0523. For EI-MS data see Table 8.

Reaction of Normal Sulfonylchloride 13 with Stoichiometric Amount of Amines

t-Butylamine: The sulfonyl chloride 13 (0.24 g, 1.17 mmol) was dissolved in dry dichloromethane (12 mL). A solution of *t*-butylamine (0.085g, 1.16mmol) and triethylamine (0.17 g, 1.75 mmol) in dichloromethane (12 mL) was added drop-wise. The progress of the reaction was followed by TLC (eluent, dichloromethane). After the addition of 9 mL of the amine solution TLC showed the formation of the Schiff base 22. The addition of the amine was stopped and the reaction mixture was worked up as usual. The product was crystallized from benzene-petroleum ether mixture to obtain 2,3-dihydro-2-*t*-butyl-3-hydroxybenzisothiazole-1,1-dioxide (33) as a colorless solid (0.2 g, 95 %), mp. 120-121 °C.

5.7. REFERENCES

1. Bowden, K. *Adv. Phy. Org. Chem.* **1993**, *28*, 171.
2. Menger, F.M.; Venkataram, U. V. *J. Am. Chem. Soc.* **1985**, *107*, 4706.
3. Valters, E. R.; Flitsch, W. **1985**, *Ring-Chain Tautomerism*, Plenum Press, NY.
4. Bhatt, M. V.; El Ashry S. H.; Somayaji, V. *Ind. J. Chem.* **1980**, *19B*, 473.
5. Bhatt, M. V.; Ravindranathan, M. *J. Chem. Soc.* **1973**, 1160.
6. Zelinin, K. N.; Aleksegev, V. V.; Gabis, T. Y.; Yakimovitch, S. I.; Pehk, T. J. *Tetrahedron Lett.* **1990**, *31*, 3927.
7. Katritzky, A. R.; Dwell, B. L.; Durst, H. D.; Knier, B. L. *J. Org. Chem.* **1988**, *53*, 3972.
8. Malpass, J. R.; Smith, C. *Tetrahedron Lett.* **1992**, *33*, 277.
9. Bowden, K.; Byme, J. M. *J. Chem. Soc. Perk. Trans. 2*, **1996**, 1921.
10. Darabantu, M.; Ple, G.; Mager, S.; Cotoră, E.; Gaina, L.; Costas, L.; Mates, A. *Tetrahedron*, **1997**, *53*, 1873.
11. Balode, D.; Valters, R. *Latv. PSR Zinat. Akad. Vestis. Khim. Ser.* **1980**, *227*, CA 93 *168175e*.
12. Valters, R.; Balode, D.; Kampare, R.; Valtere, S. *Khim. Geterotsikl Soedin.* **1981**, *1209*, CA 95, *203048f*.
13. Balode, D.; Valters, R.; Valtere, S. *Khim. Geterotsikl Soedin.* **1978**, *1632*, CA 90, *120792q*.
14. Endo, K.; Takahashi, H.; Aihara, M. *Heterocycles*, **1996**, *42*, 589.
15. Derrick, S. D.; Boehme, R.; Wong, K. M.; Nemeth, F.; Tanaka, K.; Rumberg, B.; Beekman, R. A.; Dibble, P. W. *Tetrahedron*, **1996**, *52*, 7679.
16. King, J. F.; Hawson, A.; Huston, B. L.; Danks, L. J.; Komery, J. *Can. J. Chem.* **1971**, *49*, 943.
17. Kubota, Y.; Tatsuno, T. *Chem. Pharm. Bull.*, **1971**, *19*, 1226.
18. King, J. F.; Huston, B. L.; Komery, J.; Deaken, D. M.; Harding, D. R. K. *Can. J. Chem.* **1971**, *49*, 936.
19. Shashidhar, M. S.; Bhatt, M. V. *Proc. Ind. Acad. Sci. (Chem. Sci.)*, **1989**, *101*, 319.
20. Shashidhar, M. S. *Ph. D. Thesis: "Studies in Neighboring Group Effects."* Indian Institute of Bangalore, **1986**.
21. Jennings, W.B. *Chem. Rev.* **1975**, *75*, 307.

22. Haigh, C.W.; Mallion, R. B. in *Progr. NMR Spect.* **1980**, Vol. 13, pp. 303 and references cited there in.
23. (a) Nishio, M.; Umezawa, Y.; Hirota, M.; Takeuchi, Y. *Tetrahedron* **1995**, *51*, 8665. (b) Dougherty, D.A. *Science* **1996**, *271*, 163. (c) Samanta, U.; Chandrasekhar, J.; Chakrabarti, P. (submitted).
24. Samanta, U.; Das, T.; Puranik, V. G.; Shashidhar, M. S.; Chakrabarti, P. (Submitted).
25. Nowick, J. S.; Antonovich, V.; Norhona, G.; Ziller, J. W. *J. Org. Chem.* **1995**, *60*, 1888.
26. Fuji, K. *Org. Mass Spectrum.* **1990**, *25*, 609.
27. Hendi, M. S.; Natalie Jr., K. J.; Hendi, S. B.; Campbell, J. A.; Greenwood, T. D.; Wolfe, J. F. *Tetrahedron Lett.* **1989**, *30*, 275.
28. Luzzio, F. A.; O'Hara, L. C. *Synth. Commun.* **1990**, *20*, 3223.
29. Dewar, M. J. S.; Zoebisch, E. G.; Healy, E. F.; Stewart, J. J. P. *J. Am. Chem. Soc.* **1985**, *107*, 3902.
30. Gabe, E. J.; Le Page, Y.; Charland, J.-P.; Lee, F L; White, P S *J. Appl. Crystallogr.* **1989**, *22*, 384.
31. Sheldrick, G. M. **1993**, *SHELXL93*. Program for the Refinement of Crystal Structures, University of Göttingen, Germany.